ADVANCED COATINGS FROM NATURAL-BASED POLYMERS FOR METALS

Final Report

Toshifumi Sugama

July 2000

Prepared for the
U.S. Army Research Office
P.O. Box 12211
Research Triangle Park, NC 27709

Energy Resources Division
Energy Sciences & Technology Department
Brookhaven National Laboratory
Upton, New York 11973

This work was performed under the auspices of the U.S. Department of Energy
Washington, D.C., under Contract No. DE-AC02-98CH10866

ADVANCED COATINGS FROM NATURAL-BASED POLYMERS FOR METALS

Final Report

Toshifumi Sugama

July 2000

Prepared for the
U.S. Army Research Office
P.O. Box 12211
Research Triangle Park, NC 27709

Energy Resources Division
Energy Sciences & Technology Department
Brookhaven National Laboratory
Upton, New York 11973

This work was performed under the auspices of the U.S. Department of Energy Washington, D.C., under Contract No. DE-AC02-98CH10866

SF 298 MASTER COPY KEEP THIS COPY FOR REPRODUCTION PURPOSES

REPORT DOCUMENTATION PAGE

Form Approved
OMB NO. 0704-0188

1. AGENCY USE ONLY *(Leave blank)*	2. REPORT DATE	3. REPORT TYPE AND DATES COVERED
	7/7/00	

4. TITLE AND SUBTITLE

ADVANCED COATINGS FROM NATURAL-BASED POLYMERS FOR METALS

5. FUNDING NUMBERS

ARO MIPR 96-40

6. AUTHOR(S)

T. Sugama

7. PERFORMING ORGANIZATION NAMES(S) AND ADDRESS(ES)

Brookhaven National Laboratory
Brookhaven Science Associates
Upton, NY 11973-5000

8. PERFORMING ORGANIZATION REPORT NUMBER

9. SPONSORING / MONITORING AGENCY NAME(S) AND ADDRESS(ES)

U.S. Army Research Office
P.O. Box 12211
Research Triangle Park, NC 27709-2211

10. SPONSORING / MONITORING AGENCY REPORT NUMBER

ARO 34578.8-MS

11. SUPPLEMENTARY NOTES

The views, opinions and/or findings contained in this report are those of the author(s) and should not be construed as an official Department of the Army position, policy or decision, unless so designated by other documentation.

12a. DISTRIBUTION / AVAILABILITY STATEMENT

Approved for public release; distribution unlimited.

12 b. DISTRIBUTION CODE

13. ABSTRACT *(Maximum 200 words)*

In trying to replace coating materials or processes that generate environmentally degrading pollutants or emissions, the focus centered on the molecular modifications of the environmentally green natural polysaccharide biopolymers originating from pectin, starch, and chitosan as renewable agricultural and marine resources, and on assessing their potential as the corrosion-preventing water-based coatings for aluminum (Al) substrates. The modified polysaccharide coatings resolved the following five undesirable properties confronting the unmodified ones; (1) the settlement and growth of microorganisms in its aqueous solution, (2) the high susceptibility of film to moisture, (3) the poor chemical affinity of films for Al surfaces, (4) the weak adherence to polymeric topcoatings, and (5) the biodegradation of films caused by fungal growth, thereby resulting in a great film-forming performance, low susceptibility to moisture, low ionic conductivity, and excellent salt-spray resistance.

14. SUBJECT TERMS	15. NUMBER IF PAGES
Coating, Corrosion, Aluminum, Biopolymer, Starch, Chitosan	7
	16. PRICE CODE

17. SECURITY CLASSIFICATION OR REPORT	18. SECURITY CLASSIFICATION OF THIS PAGE	19. SECURITY CLASSIFICATION OF ABSTRACT	20. LIMITATION OF ABSTRACT
UNCLASSIFIED	UNCLASSIFIED	UNCLASSIFIED	UL

STATEMENT OF WORK

Current and pending environmental, health, and occupational safety regulations impose serious constraints on industries producing corrosion protective coating. One such example is reduce volatile organic compound (VOC) in the coating. In addition, hexavalent Cr and Pb compounds are environmentally hazardous, and there are pressures to eliminate their use in corrosion barriers for metals. As a result, more effective and environmentally benign corrosion protecting coating systems are needed for metals.

Under U.S. Army Research Office (AGO) sponsorship, on Contract Numbers, MIPR7HDOEARO40, MIPR8FDOEARO34, and MIPR9GDOEARO43, Brookhaven National Laboratory (BNL) performed research program aimed at gaining an understanding of the fundamental reaction pathways that are the key to the successful transformation of hydrophilic natural polysaccharide polymers into nonbiodegradable and hydrophobic ones. The natural polymers used in this program were the corn-or potato-starch and crab or shrimp shells-chitosan obtained from renewable agricultural and marine resources. Also, considerable attention of research program was paid to the formulation and characterization of transformed natural polymers for use as environmentally benign water-based coatings that mitigate the corrosion of aluminum (Al) alloys.

As for the resources of these natural polymers, world wide, a 1995 survey on the consumption of starch as a natural polymer indicated total usage of ~ 1850 million ton per year. By the year 2000, its products are estimated to reach about 2000 million tons. Because the source of starch comes from the seeds and roots of plants, it is abundant, comparatively inexpensive, and relatively stable in quality and price. In the United States, the main source of starch is corn where demand is about ten times higher than all the other sources from tapioca, sage, wheat, potato, and rice. US corn impacts the world because this county produces more than one-third of the world's corn and exports as much as 30 % of its production. This corn represents 80 % of exports from all countries of the world. On the other hand, chitosan, which is a family of polysaccharide, is well known as a low-cost, marine polymer, and is produced from the crab or shrimp shells at an estimated amount of one billion tons per year. Thus, using these natural polymers as extender and replacements for synthetic polymers not only yield economic benefit, but

also reduce our dependence on petrochemical-derived products. However, there are drawbacks in using natural polymers as protective coatings because they have the following five undesirable features, (1) the settlement and growth of microorganisms in its aqueous solution, (2) the high susceptibility of films to moisture, (3) the poor chemical affinity of films for Al surfaces, (4) the weak adherence to polymeric topcoatings, and (5) the biodegradation of films caused by fungal growth. Thus, chemical modification and processing of natural polymers, such as grafting and cross-link conformations, are needed to design and assemble the macromolecular structures that ensure adequate protection.

SUMMARY AND RESULTS

To design the nonbiodegradable and hydrophobic polysaccharide macromolecule structure, three synthetic technologies were developed at BNL: The first technology involved reconstituting an oxidation-derived fragmental polymer to include Ce ion; the second one was by grafting synthetic water-soluble polymers onto polysaccharide through a ring opening-condensation reaction pathway; and the third one was the synthesis of new-type polymers through blending polybase- and polyacid-saccharide. A general description of these synthetic technologies and the performance of the coatings made from the synthesized polymers can be drawn below.

1. Oxidation-Reconstituting Reaction Route

In the oxidation of potato-starch (PS) polymers, the conversion of PS colloidal solutions containing cerium (IV) ammonium nitrate (CAN) as an oxidizing agent onto solid states by heating in the presence of atmospheric oxygen at 150°C introduced functional C=O derivatives formed by the cleavage of glycol C-C bonds in the glycosidic rings in terms of ring openings. Progressive oxidation of CAN-modified PS by thermal treatments at 200 and 300°C not only resulted in the incorporation of oxygen into the C=O derivatives, but also caused the breakage of C-O-C linkages in the open rings. Such a highly oxidizing process led to the generation of intermediate carboxylate (COO^-) derivatives which finally transformed into cerium-bridged carboxylate complexes formed by reactions between the Ce^{4+} released from CAN and the COO^-. When such an oxidized PS film was applied a the primer coating of aluminum substrates, the following generalizations can be made about the specific characteristics of this primer, (1) the ranking of oxidation-induced functional derivatives in reducing the ionic conductivity generated by NaCl electrolyte passing through the film layers, was in the order of cerium-

complexed carboxylate > carboxylate > carbonyl > non-oxidized PS, suggesting that the complexed carboxylate films displayed a far better protection of aluminum (Al) against corrosion, then did non-oxidized PS films, and (2) in the adherence aspect of intermediate primer layers to both polyurethane (PU) top-coat and Al substrate sites, all the functional derivatives contributed significantly to improving the adhesive bonding. This links PU and Al tightly, and the result is the cohesive failure in which the loss of adhesion occurs in the PU layers.

2. Grafting Reaction Route

To graft the synthetic polymers onto the polysaccharide, the monomeric N-[-3-(triethoxysilyl) propyl]-4,5-dihydroimidazole (TSPI), polyacrylamide (PAM), and polyitaconic acid (PIA) were used as the graft-forming polymeric reagents.

2.1 TSPI

Precursor hydrolysate solutions with a pH of 8.5-8.9 were prepared by incorporating TSPI into a 1.0 wt% potato starch (PS) aqueous solution. The monomeric TSPI solutions considered consisted of 9.5 wt% TSPI, 3.8 wt% CH_3OH, 1.0 wt% HCL, and 85.7 wt% water. In this system, TSPI played an important role in preventing the settlement and growth of micro-organisms in PS aqueous solution. One of the important properties of this precursor solution was that the surface tension of PS hydrolysate can be reduced by adding the TSPI hydrolysate, thereby assuring excellent wetting behavior on Al surfaces. The high magnitude of this wettability was responsible for the fabrication of a thin solid film over the Al surfaces. When the precursor solution-solid phase conversion occurred at 200°C in air, grafting of TSPI-derived polyorgansiloxane (POS) polymer onto the PS were produced by dehydrating condensation reactions between the silanol groups in the hydrolysate of TSPI, and the OH groups of glycol and CH_3OH in the glucose units. Such reactions of glycol with one OH of the glycol groups also led to the cleavage of glycol C-C bonds, causing the opening of glycosidic rings. Thus, an increase in the number of POS grafts shifted the melting point of PS to a lower temperature, thereby forming the molecular configuration of PS chains with few hydrogen bonds between PS and water. The coating films with a high degree of grafting displayed a low susceptibility to moisture, improved impedance (in cm^2) by two orders of magnitude over that of the Al substrate, and conferred salt-spray resistance for 288 hours.

2.2. PAM

The PAM-modified corn starch-derived dextrine (DEX) paints as a film-forming precursor solution were prepared by incorporating a proper amount of PAM into the colloidal DEX aqueous solution. The liquid coating layers were deposited onto the Al surfaces using a simple dipping-withdrawing coating technology and converted into the solid layers by heating them at 150 or 200 C in air. At 150 C, the secondary amide bonds yielded by the reaction between the primary amide group in PAM and one hydroxyl group of glycol in DEX led to grafting of the PAM onto the DEX. Although increasing the temperature to 200 C caused opening of the glycosidic rings due to bond breakage between the alcohol carbon and the secondary amide carbon, the grafting conformation acted to inhibit the fragmentation of glucose units by oxidation-caused scission of the C-O-C linkages in the DEX. An increase in the degree of grafting resulted in the formation of coating films that were less susceptible to moisture. Furthermore, the Al metal in the substrate favorably interacted with the amide oxygen in the PAM-grafted DEX coatings, creating interfacial Al-O bonds formed by a charge transferring reaction in which electrons were transferred from the Al atoms to the electron accepting oxygen in the amide groups. Two important factors for highly grafted DEX coatings, a lesser susceptibility to moisture and an interfacial bond at metal/coating joints, contributed significantly to minimizing the permeability of electrolyte species through the coating layers.

2.3. PIA

Partially N-acetylated chitosan (CS) biopolymer consisting of ~ 80 % poly(D-glucosamine) and ~ 20 % poly(N-acetyl-D-glucosamine) is a derivative of the polysaccharide chitin marine biopolymer, which originates from the structural components of crustaceans, such as shrimp, lobster, and crab. In seeking ways of applying the CS biopolymer as renewable resource to an environmentally green water-based coating system for the aluminum (Al) substrates, emphasis was directed towards its molecular modification with poly(itaconic acid) (PIA), which is among the synthetic polyacid electrolytes. Adding a certain amount of HCL to the CS in aqueous medium not only enhances its solubility, but also served to remove acetyl groups from the linear CS polymer structure. The primary amine, NH_2, groups in the deacetylated CS, is polybase electrolyte having a highly positive charge density. The carboxylic acid, COOH, groups in the PIA had a strong chemical affinity for the basic NH_2 groups in the CS and formed secondary amide linkages that grafted the PIA polymer onto the linear CS chains and crosslinked between the CS chains, when mixtures of these two aqueous solutions were heated at 200 C in air. An increase in the degree of grafting and cross-link provided the

formation of the coating films that are less susceptible to moisture and to the infiltration of corrosive electrolyte species in the coating layer, conferring good protection of Al metal against corrosion. In addition, the surfaces of Al substrate preferentially reacted with the PIA, rather than the CS. This interfacial interaction could be accounted for by the formation of -COO-Al metal linkages by the acid-base reaction between the COOH groups (proton donor) in the PIA and the OH groups (proton acceptor) on the hydroxylate Al surfaces. Consequently, this coating film, deposited on the Al surfaces had a lesser sensitivity to moisture, and imposed pore resistance (in ohm-cm^2) of an order of magnitude higher than those of single CS and PIA coatings, and conferred salt-spray resistance for 694 hours.

3. Acid-Base Condensation Reaction Route

In this study, the two different polysaccharide biopolymers, poly(D-glucosamine) and poly(D-glucose) were used. The former biopolymer, called chitosan, is a structural component of the shells of crustaceans, such as lobsters, crabs, and shrimps. When this marine chitosan is dissolved in an aqueous medium at pH <6.5, it becomes a liner polybase electrolyte with a highly positive charge density. The corn-starch-derived dextrine, attributed to poly(D-glucose), is dissolved in an aqueous medium by adding proper amounts of oxidizing agents. The oxidation of dextrine not only promotes the rate of its solubilization in water, but also leads to the incorporation of oxygen functional groups, such as carbonyl and carboxylic acid, into the biopolymer's structure. Thus, the oxidized dextrine becomes a polyacid as a counter electrolyte of the chitosan polybase. These two opposite electrolyte biopolymer were mixed together to initiate a acid-base condensation reaction. This reaction generates the formation of amide linkages that serve in forming new-type polysaccharide polymers. An increase in the rate of acid-base reaction plays an important role in forming uniform, defect-free coating films that are unsusceptible to moisture, thereby conferring good protection for Al against corrosion.

ACKNOWLEDGMENTS

The author wish to acknowledge the support and guidance received from Dr. Robert R. Reeber of the U.S. Army Research Office, Research Triangle Park, NC.

List of Program Presentations, Publications, and Patents

Papers Presented

T. Sugama, Oxidized Dextrine Coatings for Preventing Corrosion of Aluminum. Proceedings of the 1997 Tri-Service Conference on Corrosion, Wrightsville Beach, North Carolina, November 17-21, 1997.

T. Sugama, Poly(acid)-modified Chitosan Marine Polymer Coatings for Aluminum Substrates. Proceedings of the 1999 Tri-Service Conference on Corrosion, Myrtle Beach, South Carolina, November 15-19, 1999.

Published

T. Sugama, Pectin Copolymers with Organsiloxane Grafts as Corrosion-Protective Coatings for Aluminum. Materials Letters, Vol.25, 291-299 (1995).

T.Sugama and J.E. DuVall, Polyorganisiloxane-Grafted Potato Starch Coatings for Protecting Aluminum from Corrosion. Thin Solid Films, Vol. 289, 39-48 (1996).

T. Sugama, Oxidized Potato-Starch Films as Primer Coatings of Aluminum. Journal of Materials Science, Vol. 32, 3995-4003 (1997).

T. Sugama and T. Hanwood, Polacrylamide-Grafted Dextrine Copolymer Coatings. Journal of Coatings Technology, Vol. 70, 69-78 (1998).

T. Sugama and S. Millian-Jimoney, Dextrine-modified Chitosan Marine Polymer Coatings. Journal of Materials Science, Vol. 34, 2003-2014 (1999).

T. Sugama and M. Cook, Poly(itaconic acid)-modified Chitosan Coatings for Mitigating Corrosion of Aluminum Substrates. Progress in Organic Coatings, (in press).

Patents

T. Sugama, Organosiloxane-grafted Natural polymer Coatings. United State Patent Number 5,844,058 on Dec. 1, 1998.

T. Sugama, Chitosan Marine Polymer-based Coatings. (in pending).

List of Supported Students and Teachers

Summer Student

M. Cook	Department of Chemistry, Polytechnic University

Semester Students

S. Milian-Jimenez	Department of Chemistry, Washington College
P. Hayenga	Chemical Engineering Department, Columbia Basin College

High School Teachers

J. E. DuVall	Green Valley School, Henderson, NV
T. Hanwood	Crown Height School, Brooklyn, NY
M. Gerena	Oliver W. Holmer School, Long Island City, NY

APPENDIX A

PUBLICATIONS

ELSEVIER

Thin Solid Films 289 (1996) 39–48

thin solid films

Polyorganosiloxane-grafted potato starch coatings for protecting aluminum from corrosion

T. Sugama [a], J.E. DuVall [b]

[a] *Energy Efficiency and Conservation Division, Department of Applied Science, Brookhaven National Laboratory, Upton, NY 11973, USA*

[b] *Green Valley High School, 460 N. Arroyo Grande Henderson, Henderson, NV 89014, USA*

Received 23 November 1995; accepted 22 February 1996

Abstract

Polyorganosiloxane (POS) grafted polysaccharide copolymers were synthesized through a heat-catalyzed dehydrating condensation reaction between the hydrolysates of potato starch (PS) as source of polysaccharide and *N*-[3-(triethoxysily)propyl]-4,5,-dihydroimidazole (TSPI) as the antimicrobial agent and source of the graft-forming POS at 200 °C in air. The grafting of POS onto PS followed by the opening of glycosidic rings significantly improved the thermal and hydrophobic characteristics of PS. The degree of wettability of Al surfaces by PS solution increased as the TSPI hydrolysate was incorporated into PS, thereby fabricating a thin uniform solid film over the Al substrate suitable for the protection of Al against corrosion. Consequently, the POS-grafted PS coatings derived from the precursor solution with a [PS]/[TSPI] ratio of 90/10 conferred an impedance of greater than 10^5 Ω cm^2 and salt-spray resistance of 288 h.

Keywords: Polyorganosiloxane; Potato starch; Coating; Aluminum

1. Introduction

In applying environmentally benign natural polymers as water-based coating systems to protect Al alloys from corrosion, we have previously studied the chemical modification of polygalaturonic acid methyl ester (pectin, PE) which is a family of natural polymers [1]. The major aim in modifying PE was to resolve the following three undesirable problems: (1) the settlement and growth of micro-organisms in PE aqueous solutions, (2) the high susceptibility of PE films to moisture, and (3) the poor chemical affinity of PE polymers for Al surfaces. We succeeded in overcoming these drawbacks by incorporating a sol solution derived from mineral acid-catalyzed hydrolysis of *N*-[3-(triethoxysily)-propyl]-4,5,-dihydroimidazole (TSPI) in aqueous medium, into the PE solution. Acting as an antimicrobial agent, the hydrized TSPI not only prevented the growth of micro-organisms in the PE solution, but also played an essential role in ensuring that the TSPI-modified PE coatings adequately protected Al from corrosion. Such protection was due mainly to the conformation of PE copolymer with polyorganosiloxane (POS) grafts from the chemical reaction between the OH or COOH groups in PE, and the silanol end groups in POS, which were formed by a polycondensation reaction between the hydrolysates of TSPI. In addition, the silanol end groups in the POS graft reacted favorably with the Al_2O_3 at the surface of Al substrates to create interfacial covalent oxane bonds, thereby improving the adherence of the coating films to the Al.

Worldwide, a 1985 survey on the consumption of starch as a natural polymer indicated total usage of approximately 1700 million tons per year [2]. By the year 2000, its products are estimated to reach about 2000 million tons. Because the source of starch is the seeds and roots of plants as renewable agricultural resources, it is abundant, comparatively inexpensive, and relatively stable in quality and price. Thus, using starch as an extender and replacement for synthetic polymers might reduce our dependence on petrochemically derived products. Starch is a mixture of amylose and amylopectin. The former is a linear homopolysaccharide which is made up of several hundred glucose units linked by (1→4)-α-D-glycosidic linkages, and the latter is a branched homopolysaccharide of glucose units with (1→6)-α-D-glycosidic linkages at the branching points and (1→4)-α-D-glycosidic linkages in the linear region [3]. The hydrated linear amylose molecules tend inherently to align. Once the aligned configuration is formed, the intramolecular hydrogen bonds generated between the linear chains lead to the agglomeration and crystallization of amylose chains, thereby resulting in a low solubility in water. Similarly, the molecular arrangement of linear portions in the branched amylopectin introduces some degree of crystallinity into the hydrated starch [4].

PII S0040-6090(96)08814-1

However, the solubility of amylopectin in water is much higher than that of amylose. Typical starches have the proportions of 20%–30% amylose and 70%–80% amylopectin.

Several investigators [5–9] reported that a better way to modify starch with synthetic polymers or monomers at the molecular level, compared with physical blending, is graft copolymerization in an aqueous or non-aqueous medium. Starch structures were modified through the reaction of their hydroxyl groups with functional groups of the synthetic polymers, such as carboxylic acid, anhydride, epoxy, urethane, or oxazoline, and by free-radical ring-opening polymerization occurring between their glucose rings and the vinyl monomers.

Based on this information, our emphasis in the present study was directed toward evaluating the ability of antimicrobial TSPI-modified starch films to protect Al alloys from corrosion. The evaluations were carried out using A.C. electrochemical impedance spectroscopy and salt-spray resistance tests. These data were then correlated with several physicochemical factors, such as the spreadability of the modified starch aqueous solution on the Al substrate surface, the magnitude of the susceptibility of solid coating film surfaces to moisture, the molecular conformation of the modified starch, its thermal decomposition, and the surface morphology of films. In addition, we investigated the effect of TSPI as antimicrobial agent on preventing the settlement and growth of micro-organisms in aqueous starch solution.

2. Experimental details

2.1. Materials

The starch used was potato starch (PS) from ICN Biomedical Inc. For modifying PS, monomeric *N*-[3-(triethoxysily)propyl]-4,5,-dihydroimidazole (TSPI) was supplied by Huls America Inc. A 1.0 wt.% PS solution dissolved in deionized water at 80 °C was modified by incorporating various amounts of the TSPI solution consisting of 9.5 wt.% TSPI, 3.8 wt.% CH_3OH, 1.0 wt.% HCl, and 85.7 wt.% water. We employed six ratios of PS to TSPI of 100/0, 99/1, 97/3, 95/5, 90/10, and 85/15 by weight. The lightweight metal substrate was a 6061-T6 aluminum (Al) sheet containing the following chemical constituents: 96.3 wt.% Al, 0.6 wt.% Si, 0.7 wt.% Fe, 0.3 wt.% Cu, 0.2 wt.% Mn, 1.0 wt.% Mg, 0.2 wt.% Cr, 0.3 wt.% Zn, 0.2 wt.% Ti, and 0.2 wt.% other elements.

2.2. Coating technology

The Al surfaces were coated by TSPI-modified and unmodified PS films in the following sequence. As a first step to remove surface contaminants, the Al substrates were immersed for 20 min at 80 °C in an alkaline solution consisting of 0.4 wt.% NaOH, 2.8 wt.% tetrasodium pyrophosphate, 2.8 wt.% sodium bicarbonate, and 94.0 wt.% water. The alkali-cleaned Al surfaces were washed with deionized water at 25 °C for 5 min, and dried for 15 min at 100 °C. Then the substrates were dipped into a soaking bath of solution at room temperature, and withdrawn slowly. The wetted substrates were then heated in an oven for 120 min at 200 °C to yield thin solid films. The heating temperature of 200 °C was selected on the basis of the results of our previous study on the most effective curing temperature for pectin copolymers with polyorganosiloxane grafts for improving their hydrophobic characteristics and protecting the metal against corrosion [1].

2.3. Measurements

Because the PS solution is a suitable nutrient for fungal and bacterial growth, the effect of adding TSP to prevent the growth and colonization of micro-organisms was observed, using scanning electron microscopy (SEM). The surface tension of the unmodified and TSPI-modified PS solutions was measured with a Genco-DuNouy tensiometer model 70535. Solutions with an extremely high or low pH are not suitable for use as coatings of metal surfaces because of the corrosion of metal by such solutions. Thus it is very important to measure the pH of coating solutions prior to depositing them onto the metal surface. To understand the molecular structure of TSPI-modified PS, the films deposited onto Al surfaces were investigated by specular reflectance Fourier transform IR (SRFT-IR) spectrophotometry, and X-ray photoelectron spectroscopy (XPS). The combined techniques of scanning calorimetry (DSC), thermogravimetric analysis (TGA), and differential thermal analysis (DTA) were used to assess the changes in the melting point of PS as a function of TSPI concentration, and also to determine the thermal decomposition characteristics of modified and unmodified PS polymers. The degree of crystallinity of the polymers was estimated using X-ray powder diffraction (XRD). We recorded the changes in the magnitude of wettability and spreadability of Al surfaces by PS solutions modified with various amounts of TSPI by measuring the contact angle within the first 30 s after dropping the solution onto the Al surface. The same technique was employed to obtain the water-wettability of polymer film surfaces; this gave us information on the degree of susceptibility of modified and unmodified PS film surfaces to moisture. Information on the surface morphology and chemical composition of films deposited onto Al was obtained by SEM and energy-dispersive X-ray (EDX) analysis.

A.C. electrochemical impedance spectroscopy (EIS) was used to evaluate the ability of coating films to protect Al from corrosion. The specimens were mounted in a holder, and then inserted into an electrochemical cell. Computer programs were prepared to calculate theoretical impedance spectra and to analyze the experimental data. Specimens with a surface area of 13 cm^2 were exposed to an aerated 0.5 N NaCl electrolyte at 25 °C, and single-sine technology with an input A.C. voltage of 10 mV (rms) was used over a frequency

range of 10 kHz to 10^{-2} Hz. To estimate the protective performance of coatings, the pore resistance R_{po} was determined from the plateau in Bode-plot scans (impedance $\Omega\,cm^2$ vs. frequency Hz) that occurred at low frequency regions. Salt-spray tests of the unmodified and modified PS-coated Al panels (75 mm × 75 mm in size) were performed in accordance with ASTM B 177, using a 5% NaCl solution at 35 °C.

3. Results and discussion

3.1. Properties of solutions and films

The PS polymers contain C, H, and O, among other elements, as suitable nutrients for fungal and bacterial growth. When this polymer comes into contact with water, inevitably the growth of micro-organisms already present in the water is stimulated, and they flourish, forming colonies. A serious problem in using such colonized polymer solutions as coating materials is that the microbial bioparticles incorporated into the layers of the dried coating film promote the rate of water transportation, thereby resulting in its failure as corrosion-protective coatings. Thus, the addition of an antimicrobial agent to the PS solution is needed to prevent the growth of micro-organisms.

In this study, monomeric TSPI was employed as the antimicrobial agent. To assess its effectiveness in inhibiting microbial growth, 20 g aqueous solutions with [PS]/[TSPI] ratios of 100/0 and 97/3 were placed in culture flasks, and then left for 2 months at 25 °C in atmospheric environments. Subsequently, these solutions were deposited onto the Al substrate surfaces by dip-withdrawal coating methods, and then dried for 24 h in a vacuum oven at 40 °C to transform them into solid films for SEM observations. The SEM image (not shown) from the unmodified PS coating disclosed a continuous coverage of extensive fungal clusters over the Al. A strikingly different feature was found when the PS was modified with a 3 wt.% TSPI solution; there was no fungal growth in these 97/3 ratio films. This finding strongly suggested that the incorporation of TSPI as an antimicrobial agent prevents the growth of micro-organisms in the PS solution.

Table 1 shows the changes in surface tension of solutions as a function of [PS]/[TSPI] ratio at 25 °C, and also the pH values. The addition of the TSPI solution to the PS solution tends to decrease the surface tension, from 72.3 dyne cm^{-1} for the unmodified PS solution, to 54.7 dyne cm^{-1} for 15 wt.% TSPI-modified PS. The pH of the unmodified PS solution was 6.4; however, when this solution was modified with 1 wt.% TSPI solution, its pH shifted to a weak base site. The pH values of all TSPI-modified PS solutions ranged from 8.5 to 8.9.

To gain information on the interfacial reaction mechanisms between PS and TSPI, and the chemical conformation of the reaction products, we investigated the samples prepared in accordance with the following method, by SRFT-IR. First, the PS solution was deposited onto the Al surfaces by dip-withdrawal coating methods, and then left for 1 h in an oven at 100 °C to transform it into a solid film. Then, the PS-coated Al substrates were dipped into a 2 or 5 wt.% TSPI solution, and the TSPI-wetted PS coatings were treated for 2 h with heating at 200 °C for SRFT-IR explorations.

Table 1
Changes in surface tension and pH of PS solutions modified with TSPI solutions

[PS]/[TSPI]	Surface tension (dyne cm^{-1})	pH
100/0	72.3	6.4
99/1	62.4	8.5
97/3	58.9	8.7
95/5	55.4	8.9
90/10	54.8	8.9
85/15	54.7	8.9

Fig. 1 depicts the IR spectra for the 2 and 5 wt.% TSPI-coated PS samples, over the three frequency ranges 4000–3000, 1800–1570, and 1220–970 cm^{-1}. For comparison, the spectra of 200 °C heated bulk PS and TSPI coating films as reference samples are also illustrated in this figure. A typical spectrum of the bulk PS reference coating showed absorption

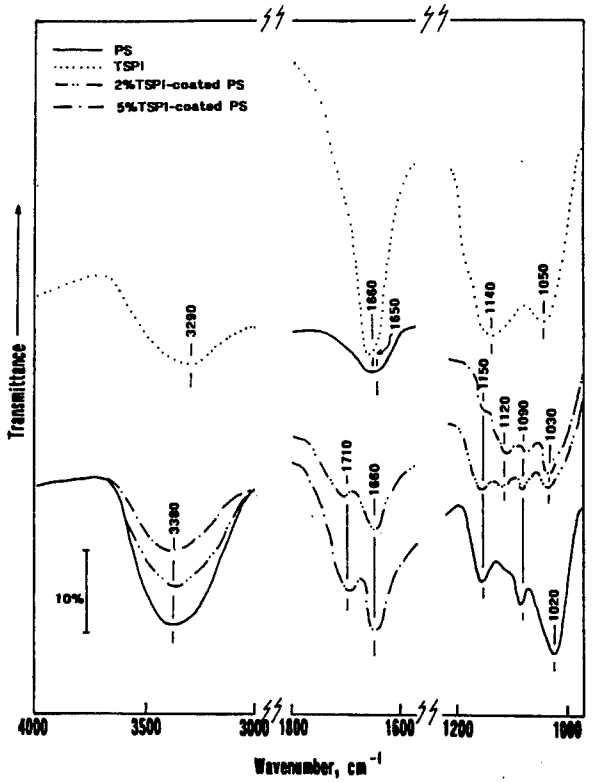

Fig. 1. SRFT-IR spectra for bulk PS and TSPI coating films, and 2% and 5% TSPI-coated PS films.

bands at 3380 cm^{-1}, revealing the OH groups in the glucose units, at 1660 cm^{-1} which can be ascribed to the bending vibration of H–O–H in the adsorbed H_2O, and also at 1150, 1090, and 1020 cm^{-1}, reflecting the stretching mode of C–O–C linkages in the glycosidic rings [10]. As described in our previous study [11], the spectrum of bulk TSPI film involved the OH stretching band in the adsorbed H_2O at 3290 cm^{-1}, the –C=N– band in dihydroimidazole coexisting with the H–O–H bending in H_2O at 1660 cm^{-1}, the Si–O–C bond in the Si-joined alkoxy groups at 1140 cm^{-1}, and the Si–O–Si linkages at 1050 cm^{-1}. When PS was coated with 2 wt.% TSPI, the features of the IR spectrum that differed from those of the reference samples were as follows: (1) a decrease in intensity of the absorption band at 3380 cm^{-1}, (2) the development of three new bands at 1710, 1120, and 1030 cm^{-1}, and (3) a striking reduction in intensity of the C–O–C linkage-related bands in the frequency region 1200–1000 cm^{-1}. Increasing the concentration of TSPI to 5 wt.% led to a further decrease in intensity of the OH and C–O–C bands, while a marked growth of these new bands can be seen in the spectrum. The contributor to the new band at 1710 cm^{-1} is likely to be the C=O groups [12]. In contrast, the Si-alkoxy compounds and siloxanes have strong bands in the ranges 1170–1110 cm^{-1} and 1110–1000 cm^{-1} respectively [13]. Thus it is possible to assume that the new bands at 1120 and 1030 cm^{-1} reveal the formation of Si–O–C and Si–O–Si linkages respectively. If this interpretation is correct, the Si–O–C linkage not only belongs to that in the TSPI, but may also be due to the reaction products formed by the interaction between PS and TSPI. The Si–O–Si linkage is the embodiment of the formation of polysiloxane structures. In a study of the mechanism of graft copolymerization onto polysaccharide initiated by the metal ion oxidation reaction, Doba et al. [14], demonstrated that oxidation of glycol groups in the glycosidic rings by ionic metal species cleaved the glycol C–C bond. The opening of the rings caused by such a cleavage not only generated a free radical which promoted the grafting of the vinyl monomers onto the polysaccharides, but also provided the formation of C=O groups. Also, they reported that no free radicals were found at the C position of $-CH_2OH$ groups in the glucose units. Relating this finding to the fact that the spectrum of the bulk PS film does not show a clear feature of C=O bands, the development of C=O groups in the TSPI-coated PS is thought to involve the formation of Si–O–C linkages yielded by a dehydrating condensation reaction between the one hydroxyl, OH, of glycol groups and the silanol group, Si–OH, in the hydrolysate of TSPI, followed by opening of the ring. However, there is no evidence as to whether a free radical was generated. Moreover, such a condensation reaction may also occur between the OH of the $-CH_2OH$ group in the glucose units and the OH of the silanol group to form the Si–O–C linkages. Because the polysiloxane structure is present in the reaction products, the creation of these linkages virtually demonstrates that the polyorganosiloxanes (POS) were grafted onto the PS.

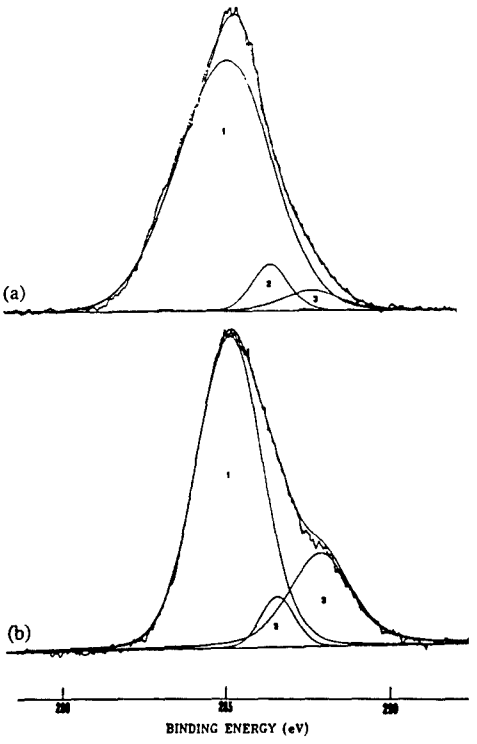

Fig. 2. XPS C_{1s} core-level spectra for bulk PS (a) and TSPI-modified PS (b) coating surfaces at 200 °C; the peak positions for curves 1, 2, and 3 correspond to 285.0, 286.5, and 288.0 eV respectively.

To ascertain further that C=O groups were generated, we inspected the XPS C_{1s} core-level excitations for the 200 °C heated film surfaces with [PS]/[TSPI] ratios of 100/0 and 85/15. In this core-level spectrum, the scale of the binding energy (BE) was calibrated with the C_{1s} of the principal hydrocarbon-type carbon peak fixed at 285.0 eV as an internal reference standard. A curve deconvolution technique, using a Du Pont curve resolver, was employed to substantiate the information on the carbon-related chemical states from the spectrum of the carbon atom. The C_{1s} region of bulk PS surfaces (Fig. 2) had the three resolvable Gaussian components at the BE positions of 285.0, 286.5, and 288.0 eV denoted as peak areas '1', '2', and '3'. The major peak at 285.0 eV is associated with the C in CH_2 and CH groups as the principal component. According to the literature [15], the second intense peak at 286.5 eV is attributable to the C in $-CH_2O-$ (e.g. alcohol and ether), while a very weak signal, emerging at 288.0 eV, originates from C in the C=O groups. Although the thermal treatment of PS film at 200 °C in an air may introduce C=O into the PS surface as an oxidation product, we assume from the curve features that the number of groups is very low. In contrast, the curve structure of TSPI-modified PS film is quite different from that of bulk PS film; in particular, (1) there is a significant growth of the C=O peak and (2) there is a marked decay of the C–O signal intensity. Thus, these findings strongly support the results from the IR study; namely, the grafting of POS onto PS

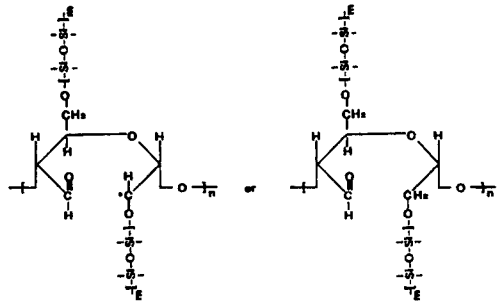

Scheme 1. Hypothetical graft structure.

Table 2
Changes in enthalpy which represent the rate of PS hydration as a function of [PS]/[TSPI] ratio

[PS]/[TSPI]	Enthalpy ΔH(kJ g^{-1})
100/0	0.325
99/1	0.266
97/3	0.240
95/5	0.176
90/10	0.136
85/15	0.119

promotes the development of C=O groups within the PS structure, thereby causing opening of the ring.

From this information, we propose the hypothetical graft structure shown in Scheme 1. However, it is not clear whether the opening of the ring leads to the formation of a free radical or a saturated group.

Next, our attention was centered on the thermal characteristics, such as the melting point, thermal degradation, and stability of 200 °C heated samples with [PS]/[TSPI] ratios of 100/0, 99/1, 95/5, 90/10, and 85/15. Fig. 3 illustrates the DSC endothermic phase transitions occurring in these samples at temperatures ranging from 25 to 170 °C. As reported by Lelievre [16] and Donovan [17], the temperature of the endothermal peak for hydrated starches depended primarily on the degree of hydration; namely, the starch with a low degree of hydration had the endothermal peak at higher temperature. They interpreted the shift in the endothermal peak to a high temperature site as corresponding to an increase in the melting point of starch. From this information, the endothermal peak at 120 °C for bulk PS (100/0 ratio) was similar to that obtained from their samples containing a minimum amount of water. When the PS was modified with TSPI, the endothermic temperature, expressed as the melting point T_m, decreased with an increasing amount of TSPI, suggesting that T_m shifts to lower temperatures as the number of POS grafts per PS chain unit is increased. In the other words, the cleavage of glycol C–C bonds by grafting POS on the glycosidic rings might cause a decrease in T_m, reflecting a low rate of PS hydration. The enthalpy ΔH of this phase transition was computed using the following formula [18,19]: $\Delta H = TRA/hm$, where T, R, A, h, and m refer to the temperature scale (°C inch^{-1}), the range sensitivity (mcal s^{-1} inch^{-1}), the peak area (inch^2), the heating rate (°C s^{-1}), and the sample weight (mg) respectively. The changes in ΔH as a function of the proportion of PS to TSPI are given in Table 2. A given result showed that the ΔH value decreases with an increasing amount of TSPI incorporated into PS. Because the ΔH value reflects the total energy consumed for breaking the intermolecular hydrogen bonds generated between starch and water [4,17], we assume that a high degree of POS grafts might lead to the molecular configuration of PS chains with fewer hydrogen bonds.

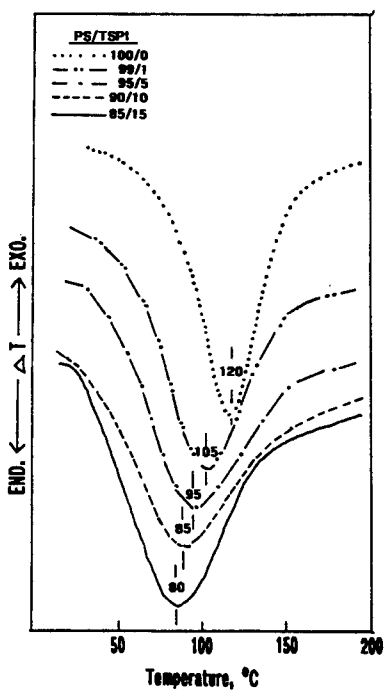

Fig. 3. Shift in the endothermal temperature of PS to low values when the proportion of TSPI to PS was increased.

A thermal analysis, combining TGA and DTA, revealed the decomposition characteristics during pyrolysis of 200 °C heated samples (Fig. 4). The TGA curve (top) for the bulk PS showed a certain rate of weight loss between 100 and 250 °C, followed by large reductions in the two temperature ranges 300–450 °C and 450–600 °C, and then a small decrease between 600 and 700 °C. The weight loss occurring at each individual stage in the four-step decomposition process had the following values: approximately 10% at temperatures up to 200 °C, 19% between 200 and 450 °C, 16% between 450 and 600 °C, and 3% between 600 and 700 °C. By comparison with the TGA curve of bulk PS, changes in the features of the curve can be seen in samples in which TSPI was incorporated. The addition of TSPI to PS greatly reduces the weight loss at the first decomposition stage. Considering that the weight loss at temperatures up to 200 °C was due mainly to dehydration of the samples, we believe that the 200 °C

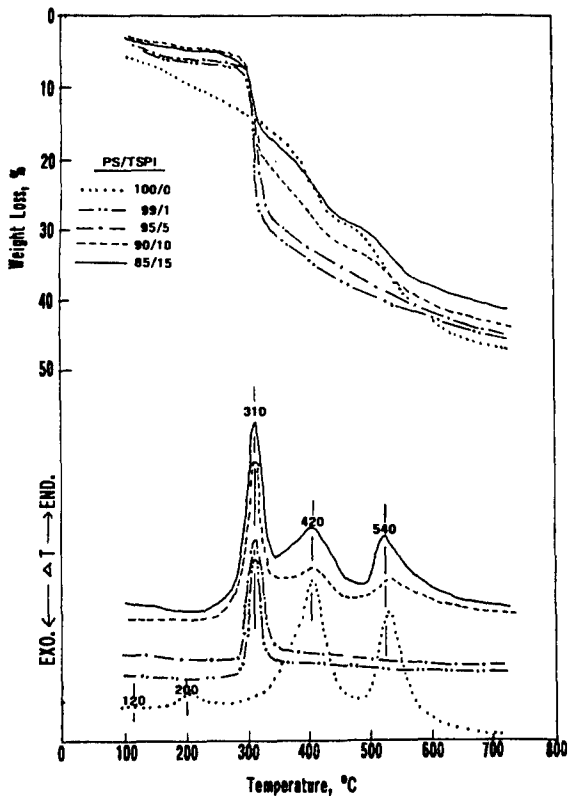

Fig. 4. TGA and DTA curves for 200 °C heated bulk PS and TSPI-modified PS polymers.

heated samples with a high proportion of TSPI to PS had a lesser uptake of moisture. For all the TSPI-modified PS samples, the onset temperature of the second decomposition stage was near 280 °C. Beyond this, of particular interest is the result that the curves of the 99/1 and 95/5 ratio samples are different from those of the 90/10 and 85/15 ratio samples. The latter samples had two additional decomposition stages at temperatures ranging from 310 to 600 °C; by contrast, the 99/1 and 95/5 ratio samples were characterized by a large decrease between 280 and 340 °C, followed by a gradual loss in weight after 340 °C. In these additional stages, one of the decompositions occurs between 310 and 470 °C, and the other was in the range 470–600 °C. As reported in our previous study on the thermal decomposition of TSPI-derived POS polymers [20], these additional decomposition stages belong to the POS polymers. Thus, a high proportion of TSPI to PS seems to provide individual POS formation segregated from the POS-grafted PS polymer systems. If this interpretation is correct, the decomposition occurring between 280 and 340 °C may correspond to the formation of POS-grafted PS polymers as the reaction products. In fact, no such decomposition was found from the bulk PS samples. The DTA curves (bottom) accompanying the TGA data strongly supported the information described above. The curve of bulk PS indicated the presence of four endothermic peaks at 120, 200, 420 and 540°C. Because a DTA endothermic peak represents the phase transition temperature caused by the thermal decomposition of chemical compounds, the peaks at 120 and 200°C reveal the dehydration of PS, while the removal of carbonaceous groups from the PS structure may be associated with the peaks at 420 and 540 °C. In contrast, the 99/1 and 95/5 ratio samples had only one endothermic peak at 310 °C. This peak might reveal the decomposition of POS-grafted PS polymers. No peaks at 420 and 540 °C were recorded on the DTA curves. Assuming that the peak at 310 °C is related to the grafted PS polymers, the increase in its line intensity resulting from the incorporation of a large amount of TSPI into PS reveals that the extent of POS grafting is promoted by an increased amount of TSPI. The peaks at 420 and 540 °C for the 90/10 and 85/15 ratio samples are assignable to the phase transition temperatures of POS itself isolated from the grafted PS. The intensity of these peaks increased with an increase in the proportion of TSPI to PS, implying that the extent of non-grafted bulk POS existing in the whole polymer structure increased as an excessive amount of TSPI was added to PS.

As described in Section 1, it is well documented that the hydration of starch introduces crystallinity into the amylose portion and linear branching of amylopectin. Thus, we investigated the degree of crystallinity of unmodified and TSPI-modified PS samples after heating at 200 °C, by XRD. The resulting XRD patterns, ranging from 0.256 to 0.590 nm (not shown), gave us the information that all the samples are essentially amorphous. Because the formation of an amorphous phase is due mainly to the low rate of hydration of starch, we assumed that the two major factors, the treatment at 200 °C and the opening of glycosidic rings by grafting of POS onto the PS, may cause poor hydration of starch.

3.2. *Characteristics of coatings*

Based on the information described above, our emphasis was now directed toward determining the characteristics of the TSPI-modified PS coating films deposited onto the Al substrate surfaces. The characteristics investigated were the magnitude of wettability and spreadability of the Al surfaces by the PS solutions modified with TSPI, the morphological features and elemental compositions of the coating films, and the susceptibility of the film surface to moisture. All of the data obtained were correlated directly with the results from the corrosion-related tests, such as electrochemical impedance spectroscopy (EIS) and salt-spray resistance.

In forming uniform, continuous coating films, the magnitude of wettability and spreadability of the alkali-cleaned Al surfaces by TSPI-modified PS solutions is among the most important factors governing good protective-coating performance. In our earlier study on the chemical composition of Al surfaces treated with a hot alkali solution [21], we reported that such a surface preparation method introduces an oxide layer into the outermost surface sites of Al. Hence, the magnitude of wettability of the unmodified and TSPI-modified PS solutions over the Al oxide layers was estimated

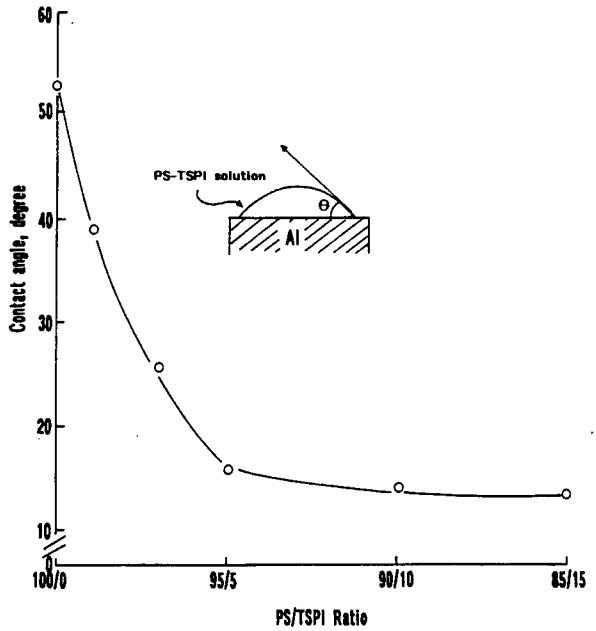

Fig. 5. Contact angles for various different [PS]/[TSPI] ratio solutions dropped onto the Al substrate surface.

from the average value of the advancing contact angle θ (deg) on this surface. A plot of θ as a function of the [PS]/[TSPI] ratios is given in Fig. 5. Because a low contact angle implies better wetting, the resultant θ–ratio data exhibited an interesting feature, namely the wetting behavior was improved by increasing the proportion of TSPI to PS. In fact, a very low θ value of less than 18°, compared with that of the 100/0 ratio, was measured from the 95/5, 90/10, and 85/15 ratio solutions, suggesting that the chemical affinity of the PS solution for the Al oxide surface was significantly improved by the incorporation of TSPI.

Surface imaging and elemental analyses of 200 °C treated 100/0, 95/5, 90/10, and 85/15 ratio films on Al substrates were carried out by SEM and EDX. The SEM image of the 100/0 ratio film (Fig. 6, top) showed a rough thick coating film. The EDX spectrum, concomitant with the SEM image, for this film, showed four dominant lines corresponding to C, O, Al, and Au. The Au corresponds to the sputtering material over the film surfaces. Because EDX is useful for quantitative analysis of elements which exist in the subsurface layer up to about 1.5 μm in thickness, the Al element virtually belongs to the underlying substrate, while the C and O elements are assignable to the PS film. Hence, the thickness of this film is less than 1.5 μm. In contrast, the SEM image of coatings derived from the 95/5 ratio shows a continuous film covering the Al (Fig. 6, bottom). The disclosure of a rough underlying Al surface expresses the formation of a thin transparent film. As expected, the EDX spectrum of this film had a dominant Al peak, and weak C, O, and Si signals which reveal the formation of POS-grafted PS polymer films. Relating this finding to the fact that the spreadability of PS solution over the Al was significantly improved by incorporating TSPI, such a high magnitude of spreadability of TSPI-modified PS solutions perhaps enabled the fabrication of a thin coating film on Al. However, the thickness of the film was not determined in this study. In comparison with the 95/5 ratio film, no distinctive features were seen in the SEM images (not shown) of the 90/10 and 85/15 ratio films. The EDX spectra of these films demonstrated that a very thin film was formed from 90/10 and 85/15 ratio solutions because of the indication of a further intense Al signal.

One of the important factors indispensable for good protective coating systems is the hydrophobic characteristic that the assembled coating film surfaces are not susceptible to moisture. To obtain information on this characteristic, we measured the contact angle of a water droplet on the 200 °C treated 100/0, 95/5, 90/10, and 85/15 ratio film surfaces. If the contact angle was low, we concluded that the film is susceptible to moisture. A high degree of susceptibility may allow hydrolytic decomposition of the film and the penetration of water through the coating layers. A plot of the contact angle against the [PS]/[TSPI] ratio showed (Fig. 7) that a decrease in this ratio enhanced the contact angle, corresponding to a low degree of wettability of the film surface. The highest value of contact angle in this test series was obtained from the 90/10 and 85/15 ratio coatings, reflecting their low susceptibility to moisture.

All these data were correlated directly with the results from electrochemical impedance spectroscopy (EIS) for the 100/0, 95/5, 90/10, and 85/15 ratio coated Al specimens at 200 °C. An uncoated Al substrate was also used as reference sample. Fig. 8 compares the Bode-plot features (the absolute value of impedance Z Ω cm^2 vs. frequency Hz) of these specimens before exposure. Particular attention in the overall impedance curve was given to the impedance value of the element Z, which can be determined from the plateau in the Bode plot occurring at sufficiently low frequencies [22]. The impedance of the uncoated Al substrate was approximately 3.0×10^3 Ω cm^2 at a frequency of 0.0 Hz. Once the Al surface was coated with the unmodified and TSPI-modified PS films, the impedance in terms of the pore resistance R_{po} of the coatings increased by one or two orders of magnitude over that of the substrate. The R_{po} values reflect the magnitude of ionic conductivity generated by the electrolyte passing through the coating layers; a high value of R_{po} corresponds to a low degree of penetration of electrolyte into the coating film [23]. The data demonstrated that the changes in magnitude of the conductivity depend on the [PS]/[TSPI] ratio. The data also showed that the curve for the 90/10 ratio derived coating closely resembled that of the 85/15 ratio coating, suggesting that the ability of the 90/10 ratio coating to prevent the penetration of electrolyte is almost the same as that of the 85/15 ratio coating. From comparison of the R_{po} values at 5×10^{-2} Hz, we found the effectiveness of these ratios in ensuring a low degree of penetration of electrolyte to be in the following order: 85/15 = 90/10 > 95/5 > 100/0. Thus, the 85/15 and 90/10 ratio-derived coating films displayed good protection of Al against corrosion.

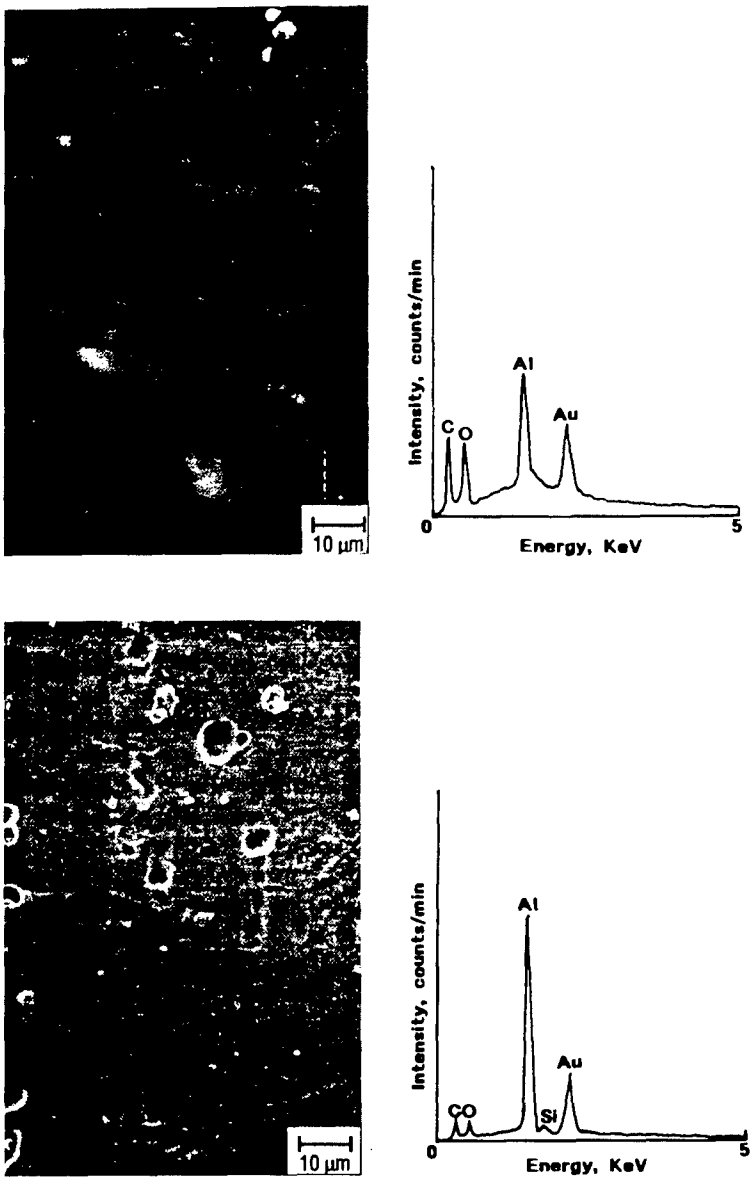

Fig. 6. SEM images coupled with EDX spectra for 200 °C treated film surfaces with 100/0 (top) and 95/15 (bottom) ratios.

To support the EIS data, we carried out salt-spray resistance tests for all the coated specimens. Traces of rust stains were generally looked for in evaluating the results from tested specimens. Table 3 shows the results reported as the total exposure time to the generation of rust stains on the Al surface. The surfaces of the 100/0, 99/1 and 97/3 ratio coatings were corroded after exposure to the salt fog for only 24 h. By comparison with these coatings, better protective performance of 48 h was obtained from the 95/5 ratio-coated specimens. In contrast, the deposition of the 90/10 and 85/15 ratio coatings onto Al contributed remarkably to protecting it from salt-induced corrosion for 288 h. This finding was similar to the results of EIS; the most effective thin coating films for protecting Al alloys against corrosion can be prepared using solutions with the 90/10 and 85/15 ratios.

4. Conclusion

To apply polyorganosiloxane (POS) polymers grafted onto polysaccharide as thin coating films which afford adequate protection of aluminum (Al) alloys against corrosion, precursor hydrolysate solutions with a pH of 8.5–8.9 were prepared by incorporating monomeric *N*-[-3-(triethoxysilyl)propyl]-4,5,-dihydroimisazole (TSPI) as the source of graft-forming POS into a 1.0 wt.% potato starch (PS) aqueous solution (as the source of polysaccharide). The monomeric TSPI solutions considered consisted of 9.5 wt.% TSPI, 3.8 wt.% CH_3OH, 1.0 wt.% HCl, and 85.7 wt.% water. In this system, TSPI played an important role in preventing the settlement and growth of micro-organisms in PS aqueous solution. One of the important properties of this precursor

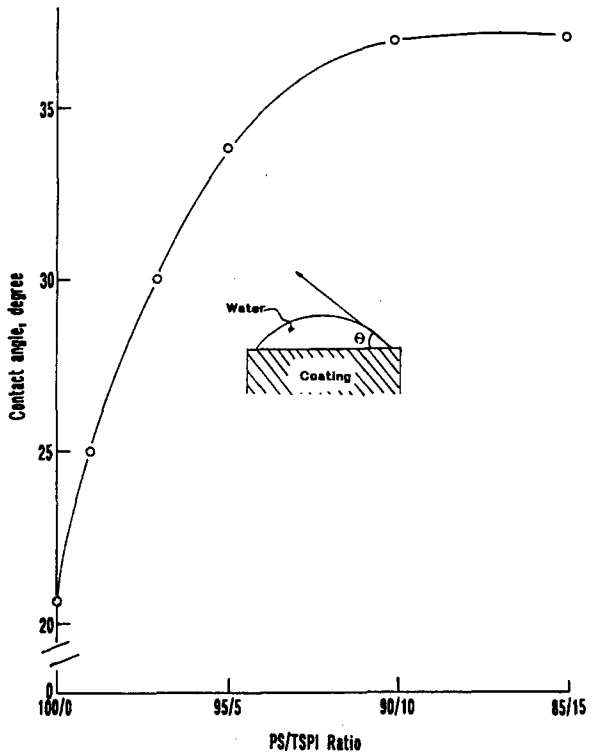

Fig. 7. Contact angle of a water droplet on 200 °C treated coating films with various different [PS]/[TSPI] ratios.

solution was that the surface tension of PS hydrolysate can be reduced by adding the TSPI hydrolysate, thereby assuring excellent wetting behavior on Al surfaces. The high magnitude of this wettability was responsible for the fabrication of a thin solid film over the Al surface. When the precursor solution–solid phase conversion occurred at 200 °C in air, grafting of TSPI-derived POS polymer onto the PS was produced by dehydrating condensation reactions between the silanol groups in the hydrolysate of TSPI, and the OH groups of glycol and CH_2OH in the glucose units. Such reactions of silanol with one OH of the glycol groups also led to the cleavage of glycol C–C bonds, causing the opening of glycosidic rings. Thus, an increase in the number of POS grafts shifted the melting point of PS to a lower temperature, thereby forming the molecular configuration of PS chains with few hydrogen bonds between PS and water. Although the onset of major thermal decomposition of POS-grafted PS polymers occurred near 280 °C, the loss in weight of POS–PS copolymers occurring between 280 and 700 °C depended mainly on the number of POS grafts; a high degree of grafting corresponded to a low rate of weight reduction. However, the addition of an excessive amount of TSPI to PS caused the phase segregation of non-grafted POS polymers from the copolymer phases. Nevertheless, the most effective amorphous coating films for preventing the corrosion of Al were derived from precursor solutions with [PS]/[TSPI] ratios of 90/10 and 85/15. These coating films deposited onto the Al surface displayed a low susceptibility to moisture, improved impedance (in Ω cm^2) by two orders of magnitude over that of the substrate, and conferred salt-spray resistance for 288 h.

Table 3
Salt-spray resistance tests for TSPI-modified PS coatings

[PS]/[TSPI]	Salt-spray resistance (h)
100/0	24
99/1	24
97/3	24
95/5	48
90/10	288
85/15	288

Acknowledgements

This work was performed under the auspicious of the US Department of Energy, Washington, DC under Contract No.

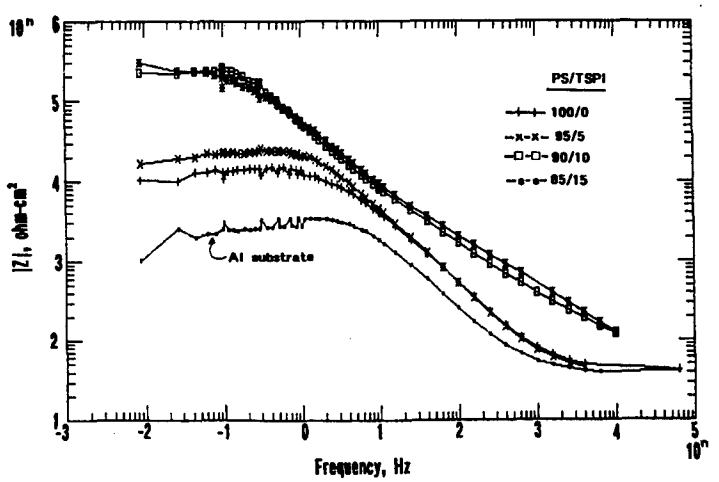

Fig. 8. Bode-plots for a bare Al substrate and Al specimens coated with films with 100/0, 95/5, 90/10, and 85/15 ratios.

DE-AC02-76CH00016, and supported by the US Army Research Office Program MIPR-ARO-117-95.

References

[1] T. Sugama, *Mater. Lett., 25* (1995) 291.
[2] F.W. Schenck and R.E. Hebeda, *Starch Hydrolysis Products*, VCH, New York, 1992, p. 32.
[3] W. Jarowenko, in I. Skeist (ed.), *Handbook of Adhesives*, Van Nostrand Reinhold, New York, 1977, p. 192.
[4] T. Bluhm, Y. Deslander, R.H. Marchessault and P.R. Sundaragan, in S.P. Rowland (ed.), *Water in Polymer*, American Chemical Society, Washington, DC, 1980, p. 253.
[5] R. Mehrotra and B. Ranby, *J. Appl. Polym. Sci., 21* (1977) 3407.
[6] G.F. Fanta, D. Trimnell and J.H. Salch, *J. Appl. Polym. Sci., 49* (1993) 1679.
[7] C.L. Swanson, G.F. Fanta and J.H. Salch, *J. Appl. Polym. Sci., 49* (1993) 1683.
[8] M. Lin, R. Cheng, J. Wu and C. Ma, *J. Appl. Polym. Sci., 31* (1993) 3181.
[9] U.R. Vaidya and M. Bhattacharya, *J. Appl. Polym. Sci., 52* (1994) 617.
[10] K. Nakanishi and P.H. Solomon, *Infrared Absorption Spectroscopy*, Holden-Day, San Francisco, CA, 1977, p. 185.
[11] T. Sugama and C. Taylor, *J. Mater. Sci., 27* (1992) 1723.
[12] L.J. Bellamy, *The Infra-red Spectra of Complex Molecules*, Chapman and Hall, London, 1975, p. 149.
[13] A.L. Smith, *Spectrochim. Acta, 16* (1960) 87.
[14] T. Doba, C. Rodehed and B. Randy, *Macromolecules, 17* (1984) 2512.
[15] D. Briggs and M.P. Seah, *Practical Surface Analysis by Auger and X-ray Photoelectron Spectroscopy*, Wiley, New York, 1983, p. 385.
[16] J. Lelievre, *J. Appl. Polym. Sci., 18* (1973) 293.
[17] J.W. Donovan, *Biopolymers, 18* (1979) 263.
[18] M.J. O'Neal, *Anal. Chem., 36* (1964) 1238.
[19] M.G. Wyzgoshi, *J. Appl. Polym. Sci., 25* (1980) 1455.
[20] T. Sugama and N. Carciello, *J. Non-Cryst. Solids, 134* (1991) 58.
[21] T. Sugama, J.R. Fair and A.P. Reed, *J. Coat. Technol., 65* (1993) 27.
[22] W.J. Loreny and F. Mansfeld, *Corros. Sci., 21* (1981) 647.
[23] F. Mansfeld, M.W. Kendig and S. Tsai, *Corrosion, 38* (1982) 478.

Guide for Authors

Manuscript Preparation

Three copies of the manuscript should be submitted, in double-spaced typing on pages of uniform size with a wide margin on the left. Some flexibility of presentation will be allowed but authors are urged to arrange the subject matter clearly under such headings as Introduction, Experimental details, Results, Discussion, etc. Each paper should have an abstract of 100–200 words.

References should be numbered consecutively (numerals in square brackets) throughout the text and collected together in a reference list at the end of the paper. Journal titles should be abbreviated according to the Chemical Abstracts Service Source Index, 1970 edition, and supplements. The abbreviated title should be followed by volume number, year (in parentheses) and page number.

Authors in Japan please note that information about how to have the English of your paper checked, corrected and improved (*before submission*) is available from: Elsevier Science Japan, Editorial Service, 1-9-15 Higashi Azabu, Minato-ku, Tokyo 106, Japan; Tel: +81-3-5561-5032; Fax: +81-3-5561-5045; E-mail: KYF04037@niftyserve.or.jp

Submission of Electronic Text

The final text should be submitted on a 3.5 in or 5.25 in diskette (in addition to a hard copy with original figures). Double density (DD) or high density (HD) diskettes formatted for MS-DOS or Apple Macintosh compatibility are acceptable, but must be formatted to their capacity before the files are copied on to them. The files should be saved in the native format of the wordprocessing program used. Most popular wordprocessor file formats are acceptable. It is essential that the name and version of the wordprocessing program, type of computer on which the text was prepared, and format of the text files are clearly indicated.

Illustrations

Line drawings should be in a form suitable for reproduction, drawn in black ink on drawing paper (letter height, 3–5 mm). They should preferably all require the same degree of reduction, and should be submitted on paper of the same size as, or smaller than, the main text to prevent damage in transit. Photographs should be submitted as clear black-and-white prints on glossy paper. Each illustration must be clearly numbered.

Illustrations can be printed in colour when they are judged by the Editor to be essential to the presentation. The publisher and the author will each bear part of the extra costs involved. Further information concerning colour illustrations and the costs to the author can be obtained from the publisher.

Legends to the illustrations must be submitted in a separate list.

All tables and illustrations should be numbered consecutively and separately throughout the paper.

Language

Papers will be published in English only.

Proofs

Authors will receive proofs, which they are requested to correct and return as soon as possible. Authors should answer clearly any question in the proofs. No new material may be inserted in the text at the time of proofreading.

Offprints

Twenty-five offprints will be supplied free of charge to the author(s). Additional offprints can be ordered at prices shown on the offprint order form which accompanies the proofs.

Further Information

All questions arising after acceptance of a paper, especially those concerning proofs, should be directed to Elsevier Editorial Services, Mayfield House, 256 Banbury Road, Oxford, OX2 7DH, UK (Tel: +44 (0) 1865 314900, Fax: +44 (0) 1865 314990, Telex: 837986).

Abstracting – Indexing Services

This journal is cited by the following Abstracting and/or Indexing Services.

Metal Abstracts, Chemical Abstracts, Physics Abstracts, Current Contents – Physical and Chemical Sciences, Current Contents – Engineering, Technology and Applied Sciences, Engineering Index, Cambridge Scientific Abstracts, Physikalische Berichte, Science Citation Index, Research Alert™, PASCAL (Centre National de la Recherche Scientifique), Fiz Karlsruhe.

Pre-publication abstracts of articles in Thin Solid Films and other related journals are now available weekly in electronic form via CoDAS, a new direct alerting service in condensed matter and materials science run jointly by Elsevier Science Publishers and Institute of Physics Publishing. For details on a free one-month subscription contact Paul Bancroft on fax +44 117 9294318 or e-mail bancroft@ioppublishing.co.uk.

0040-6090/96/$15.00

♾ The paper used in this publication meets the requirements of ANSI/NISO Z39.48-1992 (Permanence of Paper).

Printed in The Netherlands

JOURNAL OF MATERIALS SCIENCE 32 (1997) 3995–4003

Oxidized potato-starch films as primer coatings of aluminium

T. SUGAMA
Energy Efficiency and Conservation Division, Department of Applied Science, Brookhaven National Laboratory, Upton, NY 11973, USA

Potato-starch (PS) films for use as primer coatings of aluminium substrates were prepared in two steps, chemical–thermal–catalysed oxidation routes. The PS was modified with cerium (IV) ammonium nitrate (CAN) as a chemical oxidizer, followed by thermal oxidation at 150 °C in the presence of atmospheric oxygen; this led to the formation of a functional carbonyl derivative caused by cleavage of the glycol C–C bonds in glycosidic rings, thereby resulting in the ring openings. Increasing oxidation by raising the temperature to 200 and 250 °C promoted the conversion of carbonyl into carboxylate derivatives, while facilitating the breakage of C–O–C linkages in the open rings. The latter phenomenon reflected the formation of another carboxylate. The intermediate carboxylate derivatives favourably reacted with Ce^{4+} ions released from CAN to form cerium-bridged carboxylate complexes. Cerium-complexed carboxylate films used as primer coatings not only afforded some protection of aluminium substrates against corrosion, but also displayed excellent adhesion to both the polyurethane (PU) top-coating and aluminium sites. The latter demonstrated that the loss of adhesion at PU/primer/aluminium joints occurs in the PU layers, representing the mode of cohesive failure.

1. Introduction

Current and pending environmental, health and occupational safety regulations impose serious constraints on industries producing corrosion-protective coatings. One such example is the requirement that all paints containing $>250\,g\,l^{-1}$ volatile organic compound (VOC) emissions are removed from the market. In addition, chromium and lead compounds are environmentally hazardous, and there is growing pressure to eliminate their use in corrosion barriers for metals and as fillers and pigments in paints [1]. Particular attention is being paid to the large amount of hexavalent chromium as hazardous waste generated from chromium-conversion coating technologies which are commonly used as corrosion protection of anodized aluminium alloys. As a result, effective, environmentally benign material systems are needed as corrosion-protective coatings on metals.

In an attempt to mitigate such environmental impacts, our emphasis has focused on the usefulness of environmentally benign natural polymers, such as pectin and starch, as water-based coating systems to protect de-anodized aluminium from corrosion. Regarding the natural polymers, worldwide, a 1985 survey on the consumption of starch as a natural polymer indicated a total usage of $\approx 1700 \times 10^6$ ton y^{-1} [2]. By the year 2000, its products are estimated to reach about 2000×10^6 tons. Because the source of starch comes from the seeds and roots of plants as renewable agricultural resources, it is abundant, comparatively inexpensive, and relatively stable in quality and price. Thus, using starch as an extender and replacement for synthetic polymers might reduce our dependence on petrochemical-derived products. However, the direct use of natural polymers as protective coatings without any molecular modifications has three undesirable problems: (1) the settlement and growth of microorganisms in its aqueous solutions, (2) the high susceptibility of films to moisture, and (3) the poor chemical affinity of natural polymers for aluminium surfaces.

We succeeded in overcoming these drawbacks by grafting polyorganosiloxane (POS) polymers on to the natural polymer chains [3]. Such graftings were attained through heat-catalysed dehydrating polycondensation reactions between the OH or COOH groups in natural polymers and the silanol end groups in POS.

On the other hand, as already reported by several investigators [4–6], the graft copolymerization of vinyl monomers, such as acrylonitrile and methyl methacrylate, on to starch, can be initiated by cerium (IV) and manganese (III) salts as oxidizing agents. Specifically, these agents not only incorporated oxygen-based functional derivatives, such as aldehydic, ketonic, and carboxyl groups, into the starch, but also contributed to converting these functional derivatives in the oxidized starch into enolic groups. Finally, the reaction between enols and Ce^{4+} or Mn^{3+} led to the generation of free radicals caused by the opening of glycosidic rings in the starch, thereby propagating the rate of radical polymerization in assembling the grafting conformation of vinyl polymers on to the starch.

0022–2461

From this information, our particular interest was to investigate the role of the oxygen-based functional derivatives formed in the oxidized starch polymers without any grafted conformation, in applications as primer coatings of aluminium substrates. The combined techniques of chemical and thermal oxidations were employed to promote the rate of oxidation of starch polymers; namely, in the former process Ce (IV) salt was used as the chemical oxidizing agent, while the latter was accomplished by heating them in the presence of atmospheric oxygen at elevated temperatures.

Attention was paid to the characteristics of the oxidized starch coatings in protecting aluminium from corrosion and in adhering to the polyurethane top-coatings. To obtain this information, our studies included the changes in molecular conformation of starch polymers as a function of oxidation, the rate of electrolyte penetration passing through the coating film for evaluating its ability to prevent corrosion of aluminium, its salt-spray resistance, and the chemistry at interfaces between the oxidized starch primer and the polyurethane or aluminium to understand its adherence behaviour.

2. Experimental procedure

2.1. Materials

The starch used was potato starch (PS) from ICN Biomedical, Inc. Cerium (IV) ammonium nitrate $[(Ce(NH_4)_2(NO_3)_6]$ (CAN), supplied from Alfa, was used as the oxidizing agent. Chemical oxidation of a 1.0 wt % PS colloidal solution dissolved in deionized water at 80 °C was achieved by adding CAN at 0.03%, 0.07%, 0.15% and 0.30% by weight of the total PS solution. The lightweight metal substrate was a 6061-T6 aluminium sheet containing the following chemical constituents: 96.3 wt % Al, 0.6 wt % Si, 0.7 wt % Fe, 0.3 wt % Cu, 0.2 wt % Mn, 1.0 wt % Mg, 0.2 wt % Cr, 0.3 wt % Zn, 0.2 wt % Ti, and 0.2 wt % other elements. Commercial-grade polyurethane (PU) M313 resin, supplied by the Lord Corporation, was applied as an elastomeric top-coating. The PU was polymerized by incorporating a 50% aromatic amine curing agent, M201. The topcoat system was then cured in an oven at 80 °C.

2.2. Coating technology

The aluminium surfaces were coated by CAN-modified and unmodified PS films in the following sequence. As a first step to remove surface contaminants, the aluminium substrates were immersed for 20 min at 80 °C in an alkaline solution consisting of 0.4 wt % NaOH, 2.8 wt % tetrasodium pyrophosphate, 2.8 wt % sodium bicarbonate, and 94.0 wt % water. The alkali-cleaned aluminium surfaces were washed with deionized water at 25 °C for 5 min, and dried for 15 min at 100 °C. Then, the substrates were dipped into a soaking bath of solution at room temperature, and withdrawn slowly. The wetted substrates were then heated in an oven for 120 min at 150, 200 and 250 °C, to yield thin solid films. Also, this heating process promoted the rate of thermal oxidation of the films.

2.3. Measurements

To understand the changes in molecular structure of CAN-modified and unmodified PS as a function of temperature, discs for Fourier transform-infrared (FT-IR) analysis were prepared by mixing 200 mg KBr and 2–3 mg powdered PS sample that had been granulated to a size of < 0.074 mm. An X-ray photoelectron spectroscopy (XPS) study on the surfaces of these PS films was carried out to support the FT-IR data. XPS was also used to identify the locus of failure at the PU/PS/Al joints. The thickness of films deposited to the aluminium was determined by a surface-profile measuring system.

A.C. electrochemical impedance spectroscopy (EIS) was used to evaluate the ability of the coating films to protect aluminium from corrosion. The specimens were mounted in a holder, and then inserted into an electrochemical cell. Computer programs were prepared to calculate theoretical impedance spectra and to analyse the experimental data. Specimens with a surface area of 13 cm^2 were exposed to an aerated 0.5 N NaCl electrolyte at 25 °C, and single-sine technology with an input a.c. voltage of 10 mV (r.m.s.) was used over a frequency range of 10 kHz to 10^{-2} Hz. To estimate the protective performance of coatings, the pore resistance, R_{po}, was determined from the plateau in Bode-plot scans (impedance (Ωcm^2) versus frequency (Hz)) that occurred at low-frequency regions. The salt-spray tests of unmodified and modified PS-coated aluminium panels (75 mm × 75 mm, size) were performed in accordance with ASTM B 117, using a 5% NaCl solution at 35 °C.

3. Results and discussion

3.1. Oxidation of PS

Fig. 1 shows the FT-IR absorption spectra of the unmodified and 0.07, 0.15, and 0.3 wt % CAN-modified PS samples at 150 °C, over the frequency range of 4000–1000 cm^{-1}. For unmodified PS polymers, denoted as 0%, a typical spectrum enclosed absorption bands at 3420 cm^{-1}, revealing the O–H stretching vibration of OH groups in the glucose units, at 2930 cm^{-1}, and 1460 and 1370 cm^{-1} which can be ascribed to the C–H stretching and bending modes of the methylene, respectively, at 1640 cm^{-1}, originating from the bending vibration of H–O–H in the absorbed H_2O, and also at 1150, 1090, and 1020 cm^{-1}, reflecting the stretching mode of C–O–C linkages in the glucosidic rings. Similar spectral features were seen with the 0.07 wt % CAN-oxidized PS samples. Increasing the concentration of CAN to 0.15 and 0.3 wt % resulted in the appearance of a new absorption band at 1720 cm^{-1}, corresponding to the C=O groups, while the C–H bending mode at 1370 cm^{-1} somewhat shifted in frequency to a low wave number site at 1320 cm^{-1}. This information implied that a high rate of oxidation of PS polymers, induced by adding a certain amount of CAN, favourably

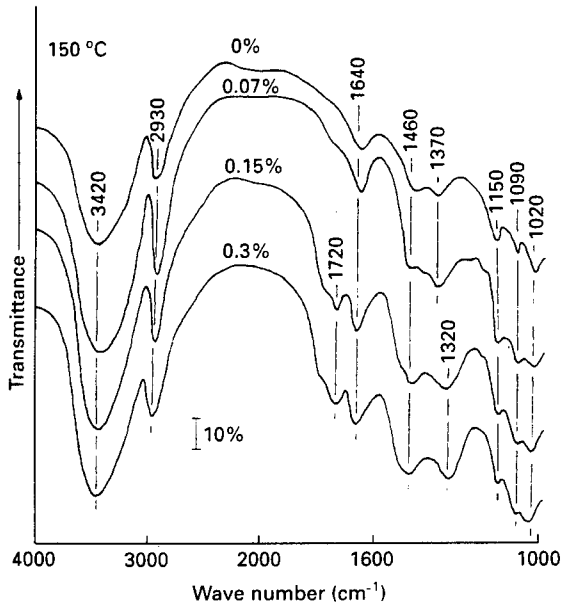

Figure 1 FT-IR absorption spectra of 0, 0.07, 0.15, and 0.3 wt % CAN-modified PS at 150 °C.

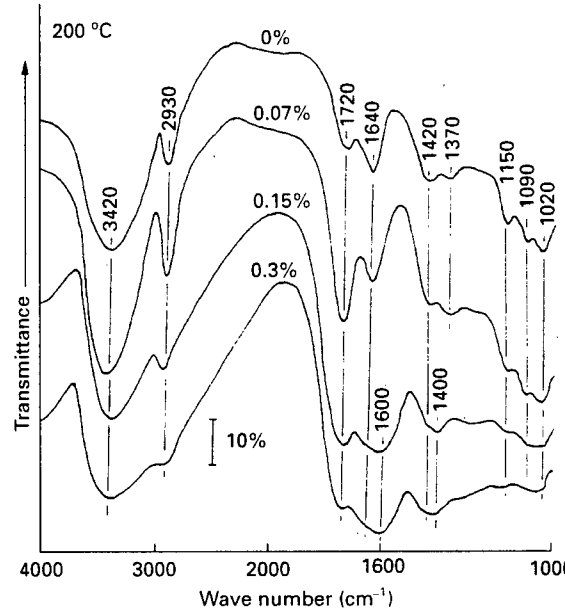

Figure 2 Comparison between IR spectral features of 0, 0.07, 0.15 and 0.3 wt % CAN-modified PS at 200 °C.

introduces the C=O groups into its molecular structure. Doba *et al.* [5] have reported that the C=O groups were formed by oxidation-caused cleavage of glycol C–C bond in the glycosidic rings. The subsequent opening of the rings caused by such cleavage not only led to the formation of C=O groups, but also generated free-radicals which promoted the rate of grafting of the vinyl monomer on to the PS. Fig. 2 depicts the FT-IR spectra of these samples treated at 200 °C. As is seen, although the CAN was unmodified, the spectrum of the bulk PS polymers was representative of the growth of C=O band at 1720 cm^{-1}. This finding clearly demonstrated that the incorporation of additional oxygens into the PS by thermal oxidation at 200 °C also provides the formation of C=O groups, corresponding to the opening of the rings by cleavaging the glycol C–C bond. As expected, PS modified with 0.07 wt % CAN revealed a further growth of the C=O band.

Next, attention centred on the spectral features of the 0.15 and 0.30 wt % CAN-modified PS samples which were quite different from those of the 0 and 0.07 wt % CAN samples: in particular, there was (1) a striking reduction in the intensity of the methylene-related bands at 2930, 1420 and 1370 cm^{-1}, and also of the C–O–C linkage-associated bands in the range 1120–1000 cm^{-1}, and (2) the emergence of strong new bands near 1600 and 1400 cm^{-1} frequencies, while the peak intensity of the C=O band became weaker. Regarding result 2, these new bands might be attributable to the formation of carboxylate groups in which the absorptions at 1600 and 1400 cm^{-1} are due to the asymmetric and symmetric stretching of COO^-, respectively [7]. If such assignments are correct, we assumed that the incorporation of more oxygens into the PS by the combination of chemical and thermal oxidations not only transforms the C=O into carboxylate groups, but also causes oxidation-induced breakage of C–O–C linkages, reflecting result 1,

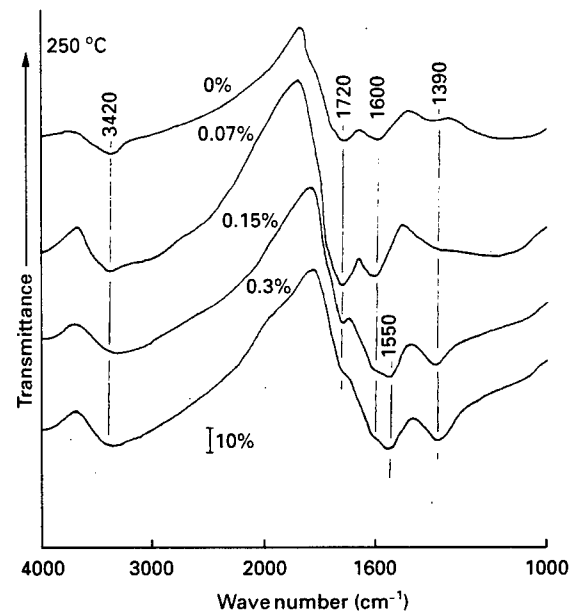

Figure 3 Changes in spectral features of 0, 0.07, 0.15 and 0.3 wt % CAN-modified PS at 250 °C.

thereby resulting in the decomposition of ring structures, and correspondingly, the removal of methylene groups from the PS. This breakage may also create C=O and carboxylate derivatives. A further increase in temperature to 250 °C enhanced the extent of the conversion of C=O into carboxylate. As shown in Fig. 3, although there was no modification with CAN, its spectrum had carboxylate bands at 1600 and 1390 cm^{-1}. With CAN-modified PS samples, the comparison between the spectral features clearly verified that the extent of peak intensity of the C=O band at 1720 cm^{-1} tends to reduce with an enhanced intensity of the carboxylate band in the range

1600–1550 cm^{-1}. Hence, the extent of C=O to carboxylate conversion seems to depend on the rate of oxidation of PS. Furthermore, a highly oxidized PS led to the decomposition of the ring structure because of the disappearance of the C–O–C linkage-associated bands ranging from 1150 to 1020 cm^{-1}, and reducing considerably the OH group-related band at 3420 cm^{-1}. As a result, it is possible to assume that the breakage of C–O–C linkages caused by incorporating an abundance of oxygen may serve in forming additional carboxylate derivatives.

This information was supported by identifying the chemical states of unmodified and 0.3 wt % CAN-modified PS film surfaces after exposing them for 2 h in air at 150 and 250 C, by XPS. In XPS core-level spectra, the scale of the binding energy (BE) was calibrated with the C1s of the principal hydrocarbon-type carbon peak fixed at 285.0 eV as an internal reference standard. A curve deconvolution technique, using a Du Pont curve resolver, was employed to substantiate the information on the carbon-related chemical states from the spectrum of the carbon atom. For the unmodified PS samples (Fig. 4), the C1s spectrum at 150 C had two resolvable Gaussian components at the BE positions of 285.0 and 286.5 eV, denoted as peak areas 1 and 2. The major peak at 285.0 eV is associated with the carbon in CH_2 and CH groups as the principal component. The secondary intensive peak at 286.5 eV originates from the carbon in $-CH_2O-$ (e.g. alcohol and ether). Noticeable changes in the shape of the C1s region were observed in the 250 C treated samples. The spectrum was characterized by the excitation of two new signals at 288.3 and 289.6 eV, corresponding to peak areas 3 and 4, respectively, and also by a striking attenuation of the area 2 signal. The possible assignments of signals at 288.3 and 289.6 eV are due to the carbon in C=O and COO^- groups, respectively [8]. Assuming that the assignments of these peaks are correct, this information strongly supported the data obtained from the FT-IR studies: namely, the susceptibility of PS to oxidation at 250 C led to the development of C=O and COO^- groups, while the elimination of the alcohol and ether groups from the rings was reflected in a striking decay of the peak area at 286.5 eV. In other words, both the alcohol and ether groups may be converted into C=O and carboxylate derivatives by oxidation. In contrast, a quite different overall curve structure was seen from modified PS film surfaces at 150 and 250 C (Fig. 5). At 150 C, the curve

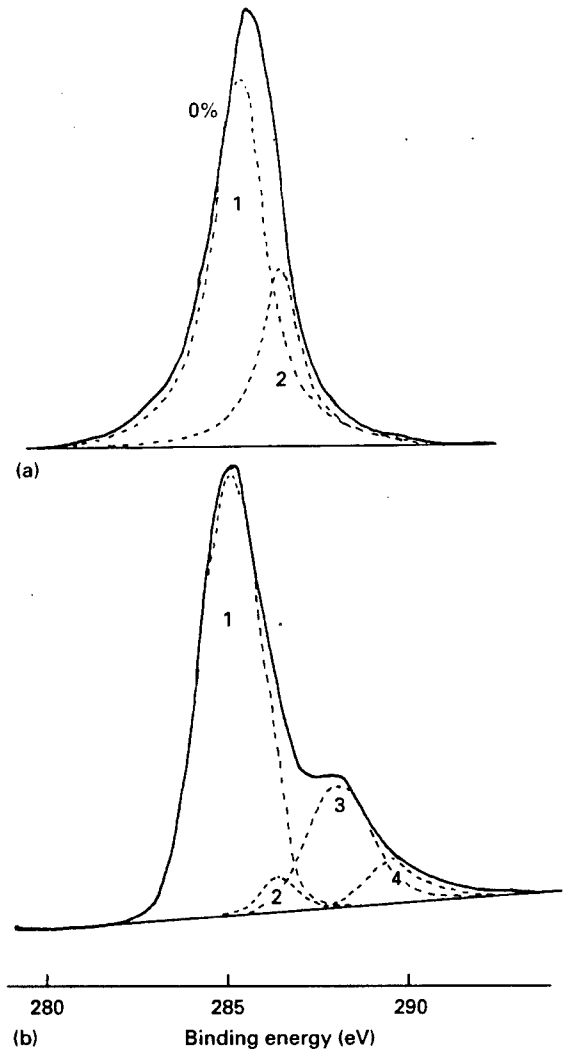

Figure 4 C1s core-level spectra for (a) 150 and (b) 250 °C oxidized bulk PS samples. 1, 285 eV; 2, 286.5 eV; 3, 288.3 eV; 4, 289.6 eV.

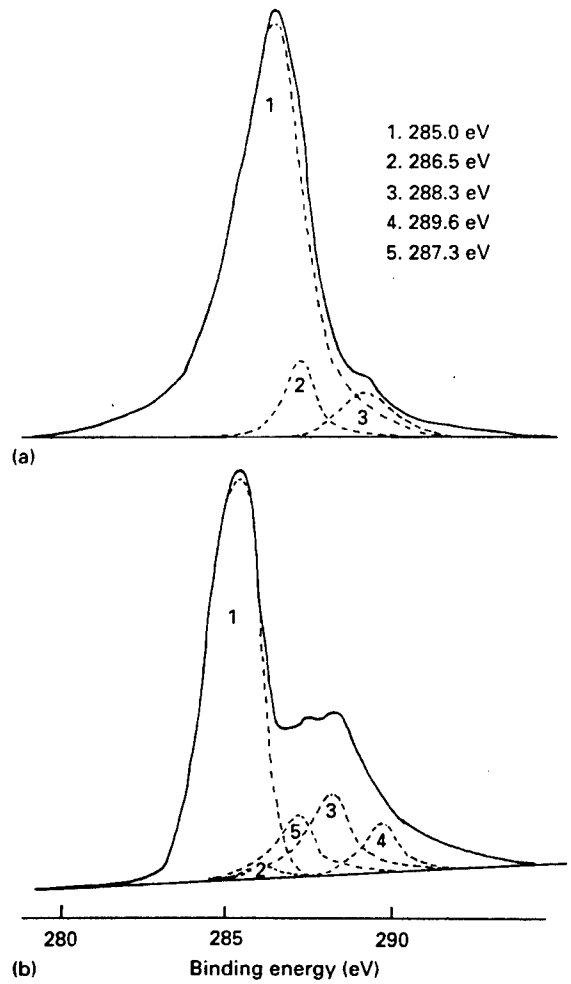

Figure 5 C1s region for 0.3 wt % CAN-modified PS samples at (a) 150 and (b) 250 °C. For key, see Fig. 4.

included the C=O related peak (area 3) at 288.3 eV, suggesting that even though the temperature of heat treatment was relatively low, adding CAN progressively promotes the rate of oxidation of PS to introduce C=O derivatives into the ring structure. A further promotion in oxidation by heating the samples to 250 °C resulted in an interesting spectral feature; namely, two new signals at 289.6 and 287.3 eV, belonging to areas 4 and 5. The former signal is assignable to the carbon in carboxylate groups. According to the literature [9], the contributor to the latter signal, which is located in BE positions between $-CH_2O-$ and C=O groups, may be due to the carbon in the metal-complexed carboxylate compounds. In this PS system, the only source of metal species comes from the CAN; it is cerium. Thus, the possible formulas of cerium complexed carboxylate are as follows

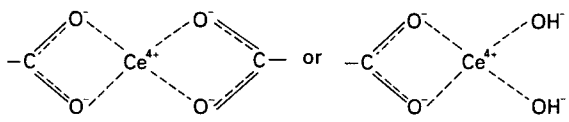

One formula is that in which Ce^{4+} ions released from CAN in an aqueous medium favourably complex with the carboxylate anions (COO^-) to form Ce^{4+} salt-bridge structures which link two adjacent carboxylates; the other formula represents a half-salt conformation containing two OH groups. Accordingly, such cerium-complexed carboxylates might be produced through the following oxidation pathways: first, the C=O derivatives are developed by preferential oxidation of glycol groups in the glycosidic rings by Ce^{4+} ions in the presence of atmospheric oxygen at low temperature; while the cleavage of the glycol C–C bond occurs followed by opening the ring. Second, enhancing the rate of oxidation by increasing the temperature not only leads to the conversion of C=O into carboxylate derivatives, but also causes the breakage of the C–O–C linkages in the ring. The latter phenomenon further promotes the formation of carboxylate because of the oxidation of alcohol and ether groups present in ring, thereby resulting in the decomposition of PS structure. Finally, the carboxylate anions (COO^-) favourably react with Ce^{4+} to form Ce^{4+} salt-bridge conformations which play an essential role in binding the COO^- ions.

The XPS study was extended to inspect the $Ce3d_{5/2}$ region of the 0.3 wt % CAN-modified PS film surfaces at 150 and 300 °C (Fig. 6). At 150 °C, the spectrum included two signals at 884.6 and 882.4 eV; the possible assignment of the latter signal is the cerium in the CeO_2 [10]. Although no information was found in the literature on surface sciences, the former signal may be due to the cerium in the cerium-complexed carboxylate compounds. Increasing the oxidizing temperature to 300 °C corresponded to a marked growth of the overall curve, suggesting that a large amount of the oxidized and complexed compounds was formed on the film's surfaces.

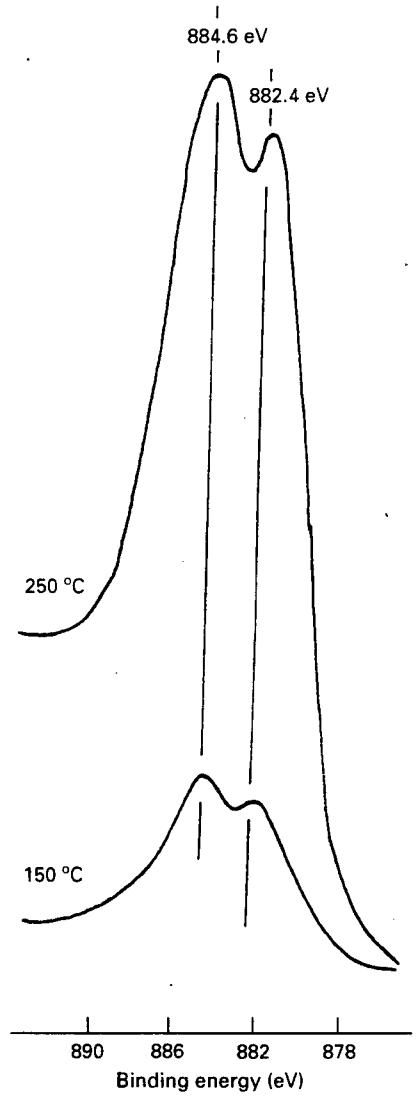

Figure 6 $Ce3d_{5/2}$ region for 0.3 wt % CAN-modified PS samples at 150 and 300 °C.

3.2. Corrosion protection

The research subject focused on investigating the ability of the oxidized PS coating films deposited on the aluminium substrate surfaces to protect them from corrosion. As described in Section 2, the coating films were prepared by dipping alkali-cleaned aluminium substrates into unmodified, and 0.07, 0.15, and 0.3 wt % CAN-modified PS solutions, followed by heating for 120 min in an air oven at 150, 200, and 250 °C. The thickness of films deposited on the aluminium ranged from ≈ 1.0 to ≈ 2.5 μm. Two corrosion-related tests, a.c. electrochemical impedance spectroscopy (EIS) and salt-spray resistance, were carried out to evaluate the effectiveness of coating films in reducing the rate of corrosion of aluminium.

In EIS examination, our attention focused on the impedance value of the element, $|Z|$, in the Bode-plot features (the absolute value of impedance, $|Z|$, $\Omega\,cm^2$, versus frequency, Hz); this value can be determined from the plateau in the Bode plot occurring at a frequency of 10^{-1} Hz for modified PS coatings, and at 10^0 Hz for unmodified PS and uncoated aluminium

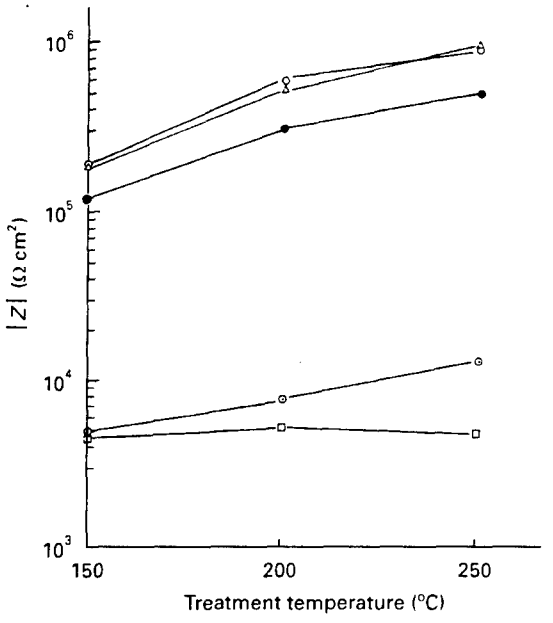

Figure 7 Changes in impedance, $|Z|$, values for CAN-modified and unmodified PS coatings as a function of thermal-oxidation temperature. (□) Aluminium substrate, modified with (⊖) 0%, (●) 0.07%, (△) 0.15% and (○) 0.30% CAN.

specimens. Fig. 7 shows the changes in $|Z|$ value as a function of thermal-oxidation temperature of the film. The impedance of the uncoated aluminium substrates treated at these temperatures ranged from $\approx 4.5 \times 10^3$ to $\approx 5.4 \times 10^3\ \Omega cm^2$. When the aluminium surfaces were coated with unmodified and CAN-modified PS films, the data demonstrated that the value of $|Z|$ depended mainly on two parameters, the concentration of CAN and the temperature; i.e. the increases in the concentration of CAN and treatment temperature reflected an increasing $|Z|$ value. Although the $|Z|$ value for the unmodified PS films gradually rises with an increase in temperature, the highest value at 250 °C was only $\approx 1.3 \times 10^4\ \Omega cm^2$. In contrast, all the CAN-modified coatings displayed an impedance of $> 10^5\ \Omega cm^2$, especially the 250 °C treated 0.15 and 0.3 wt % CAN coatings which have an impedance near $1 \times 10^6\ \Omega cm^2$, corresponding to an improvement of approximately two orders of magnitude over that of the unmodified PS. Because the $|Z|$ values reflect the extent of ionic conductivity generated by the electrolyte passing through the coating layers, a high value of $|Z|$ appears to imply a low degree of penetration of electrolyte into the coating films. Hence, from a comparison of $|Z|$ values, the most effective PS coatings for reducing the rate of penetration of NaCl electrolyte can be prepared by adding 0.15 and 0.3 wt % CAN oxidizing agents at 250 °C, thereby resulting in some degree of protection of aluminium against corrosion.

The information on the EIS was supported by salt-spray resistance tests for all the coated aluminium panels. A trace of rust stain was generally looked for in evaluating the results for salt-sprayed specimens. As shown in Table I, the results were reported as the total exposure time at the date of the generation of the rust stain from the aluminium surfaces. All the unmodified

TABLE I Salt-spray resistance of aluminium substrates coated with CAN-modified and unmodified PS at 150, 200 and 250 C

CAN (wt %)	Treatment temperature of film (°C)	Salt-spray resistance (h)
0	150	< 24
0	200	< 24
0	250	< 24
0.07	150	< 24
0.07	200	30
0.07	250	48
0.15	150	30
0.15	200	48
0.15	250	168
0.30	150	30
0.30	200	48
0.30	250	168

PS coatings at 150, 200 and 250 C failed in an exposure period of only 24 h. Although the surface of the 0.07 wt % CAN-modified PS coating at 150 C was corroded after exposure to the salt fog within 24 h, the increase in treatment temperature of this coating extended the protection to 30 and 48 h at 200 and 250 C, respectively. By comparison with the 0.07 wt % CAN coatings, an increased amount of CAN at high temperature afforded good protection. In fact, the coatings modified with 0.15 and 0.3 wt % CANs at 250 C had a salt-spray resistance for 168 h.

Relating this finding to the molecular structure of coatings, it is very interesting to note that the extent of corrosion protection afforded by the PS coating depends primarily on the complexity of the Ce^{4+} salt-bridge carboxylate conformations formed by the oxidation of CAN-modified PS; coating films containing a large number of cerium-complexed carboxylate displayed a better protection of aluminium from the corrosion, than those of a poor complexity and an uncomplexed carboxylate.

3.3. Adhesion

Assuming that these thin complex films in the range of approximately 1.0–2.5 μm are used as primer coatings of aluminium, our attention then focused on their adherence to polymeric top-coatings. In this study, only polyurethane (PU) polymer was applied as elastomeric top-coating material. To gain information on the adherent behaviour of primers, the samples were prepared in the following manner. The surfaces of the alkali-cleaned aluminium substrates were treated with 0.3 wt % CAN-modified and unmodified PS primers, and then heated for 2 h at 150, 200 and 250 °C. PU, ≈ 2 mm thick, was coated over the primed aluminium surfaces, and then cured in an oven at 80 °C. As described in our previous paper [11], the identification of the failure locus occurring at the interfaces of PU topcoat/PS primer/Al substrate joint systems provides information on evaluating the interfacial adhesive performance; namely, the most ideal failure mode is a cohesive one in which the loss of adhesion occurs in the PU layers, thereby developing a great bond strength at interfaces between the primer and PU or

TABLE II Atomic composition (at %) of interfacial aluminium sites removed from PU coatings in PU top-coat PS Primer Al substrate joint systems

CAN (wt%)	Temperature (°C)	Al	C	N	O
0	150	7.64	49.21	0.00	43.15
0	200	0.00	72.77	2.08	25.15
0	250	0.00	75.13	2.13	22.73
0.3	150	0.00	72.55	2.95	24.50
0.3	200	0.00	73.77	3.49	22.74
0.3	250	0.00	73.70	3.51	22.79

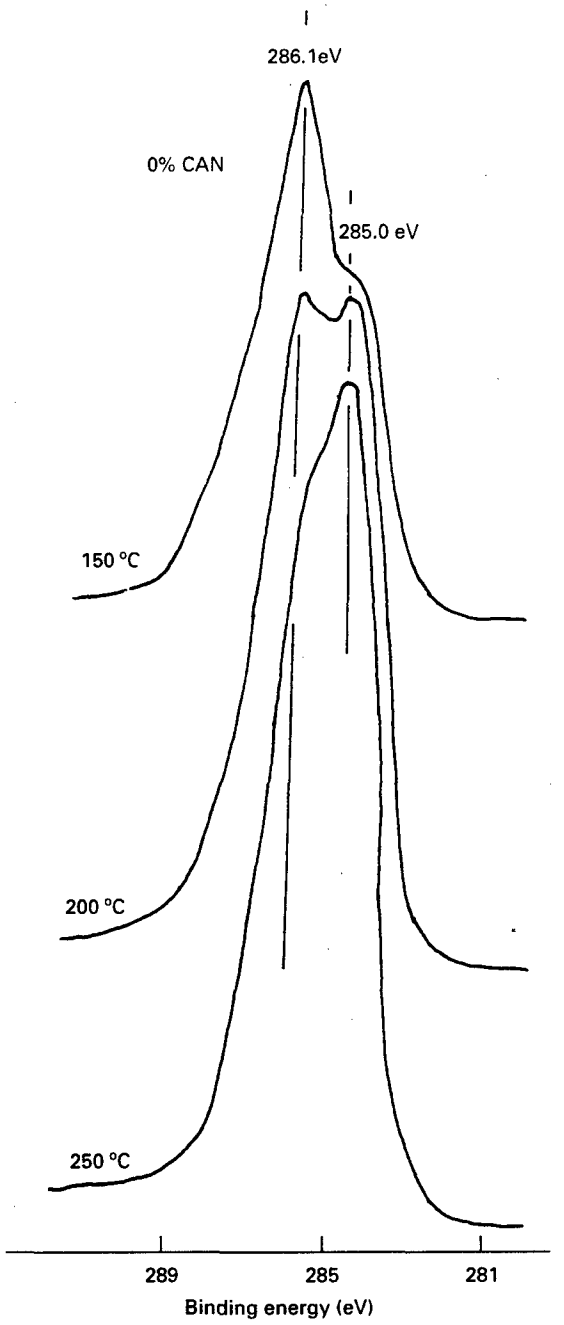

Figure 8 C1s region for interfacial aluminium surfaces removed from PU top-coatings in PU/150, 200, and 250 °C oxidized bulk PS primer/Al joint systems.

aluminium. Thus, the PU coatings adhering to the primer were physically separated from the primed aluminium surfaces. After removing PU, the interfacial aluminium surface sites were examined to identify the locus of bond failure. These data were obtained from a comparison between the XPS peak areas, which were converted into the atomic concentrations by means of the differential cross-sections for core-level excitation of the respective elements. The internally generated Al2p, C1s, N1s and O1s peak areas were used to obtain the atomic per cents. The C1s region also was investigated to substantiate further the mode of failure.

The changes in the XPS atomic composition and the spectral features of the C1s region as function of oxidizing temperature of primers are given in Table II, and in Figs 8 and 9. For the unmodified PS primers denoted as 0 wt % CAN (Table II), the atomic composition of the interfacial aluminium site with a 150 °C treated primer was characterized by having 7.64% aluminium, a large amount of carbon and oxygen, and 0% nitrogen. The sources of aluminium and oxygen elements come from the aluminium oxide layers existing at the outermost surface site of the underlying aluminium substrates [11]. In connection with the presence of carbon, the oxygen can also be associated with the PS primer. The PU has two nitrogen-related groups, isocyanate (–NCO) and urethane ($-NHCO_2$). Thus, the lack of a nitrogen signal seems to suggest that the amount of PU remaining on the primed aluminium after removing PU is very small, if any. In other words, most PU layers were isolated from the primed aluminium surfaces during the failure. Using the 200 °C treated primers, the differences in elemental distribution, compared with that of the 150 °C treated one, were as follows: (1) the presence of a certain amount of nitrogen, (2) a marked increase in the amount of carbon, (3) no aluminium signal, and (4) a pronounced reduction of the oxygen atom. From finding (3), it is conceivable that failure occurs through the coating layers away from the underlying aluminium. This information verified that the primer treated at 200 °C had some chemical affinity with the aluminium surfaces. Such an affinity probably develops a good adhesive force at interfaces between the primer and aluminium. This interfacial bond strength might be greater than those of primer and PU layers. However, there is no evidence whether the disbandment takes place in the primer, PU, or their mixed layers.

Nevertheless, it is apparent that the oxidation of PS in the presence of atmospheric oxygen at 200 °C causes the formation of C=O derivatives. Thus, a possible interpretation for the good bonding behaviour of PS to the aluminium may be due to a high reactivity of the C=O derivative as a functional group with the Al_2O_3 as the top-surface layers of aluminium. At 250 °C, the atomic composition closely resembled that of the aluminium interface at 200 °C.

To support this information, we assessed the chemical states at the BE positions of photoelectron signals which emerged in the C1s region. As seen in Fig. 8, the C1s curve of the 150 °C primed aluminium interfaces

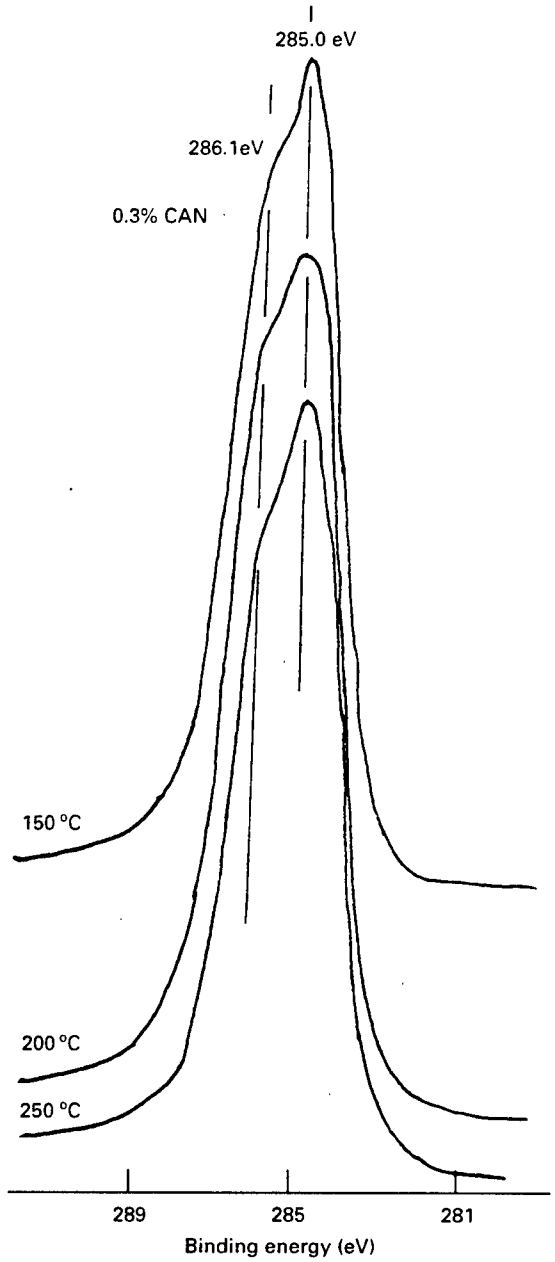

Figure 9 C1s spectra for interfacial aluminium surfaces separated from PU top-coatings in PU/thermally oxidized 0.3 wt % CAN primer/Al joint systems.

separated from the PU showed the excitations of two distinctive peaks at 286.1 and 285.0 eV. The latter shoulder peak, as a minor component, is assignable to the carbon in the $-CH_2-$ compounds. When the contributors to the major carbon peak at 286.1 eV were considered, it is possible that they encompassed the four carbon-related groups, the alcohol and ether carbons in the primer, and the diphenylic carbons joined to oxygen and nitrogen, such as $\equiv C-O-$ and $\equiv C-N=$ in the PU. However, as mentioned in the atomic composition study (Table II), there are no nitrogen atoms originating from the PU. Thus, the carbon peak at 286.1 eV is more likely to be associated with that in the primer, rather than in the PU. Assuming that this interpretation is reasonable, the loss of adhesion is not only due to the cohesive failure through the primer layers adjacent to the underlying aluminium, but also occurs at the interfaces between primer to the aluminium, as adhesive failure. Such a failure mode, which can be described as a mixed mode of cohesive and adhesive ones, suggested that the extent of the adherence of primer to the aluminium is poor, thereby creating a weak primer metal boundary layer. In other words, the magnitude of the interfacial bonding between the primer and aluminium is lower than that for the PU-to-primer interfacial bond. By comparison with that at 150 C, the curve from the aluminium interface at 200 C exhibited a doublet feature in which the peak intensity at 286.1 eV is almost the same as that at 285.0 eV, while the area in the overall curve had grown significantly. Relating this finding to the fact that the interfacial aluminium surfaces have some nitrogen atoms (Table II), it was inferred that the failure may propagate through the PU primer mixed layers. These data substantially supported the finding that the functional C=O derivative formed by the oxidation of PS at 200 C enhances its chemical affinity with the Al_2O_3. At 250 C, a specific feature of the C1s spectrum was that the peaks at 285.0 and 286.1 eV become the principal and shoulder signals, respectively. Although the data are not shown in any of the figures, the C1s region of PU itself showed a spectral feature similar to that taken from the aluminium interface at 250 C. Hence, the cohesive failure through the PU layers can be proposed as the disbandment mode in this coating system. Such information engendered the interesting concept that the 250 C treated primer promotes the adherence to both the PU and aluminium sites. Because a further oxidation of C=O derivative at 250 C converts it into the COO^- derivative, it is believed that the intermediate primer layers, consisting of a mixture of these functional derivatives, perhaps act to link tightly between the PU and aluminium substrate. Also, from this failure mode, the interfacial bond strengths developed at interfaces between primer and aluminium or PU appear to be much stronger than that of the PU itself. As a result, primers containing a large number of oxidation-derived C=O, and COO^- groups contribute significantly to improving the interfacial bonding of both the PU and aluminium sides, reflecting the formation of the most effective intermediate layers as interfacial tailoring.

Returning to Table II, when the 0.3 wt % CAN-modified PS s were applied as primer coatings, the surface chemical composition for all the aluminium interfaces at 150, 200, and 250 C had a similar elemental distribution; there was no aluminium, 72.55%–73.70% C, 2.95%–3.51% N, and 24.50%–22.79% O. As is evident from the absence of aluminium, disbandment is generated in the coating layers. In support of this information, a comparison between the C1s spectral features taken from these interfacial samples is shown in Fig. 9. As expected, all the spectra showed the PU-related curve feature, implying that the loss of adhesion occurs in the PU layers as the mode of cohesive failure. Relating this finding to the IR and XPS data, the major chemical factor of the primer

contributing to a high adhesive performance was due to the incorporation of functional C=O and cerium-complexed carboxylate derivatives into the PS by CAN-catalysed oxidation, followed by thermal oxidation in air at high temperature.

4. Conclusion

In the oxidation of potato-starch (PS) polymers, the conversion of PS colloidal solutions containing cerium (IV) ammonium nitrate (CAN) as an oxidizing agent into solid states by heating in the presence of atmospheric oxygen at 150 C introduced functional C=O derivatives formed by the cleavage of glycol C–C bonds in the glycosidic rings in terms of ring openings. Progressive oxidation of CAN-modified PS by thermal treatments at 200 and 300 C not only resulted in the incorporation of oxygen into the C=O derivatives, but also caused the breakage of C–O–C linkages in the open rings. Such a highly oxidizing process led to the generation of intermediate carboxylate (COO^-) derivatives which finally transformed into cerium-bridged carboxylate complexes formed by reactions between the Ce^{4+} released from CAN and the COO^-.

When such an oxidized PS film is applied as the primer coating of aluminium substrates, the following generalizations can be made about the specific characteristics of this primer. (1) the ranking of oxidation-induced functional derivatives in reducing the ionic conductivity generated by NaCl electrolyte passing through the film layers, was in the order of cerium-complexed carboxylate > carboxylate > carbonyl > unoxidized PS, suggesting that the complexed carboxylate films displayed a far better protection of aluminium against corrosion, than did unoxidized PS films, and (2) in the adherence aspect of intermediate primer layers to both polyurethane (PU) top-coat and aluminium substrate sites, all the functional derivatives contributed significantly to improving the adhesive bonding which links tightly between the PU and aluminium, thereby resulting in the cohesive failure in which the loss of adhesion occurs in the PU layers.

Accordingly, the oxidation of environmentally benign nature polymers is a very attractive process for fabricating intermediate primer films which afford some degree of protection of aluminium from corrosion, and ensure the development of a strongly linked boundary layer.

Acknowledgements

This work was performed under the auspices of the US Department of Energy, Washington, DC under Contract DE-AC02-76CH00016, and supported by the US Army Research Office Program MIPR-96-40.

References

1. J. M. WINTON, M. HOZEL, J. CAMPBELL, C. EHRLE, J. R. HART, L. LAZORHO and K. PORTNOY, *Chemical Week* **14** (1987) 30.
2. F. W. SCHNCK and R. E. HEBEDA, "Starch Hydrolysis Products" (VCH, New York, 1992) p. 32.
3. T. SUGAMA, *Mater. Lett.* **25** (1996) 291.
4. R. MEHROTRA and B. RANBY, *J. Appl. Polym. Sci.* **21** (1977) 1647.
5. T. DOBA, C. RODEHED and B. RANDY, *Macromolecule* **17** (1984) 2512.
6. J. P. GAO, R. C. TIAN, J. G. YU and M. L. DUAN, *J. Appl. Polym. Sci.* **53** (1994) 1091.
7. L. J. BELLAMY, "The Infra-red Spectra of Complex Molecules" (Chapman and Hall, London, 1975) p. 183.
8. D. BRIGGS and M. P. SEAH, "Practical Surface Analysis by Auger and X-ray Photoelectron Spectroscopy" (Wiley, New York, 1984) p. 385.
9. J. W. BARTHA, P. O. HAHN, F. LEGOUES and P. S. HO, *J. Vac. Sci. Technol.* **3** (1985) 1390.
10. J. F. MOULDER, W. F. STICKLE, P. E. SOBOL and K. D. BOMBEN, "Handbook of X-ray Photoelectron Spectroscopy" (Perkin-Elmer Corporation, Minnesota, 1992) p. 218.
11. T. SUGAMA, L. E. KUKACKA and N. CARCIELLO, *Int. J. Adhes. Adhesives* **8** (1988) 101.

Received 23 July
and accepted 23 October 1996

Polyacrylamide-Grafted Dextrine Copolymer Coatings

T. Sugama and T. Hanwood—Brookhaven National Laboratory*

Polyacrylamide (PAM)-grafted dextrine (DEX) copolymers were prepared by heating a film-forming precursor solution consisting of PAM, corn starch-derived DEX, cerium (IV) nitrate hexahydrate, and water, at 150° or 200°C; these solutions were applied as water-based primer coating systems to aluminum (Al) substrates. Grafting PAM on the DEX not only inhibited the fragmentation of DEX structures caused by oxidation at 200°C in air, but also aided in fabricating coating films that were less susceptible to moisture and minimized the rate of permeation of electrolyte species through the film layers. In addition, the grafted DEX coating films favorably reacted with the Al substrate to form Al-O bonds at interfaces. Consequently, Al panels coated with a highly grafted DEX copolymer had a salt-spray resistance of 600 hr.

INTRODUCTION

Current and pending environmental, health, and occupational safety regulations impose serious constraints on industries producing corrosion protective coatings. One such example is to reduce volatile organic compound (VOC) in the coating.[1] In addition, chromium and lead compounds are environmentally hazardous, and there are pressures to eliminate their use in corrosion barriers for metals. As a result, more effective and environmentally benign corrosion protecting coating systems for steel and lightweight metals such as aluminum, magnesium, and zinc are needed.

In studying the application of environmentally acceptable potato-starch (PS) as a water-based primer coating system to protect aluminum (Al) alloys from corrosion, we previously sought ways to modify it chemically and investigated the characteristics of modified PS films.[2,3] The modifications were made by the following two methods: (1) grafting polyorganosiloxane (POS) polymers derived from synthetic water-soluble monomers onto the PS; and (2) assembling a cerium (Ce)-complexed PS structure synthesized by the two steps, chemical- and thermal-catalyzed oxidation routes. Using the former method, the graft was accomplished through heat-catalyzed dehydrating condensation reactions between the silanol end groups in the POS, and the OH groups of glycol and CH_2OH in the PS macromolecule known as polysaccharide, which are made up of several hundred glucose units. A complex of Ce with the starch was prepared by incorporating Ce ammonium nitrate (CAN), as a chemical oxidizing agent, into the colloidal PS solution, followed by thermal oxidation in the presence of atmospheric oxygen. This oxidation processing generated functional C=O and COO^- derivatives formed by opening of glycosidic rings in the starch. The COO^- derivatives had a strong chemical affinity for the Ce^{4+} released from CAN and formed a Ce-bridged carboxylate complex conformation in the oxidized starch. These modifications successfully resolved the following five undesirable problems that arose when starch was directly used as a protective primer without molecular modification: (1) the settlement and growth of microorganisms in its aqueous solution; (2) the high susceptibility of films to moisture; (3) the poor chemical affinity of film for Al surfaces; (4) the weak adherence to polymeric topcoatings; and (5) the biodegradation of films caused by fungal growth. There was no doubt that such modifications significantly enhanced the potential of PS for use in corrosion-protective primers.

However, one drawback in the film-forming performance of PS-based materials was the difficulty in fabricating uniform, continuous films on the Al surfaces in the repeated coating processes. The major reason for this was the low solubility of PS in water, which caused the precipitation and segregation of insoluble colloidal PS particles brought about by their coalescence and aggregation.

*Energy Efficiency and Conservation Division., Dept. of Applied Science, Upton, NY 11973.

This work was performed under the auspices of the U.S. Department of Energy, Washington, D.C. under Contract No. DE-AC02-98CH10886 and supported by the U.S. Army Research Office Program MIPR-7HDOEAR040.

Table 1—Mix Formulation and pH Value of PAM-Modified and UnModified DEX Solutions

DEX/PAM Ratio	Formulation		pH
	DEX Solution	PAM Granular	
100/0	50 g	0.00 g	4.11
90/10	50 g	0.05 g	4.18
80/20	50 g	0.13 g	4.28
70/30	50 g	0.21 g	4.31
60/40	50 g	0.33 g	4.50
0/100	—	0.33 g	5.51

As part of our ongoing research to aimed at developing a uniform, continuous hydrophobic natural polymer film that provides an adequate protection of Al against corrosion, we next investigated the dextrins [DEX, $(C_6H_{10}O_5)_n$] which are a water-soluble polysaccharide derived from cornstarch by its dextrination processes involving thermal acid hydrolysis, molecular rearrangement, and repolymerization.[4] In the United States,[5] the main source of starch comes from corn for which its demand is about 10 times higher than all the other sources from topicoca, sago, wheat, potato, rice, et al. U.S. corn impacts prices worldwide because the country produces more than one-third of the world's corn and exports as much as 30% of its production. This fact represents 80% of exports from all countries of the world. Hence, it is economically worthwhile to use the DEX as starch hydrolysates from corn because of its relatively low cost and renewable agricultural resource.

The emphasis of our current study focused on assessing the characteristics of a copolymer made from blending CAN-oxidized DEX with synthetic water-soluble polyacrylamide for use as the primer coating film on Al surfaces. The factors investigated included the changes in thermal behavior, molecular configuration, susceptibility to moisture, and chemistry at the interfaces between the copolymer and Al for the films made by varying the proportion of oxidized DEX to polyacrylamide $[(CH_2CHCONH_2)_n]$. The data obtained were integrated and correlated directly with the ability of these coating films to inhibit corrosion of the Al.

EXPERIMENTAL METHODS

Materials

Dextrin (DEX) powder, supplied by INC Biomedical, Inc., was a white-type DEX derived from the cornstarch. Cerium (IV) nitrate hexahydrate $[Ce(NO_3)_3.6H_20]$, obtained by Alfa, was used as the oxidizing agent. DEX colloidal solution was prepared by agitating the mixture of a 1 g DEX and 99 g deionized water for 3 hr at 70°C, and then allowing it to stand for 24 hr at room temperature. This was followed by the addition of CAN at 0.2% by weight of the total DEX solution; the pH of this solution was 4.11. As a synthetic water-soluble reactive polymer, polyacrylamide (PAM) with M.W. 200,000 was supplied by Scientific Polymer Products, Inc. A proper amount of PAM granules was added to the DEX colloidal solution, and then agitated by a magnetic stirrer until they were completely dissolved in this solution at room temperature. The mix formulations and the pH of these PAM-modified and unmodified DEX solutions designed in this study are given in *Table* 1. For purpose of comparison, one reference solution consisting of 0.33 g PAM and a 50 g deionized water was used as a DEX/PAM ratio sample of 0/100; the pH was a 5.51. Although adding a proper amount of CAN to PAM may improve its ability to protect metal from corrosion, no CAN was incorporated in a 0/100 ratio coating. The lightweight metal substrate was a 6061-T6 aluminum (Al) sheet containing the following chemical constituents: 96.3 wt% Al; 0.6 wt% Si; 0.7 wt% Fe; 0.3 wt% Cu; 0.2 wt% Mn; 1.0 wt% Mg; 0.2 wt% Cr; 0.3 wt% Zn; 0.2 wt% Ti; and 0.2 wt% other elements.

Coating Technology

The coating film deposition to the Al surfaces was carried out in the following sequence: First, to remove surface contaminants, the Al substrates were immersed for 20 min at 80°C in an alkaline solution consisting of 0.4 wt% NaOH, 2.8 wt% tetrasodium pyrophosphate, 2.8 wt% sodium bicarbonate, and 94.0 wt% water. The alkali-cleaned Al surfaces were washed with deionized water at 25°C, and dried for 15 min at 100°C. Next, the substrates were dipped into a soaking bath of DEX solution at room temperature, and withdrawn slowly. The wetted substrates were then heated in an oven for 120 min at 150° or 200°C, to yield thin solid films.

Measurements

The thickness of the PAM-modified and unmodified DEX films deposited on the Al surfaces was determined using a surface profile measuring system. Differential scanning calorimetry (DSC) gave information on the endothermic and exothermic phase transitions of modified and unmodified DEX polymers. DSC was run using the non-isothermal method at a constant rate of 10°C/min over the temperature range of 25° to 370°C. Thermogravimetric analysis (TGA) was used to assess the thermal decomposition characteristics of these polymers. The molecular configuration and conformation of 150°- and 200°C-treated polymers was investigated by Fourier-transformation infrared (FTIR). The contact angle was measured by dropping water onto the polymer film surfaces to determine the extent of susceptibility of their surfaces to moisture. The values of contact angle were measured within the first 20 sec after dropping it onto the surfaces. X-ray photoelectron spectroscopy (XPS) was employed to explore the chemistry at the interfaces between the polymer film and Al substrate. AC electrochemical impedance spectroscopy (EIS) was used to evaluate the ability of the coating films to protect the Al from corrosion. The specimens were mounted in a holder, and then inserted into an electrochemical cell. Computer programs were prepared to calculate theoretical impedance spectra and to analyze the experimental data. Specimens with a surface area of 13 cm^2 were exposed to an aerated 0.5 M NaCl electrolyte at 25°C, and single-sine technology with an input AC voltage of 10 mV (rms) was used over a frequency range of 10 Khz to 10^{-2} Hz. To

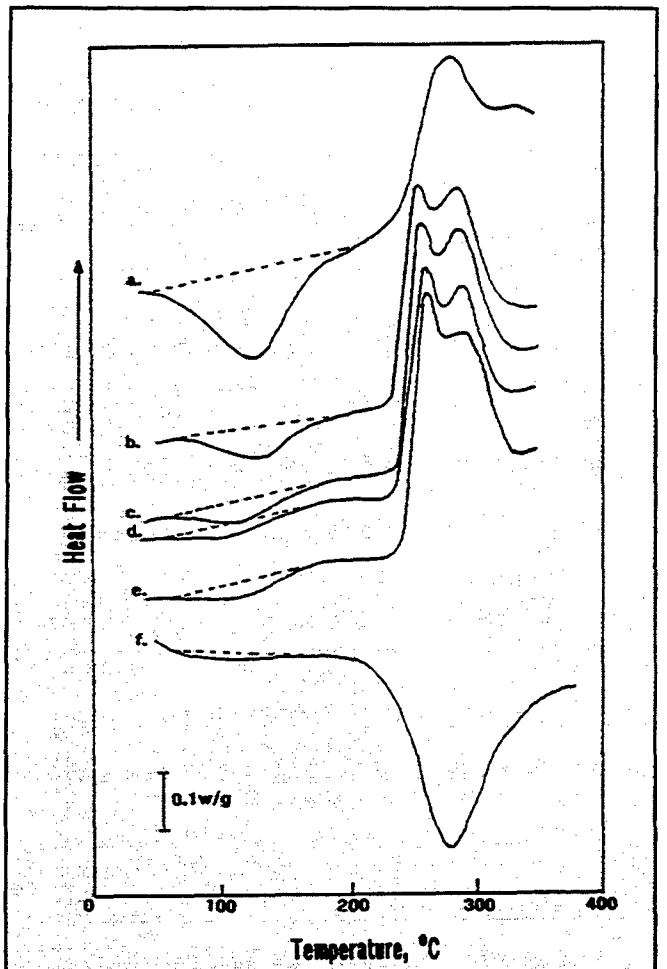

Figure 1—DSC curves for 150°C-treated polymers with DEX/PAM ratio of (a) 100/0; (b) 90/10; (c) 80/20; (d) 70/30; (e) 60/40; and (f) 0/100.

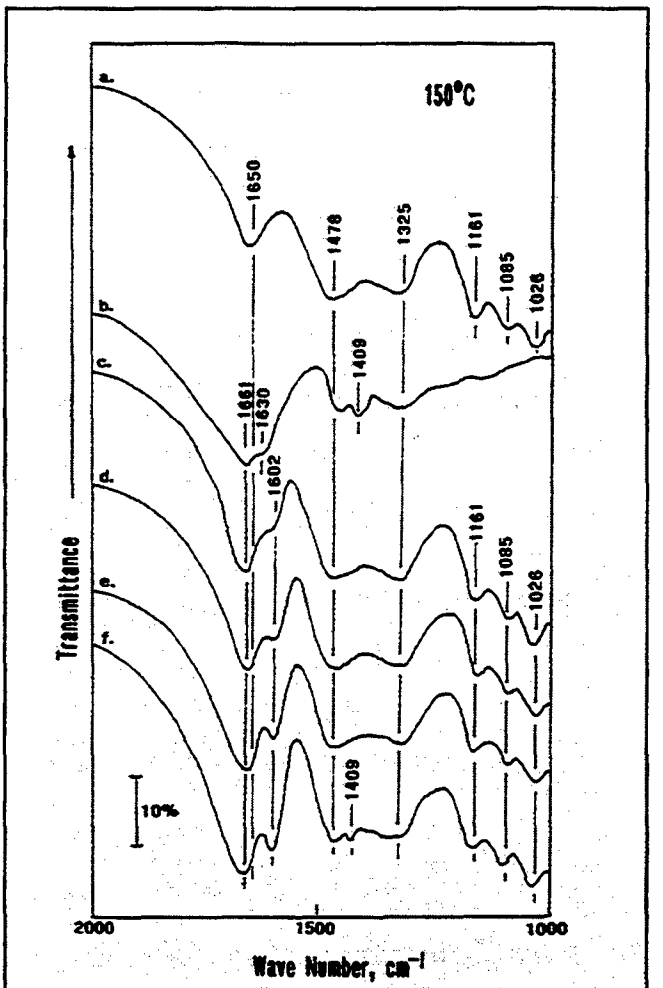

Figure 2—FTIR spectra for (a) 100/0; (b) 0/100; (c) 90/10; (d) 80/20; (e) 70/30; and (f) 60/40 ratio polymers at 150°C.

estimate the protective performance of coatings, the pore resistance, Rp, (Ω-cm^2), was determined from the plateau in Bode-plot scans that occurred at low frequency regions. The salt-spray tests of the coated Al panels (75 mm × 75 mm, size) were performed in accordance with ASTM B 117, using a 5 wt% NaCl solution at 35°C.

RESULTS AND DISCUSSION

PAM-Modified DEX Copolymers

The thermal analyses by DSC were carried out as the first approach to gaining information on the structural arrangement of the PAM-modified DEX polymers, with DEX/PAM ratios of 100/0, 90/10, 80/20, 70/30, 60/40, and 0/100. *Figure* 1 shows the DSC curves at temperatures ranging from 25° to 370°C from the 150°C-heated polymer samples. The DSC tracings for all the samples involved two phase transitions: one was the endothermic transition occurring at the temperature between ~30° and ~200°C and the other was related to the exothermic one in the temperature range 230° to 320°C. As reported by Bluhm[6] and Donovan,[7] the endothermal energy, ΔH, computed from the integrated peak area depended primarily on the degree of the starch's hydration. In other words, the ΔH value reflected the total energy consumed for breaking the intermolecular hydrogen bonds between starch and water. The ΔH was obtained from the following formula[8]: $\Delta H = T \times R \times A/h \times m$, where T, R, A, h, and m refer to the temperature scale (°C inch^{-1}), the range sensitivity (mcal s^{-1} inch^{-1}), the peak area (inch^2), the heating rate (°C s^{-1}), and the sample's weight (mg), respectively. The changes in ΔH as a function of the proportion of DEX to PAM are given in *Table* 2. A given result showed that the ΔH value decreases with an increasing amount of PAM incorporated into DEX. Thus, the incorporation of larger amounts of PAM led to the molecular configuration of DEX chains with a lower degree of hydration. Particular interest in the exothermic transition centered on the feature of the doublet curve apparent in the PAM-modified DEX polymers. The bulk DEX had a single peak of temperature of ~270°C. By comparison, all the modified DEX polymers had an additional peak at a temperature near 250°C in the overall exothermal curve. The data also showed that the

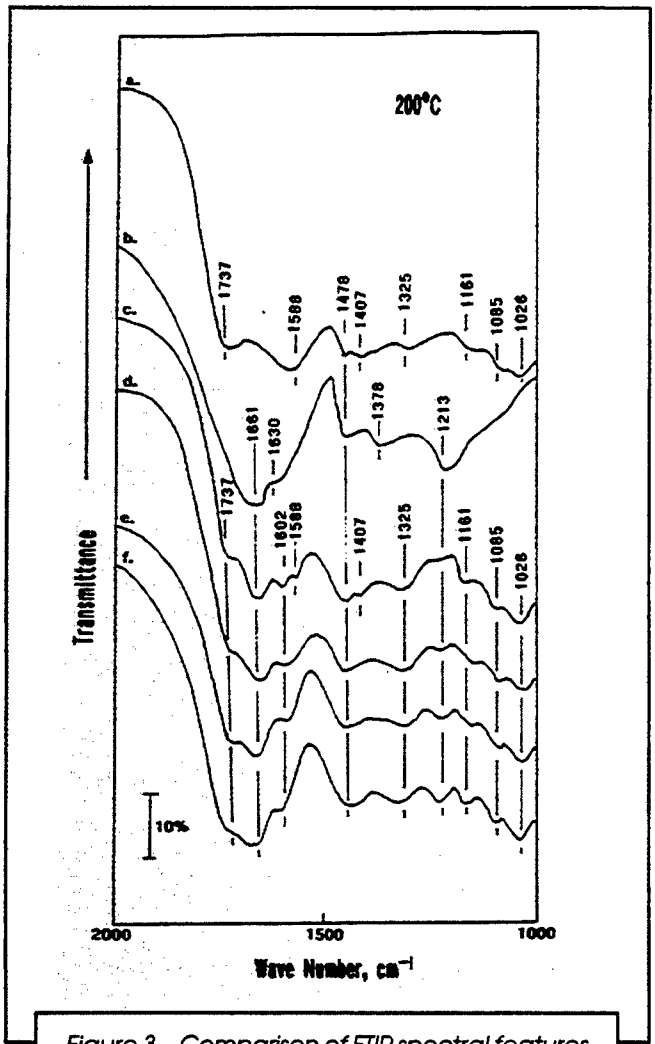

Figure 3—Comparison of FTIR spectral features for (a) 100/0; (b) 0/100; (c) 90/10; (d) 80/20; (e) 70/30; and (f) 60/40 ratio polymers at 200°C.

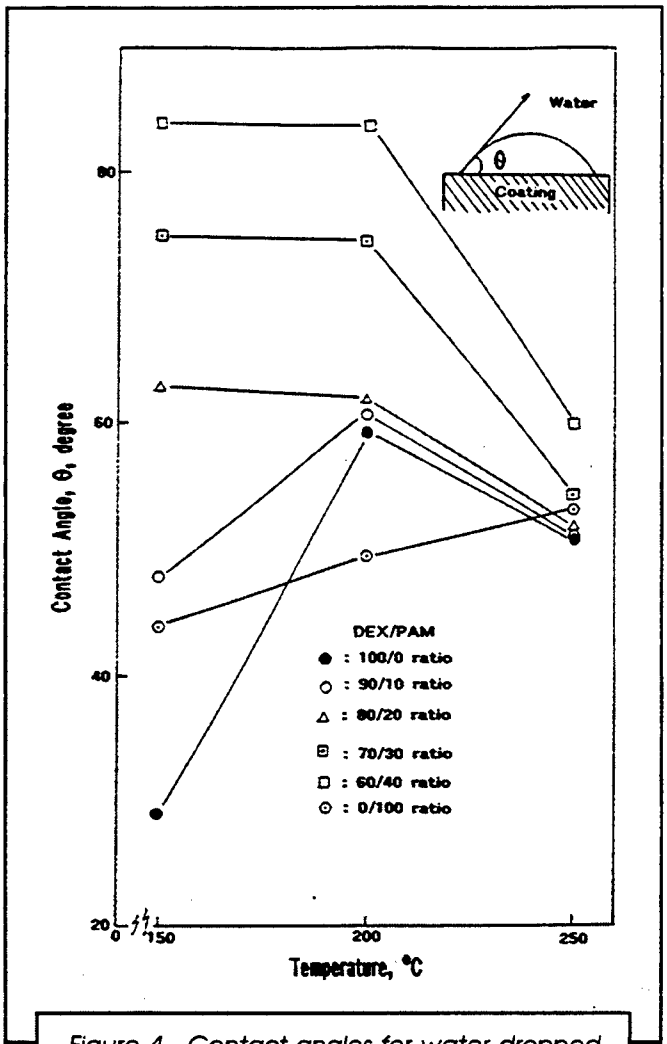

Figure 4—Contact angles for water dropped on the 150°-, 200°-, and 250°C-treated coating film surfaces.

intensity of this new peak become much stronger as the proportion of DEX to PAM was reduced; meanwhile, its intensity at ~ 270°C decreased. Because the exothermal peak is attributable to the evolution of carbonaceous species gasified by thermal decomposition of the polymers, this new peak may be associated with the decomposition of the copolymers yielded by the reaction between the PAM and the DEX. The decomposition of these samples began around 230°C and ceased near 340°C. The TGA analyses strongly supported this information; TGA curves (not shown) for all the 150°C-treated DEX/PAM blends indicated the large reductions of weight loss in the two temperature ranges 230-290°C and 290-360°C. The total loss in weight occurring at the first stage (230-290°C) in this two-step decomposition process was substantially enhanced when the DEX-PAM ratio was reduced; by contrast, loss at the second decomposition stage (290-360°C) decreased with an increase in portion of PAM in the blend polymers. Relating this finding to the results from DCS, the decomposition occurring between 230° and 290°C may reflect the formation of DEX/PAM copolymers as reaction products; no such decomposition was found in single DEX and PAM polymers. Hence, we assumed that the decomposition in the second phase involves the unreacted DEX polymers. Nevertheless, the allowed temperature to fabricate the modified DEX films appears to be no more than 230°C.

To identify possible reaction products between DEX and PAM and visualize their structures, we conducted FTIR analyses for the PAM-modified DEX polymers at 150° and 200°C, over the frequency range of 2,000 to 1,000 cm^{-1}. *Figure* 2 depicts their absorption spectra at 150°C. The spectral features of the unmodified DEX polymer, denoted as "a," reveals glucosidic rings in the polysaccharide; namely, the absorption bands at 1,650 cm^{-1}, belonging to the O–H bending vibration of H–O–H in the absorbed H_2O, at 1,478 and 1,325 cm^{-1} which can be ascribed to the C–H bending mode of the methylene, and at 1,161, 1,085, and 1,026 cm^{-1}, originating from the stretching mode of C–O–C linkages.[9] The spectrum (b) of the bulk PAM involved five major absorption peaks, at 1,661, 1,630, 1,478, 1,409, and 1,325 cm^{-1}, in this frequency range. According to the literature,[10] the contributions to the absorption bands at 1,661 and 1,630 cm^{-1} were due to the stretching vibration of C=O band and the bending vibration of NH band in the primary amides,

–CO–NH_2, respectively. The remaining three bands can be assigned to the bending mode of C–H band in the backbone methylene and methyl chains. By comparison with these bulk polymer reference samples, the spectral feature of the samples (c) with a DEX/PAM ratio of 90/10 was characterized by the appearance of a new band at 1,602 cm^{-1}. This new band is likely associated with the formation of secondary amides, –CO–NH–.[11] If this assignment is valid, the results have demonstrated that the primary amide NH_2 groups in PAM favorably reacted with the functional OH groups in DEX to form secondary amide bonds. Conceivably, the formation of such an amide bond in the blended polymers grafts the PAM onto the DEX polymer. The degree of grafting seems to be enhanced when the amount of PAM incorporated into the DEX was increased. In fact, a marked growth of this band at 1,602 cm^{-1} can be seen in the spectrum (f) from the 60/40 ratio samples, while there is still evidence of the presence of unreacted primary amide, methylene and methyl groups, as well as the C–O–C linkages related to the PAM and DEX.

At 200°C, the FTIR spectra of these samples are depicted in *Figure* 3. The spectral feature of the bulk DEX (a) was quite different from that of the 150°C-treated one: in particular, there was (1) the emergence of three new bands at 1,737, 1,588, and 1,407 cm^{-1} frequencies, and (2) a striking reduction in the intensity of the methylene-related bands at 1,478 and 1,325 cm^{-1}, and also of the C–O–C linkage-associated bands at 1,161, 1,085, and 1,026 cm^{-1}. As was evident from our previous study on the molecular alterations of Ce-containing starch caused by oxidation,[3] the new absorption band at 1,737 cm^{-1} reflected the formation of C=O groups, and other two new bands might be attributable to the asymmetric and symmetric stretching of COO^- in the Ce-complexed carboxylate groups, –COO^- Ce^{4+} –COOC–. If such interpretation is correct, we can assume that the incorporation of oxygen into the DEX by the combination of chemical and thermal oxidations not only introduces C=O and complexed carboxylate groups into its molecular structure, but also causes oxidation-induced breakage of C–O–C linkages, reflecting result (2). The C=O groups were formed by oxidation-caused cleavage of glycol C–C bond in the glycosidic rings. The subsequent opening of the rings caused by such cleavage led to the formation of C=O groups.[12] A further increase in the degree of oxidation seems to transform the C=O into the carboxylate groups. Considering that bond breakage of the C–O–C linkages results in the disintegration of glucose units in the chain conformation and in chain scission, we inferred that this may also create C=O and carboxylate derivatives. As a result, the Ce-complexed carboxylate may be formed by the hypothetical three-step reaction schemes[13,14]:

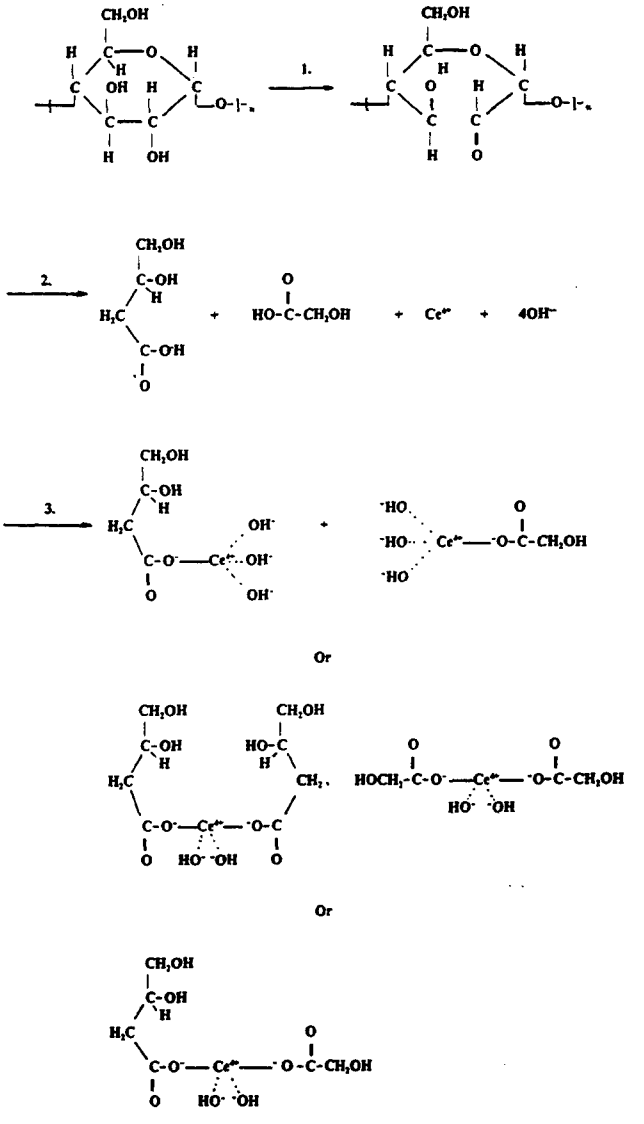

First, oxidation of the glycosidic rings initiated by the Ce ion generates aldehydic groups, –HC=O, after the opening of rings caused by cleavage of the C–C bonds in the glycol groups. Second, further oxidation of DEX leads to the breakage of the C–O–C linkages in the opening structures and in the chain, thereby resulting in the formation of two oxidized compounds, the 3,4-dihydroxybutanoic acid and glycolic acid, as the fragmental products of glucose units. Once these oxidized fragments containing functional carboxylic acid groups were present, in the final reaction step, these functional groups favorably react with hydroxylated Ce to form the Ce-complexed fragment compounds. These complexes may consist of two molecular conformations: one is a half salt configuration that the Ce^{4+} linked to the carboxylate oxygen has a coordination with three OH^- groups, and the other was a bridging structure that joined together between the fragments by Ce.

When the bulk PAM polymers were treated at elevated temperature of 200°C, the spectrum (b) showed the emergence of two new bands at 1,378 and 1,213 cm^{-1},

Table 2—Comparison Between DSC Endothermal Energies of 100/0, 90/10, 70/30, 60/40, and 0/100 Ratio Polymers

DEX/PAM Ratio	Exothermal Energy ΔH, J/G
100/0	193.6
90/10	48.9
80/20	35.2
70/30	25.1
60/40	21.1
0/100	12.4

revealing the conformation of intermolecular hydrogen bond, –NH– – – –O=C–, occurring between the neighboring amide groups in the linear chains.[11] As expected, the spectrum from the PAM-modified DEX polymer with the 90/10 ratio included almost all the bulk DEX and PAM polymer-related absorption bands, together with the typical band at 1,602 cm^{-1}, referring to the secondary amide as the reaction product between the DEX and PAM. One distinctive feature of this spectrum, compared with that of the bulk DEX samples, was the presence of a strong absorption of the C–O–C linkage-associated bands at 1,161, 1,085, and 1,026 cm^{-1}, seemingly demonstrating that the oxidation-caused bond breakage of C–O–C in the DEX is restrained by grafting PAM onto the DEX. Of particular interest in the 80/20 ratio spectrum (d) was the fact that there were no peaks at 1,588 and 1,407 cm^{-1}, originating from the formation of Ce-complexed carboxylate. The spectral features of the 70/30 (e) and 60/40 (f) ratio samples closely resembled that of the 80/20 ratio sample.

From this information, the hypothetical PAM-grafted DEX conformation at 150°C or 200°C is represented in the following reaction schemes:

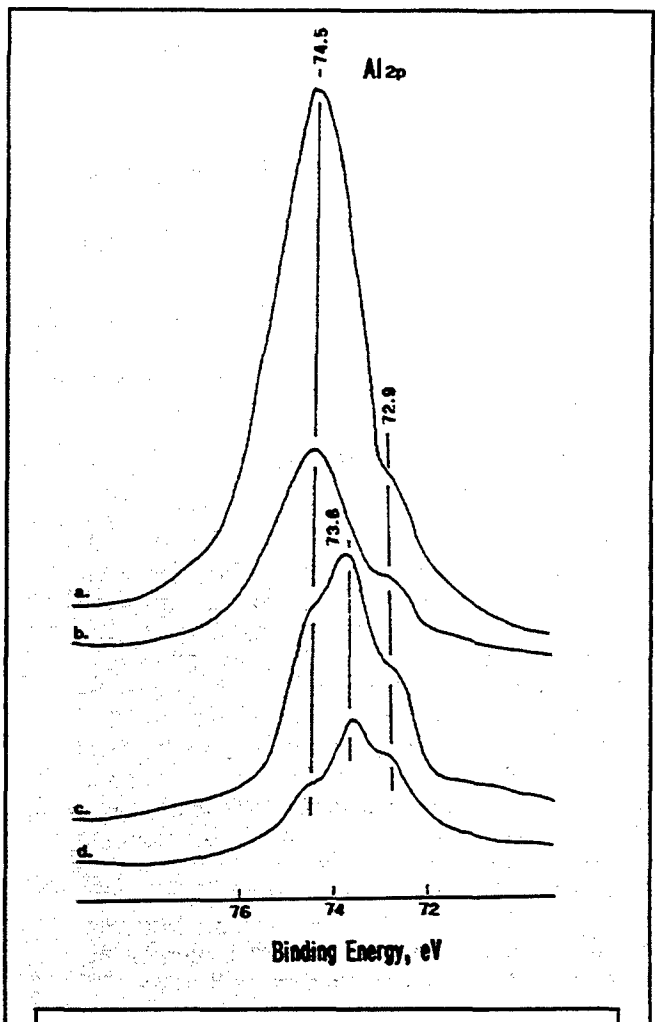

Figure 5—Al_{2p} core-level spectra for (a) Al substrate, and (b) 100/0, (c) 70/30, and (d) 0/100 ratio-coated Al.

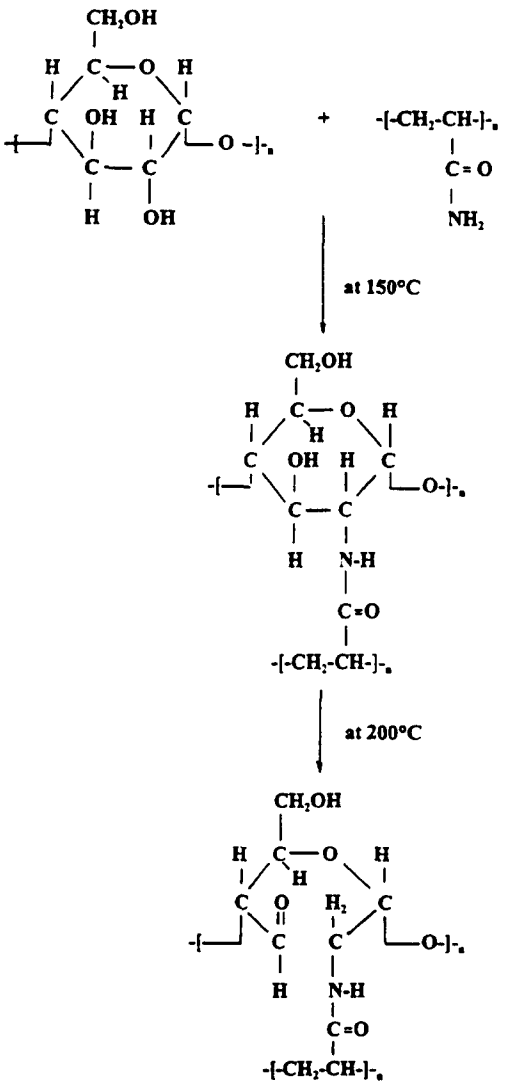

At 150°C, one hydroxyl group of glycols has a strong chemical affinity for the pendent amide group in the PAM, forming a secondary amide as the reaction product that directly grafts the PAM onto the DEX. Increasing the temperature to 200°C resulted in the bond breakage between the alcohol carbon and the secondary amide carbon. Such breakages not only led to the incorporation of the aldehydic groups into the PAM-grafted DEX conformation, but also promoted the opening of the rings. However, grafting appears to play the major role in inhibiting the formation of molecular fragments caused by the scission of C–O–C linkages. Relating this finding to the DSC results earlier, it is possible to assume that the

Table 3—Salt-Spray Resistance Tests for PAM-Grafted DEX Coatings

DEX/PAM Ratio	Salt-Spray Resistance Hours
100/0	72
90/10	144
80/20	216
70/30	432
60/40	600
0/100	72

additional exothermic peak near 250°C in the DSC curve was due to the thermal decompositions of PAM-grafted DEX conformation, but also promoted the opening of the rings. However, grafting appears to play the major role in inhibiting the formation of molecular fragments caused by the scission of C–O–C linkages. Relating this finding to the DSC results earlier, it is possible to assume that the additional exothermic peak near 250°C in the DSC curve was due to the thermal decompositions of PAM-grafted DEX copolymers.

Characteristics of the Coatings

Our emphasis was next directed towards determining the characteristics of the PAM-grafted DEX coating films deposited onto the Al substrate surfaces. Specific characteristics to be investigated were the susceptibility of the film surface to moisture, and the chemistry at interfaces between the coating film and Al.

One of the indispensable factors in good protective coating systems is the hydrophobic characteristic, so that the assembled coating film surfaces are not susceptible to moisture. The extent of their susceptibility to moisture can be estimated by assessing two physicochemical factors: one is the surface wetting properties, and the other refers to the hydrophilicity of bulk polymers. However, only the former factor was investigated in this study. Accordingly, we measured the contact angle of a water droplet on the 150°- and 200°C-treated 100/0, 90/10, 80/20, 70/30, 60/40, and 0/100 ratio film surfaces. Although thermal degradation of films might take place, we also examined the degree of wettability of 250°C-treated film surfaces by water. A high degree of wettability (i.e., low contact angle) may allow the water to permeate the coating layers. A plot of the contact angle, θ, against the treatment temperature for these film surfaces is depicted in *Figure* 4. At 150°C, all the grafted DEX film surfaces had a higher contact angle, compared with those of the individual DEX and PAM component surfaces. Furthermore, the contact angle was enhanced by decreasing the DEX/PAM ratio. In fact, the highest θ value of ~84° was determined from the 60/40 ratio, reflecting less spreadability and wettability of water over the film surfaces. This value was ~75% higher than that of the 90/10 ratio. Thus, this finding can be taken as evidence that an increase in the degree of grafting serves in providing a lower susceptibility of the film surfaces to moisture. In other words, the hydrophilic characteristics of the individual DEX and PAM coatings can be converted into hydrophobic ones by the grafting reaction between them. For the 200°C-treated film surfaces, there were no conspicuous changes in contact angle for the 60/40, 70/30, and 80/20 ratios. By contrast, the other film surfaces, especially for 100/0 ratio, revealed an increase in contact angle. This is consistent with our hypothesis at a higher level of oxidation in the absence of PAM. As expected, all coating surfaces treated at 250°C, except the 0/100 ratio, showed a noteworthy reduction of the θ value. Such a reduction perhaps is due to their thermal degradation, allowing the water to infiltrate their layers easily.

Next, our attention centered on identifying the bond structures and interaction products at the interfaces between the grafted DEX and the Al substrates. If there were no interfacial bonds, and also if the interaction products had hydrophilic characteristics, it is possible to assume that moisture would permeate through the coating layers, causing the delamination and lifting of coating films from the substrates. To gain this information, we inspected the XPS N_{1s}, Al_{2p}, and O_{1s} core-level excitations for three thin coating films with 100/0, 70/30, and 0/100 ratios deposited onto the Al substrates. These samples were prepared in the following manner: 10 g original solutions with these ratios were added to 100 g deionized water, and then were agitated for 10 min by magnetic stirrer. In preparing thin films, these dilute solutions were spun at 5,000 rpm for 45 sec, and then placed in an oven at 150°C for 10 hr. All coating films deposited on the Al were thin enough to allow direct observation of the interfaces. In fact, XPS spectra for all samples showed the Al_{2p} signal arising from the underlying Al substrates. The binding energy (BE) scale in the XPS spectra was calibrated with the C_{1s} of the principal hydrocarbon, "CH_n," peak fixed at 285.0 eV as an internal reference standard.

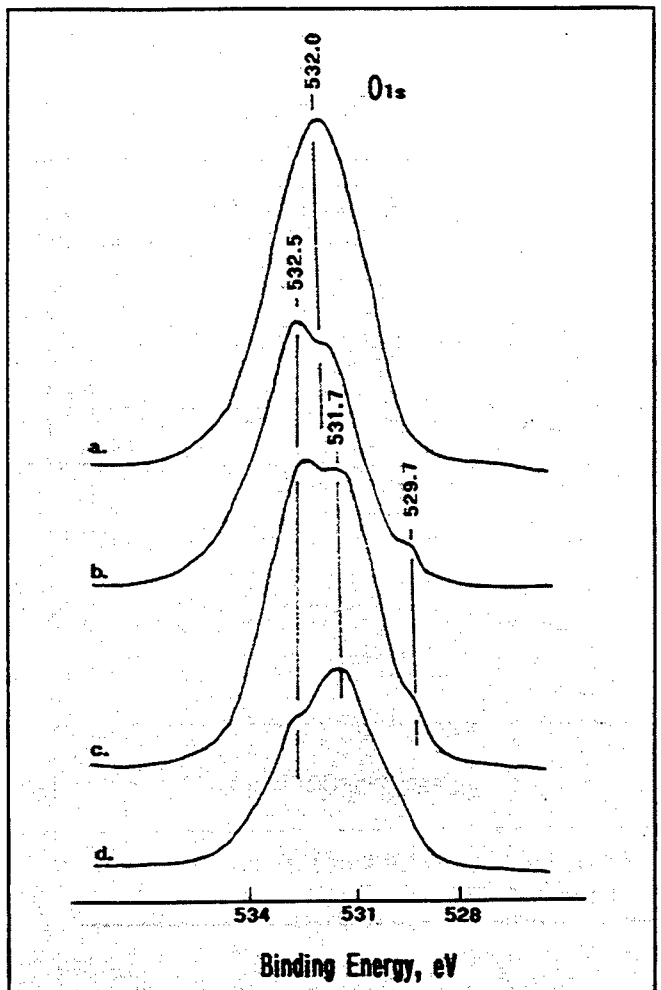

Figure 6—O_{1s} region for (a) Al, and (b) 100/0, (c) 70/30, and (d) 0/100 ratio-coated Al.

Figure 5 compares the Al_{2p} core-level spectral features of the alkali-cleaned Al substrate and of these coating

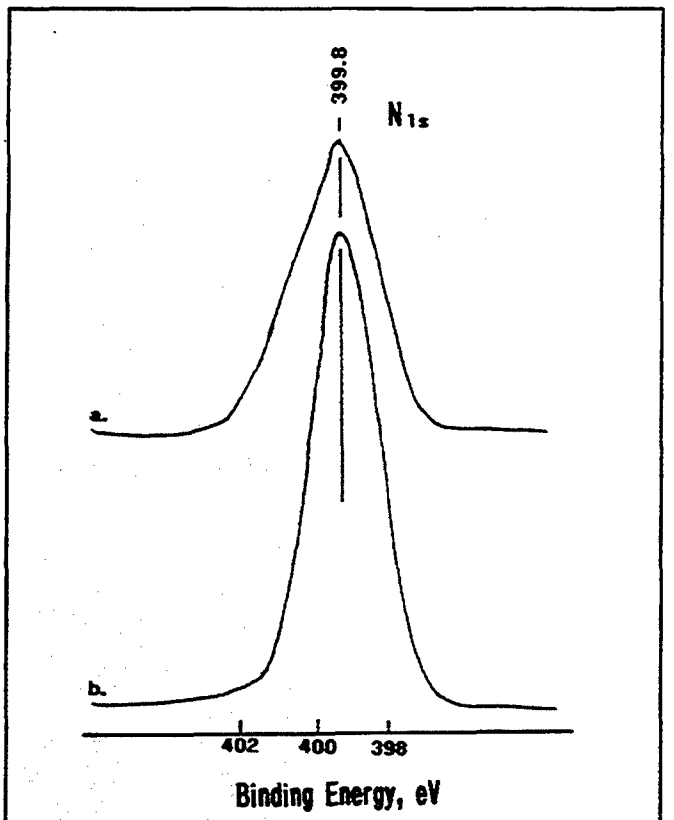

Figure 7—N_{ls} region for (a) 70/30 and (b) 0/100 ratio-coated Al.

samples. The Al_{2p} region of the cleaned Al surfaces (a) had two resolvable Gaussian components at the BE position of 74.5 and 72.9 eV. The former peak as the principal component is assignable to Al in the Al_2O_3 located on the outermost surface sides of the Al substrate, and the latter as the minor one is due to the Al metal in the substrate.[15] When the Al surfaces were covered by the 100/0 ratio coating, the spectral feature (b), excepting the decay of the overall Al_{2p} excitation, was very similar to that of the Al substrate. By comparison, noticeable changes in the shape of the Al_{2p} region were observed from the surfaces of 70/30 ratio-coated samples (c). The spectrum was characterized by the excitation of new signal of 73.6 eV, and also by a striking attenuation of the peak at 74.5 eV, corresponding to Al in the Al_2O_3, meanwhile, the Al metal-associated signal at 72.9 eV had become an intense peak. A further growth in signal intensity at 72.9 eV, together with the presence of the major peak at 73.6 eV, can be seen in the spectrum of the 0/100 ratio-coated sample (d). This information strongly manifested that the changes in the overall Al_{2p} spectrum of Al substrates caused by the coatings are more likely to be associated with the PAM, rather than the DEX. An XPS study on the formation of chemical bonds at the interfaces between polymer and Al metal demonstrated that Al has a strong affinity for the carbonyl oxygen in the amide and imide groups.[16,17] This affinity was accounted for as the charge transfer from Al to carbonyl oxygen, reflecting the formation of $Al^+ \rightarrow {}^-O\text{–}C\text{–}$. Such an interaction scheme was represented from the results of a net positive charge on the Al metal atoms caused by a shift of the Al peak to higher BE site, and, correspondingly, a negative charge on the carbonyl oxygen causing its shift to a lower BE site. Thus, we assumed that the new peak emerging at about 0.7 eV higher BE site from the Al metal peak may be attributed to a positively charged Al. If this interpretation is valid, it is conceivable that a charge transfer reaction takes place between Al and PAM. To provide further insights into the coating/Al interactions, we inspected the O_{ls} region of these samples (*Figure* 6). The spectrum (a) of the sample from uncoated Al indicated the excitation of a symmetrical signal peak at 532.0 eV, belonging to Al in the Al_2O_3. The O_{ls} region of the 100/0 ratio-coated Al samples (b) had three Gaussian peaks at 532.5, 532.0, and 529.7 eV, originating from O in the ether and hydroxyl groups,[18] in the Al_2O_3,[19] and in the CeO_2,[20] respectively. Of particular interest was a distinctly different O_{ls} spectral feature of the 70/30 ratio-coated samples (c) from that of the 100/0 sample; namely, an additional peak at 531.7 eV was incorporated in this region. Since the peak emerged at the BE position of 532.5 eV not only reveals the ether and hydroxyl oxygen atoms in the DEX, but also is assignable to the amide oxygen atom in the PAM-grafted DEX copolymers. The contributor to this additional peak is considered as the reaction products formed at interfaces between the PAM/DEX copolymer and Al. This new peak occurs at the BE position shifted to a 0.8 eV lower site from that of the amide oxygen atoms, representing the negatively charged oxygen portion in the amide groups. Furthermore, this peak position was very close to those observed from metal-linked carbonyl

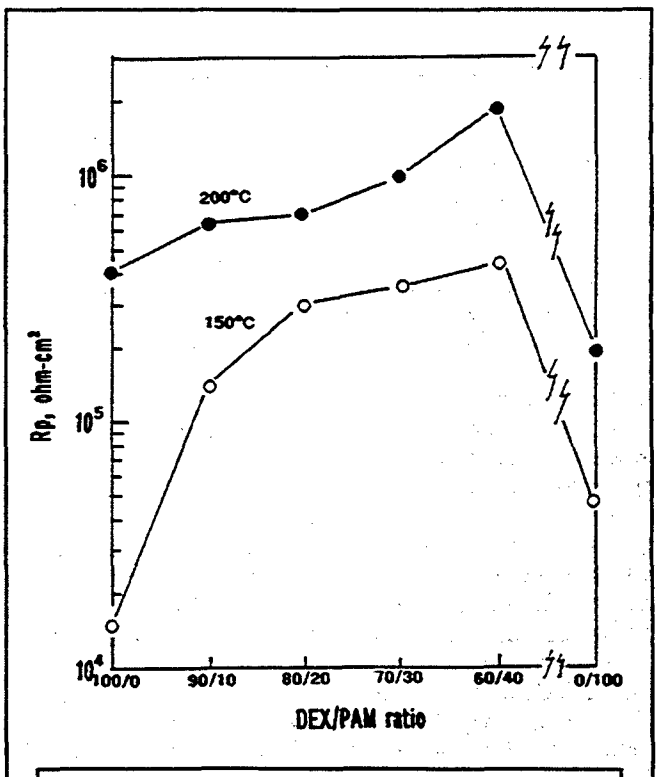

Figure 8—R_p value of Al samples coated with 100/0, 90/10, 80/20, 70/30, 60/40, and 0/100 ratios at 150° and 200°C.

groups.[17,22,23] A possible reason for the 0.8 eV decrease in BE of the amide oxygen atoms, together with the 0.7 eV enhanced energy of Al atoms, can be accounted for as a charge transfer reaction occurring between the Al and amide oxygen; the electrons were transferred from the Al atoms to the electron accepting oxygen portion in the amide groups, $Al^+ \rightarrow {}^-O\text{–}C\text{–}NH_2$. The formation of this Al-O bond was further supported from the spectrum of the 0/100 ratio samples (d). By comparison with that of the 70/30 ratio samples, the major characteristic of this spectrum was a considerable loss in intensity of the amide oxygen peak; meanwhile, the Al-O linkage at 531.7 eV become a dominant peak. From this fact, the Al atoms preferentially react with amide oxygen atoms, rather than any other atoms existing in the PAM-grafted DEX copolymers. One important question still remains concerning the role of amide nitrogen in forming the interfacial bonds between Al and PAM. *Figure 7* depicts the N_{1s} core-level spectra of the 70/30 and 0/100 ratio-coated Al samples. As seen, analysis of the N_{1s} region revealed no differences between them. They had only a single peak at 399.8 eV. Since BEs in the narrow region 399-401 eV include –CN, $-NH_2$, –OCONH–, and $-CONH_2$,[18] the amide nitrogen seems not to be reactive with Al.

Corrosion

The integration of all the data was correlated directly with the effectiveness of grafted DEX films in protecting the Al substrates from corrosion. Using a surface profile measuring system, the thickness of 100/0, 90/10, 80/20, 70/30, 60/40, and 0/100 ratio films was ~0.9, ~1.5, ~2.2, ~2.9, ~3.6, and ~4.0 μm, respectively. Although a thicker coating film may have a better corrosion-protective performance than that of a thin one, AC electrochemical impedance spectroscopy (EIS) was used to evaluate their ability as the corrosion-preventing barriers. Upon the overall Bode-plot curves [the absolute value of impedance $|Z|$ (ohm-cm^2) versus Frequency (Hz)], (not shown), particular attention was paid to the impedance value in terms of the pore resistance Rp, which can be determined from the plateau in the Bode plote occurring at sufficiently low frequency of 5×10^{-2} Hz. *Figure 8* shows the plots of Rp versus the DEX/PAM ratios. For the 150°C-treated coating films, the Rp value of the single DEX coatings was ~1.5×10^4 ohm-cm^2. When a 10% of the total amount of DEX was substituted by PAM, this value was an order of magnitude greater than that of the unmodified DEX. With further substitution, the value of Rp increased; the 60/40 ratio coatings had the highest Rp of 4.5×10^5 ohm-cm^2 in the 150°C-treated coating series. In contrast, the Rp value of the single PAM coating with the highest film thickness of ~4 μm was an order of magnitude lower than that of the 60/40 ratio sample. Since the Rp value reflects the magnitude of ionic conductivity generated by the electrolyte passing through the coating layers, a high value of Rp means a low degree of penetration of electrolyte into the coating films. Thus, although the Rp value depends on the thickness of film, the grafted DEX copolymer conformation offers improved performance on minimizing the rate of permeation of the electrolytes through the coating layers, compared with those of the individual DEX and PAM coatings. A highly grafted structure led to a low uptake of electrolytes by the coatings. Increasing the treatment temperature to 200°C provided an increased Rp value for all the coating specimens, while retaining the overall curve feature similar to that of the specimens at 150°C. This information suggested that treating the films at 200°C offers a better protection of the Al against corrosion than treatment at 150°C. The most effective coating system in reducing the permeability of electrolytes was the 60/40 ratio with a 1.8×10^6 ohm-cm^2.

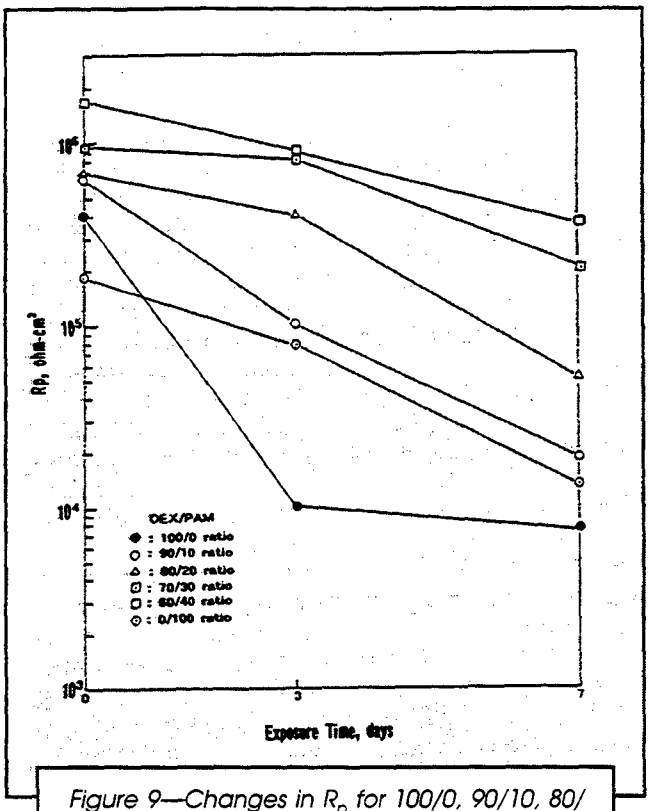

Figure 9—Changes in R_p for 100/0, 90/10, 80/20, 70/30, 60/40, and 0/100 ratio-coated Al as function of exposure times up to 7 days.

Figure 9 represents the changes in Rp at 5×10^{-2} Hz for the 200°C-treated coating specimens as a function of exposure times up to seven days in a 0.5 N NaCl solution at room temperature. All the coating systems, except for the 100/0 ratio one, showed a gradual reduction in the Rp value with increased time. Prolonged exposure period of time appears to promote the uptake of more electrolytes by the coatings. In contrast, the rate of uptake for the 100/0 ratio coatings was much higher than that of any other coatings; in fact, a marked drop in Rp to a 10^3 ohm-cm^2 level can be seen during exposures of up to three days. Upon the exposure for seven days, the effectiveness of these ratios in ensuring a low rate of infiltration of electrolytes is in the following order: 60/40 > 70/30 > 80/20 > 90/10 > 0/100 > 100/0. Implicating this finding in the FTIR contact angle and XPS data, three important factors played an essential role in conferring resistance to corrosion of the Al: first was the copolymer conformation formed by the grafting reaction between DEX and PAM; second referred to the

lesser susceptibility of the coating surfaces to moisture by the enhanced degree of grafting; and third was the interaction of grafted DEX copolymers with the Al substrates.

This information on the EIS was supported by salt-spray resistance tests for the coated panels. The results from the panels treated at 200°C are shown in *Table* 3. A trace of rust stain was generally looked for in evaluating the results for salt-sprayed panel specimens. The results were reported as the total exposure time at the date of the generation of the rust stain from the Al surfaces. As seen, the entire surfaces for the single DEX (100/0 ratio)- and PAM (0/100 ratio)-coated Al panels were corroded after exposure to the salt spray for 72 hr, corresponding to only 24 hr longer than that of the uncoated bare Al (not shown), suggesting that the ability of these coatings to protect Al against corrosion is poor. By comparison with these single coatings, the PAM-grafted DEX coating systems displayed a far better performance on reducing the rate of corrosion. With the 90/10 ratio, the resistance to salt spray extended two times to 144 hr. A further improvement in conferring resistance was observed from the coating containing increased concentrations of PAM, signifying that an increase in the grafting of PAM onto the DEX imparts improved resistance to corrosion. In fact, coatings made from 60/40 ratio served in providing a great protection of Al against corrosion for 600 hr.

CONCLUSION

By using natural dextrine (DEX) polymers derived from cornstarch as renewable agricultural resource in a water-based primer coating system to protect aluminum (Al) substrates against corrosion, the grafting of polyacrylamide (PAM) as a synthetic water-soluble reactive polymer onto the DEX was attempted to improve the properties of the DEX films as a rust-preventing barrier layer. The PAM-modified DEX paints as a film-forming precursor solution were prepared by incorporating a proper amount of PAM into the colloidal DEX aqueous solution containing Ce nitrate as the oxidizing agent. The liquid coating layers were deposited onto the Al surfaces using a simple dipping-withdrawing coating technology and converted into the solid layers by heating them at 150° or 200°C in air. At 150°C, the secondary amide bonds yielded by the reaction between the primary amide group in PAM and one hydroxyl group of glycol in DEX led to grafting of the PAM onto the DEX. Although increasing the temperature to 200°C caused opening of the glycosidic rings due to bond breakage between the alcohol carbon and the secondary amide carbon, the grafting conformation acted to inhibit the fragmentation of glucose units by oxidation-caused scission of the C–O–C linkages in the DEX. An increase in the degree of grafting resulted in the formation of coating films that were less susceptible to moisture. Furthermore, the Al metal in the substrate favorably interacted with the amide oxygen in the PAM-grafted DEX coatings, creating interfacial Al–O bonds formed by a charge transferring reaction in which electrons were transferred from the Al atoms to the electron accepting oxygen in the amide groups. Two important factors for highly grafted DEX coatings, a lesser susceptibility to moisture and an interfacial bond at metal/coating joints, contributed significantly to minimizing the permeability of electrolyte species through the coating layers. Coating films made with DEX/PAM ratio of 60/40 displayed resistance to salt spray for 600 hr.

References

(1) Winto, J.M., "Coating's 87 Changing Technology for an Environment Era," *Chemical Week*, 7, 30 (1987).
(2) Sugama, T. and DuVall, J.E., "Polyorganosiloxane-Grafted Potato Starch Coatings for Protecting Aluminum from Corrosion," *Thin Solid Films*, 289, 39 (1996).
(3) Sugama, T., "Oxidized Potato-Starch Films as Primer Coatings for Aluminum," *J. Mater. Sci.*, 32, 3995 (1997)
(4) Gulbot, A. and Mercier, C., in *The Polysaccharide*, Aspinall, G.O. (Ed.), Vol. 3, Academic Press, p. 209-283, New York, 1985.
(5) Schenck, F.W. and Hebeda, R.E., *Starch Hydrolysis Products: Worldwide Technology, Production and Application*, VCH Publishers (UK) Ltd., pp. 441-447, 1992.
(6) Bluhm, T., Deslandes, Y., Marchessault, R.H., and Sundararajan, P.R., in "Water in Polymers," Rowland, S.P (Ed.), *ACS Symposium Series 127*, American Chemical Society, pp. 253-272, Washington, D.C., 1980.
(7) Donovan, J.W., "Phase Transitions of the Starch-Water System," *Biopolymer*, 18, 263 (1979).
(8) O'Nell, M.L., "The Analysis of a Temperature-Controlled Scanning Calorimeter," *Anal. Chem.*, 36, 1238 (1964).
(9) Barker, S.A., Borne, E.J., Stacey, M., and Whiffen, D.H., "Infra-red Spectra of Carbohydrates. Part I. Some Derivatives of D-Glucopyranose," *J. Chem. Soc.*, 171 (1954).
(10) Nakanishi, K. and Solomon, P.H., "Infrared Absorption Spectroscopy," Holden-Day Inc., pp. 38-44, San Francisco, 1977.
(11) Bellamy, L.J., *The Infra-red Spectra of Complex Molecules*, Chapman and Hall, London, pp. 231-250, 1975.
(12) Doba, T., Rodehed, C., and Randy, B., "Mechanism of Graft Copolymerization onto Polysaccharide Initiated by Metal Ion Oxidation Reaction of Model Compounds for Starch and Cellulose," *Marcomolecule*, 17, 2512 (1984).
(13) Liu, M., Cheng, R., Wu, J., and Ma, C., "Graft Copolymerization of Methyl Acrylate onto Potato Starch Initiated by Ceric Ammonium Nitrate," *J. Polymer Sci.*, 31, 3181 (1993).
(14) Stinson, S.C., "Technological Innovation Thrives in Fine Chemicals Industry," *Chem. Eng. News*, 74, 35 (1996).
(15) Wagner, C.D., "X-Ray Photoelectron Spectroscopy with X-Ray Photons of Higher Energy," *J. Vac. Sci. Technol.*, 15, 518 (1978).
(16) Barha, J.W., Hahn, P.O., LeGoues, F., and Ho, P.S., "Photoemission Spectroscopy Study of Aluminum-Polyimide Interfaces," *J. Vac. Sci. Technol.*, 3, 1390 (1985).
(17) Gerenser, L.I., in "Metallization of Polymers," Sacher, E., Pireaux, J-J., and Kowalezyk, P. (Eds.), *ACS Symposium Series 440*, American Chemical Society, pp. 433-452, Washington, D.C., 1990.
(18) Briggs, D., Brewis, D.M., and Konieczko, M.D., "X-Ray Photoelectron Spectroscopy Studies of Polymer Surfaces," *J. Materi. Sci.*, 14, 1344 (1979).
(19) Tsuchida, T. and Takahashi, H., "X-Ray Photoelectron Spectroscopic Study of Hydrated Aluminas and Aluminas," *J. Mater. Res.*, 9, 2919 (1994).
(20) Moulder, J.F., Stickle, W.F., Sobol, P.E., and Bomben, K.D., "Handbook of X-Ray Photoelectron Spectroscopy," Perkin-Elmer Corp., p. 231, Minneapolis, MN, 1992.
(21) Briggs, D. and Seah, M.P., *Practical Surface Analysis by Auger and X-ray Photoelectron Spectroscopy*, John Wiley & Sons, p. 363, New York, 1983.
(22) Chou, N.J. and Tang, C.H., "Interface Reaction During Metallization of Cured Polyimide: An XPS Study," *J. Vac. Sci. Technol.*, A2, 751 (1984).
(23) Ohuchi, F.S. and Freilich, S.C., "Metal Polyimide Interface: A Titanium Reaction Mechanism," *J. Vac Sci. Technol.*, A4, 1039 (1986).

JOURNAL OF MATERIALS SCIENCE 34 (1999) 2003–2014

Dextrine-modified chitosan marine polymer coatings

TOSHIFUMI SUGAMA, SHEILA MILIAN-JIMENEZ
Energy Efficiency and Conservation Division, Department of Applied Science, Brookhaven National Laboratory, Upton, NY 11973, USA
E-mail: sugama@bnl.gov

In trying to modify partially acetylated chitosan (CS) marine polymers ground from crab or shrimp shells for use as environmentally benign water-base coatings for aluminum (Al) substrates, CS was dissolved in a solution of HCL acid, and then mixed with corn starch-derived dextrine (DEX) containing Ce nitrate as oxidizing agent in aqueous medium. This blend of polysaccharides was deposited on Al surfaces by a simple dip-withdrawing method, and then heated at 200 °C to transform the liquid layer into a solid film. The solution → solid phase transition provided the changes in the molecular conformation of CS and DEX; the former was transformed into deacetylated poly(D-glucosamine) and the latter referred to the formation of Ce-complexed carboxylate fragments. Furthermore, the chemical reactions between the NH_2 groups in deacetylated CS and the carboxylate fragments led to the creation of amide linkages that served in grafting DEX fragments onto the CS. Such fragment-grafted CS polymer coating films deduced from the proper proportions of CS to DEX offered great film-forming performance, low susceptibility to moisture, and low ionic conductivity, conferring a salt-spray resistance of 720 hours.

1. Introduction

In attempting to replace coating systems containing environmentally harmful ingredients, such as volatile organic compound (VOC) and toxic chromium and lead compounds, by environmentally acceptable water-based ones, our previous work [1, 2] focused on seeking ways to modify and design non-toxic natural polysaccharide polymers from the potato-starch and corn-starch derived dextrine as renewable agricultural resource. The modifications were made in the following two ways: One way involved reconstituting an oxidation-derived fragmental polysaccharide structure by Ce; the other way was by grafting synthetic water-soluble polymers, such as polyorganosiloxane and polyacrylamide, onto the polysaccharide. The former method employed a two-step reaction. The first step consisted of fragmentating the polysaccharide structure by incorporating Ce nitrate (CAN), as a chemical oxidizing agent, into the polysaccharide solution; this was followed by thermal oxidation in the presence of atmospheric oxygen. The second step was to assemble water-insoluble Ce-complexed conformations by the interactions between the Ce ions liberated from CAN and fragments containing oxygen functional derivatives such as C=O and COO^-. Using the latter method, the grafting was accomplished by ether- and amide-linkages formed through the condensation reactions between the silanol end groups in polyorganosiloxane or the amine pendent groups in the polyacrylamide, and the OH groups of glycol in the polysaccharide. These modifications successfully resolved the following five undesirable problems that arose when the polysaccharide was directly applied as a protective coating without any molecular modifications to the metal substrates; there were (1) the settlement and growth of microorganisms in its aqueous solution, (2) the high susceptibility of films to moisture, (3) the poor chemical affinity of films for Al surfaces, (4) the weak adherence to polymeric topcoatings, and (5) the biodegradation of films caused by fungal growth. There was no doubt that such modifications significantly enhanced the potential of polysaccharide for use in corrosion-protective coatings.

As part of our ongoing research aimed at developing an uniform, continuous hydrophobic natural polymer film that adequately protects aluminum (Al) substrates against corrosion, we next focussed on assessing the ability of chitosan [CS, poly(D-glucosamine)] ground from the crab or shrimp shells, to mitigate corrosion of Al. The CS, which is a family of polysaccharides, is well known as a low cost, renewable marine polymer, and is produced at an estimated amount of one billion tons per year [3]. However, an undesirable property of CS as the corrosion-mitigating coating films is that it absorbs a large amount of moisture in an atmospheric environment, and then forms a hydrogel [4]. Thus, the emphasis of current study centered on modifying the molecular structure of CS with corn-starch derived dextrine [DEX, poly(D-glucose)] to fabricate a material with a low susceptibility to moisture. The DEX-modified and unmodified CS polymers then were

investigated to gain information on their usefulness as water-based corrosion-preventing primer coatings for Al substrates. The factors to be investigated included changes in molecular configuration, thermal behavior, susceptibility to moisture, morphological features, and surface chemistry of films with different proportions of CS to DEX. The data obtained were integrated and correlated directly with the ability of these coating films to inhibit corrosion of Al.

2. Experimental

2.1. Materials

Chitosan (CS) with a degree of deacetylation of 75 to 85%, supplied by Sigma-Aldrich Fine Chemicals Co., was a coarse particle ground from crab or shrimp shells. Dextrin (DEX) fine powder derived from corn-starch was made by INC Biomedical, Inc. Cerium(IV) nitrate hexahydrate [CAN, $Ce(NO_3)_3 \cdot 6H_2O$], obtained from Alfa, was used as the oxidizing agent. Hydrochloric acid (HCL, 37% in water) was employed to enhance CS's solubility in water. Two aqueous solutions, 1 wt % CS and 1 wt % DEX, were separately prepared before they were blended. The former solution was made by agitating a mixture of 1 g CS, 1 g HCL, and 98 g deionized water for 3 hours at 90 °C. The latter one was prepared in the following way: First, 1 g DEX was added to 99 g deionized water at 70 °C, and mixed by a magnetic stirrer for 2 hours. Then, it was allowed to stand for 24 hours at room temperature, before incorporating CAN of 0.2% by weight of the total DEX solution into it. The seven mix formulations for these DEX-modified CS solutions were designed in this study; there were the CS/DEX ratios of 100/0, 90/10, 70/30, 50/50, 30/70, 10/90, and 0/100, by weight. The lightweight metal substrate was a 6061-T6 aluminum (Al) sheet containing the following chemical constituents; 96.3 wt % Al, 0.6 wt % Si, 0.7 wt % Fe, 0.3 wt % Cu, 0.2 wt % Mn, 1.0 wt % Mg, 0.2 wt % Cr, 0.3 wt % Zn, 0.2 wt % Ti, and 0.2 wt % other elements.

2.2. Coating technology

The coating film was deposited on the Al surfaces in the following sequence: First, to remove surface contaminants, the Al substrates were immersed for 20 min at 80 °C in an alkaline solution consisting of 0.4 wt % NaOH, 2.8 wt % tetrasodium pyrophosphate, 2.8 wt % sodium bicarbonate, and 94.0 wt % water. The alkali-cleaned Al surfaces were washed with deionized water at 25 °C, and dried for 15 min at 100 °C. Next, the substrates were dipped into a soaking bath of film-forming solution at room temperature, and withdrawn slowly. The wetted substrates were then heated in an oven for 120 min at 150 or 200 °C, to yield thin solid films.

2.3. Measurements

The thickness of the DEX-modified and unmodified CS films deposited on the Al surfaces was determined using a surface profile measuring system. Differential scanning calorimetry (DSC) gave information on the enthalpy of the first endothermic phase transition of modified and unmodified CS polymers. DSC was run using the non-isothermal method at a constant rate of 10 °C/min over the temperature range of 25 to 300 °C. The molecular configuration and conformation of 150°- and 200°-treated polymers was investigated by Fourier-transformation infrared (FT-IR) and X-ray photoelectron spectroscopy (XPS). The contact angle was measured by dropping water onto the polymer film surfaces to determine the extent of susceptibility of their surfaces to moisture. The values of contact angle were measured within the first 20 sec after dropping it onto the surfaces. Information on the surface morphology, texture, and film-forming performance of the coatings deposited onto the Al was gained by Scanning Electron Microscopy (SEM). AC electrochemical impedance spectroscopy (EIS) was used to evaluate the ability of the coating films to protect the Al from corrosion. The specimens were mounted in a holder, and then inserted into an electrochemical cell. Computer programs were prepared to calculate theoretical impedance spectra and to analyze the experimental data. Specimens with a surface area of 13 cm^2 were exposed to an aerated 0.5 M NaCl electrolyte at 25 °C, and single-sine technology with an input AC voltage of 10 mV (rms) was used over a frequency range of 10 kHz to 10^{-2} Hz. To estimate the protective performance of coatings, the pore resistance, R_p, (Ω cm^2), was determined from the plateau in Bode-plot scans that occurred at low frequency regions. The salt-spray tests of the coated Al panels (75 mm × 75 mm, size) were performed in accordance with ASTM B 117, using a 5 wt % NaCl solution at 35 °C.

3. Results and discussion

3.1. DEX-modified CS polymers

Before identifing the reaction products yielded by the chemical interactions between DEX and CS at 200 °C, we investigated the changes in chemical conformation of the CS itself at 150 and 200 °C, by FT-IR. In this study, the samples were prepared in accordance with the following method: First, a 200 g CS solution denoted as CS/DEX ratio of 100/0 was poured into glass test tubes, and then left for 24 hours in an air oven at 150 and 200 °C to form the solid polymers; Second, these polymers were ground to a particle size <0.074 mm for FT-IR exploration. Fig. 1 gives the FT-IR spectra for these samples over the frequency range from 1800 to 1000 cm^{-1}. For comparison, the spectrum of "as-received" CS powder, as the reference sample, is also illustrated in this figure. The CS reference sample (a) had absorption bands at 1654, 1549, and 1314 cm^{-1}, revealing the amide I (stretching vibration of carbonyl group, C=O), amide II (bending vibration of secondary amine group, NH), and amide III (stretching vibration of C-N bond) in the secondary amide groups, respectively, at 1590 cm^{-1} which can be ascribed to the N-H bending mode in the primary amine, NH_2, groups, at 1419 and 1372 cm^{-1}, reflecting the C-H bending modes of the methy and methylene, and also at 1149, 1078, and 1026 cm^{-1}, corresponding to the stretching

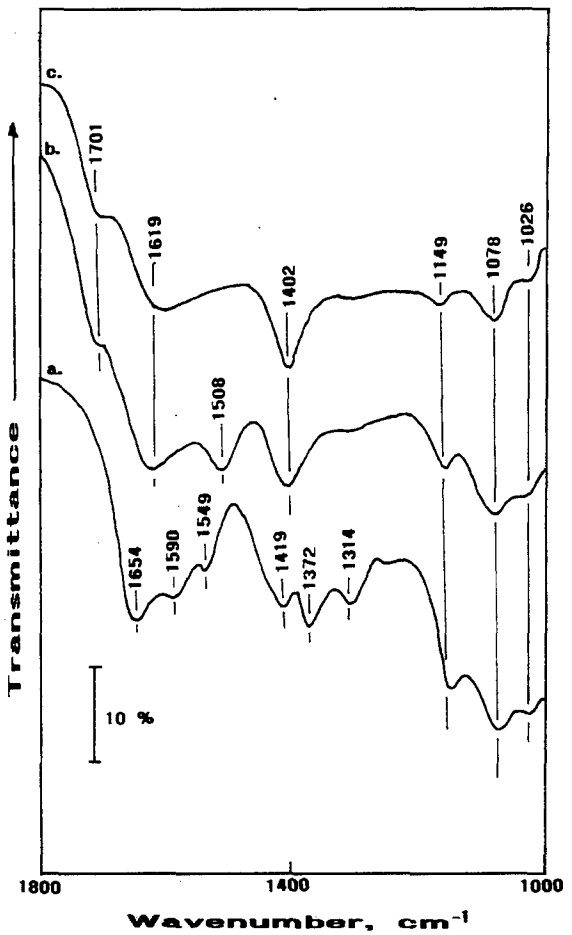

Figure 1 FT-IR absorption spectra of "as-received" CS (a) powder, 150 °C-heated CS (b), and 200 °C-heated CS (c).

vibration of C-O-C linkages in the glucosamine rings. From the representations of the secondary amide and methy groups, the "as-received" CS can be identified as partially N-acetylated chitosan,

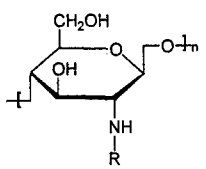

where R is $-COCH_3$ and -H.

When the CS solution was heated at 150 °C, its spectral features (b) differed notably from that of the reference sample; the differences were as follows, (1) the development of three new bands at 1701, 1508, and 1402 cm^{-1}, (2) a shift of the NH_2-associated band at 1590 cm^{-1} to a higher frequency side at 1619 cm^{-1}, (3) the disappearance of all the amide and methy group-related bands at 1654, 1549, 1419, 1372, and 1314 cm^{-1}. Regarding the result (1), the assignment of the new bands at 1701 cm^{-1} is likely to be the C=O groups [5], and that at 1508 cm^{-1} may be due to $-NH_3^+$ Cl^-, which is formed by the interaction between the primary amine and the HCL as the hydrolysis-promoter of CS [6]. A possible contributor of the new band at 1402 cm^{-1} is the $-NH_4^+$ band from the ammonium chloride salt, NH_4Cl [7]. Assuming that these assignments are valid, the result (3) gave us the following important information; the acetyl groups, CH_3OC-, seem to be removed from the partially N-acetylated CS by HCL-catalyzed hydrolysis, forming the acetic acid, CH_3COOH, and the $-NH_3^+$ Cl^- complex derivatives. The latter derivative might be transformed into the NH_4Cl salt by further hydrolysis. As is seen in the spectrum (c), increasing the temperature to 200 °C led to the elimination of $-NH_3^+$ Cl^--related band at 1508 cm^{-1}, a marked increase in intensity of the NH_4Cl absorption band at 1402 cm^{-1}, and an appreciable enhancement of C=O band at 1701 cm^{-1}, suggesting that the conformational transformation of $-NH_3^+$ Cl^- into the NH_4Cl is promoted at elevated temperatures. Since such an HCL-induced deacetylation process introduces the formation of acetic acid derivative into the polymers, we assumed that the C=O band arose from the carboxylic acid groups, COOH, within the acetic acid molecule.

This information was supported by inspecting the XPS C_{1s} and N_{1s} core-level excitations for the 150- and 200 °C-heated film surfaces with CS/DEX ratio of 100/0. The films were deposited onto the Al substrate surfaces using the coating technology described earlier. In these core-level spectra, the scale of the binding energy (BE) was calibrated with the C_{1s} of the principal hydrocarbon-type carbon peak fixed at 285.0 eV as an internal reference standard. A curve deconvolution technique, using a DuPont curve resolver, was employed to substantiate the information on the carbon- and nitrogen-related chemical states from the spectra of the carbon and nitrogen atoms. In the C_{1s} region (Fig. 2), the 150 °C-heated bulk CS films had the four resolvable Gaussian components at the BE positions of 285.0, 286.5, 288.0, and 289.5 eV. The major peak at 285.0 eV is assignable to the C in CH_n groups as the principal component. According to the literature [8, 9], the second intense peak at 286.5 eV reflects both the C in $-CH_2O$- (e.g. hydroxide and ether) and in the C-N bond, and the contributor to the third intense peak at 288.0 eV is due to the C in C=O groups, while the weak signal, emerging at 289.5 eV, originates from C in the carboxylic acid, -COOH. In contrast, the spectral feature of the 200 °C-treated film was characterized by a conspicuous growth of the C=O and COOH carbon peaks. The N_{1s} spectrum (Fig. 2) of the 150 °C CS films included the major peak at 399.8 eV, revealing the N in primary amine [10], and the two shoulder peaks at 401.2 and 402.5 eV, belonging to the N originated from the amide groups [11] and ammonium ion-based salts [12]. By comparison, the curve structure of the 200 °C films was different from that of the 150 °C ones; in particular, there was (1) a striking decay of the amide N peak at 401.2 eV and (2) an increased intensity of the ammonium salt N signal at 402.5 eV. These data strongly supported the results from the FT-IR study; namely, the HCL-catalyzed hydrolysis, followed by heat treatment at 150 and 200 °C, introduces the acetic acid and ammonium chloride derivatives into the films. These

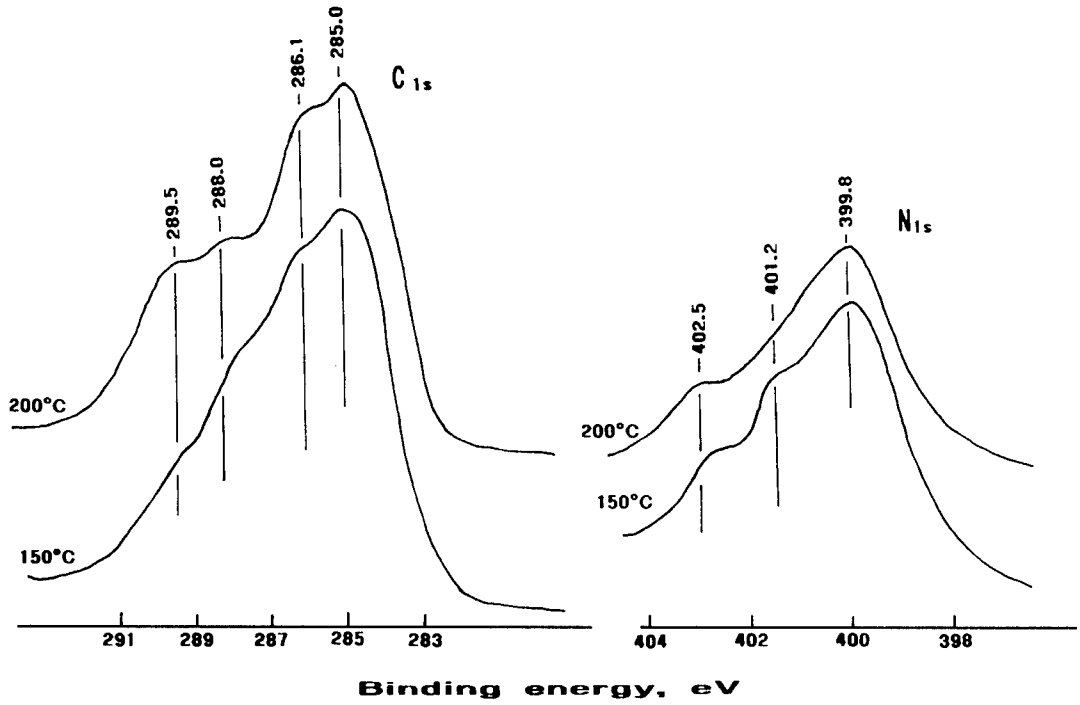

Figure 2 C_{1s} and N_{1s} core-level spectra for 150- and 200 °C-treated CS film surfaces.

derivatives may be formed by the following hypothetical deacetylation pathways:

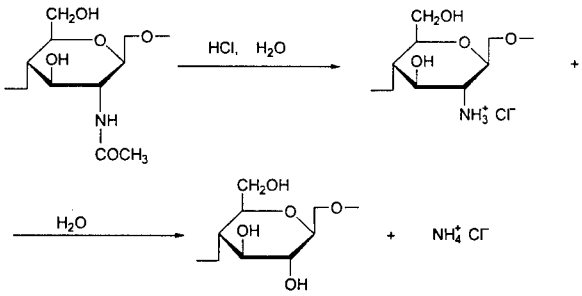

If such conformational changes take place, the molecular structure of the deacetylated CS can be illustrated as follows:

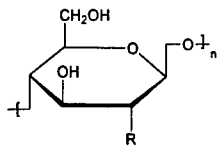

where R is NH_2 or OH. Based upon these information, our emphasis next centered on investigating the changes in the molecular conformation of the CS brought about by varying the CS/DEX ratio at 200 °C. Fig. 3 shows the FT-IR spectra of CS/DEX samples with ratios of (a) 0/100, (b) 100/0, (c) 90/10, (d) 70/30, (e) 50/50, (f) 30/70, and (g) 10/90. As described in our previous papers [1], the Ce(VI) nitrate-oxidized bulk DEX (0/100 ratio), as the reference sample, indicated the formation of a Ce-complexed carboxylate, which could be defined from the two absorption bands at 1588 and 1407 cm^{-1}. Also, this spectrum had a strong peak at 1701 cm^{-1} due to the C=O group in the carboxylic acid, and the four weak absorption bands at 1478, 1149, 1078, and 1026 cm^{-1}. The last three bands arose from the C-O-C linkage-associated groups, while the peak at 1478 cm^{-1} is ascribed to the methylene. This information suggested that Ce-linked carboxylate complexes, $-COO^- Ce^{4+} {}^-OOC-$, were generated in three-step reaction schemes [13]. First, oxidation of the glycosidic rings initiated by the Ce ion generated aldehydic groups, -HC=O, after the opening of rings caused by cleavage of the C-C bonds in the glycol groups. Second, further oxidation of DEX led to the breakage of the C-O-C linkages in the opening structures of two oxidized compounds, the 3, 4-dihydroxybutanoic acid $[(HO)_2C_3H_5COOH]$ and glycolic acid ($HOCH_2COOH$), as the fragmental products of glucose units. Once these oxidized fragments containing functional carboxylic acid groups were produced, in a final reaction step, these functional groups favorably reacted with Ce to form three Ce-bridged fragment complexes, $[(HO)_2C_3H_5COO^- Ce^{4+} {}^-OOCH_5C_3(OH)_2]\cdot 2OH^-$, $(HOCH_2COO^- Ce^{4+} {}^-OOCH_2COH)\cdot 2OH^-$, and $[(HO)_2C_3H_5COO^- Ce^{4+} {}^-OOCH_2COH]\cdot 2OH^-$ [14]. The spectrum (b) represents the bulk CS sample (100/0 ratio) in which the contributors to these absorption bands were already described in the previous pages. When a 10 wt % by weight of the total amount of CS was replaced by DEX, the spectrum (c) exhibited the incorporation of two additional bands at 1655 and 1554 cm^{-1} into the bulk CS spectrum, revealing the formation of amide I and amide II, respectively. As seen in the spectrum (d) of the 70/30 ratio sample, further replacement of the CS by DEX resulted in the growth of these bands; meanwhile, the

peak intensities of NH_2- and -NH_4^+ Cl^- -related bands at 1620 and 1402 cm^{-1} had weakened. This interesting spectrum was also showed that there were no peaks at 1588 and 1407 cm^{-1}, originating from the formation of Ce-complexed carboxylate. A possible interpretation of these findings was that the NH_2 group in the CS has a strong chemical affinity for the Ce-bridge carboxylate complexes in the DEX, so forming the amide bond, -NHCO-, as the reaction product that grafts directly the fragmental products of DEX onto the CS. The hypothetical conformation of DEX fragment-grafted CS can be represented in three reaction schemes (Fig. 4). Returning to Fig. 3, the spectral feature (e) of the 50/50 ratio sample closely resembled that of the 70/30 ratio one. As expected, incorporating an excessive amount of DEX into the CS left unreacted Ce-complexed carboxylate fragments in the samples. In fact, the spectra (f) and (g) of the 30/70 and 10/90 ratio samples, respectively, included the two absorption bands at 1588 and 1407 cm^{-1}, belonging to the fragmental Ce-bridged carboxylate complexes; concurrently, a declining intensity of the amine-, amide- and NH_4Cl-related peaks at 1655, 1620, 1554, and 1402 cm^{-1} was observed. Thus, adding a proper amount of DEX to the CS seems to be necessary to avoid staying unreactive DEX fragments in the film.

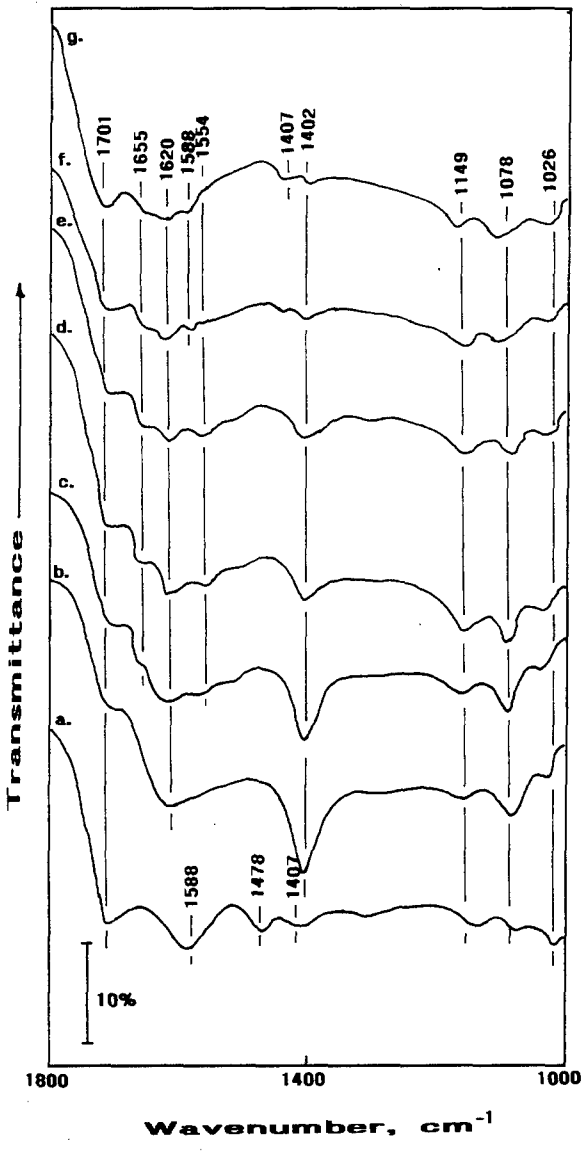

Figure 3 FT-IR spectra for the samples made with 100/0 (a), 90/10 (b), 70/30 (c), 50/50 (d), 30/70 (e), 10/90 (f), and 0/100 (g) CS/DEX ratio at 200 °C.

One concern in applying natural polymer-based coating films as corrosion-preventing barriers to the metal surfaces was the fact that they absorb a large amount of atmospheric moisture. Such a hydrophilic property, which allows water to infiltrate the film easily, is one of the undesirable factors for use as the coating materials to mitigate corrosion of the metals. Hence, our attention was centered on the uptake of the moisture by the DEX-modified CS polymers. In this study, the 200 °C-treated DEX-modified and unmodified CS powders were exposed for 10 hours in an environmental chamber under a 70% relative humidity (R.H.) at 25 °C, and then they were examined by DSC to obtain the information on the extent of water uptake. As reported by Lelievre [15] and Donovan [16], the degree of the hydration for the polysaccharide could be determined from the DSC endothermic phase transitions, such as the enthalpy (ΔH) of dehydration occurring in the samples at temperature ranging from 25 to 200 °C. Fig. 5 illustrates the DSC traces for the samples of (a) 100/0, (b) 90/10, (c) 70/30, (d) 50/50, (e) 30/70, (f) 10/90, and (g) 0/100 CS/DEX ratios after exposure in a 70% R.H. at 25 °C. The DSC curve of the unmodified bulk CS sample (100/0 ratio) showed that the onset of endothermic transition begins at around 130 °C, and ends near 250 °C; concurrently, the endothermal peak occurs at 165.3 °C. From this information, we assumed that the dehydration of moisture-absorbed bulk CS was completed at temperature range of 130–250 °C. When the CS was modified with DEX, a specific feature of the DSC curves was characterized by generating an additional endothermal peak at 134 °C. The heat flow of this new exothermal peak seemed to increase with a decreasing ratio of CS to DEX, while heat flow at 165.3 °C peak tends to decline. Furthermore, the curve (f) of the 10/90 ratio samples indicated an additional endothermal peak at 203.9 °C. From the comparison with that of the bulk DEX (g), it is possible to rationalize that this new transition peak at 203.9 °C was due to the thermal decomposition of unreacted DEX. Also, the curve of the bulk DEX had a dehydration-related peak at 110 °C in the temperature range 60–190 °C. If the postulated contributors to these exothermic transitions are valid, the peak at 134 °C is more likely to be associated with the dehydration of DEX fragment-grafted CS reaction products rather than that of the DEX fragment itself.

To estimate the extent of absorption of the moisture, the enthalpy ΔH of dehydration occurring in the first endothermic phase transition was computed using the following formula [17, 18]: $\Delta H = TRA/hm$, where T, R, A, h, and m refer to the temperature scale (°C $in.^{-1}$), the range sensitivity (mcal s^{-1} $in.^{-1}$), the peak area ($in.^2$), the heating rate (°C s^{-1}), and the sample weight (mg), respectively. The changes in ΔH as a function of the proportion of CS to DEX are given in Fig. 6. A

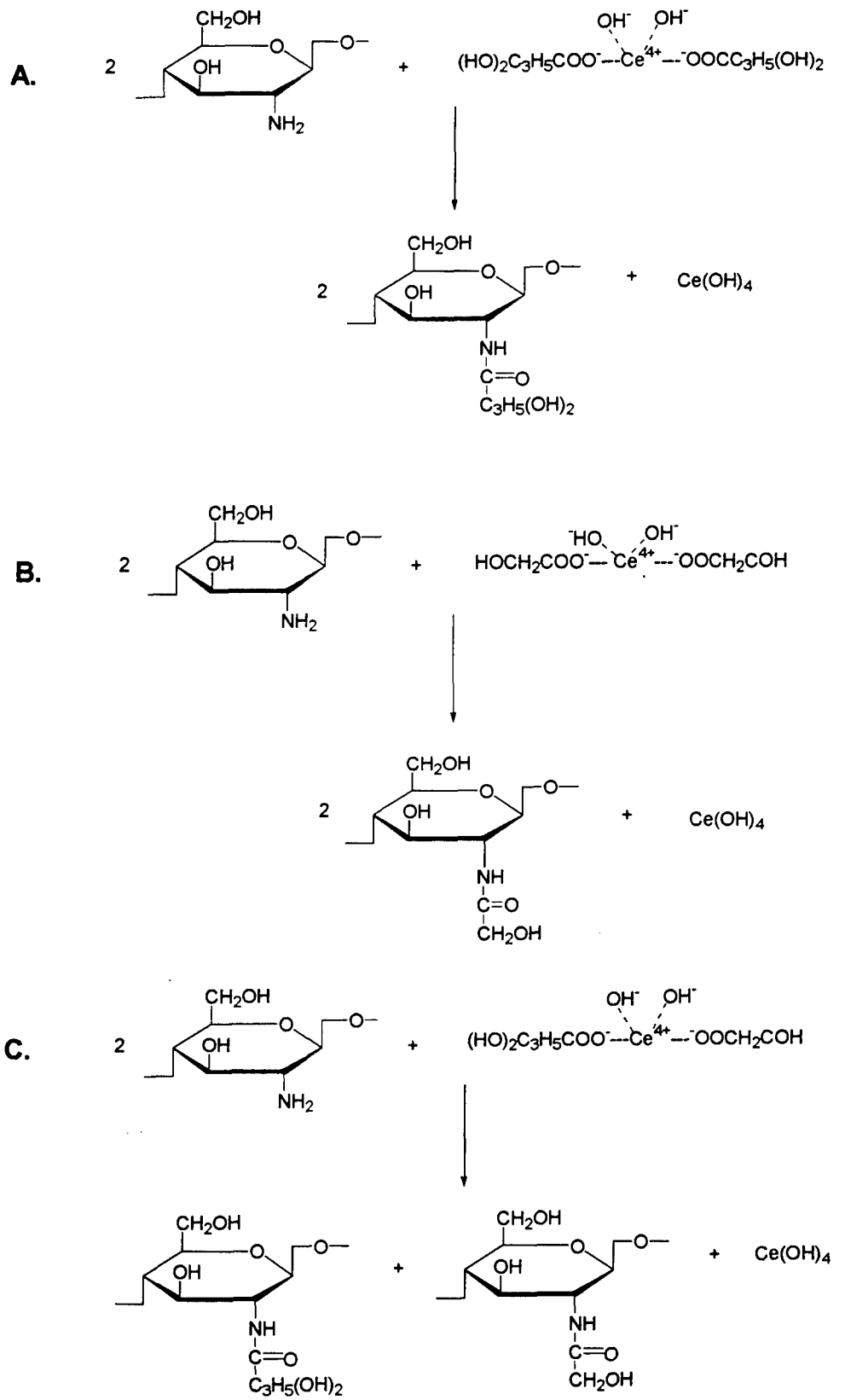

Figure 4 Hypothetical reaction schemes between D-glucosamine and Ce-bridged carboxylate complexes.

given result showed that the ΔH value was markedly reduced as the CS/DEX ratio declined from 100/0 to 70/30. The ΔH value of 0.084 kJ g^{-1} for the 70/30 ratio sample was three times lower than that of the bulk CS sample (100/0 ratio); beyond this, a further decrease in the CS/DEX ratio caused an increase in ΔH value. Because the ΔH value reflects the total energy consumed for removing all the moisture adsorbed to the CS samples, we judged that the samples with a low value of ΔH are less susceptible to water uptake. From

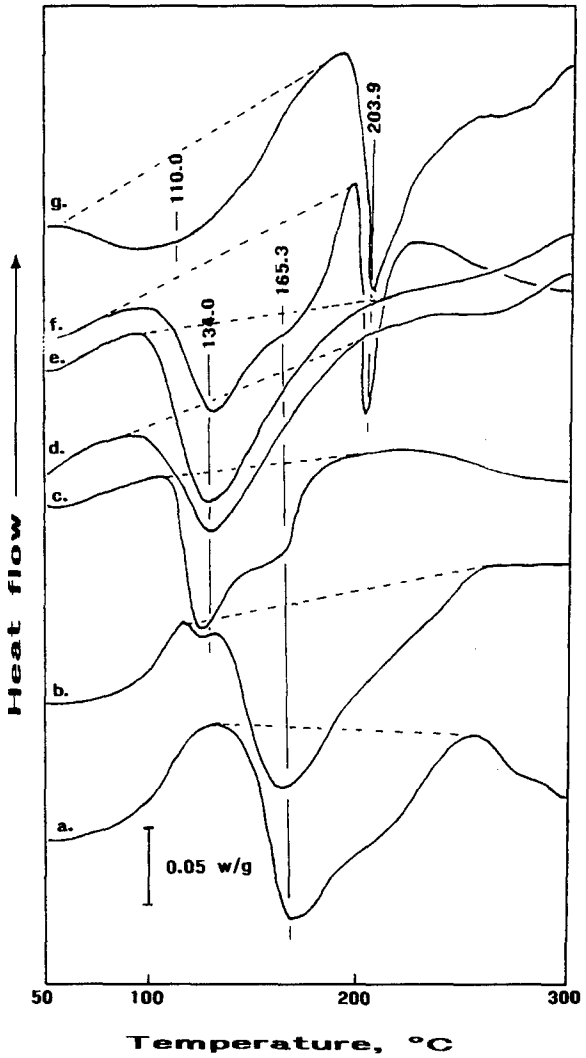

Figure 5 DSC endothermal curves for 100/0 (a), 90/10 (b), 70/30 (c), 50/50 (d), 30/70 (e), 10/90 (f), and 0/100 (g) ratio samples after exposure to a 70% R.H. at 25 °C.

this aspect, both the bulk CS and DEX samples with a very high ΔH of > 0.16 kJ g^{-1} appear to have a high susceptibility to the absorption of moisture. By comparison, the 70/30 and 50/50 ratio samples had an ΔH of less than 0.1 kJ g^{-1}, inferring that a proper proportion of CS to DEX plays an important role in reducing the magnitude of sensitivity to moisture. In other words, almost all the hydrophilic NH_2 groups present in the CS might react with all hydrophilic DEX fragments to yield the hydrophobic amide bonds as the reaction products, promoting the degree of fragment grafts on the CS. Therefore, there may be few, if any, remaining unreacted NH_2 groups and fragments in the grafted CS structure.

3.2. Characteristics of coatings

Based upon the information above, focus was now directed toward assessing the characteristics of the DEX fragment-grafted CS coating films deposited on the Al substrate surfaces. The characteristics to be assessed included the magnitude of wettability of the coating film surfaces by the water, the film-forming performance, and the morphological feature and elemental compositions of their surfaces. All the data obtained were correlated directly with the results from the corrosion-related tests, such as electrochemical impedance spectroscopy (EIS) and salt-spray resistance.

One of the important factors indispensable for good protective coating films is the hydrophobic characteristic that the assembled film surfaces are not sensitive to moisture. To gain information on this characteristic, we measured the contact angle of a water droplet on the 200 °C-treated 100/0, 90/10, 70/30, 50/50, 30/70, 10/90, and 0/100 ratio film surfaces. If the contact angel was low, we concluded that the film is sensitive to moisture. A high degree of sensitiveness may allow the water to permeate through the film easily, and, in the worst case, it may promote the hydrolysis-induced decomposition of the film. A plot of the average value of the advancing contact angle, θ (deg.), as a function of CS/DEX ratios is shown in Fig. 7. The resultant θ-ratio data exhibited that the θ value of bulk CS film (100/0 ratio) considerably increases as it was modified with the DEX, especially in the CS/DEX ratio range of 100/0 to 70/30. The 70/30 ratio coating film had the highest θ value of 60°, corresponding to a 2.9 times greater than that of the bulk CS. A further incorporation of EDX into the CS caused a declining θ value, strongly suggesting that the film with a lower sensitivity to moisture could be made by incorporating a proper amount of DEX into the CS. Thus, this finding can be taken as evidence that an increase in the degree of grafting serves in providing a less sensitive film surface to moisture. In the other words, the hydrophilic characteristics of the individual CS and DEX fragment coatings are converted into hydrophobic ones by the grafting reaction between them, inferring that the DEX fragment-grafted CS coating films made of a suitable proportion of CS to DEX will contain a minimal amount of hydrophilic unreacted fragments and D-glucosamine components. The major factor governing this conversion is the formation of amide bonds yielded by the grafting reaction, conferring a less wettability of water over the film surfaces. Also, this information substantially supported the our earlier results on the uptake of the moisture by the DEX-modified CS polymers.

Attention was next paid to exploring the surface morphology and microtexture of coating films covering Al surfaces, by SEM. In this experiment, three coating films made with 100/0, 70/30, and 10/90 ratios were deposited on Al at 200 °C. The data obtained would provide information on the film-forming performance of grafted and non-grafted CS polymer coatings. The SEM image of the brown-colored 100/0 ratio film (Fig. 8A) revealed a discontinuous microtexture containing numerous microcracks, allowing the corrosive solutions to permeate through the film layer easily. Such development of cracks in the film may be due to a high degree of shrinkage of the film encountered during drying at 200 °C, and also to the conformational changes in CS structure caused by the deacetylating reaction that introduces the formation of CH_3COOH and NH_4Cl derivatives in it. In contrast, an excellent film-forming performance was observed from the 70/30

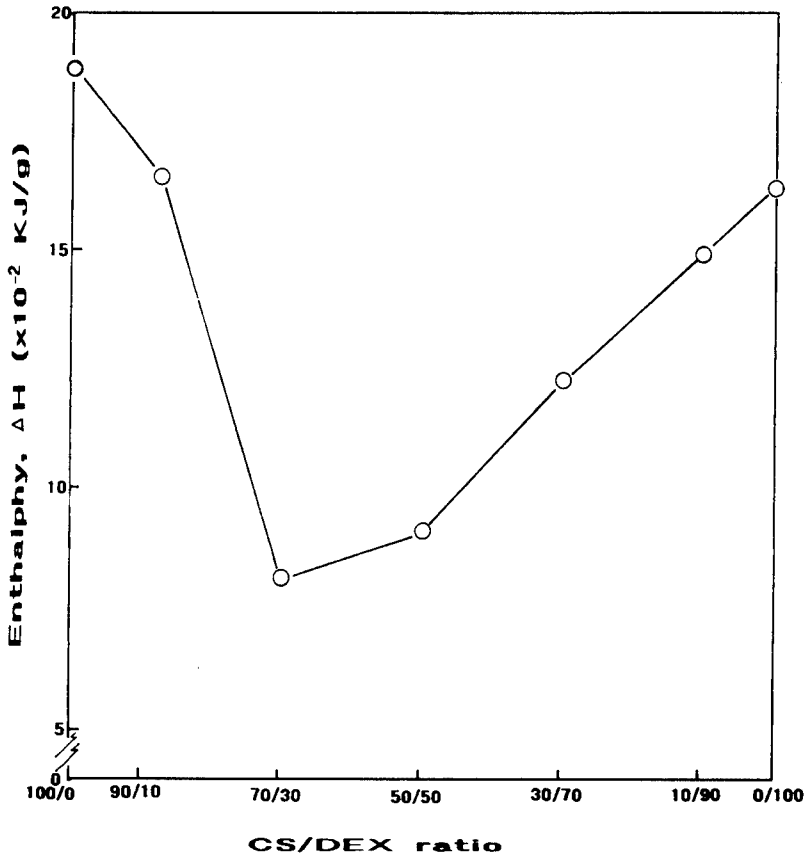

Figure 6 Changes in enthalpy which represent the magnitude of dehydration as a function of CS/DEX ratio.

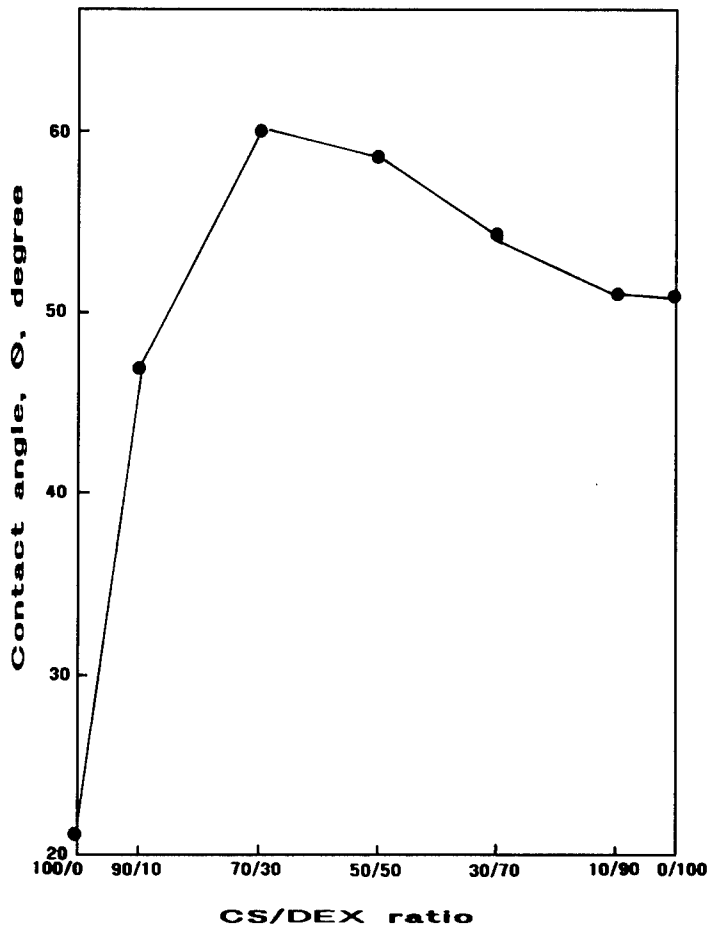

Figure 7 Contact angle of a water droplet on 200 °C-treated coating film surfaces with various different CS/DEX ratios.

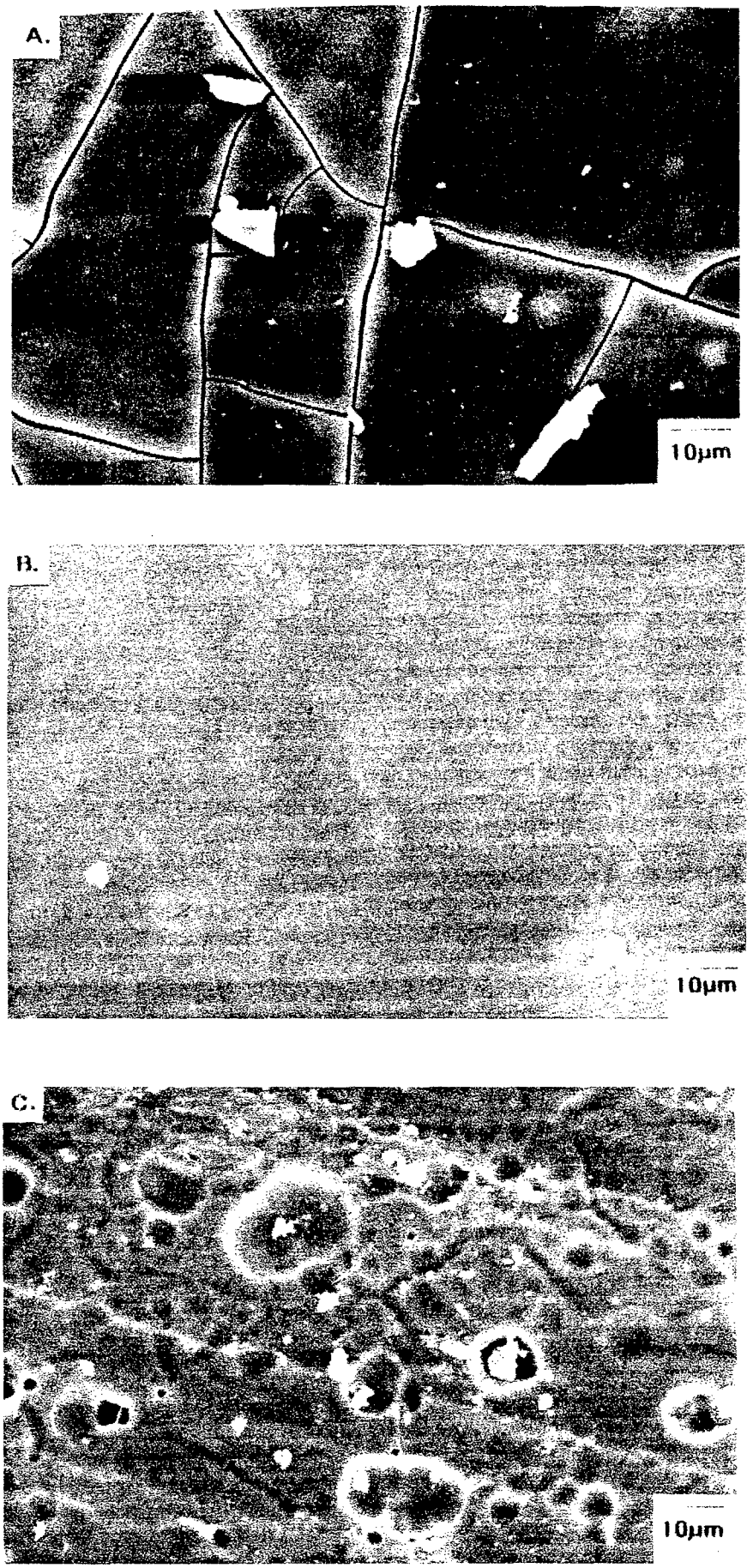

Figure 8 SEM images of 200 °C-treated 100/0 (A), 70/30 (B), and 10/90 (C) CS/DEX ratio coating films.

ratio-derived coatings, which were light brown in color (Fig. 8B); SEM disclosed a continuous, uniform film with a smooth surface morphology, seemingly suggesting that grafting the DEX fragments onto the CS serves in reducing the development of shrinkage-related stress cracks in the CS itself. There is no doubt that lack of defects and blemishes is one of the most important factors in ensuring that the coatings adequately protect the metals against corrosion. Increasing the amount of DEX in the blended systems led to the changes in color of films from brown to light yellow. With the 10/90 ratio, the SEM image (Fig. 8C) shows a continuous film covering the Al surfaces. Furthermore, the disclosure of a rough underlying Al surface signifies that a thin transparent film was formed.

All the data were integrated and correlated directly with the effectiveness of grafted CS films in protecting the Al substrates from corrosion. Using a surface-profile measuring system, the thickness of the 100/0, 90/10, 70/30, 50/50, 30/70, and 0/100 CS/EDX ratio films was ~3.2, ~2.8, ~2.4, ~1.9, ~1.6, and ~0.9 μm, respectively. Although intuitively a thicker coating film may be expected to have a better corrosion-protective performance than a thin one, AC electrochemical impedance spectroscopy (EIS) was used to evaluate their effectiveness as corrosion-preventing barriers. On the overall Bode-plot curves [the absolute value of impedance $|Z|$ ($\Omega\,cm^2$) vs. Frequency (Hz)], (not shown), our particular attention was paid to the impedance value in terms of the pore resistance, R_p, which can be determined from the plateau in the Bode plot occurring at a sufficiently low frequency of 5×10^{-2} Hz. Fig. 9 shows the plots of R_p of 200 °C-treated coating films versus the CS/DEX ratios. The R_p value (not shown) of the uncoated Al substrate was $\sim 5.0 \times 10^3\ \Omega\,cm^2$. When the Al surfaces were coated with the single CS and DEX coatings, or DEX-modified CS coatings, the R_p value increased by one or two orders of magnitude over that of the substrate. The R_p value of the single CS coatings with the thickest film of ~3.2 μm was $\sim 1.7 \times 10^4\ \Omega\,cm^2$. When a 10% of the total amount of CS was replaced by DEX, this value was an order of magnitude greater than that of the unmodified CS. With further substitution, the value of R_p increased: the 70/30 ratio coatings had the highest R_p of $4.0 \times 10^5\ \Omega\,cm^2$. However, coatings made by incorporating an excessive amount of DEX into the CS showed a decreasing R_p value. In fact, the R_p value of the 50/50 ratio coating declined ~55% to $1.8 \times 10^5\ \Omega\,cm^2$, compared with that of the 70/30 ratio. In the 10/90 ratio coating, the R_p value fell further to $1 \times 10^5\ \Omega\,cm^2$. As expected, the bulk DEX coating had a lower R_p value of $3.5 \times 10^4\ \Omega\,cm^2$, corresponding to an order of magnitude lower than that of the 70/30 ratio coating. Since the R_p value reflects the magnitude of ionic conductivity generated by the electrolyte passing through the coating layers, a high R_p value means a low degree of permeation of electrolyte into the coating films. Thus, the DEX fragment-grafted CS polymer conformation offers improved performance in minimizing the rate of permeation of the electrolytes through the coating layers, compared with those of the individual CS and DEX coatings. Hence, we believed that a grafted structure would lead to a low uptake of electrolytes by the coatings. The data also represented that the changes in the magnitude of conductivity depend on the CS/DEX ratio. Comparing R_p values, the effectiveness of these ratios in ensuring a low degree of infiltration of electrolyte was in the following order; 70/30 > 50/50 > 90/10 > 30/70 > 10/90 > 0/100 > 100/0. The most effective coating system in reducing the permeability of electrolytes was the 70/30 ratio with a $4.0 \times 10^5\ \Omega\,cm^2$.

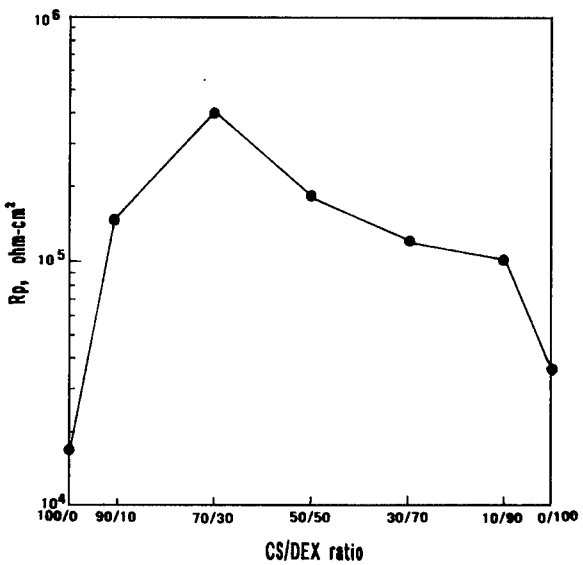

Figure 9 Pore resistance, R_p, value of Al panel samples coated with 100/0, 90/10, 70/30, 50/50, 30/70, 10/90, and 0/100 CS/DEX ratios at 200 °C.

Fig. 10 represents the changes in R_p at 5×10^{-2} Hz for the 200 °C-treated coating specimens as a function of exposure times of up to 20 days in a 0.5 N NaCl solution at room temperature. In the first five days of exposure, three coating systems, 90/10, 70/30, and 50/50 ratios, showed no changes in R_p value, compared with that of the unexposed ones. Afterwards, their R_p values gradually fell with an increasing exposure time. In contrast, the rate of uptake for all the other coating systems was much higher than that of these three coatings; in fact, a marked decrease in R_p can be seen after exposing them for 5 days. When the R_p value dropped to a less than $5 \times 10^3\ \Omega\,cm^2$, no further exposure test was made because the R_p at this level is mainly due to the anodic etching of the underlying Al. In fact, the pitting corrosion of Al caused by the failure of the coating was visually observed in these specimens. The data also indicated that the 70/30 and 50/50 ratio coatings after a 20-day exposure still maintained an $R_p > 10^4\ \Omega\,cm^2$. Implicating this finding with the data on FT-IR, XPS, DSC, and contact angle, two factors played an essential role in conferring resistance to metal corrosion: First was the polymer conformation containing amide bonds formed by the grafting reaction between Ce-complexed carboxylate in DEX fragments and NH_2 groups in CS; and second was the lesser susceptibility of the coating surfaces to moisture due to the enhanced degree of grafting, together with a minimal amount of hydrophilic unreacted fragments and CS.

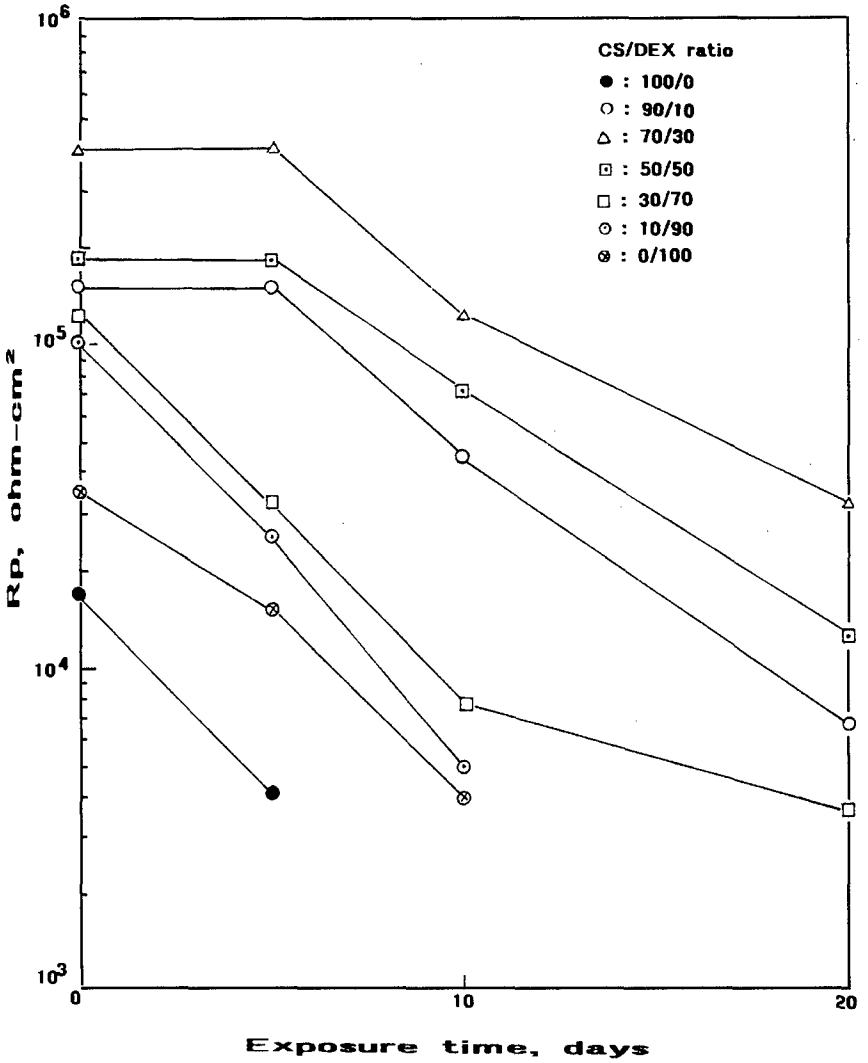

Figure 10 Change in R_p for 100/0, 90/10, 70/30, 50/50, 30/70, 10/90, and 0/100 ratio-coated Al as a function of exposures up to 20 days.

This information on the EIS was supported by salt-spray resistance tests for the coated panels treated at 200 °C (Table I). A trace of rust stain was generally looked for in evaluating the results for salt-sprayed panel specimens. The results were reported as the total exposure time at the date of the generation of the rust stain from the Al surfaces. As is seen, the entire surfaces for the single CS (100/0 ratio)- and DEX (0/100 ratio)-coated Al panels were corroded after exposure to the salt spray for 72 hours, corresponding to only 24 hours longer than that of the uncoated bare Al (not shown), suggesting that the ability of these coatings to protect Al against corrosion is poor. By comparison with these single coatings, the DEX fragment-grafted CS coating systems displayed a far better performance in reducing the rate of corrosion. With the 90/10 ratio, the resistance to salt spray extended seven times to 504 hours. A further improvement in conferring resistance was observed from the coatings containing increased concentrations of DEX, signifying that an increase in the grafting of DEX fragment onto the CS imparts improved resistance to corrosion. In fact, coatings, made from 70/30 ratio served in providing a great protection of Al against corrosion for 720 hours, However, a further incorporation of DEX into the CS caused a declining resistance to salt spray.

TABLE I Salt-spray resistance tests for DEX fragment-grafted CS coatings

CS/DEX ratio	Salt-spray resistance, hours
100/0	72
90/10	504
70/30	720
50/50	590
30/70	216
10/90	120
0/100	72

4. Conclusion

In approaching ways of using partially N-acetylated chitosan (CS) marine polymer ground from the crab or shrimp shells in a water-based coating system to protect aluminum (Al) substrates against corrosion, we modified it with natural dextrine (DEX) polymers derived from corn starch. Both are renewable resources and environmentally benign. The DEX-modified CS

paints as film-forming precursor solutions were prepared by incorporating a DEX aqueous solution containing Ce nitrate hexahydrate as the oxidizing agent into CS aqueous solution containing HCL as the hydrolyzing agent. The blended two polysaccharide polymer solutions were deposited onto the Al surfaces using a simple dip-withdrawing coating method and converted into the thin solid films by heating them at 200 °C in air. The oxidation of DEX led to the formation of two oxidized compounds, 3,4-dihydroxybutanoic acid and glycolic acid, as the fragmental products. These fragments next favorably reacted with Ce from the Ce nitrate to reconstitute Ce-complexed carboxylate fragment compounds. Adding HCL to the CS solution not only enhances its solubility in water, but also served to remove acetyl groups from the CS. The primary amine, NH_2, in the deacetylated CS, had a strong chemical affinity for the Ce-bridged carboxylate fragments to create secondary amide linkages that serve in grafting the DEX fragments onto the CS. An increase in the degree of grafting resulted in the formation of an uniform, continuous, defect-free coating films that offer a less susceptible to moisture and a low permeation of electrolyte species through the coating layers, conferring a good protection of metal against corrosion. However, incorporating an excessive amount of DEX into the CS generated undesirable coating films with a high degree of wettability of surfaces and an enhanced magnitude of ionic conductivity caused by electrolytes passing through the coating layers. These negative factors could be accounted for by the persistence of a certain amount of unreacted hydrophilic fragments in the coatings. Nevertheless, the most effective coating film for mitigating the corrosion of Al was derived from precursor solution with CS/DEX ratio of 70/30. This coating film deposited onto the Al surfaces offered a lesser sensitivity to moisture, and improved pore resistance (in Ω cm^2) by an order of magnitude higher than those of the single CS and DEX coatings, and conferred salt-spray resistance for 720 hours.

Acknowledgement

This work was performed under the auspices of the U.S. Department of Energy, Washington, D.C. under Contract No. DE-AC02-98CH10886, and supported by the U.S. Army Research Office Program MIPR 96-40.

References

1. T. SUGAMA, *J. Mater. Sci.* **32** (1997) 3995.
2. T. SUGAMA and J. E. DuVALL, *Thin Solid Films* **287** (1996) 39.
3. S. HRANO, H. INUI, H. KOSHI, Y. UNO and T. TODA, in "Biotechnology and Bioactive Polymers," edited by C. Gbelein and C. Carraher (Plenum Press, New York, 1994) p. 43.
4. I. GABRIELII and P. GATEHOLN, in Proceedings of the American Chemical Society, Division of Polymeric Materials: Science and Engineering, Vol. 79, 1998, p. 459.
5. K. NAKANISHI and P. H. SOLOMON, "Infrared Absorption Spectroscopy" (Holden-Day, San Francisco, CA, 1977) p. 38.
6. L. J. BELLAMY, "The Infrared Spectra of Complex Molecules" (John Wiley and Sons, Inc., New York, 1975) p. 289.
7. R. A. NYQUIST and R. O. KAGEL "Infrared Spectra of Inorganic Compounds" (Academic Press, New York, 1971) p. 407.
8. D. BRIGGS, D. M. BREWIS and M. B. KONIECZO, *J. Mater. Sci.* **11** (1976) 1270.
9. A. TOTH, I. BERTOTI, T. SZEKELY, J. N. SAZANOV, T. A. ANTONOVA, A. V. SHCHUKAREV and A. V. GRBANOV, *Surf. Interface Anal.* **8** (1986) 261.
10. D. BRIGGS, D. M. BREWIS and P. KNOIECZKO, *J. Mater. Sci.* **14** (1977) 1344.
11. K. B. YATSINIRSKII, V. V. NEMOSHALENKO, V. G. ALESHIN, Y. I. BRATUSHKO and E. P. MOISSENKO, *Chem. Phys. Lett.* **52** (1977) 481.
12. K. BUGER, F. TSHISMAROV and H. EBEL, *J. Electron. Spectosc. Relat. Phenom.* **10** (1977) 461.
13. S. C. STINSON, *Chemical & Engineering News* **74** (1996) 35.
14. T. SUGAMA and T. HAYWOOD, *J. Coat. Techno.*, in press.
15. J. LELIEVRE, *J. Appl. Polym. Sci.* **18** (1973) 293.
16. J. W. DONOVAN, *Biopolymers* **18** (1979) 263.
17. M. J. O'NEAL, *Anal. Chem.* **36** (1964) 1238.
18. M. G. WYZGOSHI, *J. Appl. Polym. Sci.* **25** (1980) 1455.

Received 23 October
and accepted 18 November 1998

Poly(itaconic acid)-modified Chitosan Coatings for Mitigating Corrosion of Aluminum Substrates

By

T. Sugama and M. Cook*

Materials and Chemical Science Division
Department of Applied Science
Brookhaven National Laboratory
Upton, NY 11973

* Department of Chemistry
Polytechnic University
333 Jay St., Brooklyn, NY 11201

This work performed under the auspices of the U.S. Department of Energy, Washington, D.C. under Contract No. DE-AC02-98CH10866, and supported by the U.S. Army Research Office Program MIPR9GDOEARO43

Abstract

To make a water-insoluble chitosan (CS) biopolymer, the synthetic poly(itaconic acid) (PIA) polymer was added to graft it onto the liner CS chains and to crosslink between the CS chains. The grafting and crosslinking reactions were generated by a strong chemical affinity between the NH_2 groups in the CS and the COOH groups in the PIA, leading to the formation of amide bonds. When this polymer was applied as environmentally benign water-based coatings to an aluminum (Al) substrate by a simple dip-withdrawing method, the following three factors played an essential role in mitigating the rate of corrosion of the Al: First was the polymer's conformation containing hydrophobic amide bonds, together with a minimal amount of hydrophilic unreacted COOH in PIA and NH_2 in CS; second was the lesser susceptibility of the coating films to moisture due to the enhanced degree of grafting and crosslinking; and third was the interactions at the interfaces between the grafted CS and the Al substrate, developing the formation of the -COO-Al linkage. The PIA-grafted and -crosslinked CS polymer coating films generated from the proper proportions of PIA to CS included all these factors and displayed low ionic conductivity, thereby imparting a salt-spray resistance of 694 hours for coated Al panels.

Introduction

Chitosan (CS), which is derived from the polysaccharide chitin, is well known as a low cost, renewable marine polymer because the source of chitin comes from the structural components of the shells of crustaceans, such as shrimps, lobsters, and crabs, [1]; it is the most plentiful natural polymer next to cellulose. CS is produced at an estimated amount of one billion tons per year [2]. The molecular structure of CS is represented by a beta 1→ 4 linked linear biopolymer consisting of ~ 80 % poly(D-glucosamine) and ~ 20 % poly (N-acetyl-D-glucosamine). When CS was dissolved in an aqueous medium at pH < 6.5, this biopolymer becomes a liner polybase electrolyte having a highly positive (+) charge density because it includes an amine group [3]. Such a cationic property together with its biocompatability was the reason why CS is widely used in biomedical applications, for example, a bacteriostatic agent, a flocculating agent, a drug delivery vehicle, an immobilization and encapsulation agent of toxic heavy metals, and also cosmetics. In addition, a tough, flexible CS film can be fabricated by depositing CS-dissolved aqueous solution on the substrate surfaces and then allowing it to dry. This film had a high potential for use as contact lenses and wound dressings. Thus, it seemed worthwhile to assess the usefulness of the non-toxic CS biopolymer as an environmentally green water-based coating to protect metals against corrosion. However, the major critical issue in using CS as a corrosion-preventing barrier is that it absorbs a large amount of moisture from the atmosphere, and then forms a hydrogel [4]. This transformation not only leads to biodegradation of the film, but also allows moisture to infiltrate easily into the film, causing its failure as a protective coating.

Based upon information described above, one approach to solving this problem is the incorporation of negatively charged water-soluble synthetic polyacid electrolytes into the cationic natural polybase CS electrolyte. Among the synthetic polyacid electrolytes, poly(itaconic acid) (PIA) is very attractive because it has two negatively charged carboxylic acid groups in a unit of the macromolecule. It was presumed that PIA would be a more effective

reactant than other polyacid electrolytes, such as poly(acrylic acid), poly(maleic acid), poly(3-methacryloyloxypropane-1-sulfonic acid), poly(4-vinylbenzoic acid), which contain a single anionic acid group. Thus, the focus of the current program centered on modifying the molecular structure of CS with PIA to assemble a polymeric material with a low susceptibility to moisture. The PIA-modified CS polymers than were assessed to gain information on their usefulness as water-based corrosion-preventing primer coatings for aluminum (Al) substrates. The factors to be assessed included the changes in molecular configuration, thermal behavior, susceptibility to moisture, surface chemistry of films with different proportions of CS to PIA, and chemistry at the interfaces between modified CS and Al. The data obtained were integrated and correlated directly with the ability of these coating films to inhibit corrosion of Al. Success would provide uniform, continuous, hydrophobic CS coating films that are potential candidates for replacing coating systems containing environmentally harmful ingredients, such as volatile organic compounds (VOCs) and toxic chromium and lead compounds.

Experimental Methods

Materials

Chitosan (CS) with a degree of deacetylation of 75 to 80 %, supplied by Sigma-Aldrich Fine Chemicals Co., was a coarse particle ground from crab or shrimp shells. Poly(itaconic acid) (PIA) was a fine powder with an average molecular weight of 50,000, obtained from Polysciences, Inc. Hydrochloric acid (HCl, 37 % in water) was employed to enhance CS's solubility in water. Two aqueous solutions, 1 wt% CS and 1 wt% PIA, were separately prepared before they were blended. The former solution was made by agitating a mixture of 1 g CS, 1 g HCl, and 98 g deionized water for 3 hours at 90°C. The latter one was prepared by mixing 1 g PIA and 99 g deionized water at room temperature using magnetic stirrer for 2 hours. The seven mix formulations for these PIA-modified CS solutions were designed in this study; there were the CS/PIA ratios of 100/0, 90/10, 80/20, 70/30, 50/50, 30/70, and 0/100, by weight. The lightweight metal substrate was a 6061-T6 aluminum (Al) sheet containing the following chemical consitutents; 96.3 wt% Al, 0.6 wt% Si, 0.7 wt% Fe, 0.3 wt% Cu, 0.2 wt% Mn, 1.0 wt% Mg, 0.2 wt% Cr, 0.3 wt% Zn, 0.2 wt% Ti, and 0.2 wt% other elements.

Coating Technology

The coating film was deposited on the Al surfaces in the following sequence: First, to remove surface contaminants, the Al substrates were immersed for 20 min at 80°C in an alkaline solution consisting of 0.4 wt% NaOH, 2.8 wt% tetrasodium pyrophosphate, 2.8 wt% sodium bicarbonate, and 94.0 wt% water. The alkali-cleaned Al surfaces were washed with deionized water at 25°C, and dried for 15 min at 100°C. Next, the substrates were dipped into a soaking bath of film-forming solution at room temperature, and withdrawn slowly. The wetted substrates were then heated in an oven for 120 min at 200°C to yield thin solid films.

Measurements

The thickness of the PIA-modified and unmodified CS films deposited on the Al surfaces was determined using a surface profile measuring system. Thermogravimetric analysis (TGA) was used to investigate the amount of absorbed moisture in the modified and unmodified CS polymers. TGA was run using the non-isothermal method at a constant rate of 10°C/min over the temperature range of 25° to 450°C. The molecular configuration and conformation of 200°-treated polymers was investigated by Fourier-transformation infrared (FT-IR) and X-ray photoelectron spectroscopy (XPS) . The contact angle was measured by dropping water onto the polymer film surfaces to determine the extent of susceptibility of their surfaces to moisture. The values of contact angle were measured within the first 20 sec after dropping it onto the surfaces. AC electrochemical impedance spectroscopy (EIS) was used to evaluate the ability of the coating films to protect the Al from corrosion. The specimens were mounted in a holder, and then inserted into an electrochemical cell. Computer programs were prepared to calculate theoretical impedance spectra and to analyze the experimental data. Specimens with a surface area of 13 cm^2 were exposed to an aerated 0.5 M NaCl electrolyte at 25°C, and single-sine technology with an input AC voltage of 10 mV (rms) was used over a frequency range of 10 Khz to 10^{-2} Hz. To estimate the protective performance of coatings, the pore resistance, R_p, (ohm-cm^2), was determined from the plateau in Bode-plot scans that occurred at low frequency regions. The salt-spray tests of the coated Al panels (75 mm x 75 mm, size) with no scribe were carried out in

accordance with ASTM B 117, using a 5 wt% NaCl solution at 35°C.

Results and Discussion

PIA-modified CS Polymers

To obtain information on the changes in the molecular conformation of the CS polymer brought about by varying the CS/PIA ratio at 200°C, we investigated the FT-IR spectra of CS/PIA samples with ratios of (a) 100/0, (b) 0/100, © 30/70, (d) 50/50, (e) 70/30, and (f) 80/20. Fig. 1 gives the FT-IR spectra for these samples over the frequency range from 2000 to 1000 cm^{-1}. The unmodified CS samples (a) had the following absorption bands: at 1702 cm^{-1}, revealing the stretching vibration of the carbonyl, C=O, group; at 1619 cm^{-1}, which can be ascribed to the N-H bending mode in the primary amine, NH_2, group; at 1402 cm^{-1}, reflecting the $-NH_4^+$ band from the ammonium chloride salt, $NH_4^+Cl^-$; and also at 1155, 1072, and 1020 cm^{-1}, corresponding to the stretching vibration of C-O-C linkages in the glucosamine rings. This spectrum also showed that there was no band related to the amide group in the partially N-acetylated CS,

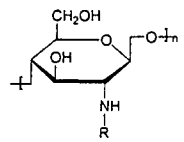

, where R is $-COCH_3$ and -H. Since the CS includes ~ 20 % N-acetyl-D-glucosamine , this result seems to suggest that the acetyl groups, CH_3OC-, were removed from the N-acetyl-D-glucosamine by HCl-catalyzed hydrolysis, followed by heat treatment at 200°C, thereby introducing the acetic acid and ammonium chloride derivatives into the CS polymers. These derivatives may be formed by the following hypothetical diacetylation pathways [5]:

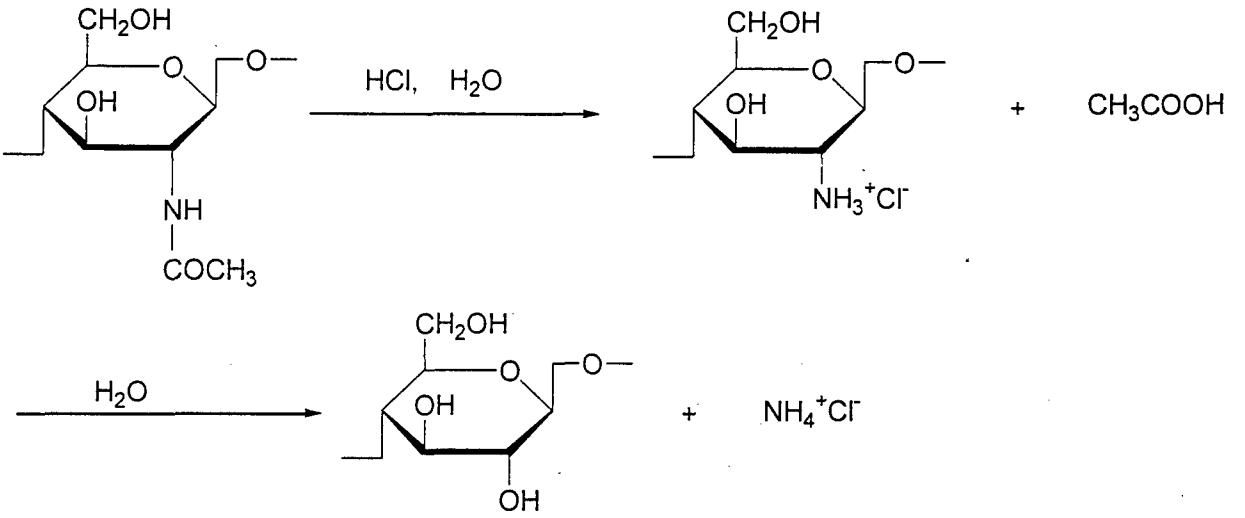

If such chemical structural changes take place, the molecular structure of the deacetylated CS can be illustrated as follows:

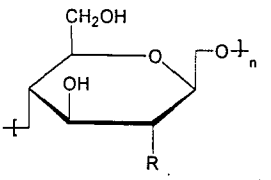

Where R is NH_2 or OH

The spectral feature of bulk PIA polymer (b) revealed that some of the carboxylic acid, -COOH, groups were transformed into acid anhydride groups by heating at 200°C. In fact, two absorption bands at 1852 and 1780 cm^{-1} reflected the stretching vibration of C=O in the itaconic anhydride group, while the band at 1191 cm^{-1} reflected the C-O-C linkage in this group. On the other hand, the frequency at 1776 cm^{-1} is associated with the C=O stretching vibration in the -COOH group, and the C-H bending modes of methylene and methyl groups in the PIA are identical to the bands at 1450 and 1392 cm^{-1}, respectively. No specific spectral feature was observed from sample (c) with CS/PIA ration of 30/70; namely, it included almost all the peaks associated with the 100/0

and 0/100 ratio samples. When 50 % by weight of the total amount of PIA was displaced by CS, the resulting spectrum (d) indicated the appearance of two new bands at 1648 and 1512 cm^{-1}. The former band is likely to be associated with the amide I (stretching vibration of carbonyl group, C=O) [6]. If this interpretation is valid, the latter band is due to the amide II (bending vibration of secondary amine group, NH). As seen in spectrum (e) of the 70/30 ratio sample, further replacement of the PIA by CS resulted in the growth of these bands. As expected, these bands became the prominent ones in the 80/20 ratio samples (f). A possible explanation for the formation of secondary amide group, -CO-NHR-, was that the NH_2 group in the CS reacts with the COOH group in the PIA, so forming the amide bond as the reaction product that links directly the PIA to the CS.

To support this information, additional experimental work was conducted by inspecting the XPS N_{1s} core-level excitation for the 200°C-heated film surfaces with CS/PIA ratios of (a) 100/0, (b) 80/20, (c) 70/30, (d) 50/50, and (e) 30/70 (Fig. 2). The films were deposited onto the Al substrate surfaces using the coating technology described in the experimental methods section. In this core-level spectrum, the scale of the binding energy (BE) was calibrated with the C_{1s} of the principal hydrocarbon-type carbon peak fixed at 285.0 eV as an internal reference standard. A curve deconvolution technique, using a DuPont curve resolver, was employed to substantiate the information on the nitrogen-related chemical states from the spectra of the nitrogen atoms. The N_{1s} spectrum (a) of the 100/0 ratio film surfaces was a symmetrical feature with a peak at the BE position of 399.8 eV, belonging to the N in primary amine [7]. When 10 % by weight of the total amount of CS was substituted for PIA, the major characteristic of the curve (b) was the emergence of new shoulder peak at 401.2 eV, revealing the N originated from the amide group [8]. The changes in its feature caused by a further substitution are as follows; in particular, there was (1) an increased intensity of the amide N signal at 401.2 eV and (2) a striking attenuation of the amine N peak at 399.8 eV. These data strongly supported the results from the FT-IR study; namely, the amine groups in CS had a strong chemical affinity for the carboxylic acid groups in PIA and formed amide linkages as the reaction product that acts to promote the branching of PIA onto the CS and to generate crosslinks between the two liner CS

conformation of PIA-linked CS can be represented in three reaction schemes (Fig. 3). Schemes No. 1 and 2 are characterized by representing a branching structure of PIA onto the liner CS polymer, and the scheme No.3 represents a cross-linking structure by PIA, which connects the two linear CS polymer chains.

One concern in applying natural polymer-based coating films as corrosion-preventing barriers to the metal surfaces was the fact that they absorb a large amount of atmospheric moisture. Such a hydrophilic property, which allows water to infiltrate the film easily, is an undesirable factor in coating materials used to mitigate corrosion of the metals. Hence, considerable attention was paid to the effectiveness of PIA in reducing the uptake of the moisture by CS. In this study, the 200°C-treated PIA-modified and unmodified CS polymer films were exposed for 24 hours in an environmental chamber under 70 % relative humidity (R.H.) at 25°C, and then they were examined by TGA to gain the information on the extent of moisture uptake. Fig. 4 depicts the TGA curves of CS/PIA 100/0 and 90/10 ratio films. The curve (bottom) for the 100/0 ratio showed a certain amount of weight loss between 25 and 250°C, followed by large reduction in the temperature range of 250 to 450°C. It is believed that the weight loss occurring at temperatures up to 250°C is due mainly to the removal of all the moisture adsorbed to the film samples. Correspondingly, the thermal decomposition of CS seems to take place at temperatures of > 250°C. As a result, the weight loss of CS films by dehydration was a 5.5 %, implying that this film adsorbed this amount of moisture during exposure to 70 % R.H.. By comparison, the uptake of moisture by a 10 wt% PIA-modified CS film (top) was only 1.6 wt%, corresponding to ~ 29 % lower than that of the unmodified CS. This fact strongly verified that PIA greatly reduces the uptake of moisture by CS. Figure 5 shows the changes in its uptake estimated from the TGA curve as a function of the proportion of CS to PIA. A given result showed that the uptake was markedly reduced as the CS/PIA ratio declined from 100/0 to 70/30. The total adsorbed moisture of 1.4 wt% for the 70/30 ratio film was ~ four times lower than that of the bulk CS film (100/0 ratio); beyond this, a further decrease in the CS/PIA ratio caused an increase in its moisture uptake. Thus, both the bulk CS and PIA films with a high uptake of > 3.5 wt% appear to be highly susceptible to the absorption of moisture. In contrast,

the 80/20 and 70/30 ratio films had uptakes of less than 1.5 wt%, inferring that a proper proportion of CS to PIA plays an important role in mitigating the magnitude of sensitivity to moisture. In other words, the hydrophilic NH_2 groups present in the CS may react with hydrophilic carboxylic acid groups in the PIA to yield hydrophobic amide bonds as reaction products, so promoting the degree of PIA grafts on the CS, and also the extent of crosslinking between the two liner CS chains by PIA.

In trying to further support this information, the extent of wettability of these film surfaces by water was estimated by determining the contact angle of a water droplet on their surfaces. If the contact angle was low, it was concluded that the film surfaces are susceptible, allowing moisture to infiltrate them easily; in the worst case, such seepage may cause hydrolysis-induced decomposition of the films. In this study, the contact angle was measured on the surfaces of the films made with the various different CS/PIA ratios before and after immersing them for up to 20 days in the water at 25 °C. A plot of the average value of the advancing contact angel, θ, (deg.), for the various CS/PIA ratio film surfaces as a function of immersion time is shown in Fig. 6. For unimmersed films, the resultant θ-ratio data exhibited that the θ value of the bulk CS film (100/0 ratio) was considerably enhanced as it was modified with PIA, especially in the CS/PIA ratio range of 100/0 to 70/30. The 80/20 ratio film had the highest θ value of 75°, corresponding to ~ 4 times greater than that of the bulk CS. Further incorporation of PIA into the CS caused a declining θ value, taking as evidence that films with a lower sensitivity to moisture could be prepared by incorporating a proper amount of PIA into the CS. Thus, this finding substantially supported the earlier TGA results on the uptake of moisture by the films; namely, an increase in the degree of grafting and crosslinking provides film surfaces that are less sensitive to moisture. In other words, the hydrophilic characteristics of the individual CS and PIA films are converted into the hydrophobic ones by the grafting and crosslinking reactions between them, inferring that the PIA-grafted and -crosslinked CS films with a suitable proportion of CS to PIA will contain a minimal number of hydrophilic carboxylic acid and amine groups. The major factor governing this conversion is the formation of amide bonds yielded by the grafting and crosslinking reactions, conferring less wettability by water over the film's surfaces. No

significant change in the contact angle was observed from the 80/20 and 70/30 ratio film surfaces in the first 10 days of exposure. When the immersion time was extended to 20 days, the θ value for these films slightly decreased. By comparison, the other films tend to show a declining θ value with increasing exposure time; in particular, both the bulk CS and PIA films were hydrolyzed during a 10-day exposure to water.

Emphasis was next directed towards determining the characteristics of the PIA-grafted and -crosslinked CS coating films deposited onto the Al substrate surfaces. The specific characteristics to be investigated were the chemistry at the interfaces between the film and Al, and also the effectiveness of the coating films in protecting the Al against corrosion. One of the indispensable factors in a good protective performance of coatings is the bonding of the grafted and crosslinked CS to the Al, so that it is very important to identify the bond structure at the interfaces between CS and Al. If there are no interfacial bonds, the moisture permeated through the coating may cause the generation of blisters, promoting the rate of delamination of the coating films from the Al substrates. To gain this information, we inspected the XPS C_{1s} and O_{1s} core-level excitations for three coating films with CS/PIA ratios of 100/0, 70/30, and 0/100 deposited onto the Al. These samples were prepared in the following manner: The Al substrates were dipped into these solutions, and then, the solution-covered substrates were dried for 1 hour in oven at 80°C to form a water-soluble xerogel film. Most of the xerogel films were removed from the Al surfaces by immersing them in deionized water; subsequently, the film-devoid Al side was dried for 1 hour in N_2 gas at 200°C for XPS examination. Fig.7 compares the C_{1s} core-level spectral features for these film-devoid Al surfaces. The C_{1s} region of the interfacial Al surfaces (a) in the 100/0 ratio coating system had the two resolvable Gaussian components at the BE positions of 285.0 and 288.0 eV. The principal peak at 285.0 eV is related to the C in the CH_2 and CH groups as the major component present at the outermost surface site. The weak signal, emerging at 288.0 eV, originates from C in the C=O groups [9]. There is no peak around 286.5 eV that would correspond to the chemical components of CS, such as the C in $-CH_2O-$ (e.g. hydroxide and ethers) and in the C-N bond [10]. This finding seems to suggest that these carbon species detected on the interfacial Al surfaces are assignable to organic contaminants. Thus, the

amount of CS film remaining on the Al is very little, if any, implying that a water-soluble CS does not bond to the Al surface. The feature of the curve taken from the 70/30 ratio film-devoid Al surfaces differed from that of the 100/0 ratio one; there was the incorporation of two new signals at 289.5 and 288.6 eV into the curve. The former signal reveals the C in the carboxylic acid, COOH, group of PIA [10], and the latter one which is situated between the C=O and the COOH peaks may belong to the C in the -COO-metal complexed conformation [11, 12]. Since the source of metal arises from the Al substrate, a possible interpretation for this complex is that the functional COOH groups in the PIA have a strong chemical affinity for the Al substrates to yield the linkages between the PIA and the Al metal. It is well known that when the Al_2O_3 layer existing at the outermost surface site of the Al metals comes in contact with water, it can be hydrated and converted into the hydrous Al oxides such as AlOOH and $Al(OH)_3$ [13-15]. Thus, the interaction between the COOH and the hydroxdylated Al may occur through the Lewis acid-base reaction pathways; there is , -COOH (proton donor) + HO-Al surface (proton acceptor) → -COO^-----^+H_2O-Al → -COO-Al linkage, in terms of interfacial covalent oxane-bond structure, that might lead to the formation of water-insoluble PIA at the interfacial boundary regions. To ascertain whether the -COO group covalently linked to the Al, the aluminum acrylate, Al $(H_2C=CHCOO)_3$, as the reference compound, was inspected by XPS. The resulting data revealed that the excitation of the peaks at 288.5 eV in the C_{1s} region and at 531.2 eV in the O_{1s} region, corresponding to the C and O originating from the -COO-Al linkage with the O-Al covalent bond. Thus, it is reasonable to assume that the interfacial reaction products containing the -COO-Al linkage might have a hydrophobic characteristic. As expected, the C_{1s} spectrum of the 0/100 ratio film-devoid Al surfaces indicated a striking growth of the signal intensity at 288.6 eV, reflecting an extensive -COO-Al linkage. This strongly demonstrated that a large amount of PIA adhering to the Al remains at the outersurface site of the substrates. To support this information, we inspected the O_{1s} core-level excitation of these samples (Fig. 8). The spectrum (a) of the 100/0 ratio-devoid Al sample showed the feature of a symmetrical single peak film at 532.0 eV, belonging to Al in the Al_2O_3 [17]. By comparison, the O_{1s} region of the 70/30 ratio film-devoid Al (b) included two additional shoulder peaks at 532.7 and 531.4 eV, while the Al_2O_3 signal at 532.0 eV retained as the major peak. Regarding the two new signals, the literature [18, 19]

suggested that the signal at 532.7 eV is related to O in the carboxylate and hyroxyl groups, while the other at 531.4 eV originates from the metal-bound O in the -COO-metal linkage. The intense signals of these new peaks can be seen in the O_{1s} region of the 0/100 ratio film-devoid Al (c). These findings strongly supported the results from the C_{1s} core-level analysis; namely, the PIA in the modified CS polymer favorably reacts with the Al substrate surfaces and diffuses over them to form a water-insoluble PIA-linked Al structure.

The integration of all the data was correlated directly with the effectiveness of PIA-grafted and -crosslinked CS films in mitigating corrosion of the Al substrates. Using a surface profile measuring system, the thickness of the 100/0, 90/10, 80/20, 70/30, 50/50, 30/70, and 0/100 ratio films was ~ 1.6, ~ 0.8, ~ 0.5, ~ 0.42, ~ 0.36, ~ 0.2, and ~ 0.24 μm, respectively. No experimental work was made to determine the changes in viscosity of the solution as a function of CS/PIA ratio. However, the viscosity of the solution seems to rise when this ratio was increased, implying that the solution made with a higher CS/PIA ratio leads to the fabrication of a thicker coating film. Although intuitively a thicker coating film may be expected to have a better corrosion-protective performance than a thin one, AC electrochemical impedance spectroscopy (EIS) was used to evaluate their effectiveness as corrosion-preventing barriers. On the overall Bode-plot curves [the absolute value of impedance $|Z|$ (ohm-cm^2) vs. Frequency (Hz)], (not shown), our particular attention was paid to the impedance value in terms of the pore resistance, Rp, which can be determined from the plateau in the Bode plot occurring at a sufficiently low frequency of 5×10^{-2} Hz. Fig. 9 illustrates the plots of Rp of films versus the CS/PIA ratios. The Rp value (not shown) of the uncoated bare Al substrate was ~ 5.0×10^3 ohm-cm^2. Once the Al surfaces were coated with the single CS and PIA polymers, or PIA-modified CS polymers, the Rp value was increased by one or two orders of magnitude over that of the substrate. The Rp value of the unmodified single CS coating denoted as 100/0 ratio was 1.5×10^5 ohm-cm^2. When a 10 % of the total amount of CS was replaced by PIA, this value rose ~ three times to 4.3×10^5 ohm-cm^2 . With further substitution, the value of Rp increased: The 80/20 ratio coatings with the film thickness of ~ 0.5 μm had the highest Rp of 1.2×10^5 ohm-cm^2 in this coating series, corresponding to an order of magnitude greater than that of an unmodified CS

coating with the highest film thickness of ~ 1.6 μm. However, the coatings made by incorporating an excessive amount of PIA into CS showed a declining Rp value . In fact, the Rp value of the 70/30 ratio coating dropped ~ 27 % to 8.8 x 10^5 ohm-cm^2. As expected, the bulk PIA coating (0/100 ratio) had the lowest Rp value of 8.0 x 10^4 ohm-cm^2. Since the Rp value reflects the magnitude of ionic conductivity generated by the electrolyte passing through the coating layers, a higher value signifies a low degree of penetration of electrolyte into the coating films. Thus, the PIA-grafted and -crosslinked CS polymer conformation offers an improved performance in minimizing the rate of permeation of electrolytes through the coating layers, compared with those of the individual CS and PIA coatings. Hence, it was believed that a grafted and crosslinked polymer structure would lead to a lower rate of the uptake of electrolytes by the coatings. The data also revealed that the changes in the magnitude of conductivity depend on the CS/PIA ratio. Comparing the Rp values, the effectiveness of these ratios in ensuring a low degree of electrolyte infiltration was in the following order; 80/20 > 70/30 >50/50 > 90/10 > 30/70 > 100/0 > 0/100. The most effective coating system was the 80/20 ratio.

Fig. 10 represents the changes in Rp at 5 x 10^{-2} Hz for the coating specimens as a function of exposure times of up to 80 days in a water at room temperature. In the first ten days of exposure, four coating systems, 90/10, 80/20, 70/30, and 50/50 ratios, showed no significant changes in Rp value, compared with that of the unexposed ones. Afterwards, their Rp values, except for the 80/20 ratio coating, fell with increasing exposure time. Despite a long exposure for 20 days, the Rp value of the 80/20 ratio specimens was almost the same as that at 10 days, suggesting that the magnitude of susceptibility of this coating to the hydrolysis during its immersion in water is less than that of all the other coatings. However, the Rp value-exposure time relation revealed that when exposure was prolonged for > 20 days, the Rp value gradually fell with increasing exposure time, inferring that extending the exposure period promotes the uptake of more electrolytes by the coatings. After exposure for 80 days, only the 80/20 ratio coating still maintained an Rp > 10^5 ohm-cm^2 . The second highest Rp value was found in the 70/30 ratio films. In contrast, the rate of its uptake for the three coating specimens, 30/70, 100/0, and 0/100 ratios, was considerably higher than that of the 80/20 and 70/30 ratio coatings; in fact,

their Rp values after 80 days exposure were in the order of 10^3 ohm-cm^2 . In particular, the Rp value of the 0/100 ratio coating specimens sharply dropped to 4.0 x 10^3 ohm-cm^2 during exposure for 20 days from the 8.0 x 10^4 ohm-cm^2 , no further exposure was made because the Rp at this level is mainly due to the anodic etching of the underlying Al. In fact, pitting due to the local corrosion of Al caused by the failure of the coating was visually observed in these specimens.

This information on the EIS was supported by the findings from salt-spray resistance tests for the coated panels (Table 1). A trace of corrosion products was generally looked for in evaluating the results. These findings were reported as the total exposure time at the date of the generation of the rust stain on the Al surfaces. As shown, the entire surfaces of the individual CS(100/0)- and PIA(0/100)-coated Al panels were corroded after exposure to the salt spray for 72 hours, corresponding to only 24 hours longer than that of the uncoated bare Al (not shown), suggesting that these coatings poorly protect Al against corrosion. By comparison, the PIA-grafted and -crosslinked CS coating systems were far better in reducing the rate of corrosion. With the 90/10 ratio, the resistance to salt spray was extended ~ 7 times to 480 hours. A further improvement was observed with coatings containing increased concentrations of PIA, signifying that an increase in the degree of the grafting and crosslinking of PIA onto the CS improves the resistance to corrosion. In fact, coatings made from the 80/20 ratio protected Al against corrosion for 694 hours. However, adding an excessive amount of PIA to the CS resulted in a less effectiveness in mitigating the corrosion of Al; the salt-spray resistance of the 30/70 ratio coatings was only 192 hours.

Implicating this finding with the data on the FT-IR, TGA, XPS, and contact angle, three factors played a key role in conferring resistance to metal corrosion: First was the polymer's conformation containing amide bonds formed by the grafting and crosslinking reactions between the carboxylic acid groups in PIA and NH_2 groups in CS; second was the lesser susceptibility of the coating films to moisture due to the enhanced degree of grafting and crosslinking, together with a minimal amount of hydrophilic unreacted COOH in PIA and NH_2 in CS; and, third was

the interaction of the COOH groups in the PIA-grafted CS polymers with the hydroxylated Al metal surfaces to form an interfacial covalent oxane-bond structure, such as -COO-Al linkages.

Conclusion

Partially N-acetylated chitosan (CS) biopolymer consisting of ~ 80 % poly(D-glucosamine) and ~ 20 % poly(N-acetyl-D-glucosamine) is a derivative of the polysaccharide chitin marine biopolymer, which originates from the structural components of crustaceans, such as shrimp, lobster, and crab, and is abundant, comparatively inexpensive, and relatively stable in quality. In seeking ways of applying the CS biopolymer as renewable resource to an environmentally green water-based coating system for the aluminum (Al) substrates, emphasis was directed towards its molecular modification with poly(itaconic acid) (PIA), which is among the synthetic polyacid electrolytes. Adding a certain amount of HCl to the CS in aqueous medium not only enhances its solubility, but also served to remove acetyl groups from the linear CS polymer structure. The primary amine, NH_2, groups in the deacetylated CS, is polybase electrolyte having a highly positive charge density. The carboxylic acid, COOH, groups in the PIA had a strong chemical affinity for the basic NH_2 groups in the CS and formed secondary amide linkages that grafted the PIA polymer onto the linear CS chains and crosslinked between the CS chains, when mixtures of these two aqueous solutions were heated at 200°C in air. An increase in the degree of grafting and crossliking provided the formation of the coating films that are less susceptible to moisture and to the infiltration of corrosive electrolyte species in the coating layer, conferring good protection of Al metal against corrosion. However, incorporating an excessive amount of PIA into the CS created undesirable features as the anti-corrosion barriers, leading to a high degree of wettability and moisture absorption of coating surfaces, and also an enhanced magnitude of ionic conductivity caused by electrolytes passing through the coating layers. These negative factors were due primarily to the persistence of a certain amount of unreacted hydrophilic PIA and CS polymers in the coating films. In addition, the surfaces of Al substrate preferentially reacted with the PIA, rather than the CS. This interfacial interaction could be accounted for by the formation of -COO-Al metal linkages by the acid-base reaction between the COOH groups (proton donor) in the PIA and the OH groups (proton acceptor) on the

hydroxylate Al surfaces. The coating films made with the CS/PIA 80/20 ratio precursor solution had all the properties needed for use as a corrosion-preventing barrier. In fact, this coating film, deposited on the Al surfaces had a lesser sensitivity to moisture, and imposed pore resistance (in ohm-cm^2) of an order of magnitude higher than those of single CS and PIA coatings, and conferred salt-spray resistance for 694 hours.

References

1. S. Hiano, H. Inui, H. Kosaki, Y. Uno, and T. Toda, in C.G. Gebelein and C.E. Carraher, Jr. (Eds.), Biotechnology and Bioactive Polymers, Plenum Press, New York, 1994, p 43.

2. I. Gabrielii and P. Gtenholm, Proceedings of the ACS Division of Polymer Materials: Science and Engineering, 79 (1998) 459.

3. P.A. Sandford and A. Steinners, in S.W. Shalaby, C.L. McCormick and G.B. Butles (Eds.), Water-Soluble Polymers, ACS Symposium Series 467, Washington, DC. 1991 p. 430.

4. X. Ou, A. Wiren, and A. Albertson, Proceedings of the ACS Division of Polymeric Materials: Science and Engineering, 79 (1998) 242.

5. T. Sugama and M. Sheila, "Dextrine-Modified Chitosan Marine Polymer Coatings", J. Mater. Sci., (in press).

6. L.J. Bellamy, "The Infra-red Spectra of Complex Molecules", Chapman and Hall, London, 1975, p. 231.

7. D. Briggs, D.M. Brewis, and P. Knoieczko, J. Mater. Sci., 11 (1976) 1270.

8. K. B. Yatsmirshii, V.V. Nenoshalenko, V.G. Aleshin, Y.I. Bratushko, and E.P. Missenko, Chem. Phys. Lett., 52 (1977) 481.

9. A. Toth, I. Bertoti, T. Sgekely, J.N. Sazanov. T.A. Antonova, A.V. Shchukarev, and A.V. Grbanov, Surf. Interface Anal., 8 (1986) 261.

10. D. Briggs, D.M. Brewis, and P. Knoeczko, J. Mater. Sci., 14 (1977) 1344.

11. J.S. Hammond, J.W. Holubka, J.W. Devries, and R.A. Dickie, Corros. Sci. 21 (1981) 239.

12. L.J. Gerenser, In E. Sacher, J-J, Pireaux, and S.P. Kowalczyk (Eds.), Metallization of Polymers, ACS Symposium Series 440, Washington DC, 1990 p. 433.

13. G.D. Davis and J. D. Venables, in A.J. Kinloch (Ed.), Durability of Structural Adhesives, Applied Science, Essex. UK, 1983 p. 43.

14. D.A. Hardwick, J.S. Ahearn and J.D. Venables, J. Mater. Sci. 19 (1984) 223.

15. R.T. Foley, Corrosion, 42 (1986) 277.

16. J.C. Bolger, in K.L. Mittal (Ed.), Adhesion Aspects of Polymeric Coatings, Plenum, New York, 1983 p.3.

17. T. Tshckda and H. Takahashi, J. Mater. Res., 9 (1994) 2919.

18. D. Briggs and M.P. Seah, "Practical Surface Analysis by Auger and X-ray Photoelectron Spectroscopy", John Wiley & Sons, New York, 1985, p. 386.

19. B. Lindberg, A. Brendtson, R. Nisson, R. Nyholm, and O. Exner, Acta Chem. Scand. A32 (1978) 353.

Table 1. Salt-spray Resistance Tests for PIA-modified CS Coatings

CS/PIA ratio	Salt-spray resistance, hours
100/0	72
90/10	480
80/20	694
70/30	624
50/50	264
30/70	192
0/100	72

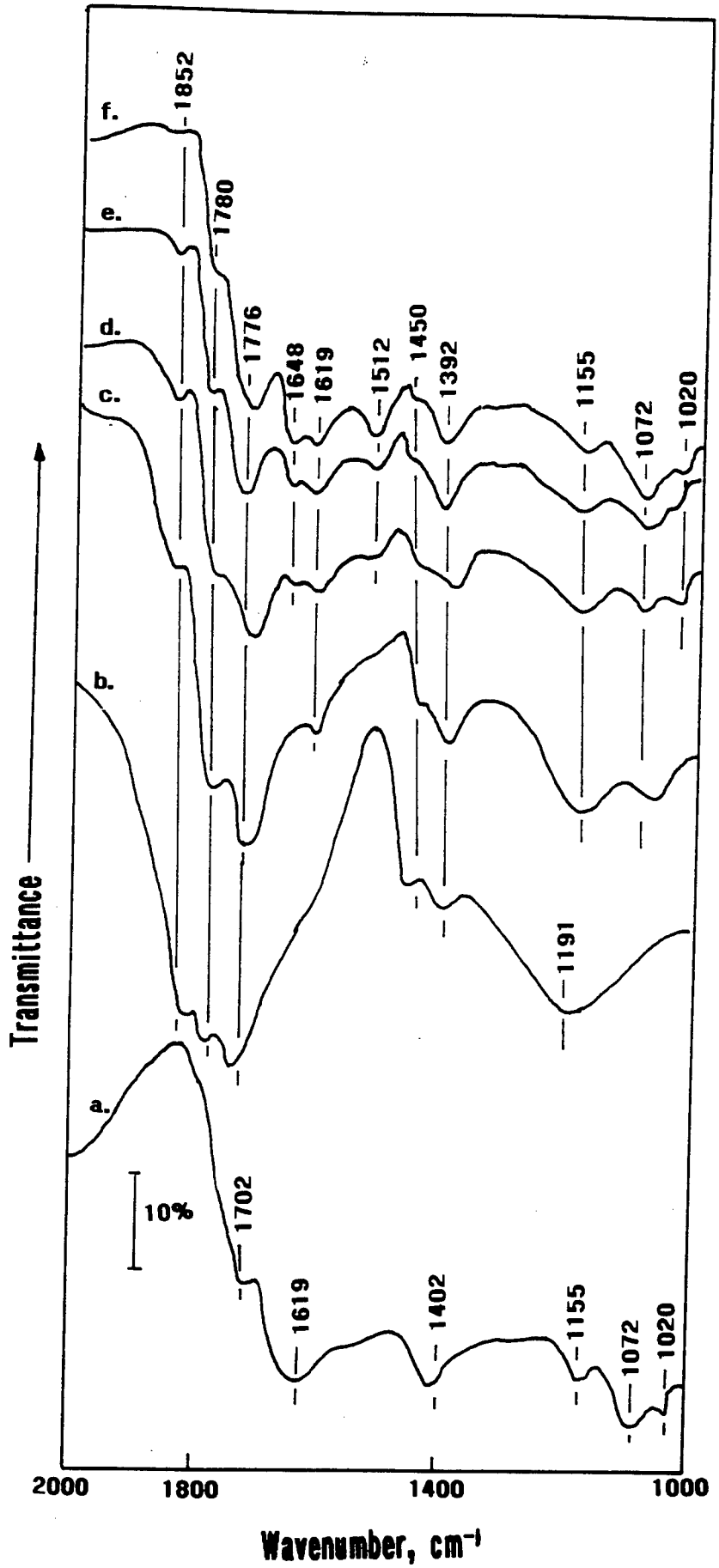

Fig. 1 FT-IR adsorption spectra for the polymer samples made with (a) 100/0, (b) 0/100, (c) 30/70, (d) 50/50, (e) 70/30, and (f) 80/20 CS/PIA ratios at 200°C.

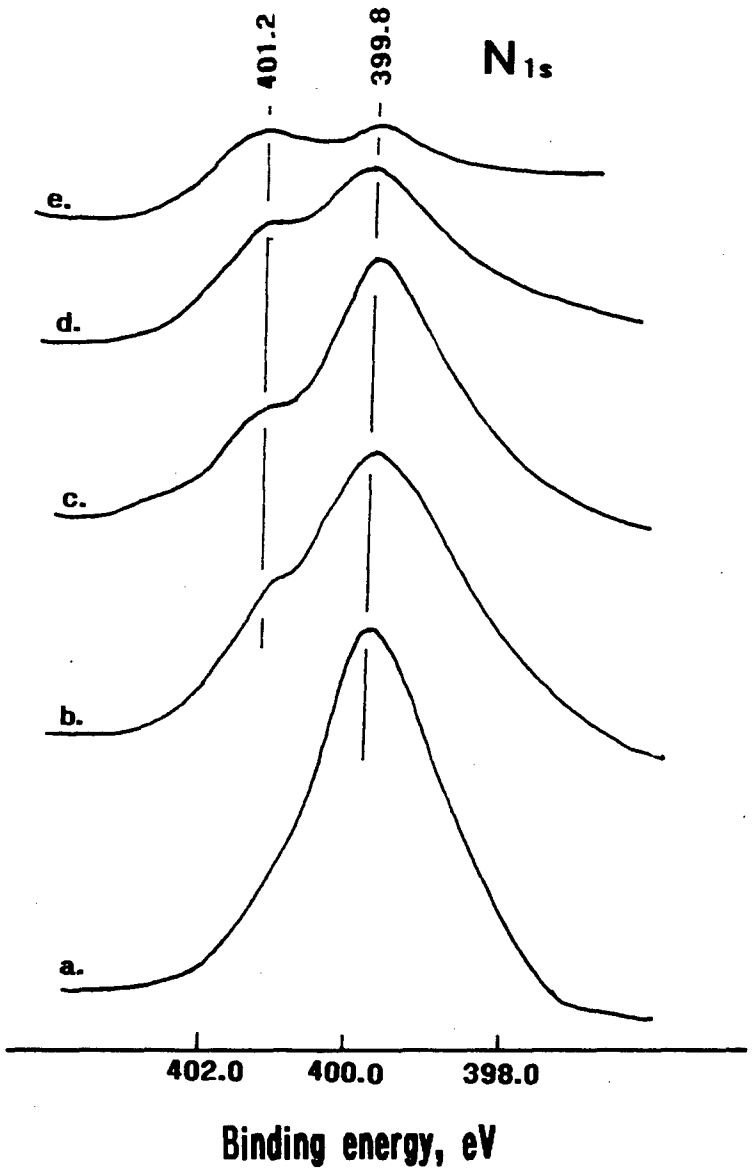

Fig. 2 N_{1s} core-level spectra for the 200°C-treated (a) 100/0, (b) 90/10, (c) 70/30, (d) 50/50, and (e) 30/70 ratio coating film surfaces.

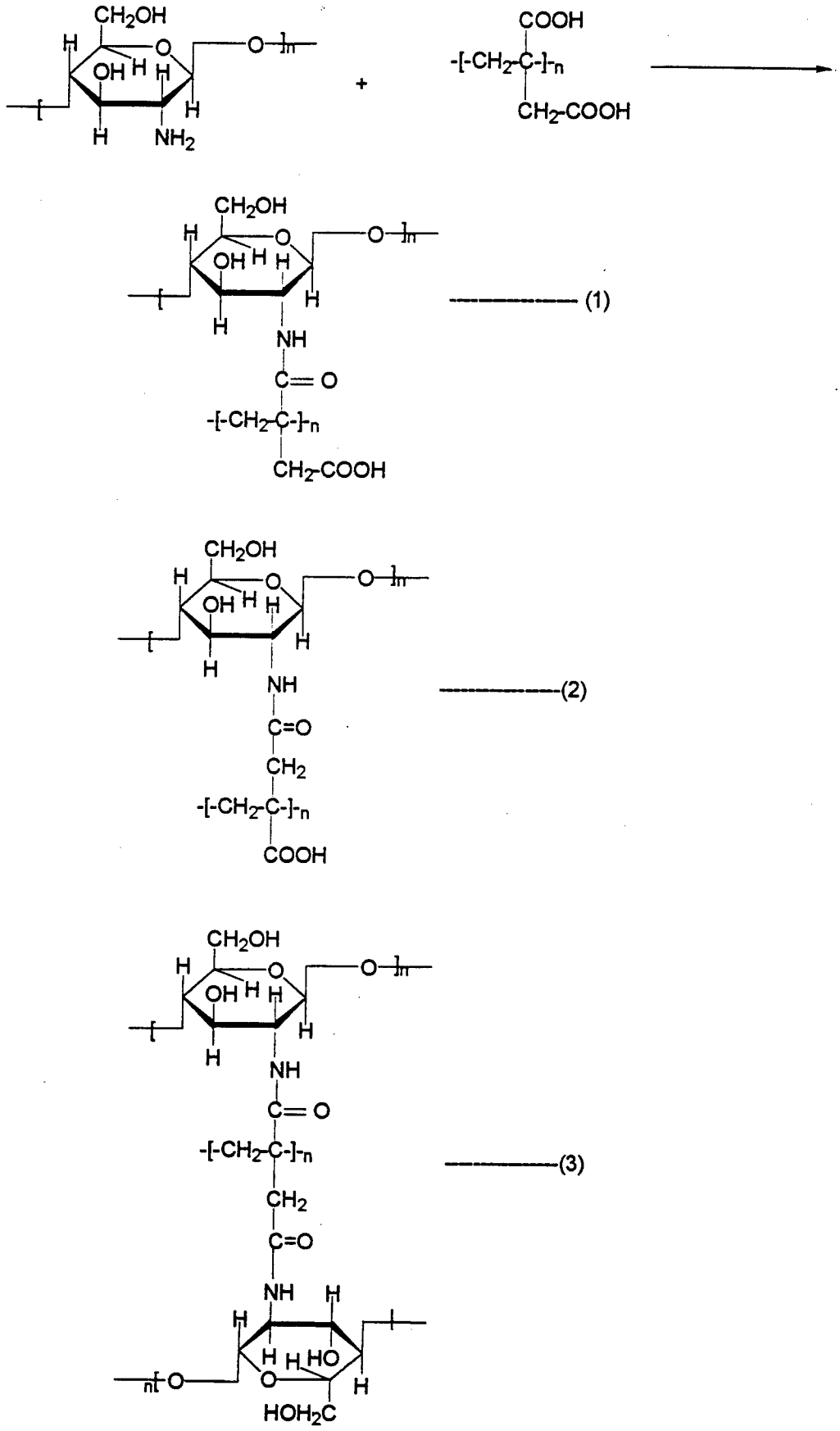

Fig. 3 Hypothetical reaction schemes between PIA and D-glucosamine.

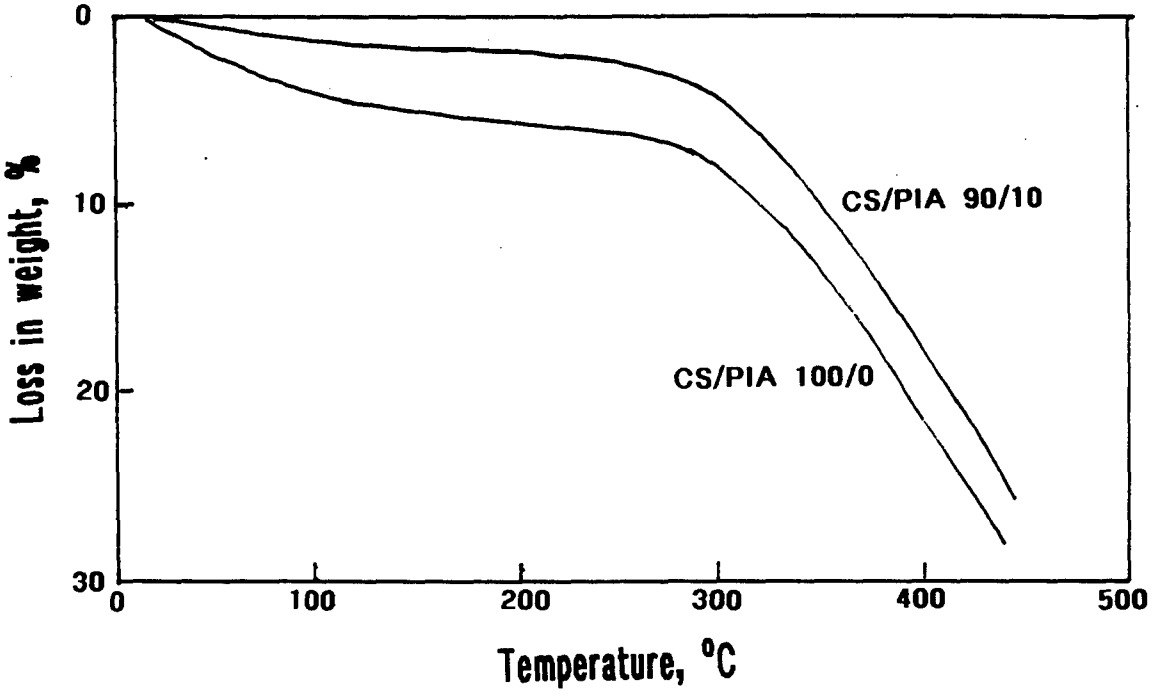

Fig. 4 TGA curves for the 100/0 and 90/10 ratio coating films after exposure for 24 hours in 70 % relative humidity at 25 °C.

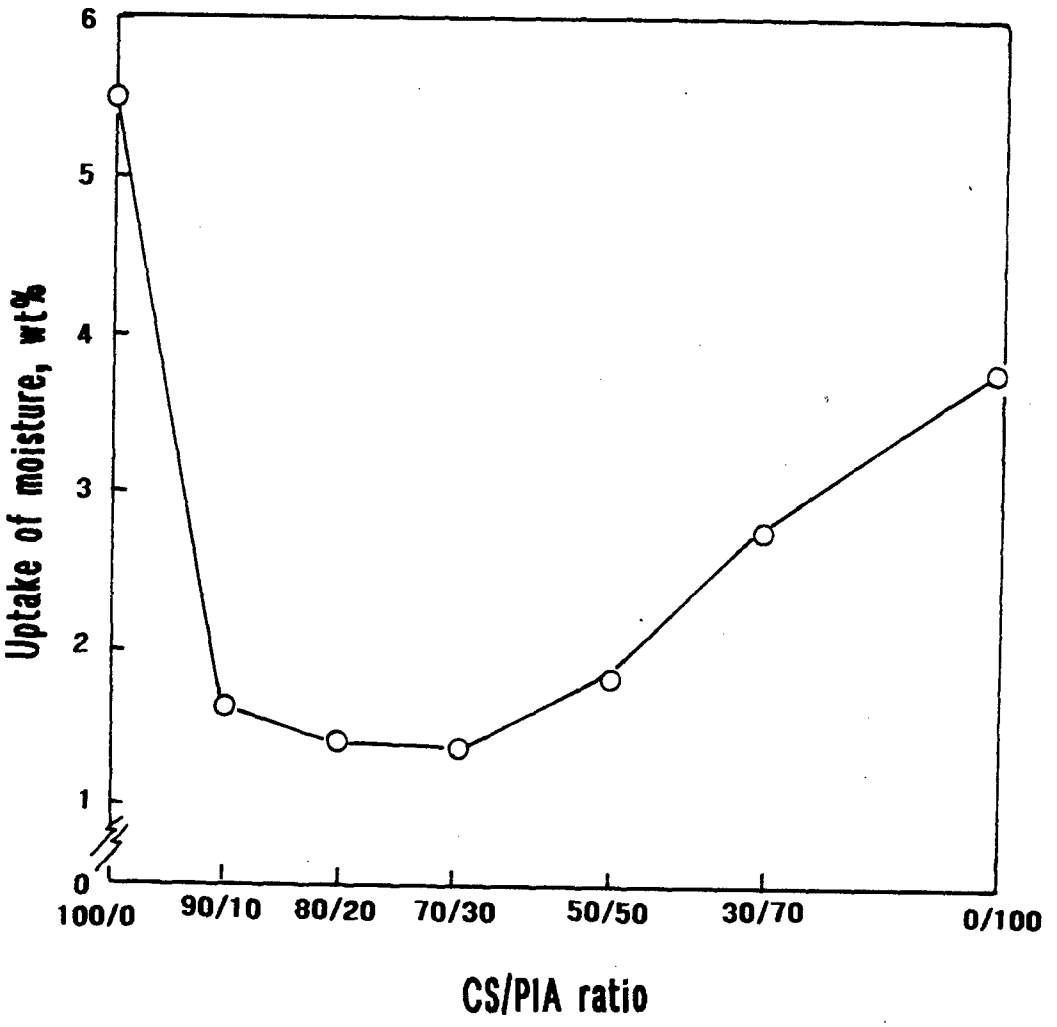

Fig. 5 Changes in the extent of moisture uptake by coating films as a function of CS/PIA ratios.

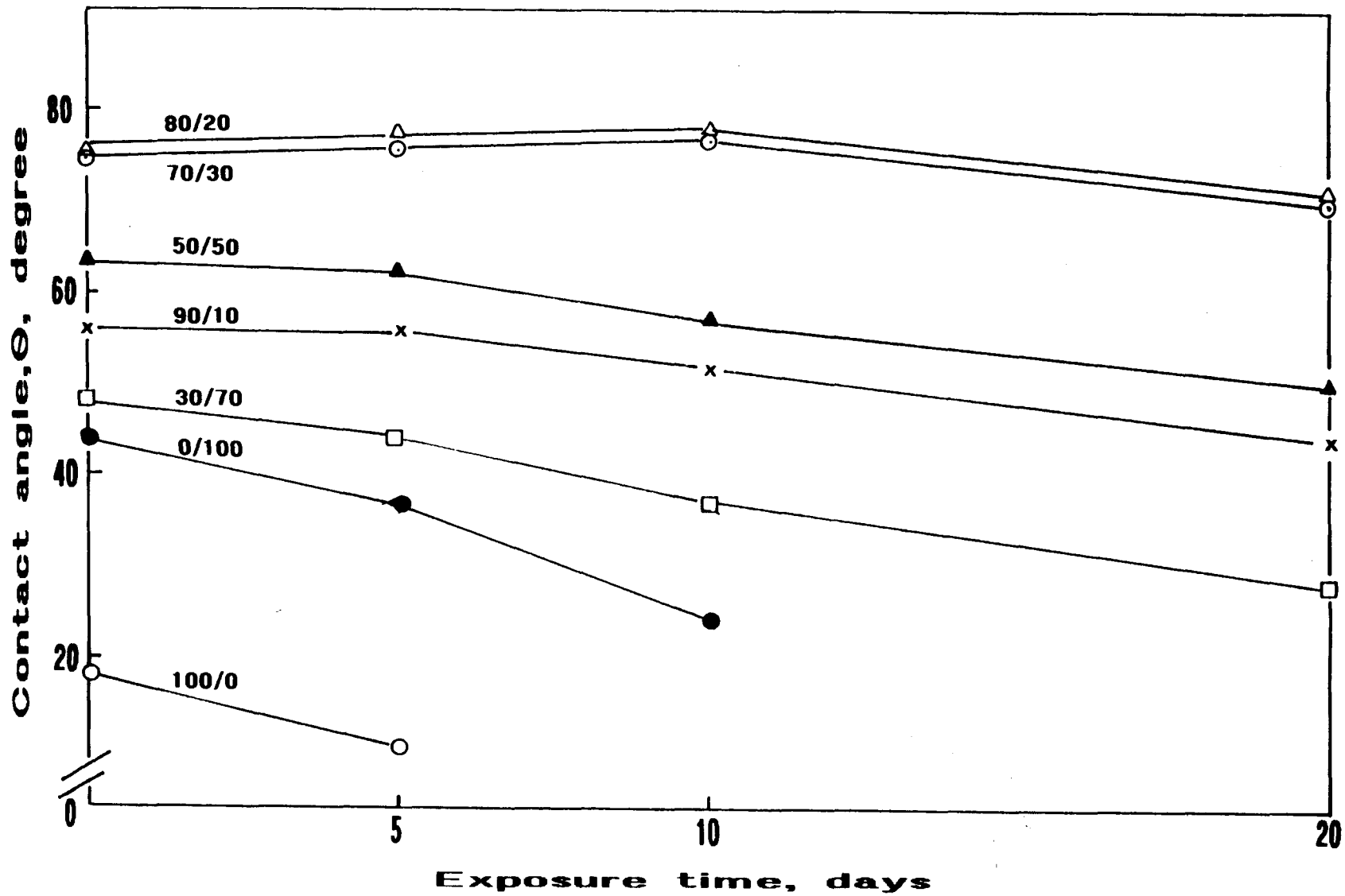

Fig. 6 Changes in contact angle of a water droplet on surfaces of coating films made with (∘) 100/0, (•) 0/100, (□) 30/70, (▲) 50/50, (⊙) 70/30, (△) 80/20, and (x) 90/10 ratios as a function of exposure time in water at 25 °C.

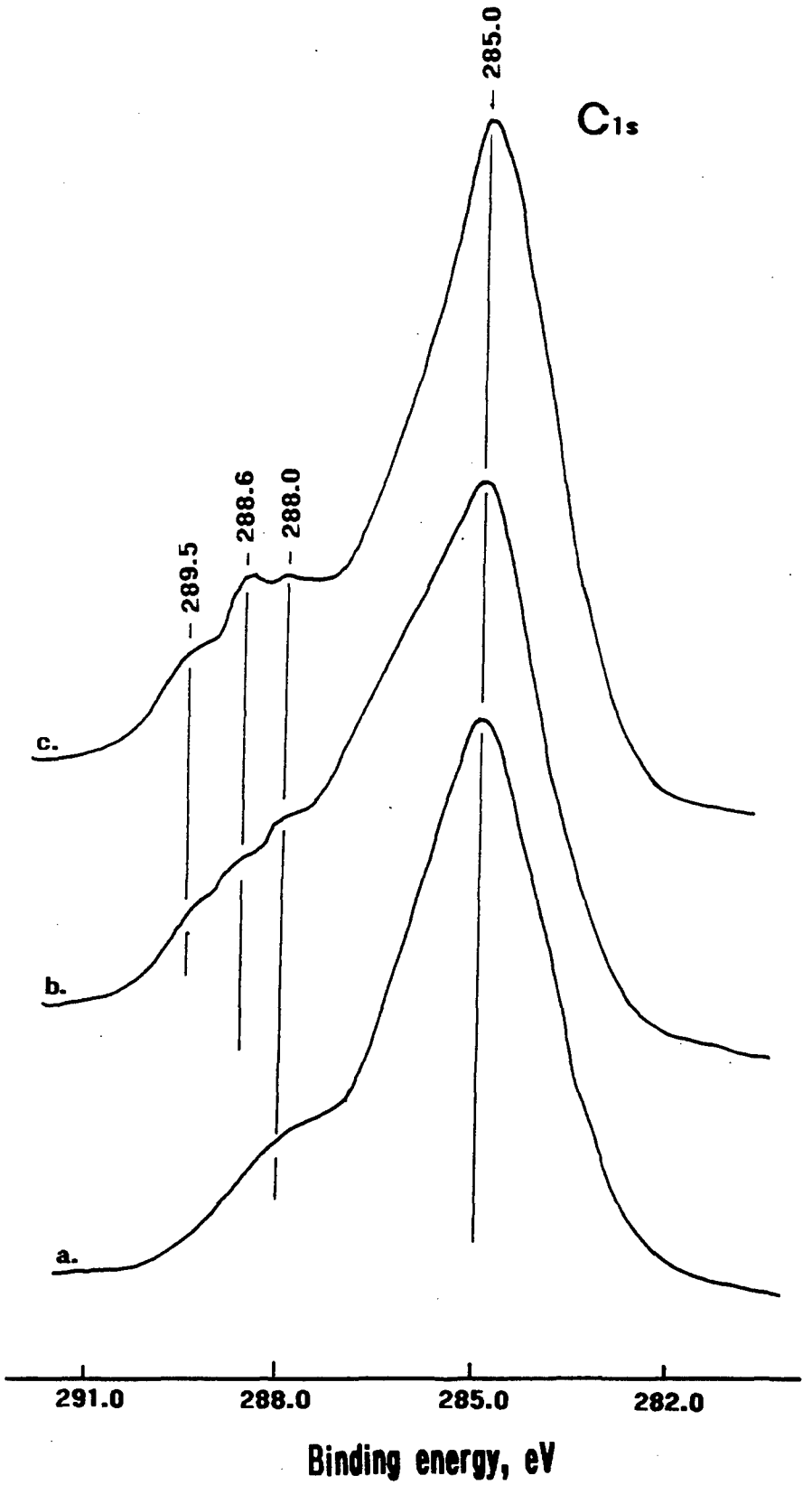

Fig. 7 C_{1s} core-level spectra for the (a) 100/0, (b) 70/30, and (c) 0/100 ratio film-devoid Al substrate sides.

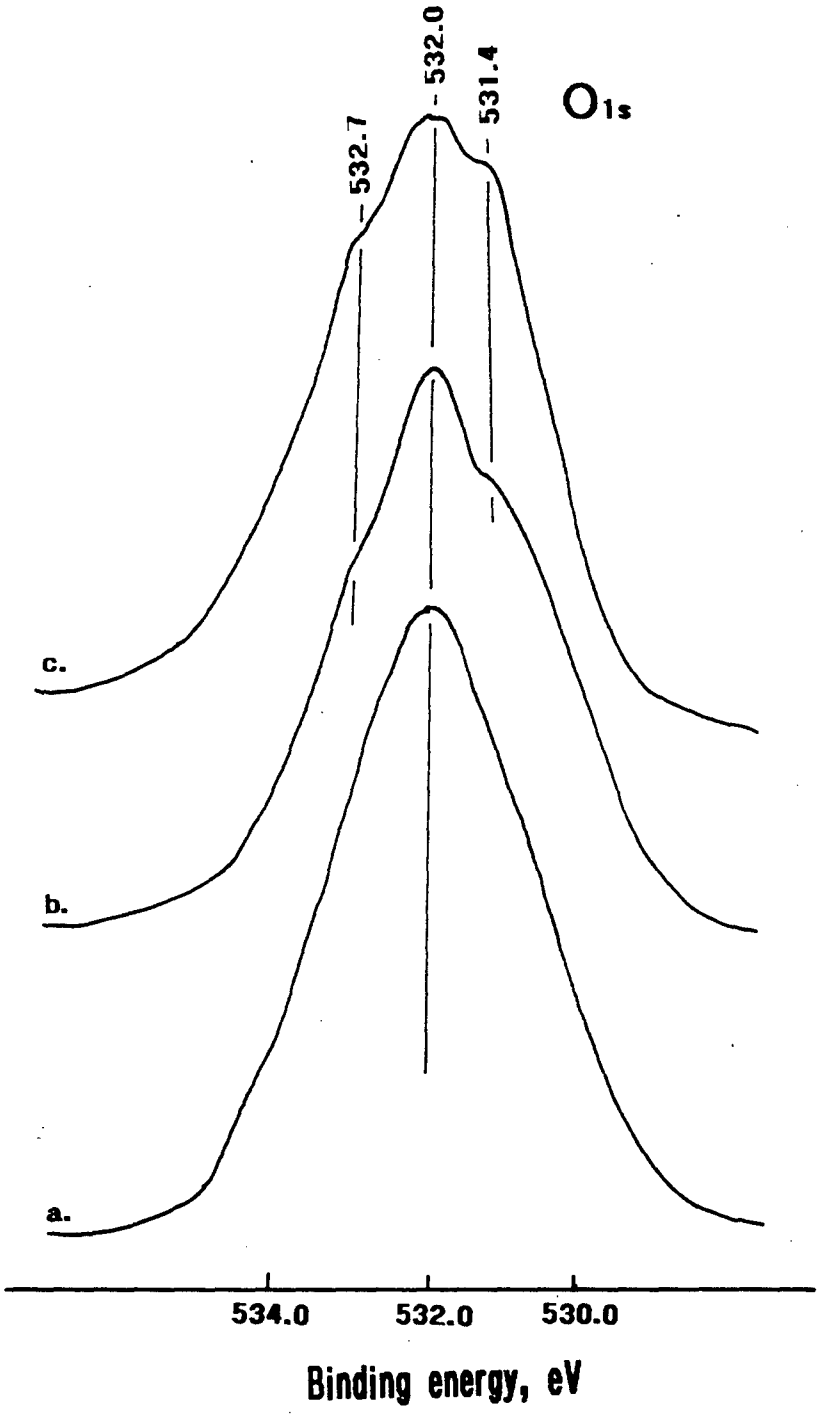

Fig. 8 O_{1s} region for the (a) 100/0, (b) 70/30, and (c) 0/100 ratio film-devoid Al substrate surfaces.

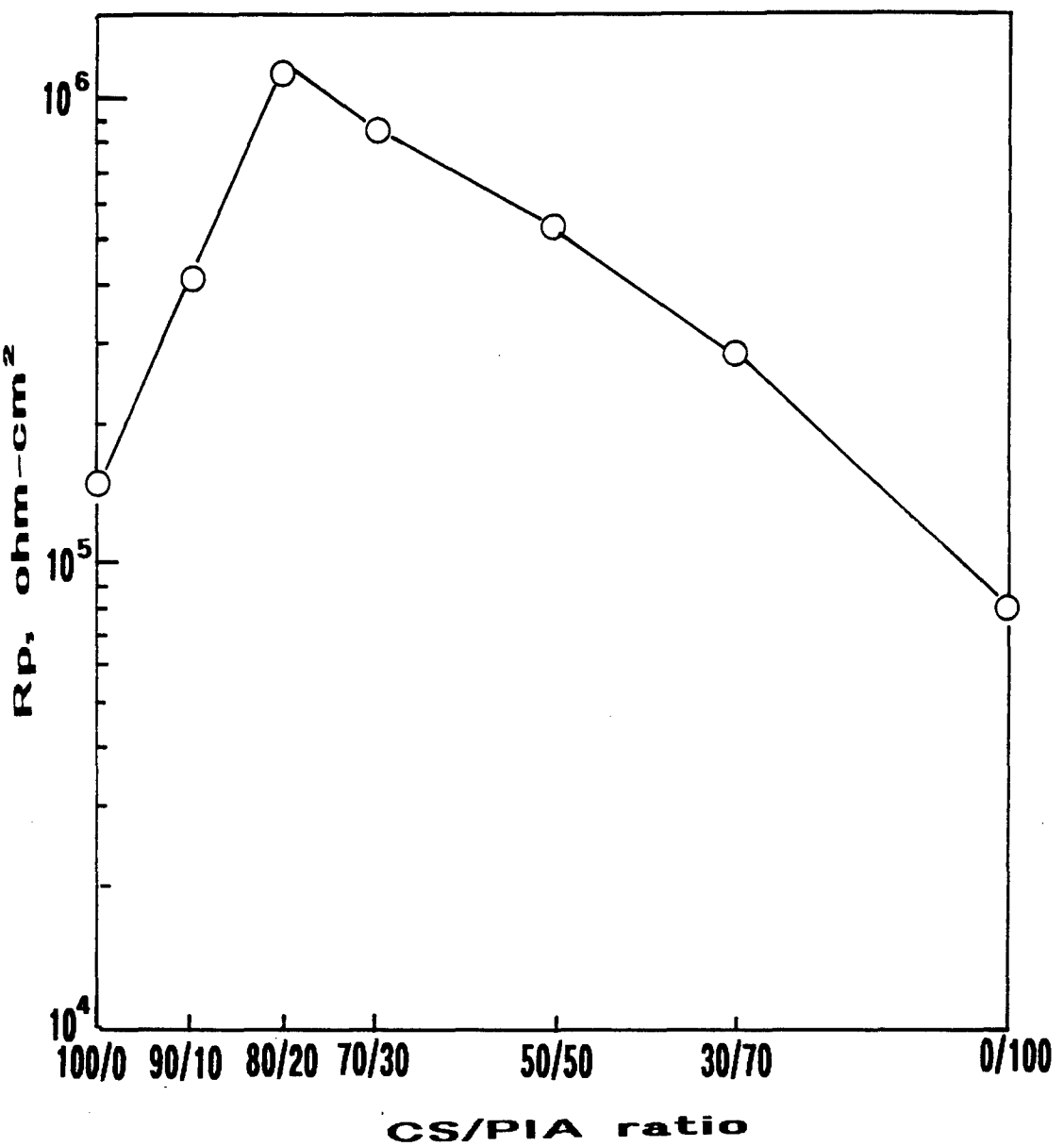

Fig. 9 Pore resistance, Rp, value of Al panel samples coated with 100/0, 90/10, 80/20, 70/30, 50/50, 30/70, and 0/100 CS/PIA ratios.

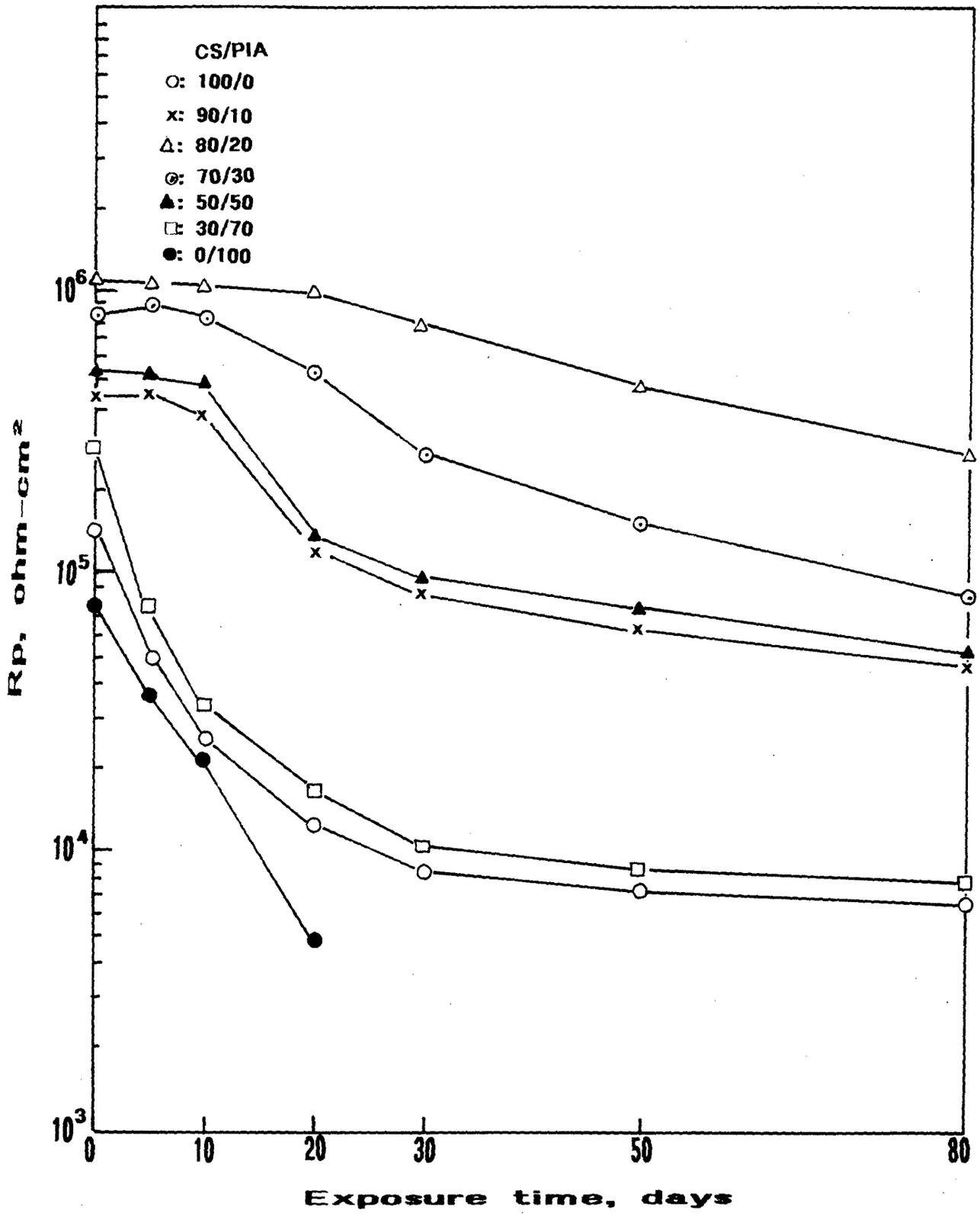

Fig. 10 Change in Rp for 100/0, 90/10, 80/20, 70/30, 50/50, 30/70, and 0/100 ratio-coated Al as a function of exposures up to 80 days.

APPENDIX B

ISSUED PATENT

US005844058A

United States Patent [19]

Sugama

[11] Patent Number: 5,844,058

[45] Date of Patent: Dec. 1, 1998

[54] **ORGANOSILOXANE-GRAFTED NATURAL POLYMER COATINGS**

[75] Inventor: **Toshifumi Sugama**, Wading River, N.Y.

[73] Assignee: **Brookhaven Science Associates**, Upton, N.Y.

[21] Appl. No.: **767,983**

[22] Filed: **Dec. 17, 1996**

[51] **Int. Cl.**[6] **C08G 79/00**; C04B 9/02; B65B 33/00

[52] **U.S. Cl.** **527/300**; 536/84; 536/101; 536/111; 536/120; 106/14.5; 427/156; 427/435

[58] **Field of Search** 527/300; 536/84, 536/101, 111, 120; 106/14.5; 427/156, 435

[56] **References Cited**

U.S. PATENT DOCUMENTS

3,556,754	1/1971	Marsden .	
4,129,722	12/1978	Iovine et al.	536/43
4,540,777	9/1985	Amort et al.	536/102
4,584,280	4/1986	Nanao et al.	501/80
4,839,449	6/1989	Billmers et al.	526/238.2
4,950,583	8/1990	Brewer et al.	430/311
4,973,680	11/1990	Billmers	536/58
5,004,791	4/1991	Billmers	527/300
5,032,683	7/1991	Dragner et al.	536/104
5,110,863	5/1992	Sugama	524/767
5,200,237	4/1993	Sugama	427/380
5,292,799	3/1994	Naito et al.	524/783
5,496,937	3/1996	Okamoto et al.	536/124

FOREIGN PATENT DOCUMENTS

0094924A2	5/1983	European Pat. Off. .
0644204A1	5/1994	European Pat. Off. .

OTHER PUBLICATIONS

Sugama et al., "Zirconocene–modified Polysiloxane–2–Pyridine Coatings", *Thin Solid Films*, 258, 1995, pp. 174–184.

Sugama, "Pectin Copolymers with Organosiloxane Grafts as Corrosion–Protective Coatings for Aluminum", *REDC Material Letters*, vol. 25, Dec. 1995, pp. 291–299.

Sugama et al., "Polyorganosiloxane–Grafted Potato Starch Coatings for Protecting Alumium from Corrosion", *Thin Solid Films*, vol. 289, Nov. 1996, pp. 39–48.

Primary Examiner—Nathan M. Nutter

Attorney, Agent, or Firm—Margaret C. Bogosian

[57] **ABSTRACT**

A new family of polysaccharide graft polymers are provided as corrosion resistant coatings having antimicrobial properties which are useful on light metals such as aluminum, magnesium, zinc, steel and their alloys. Methods of making the polysaccharide graft polymers are also included. The methods of making the polysaccharide graft polymers involve reacting a polysaccharide source with an antimicrobial agent under conditions of hydrolysis-condensation.

12 Claims, 14 Drawing Sheets

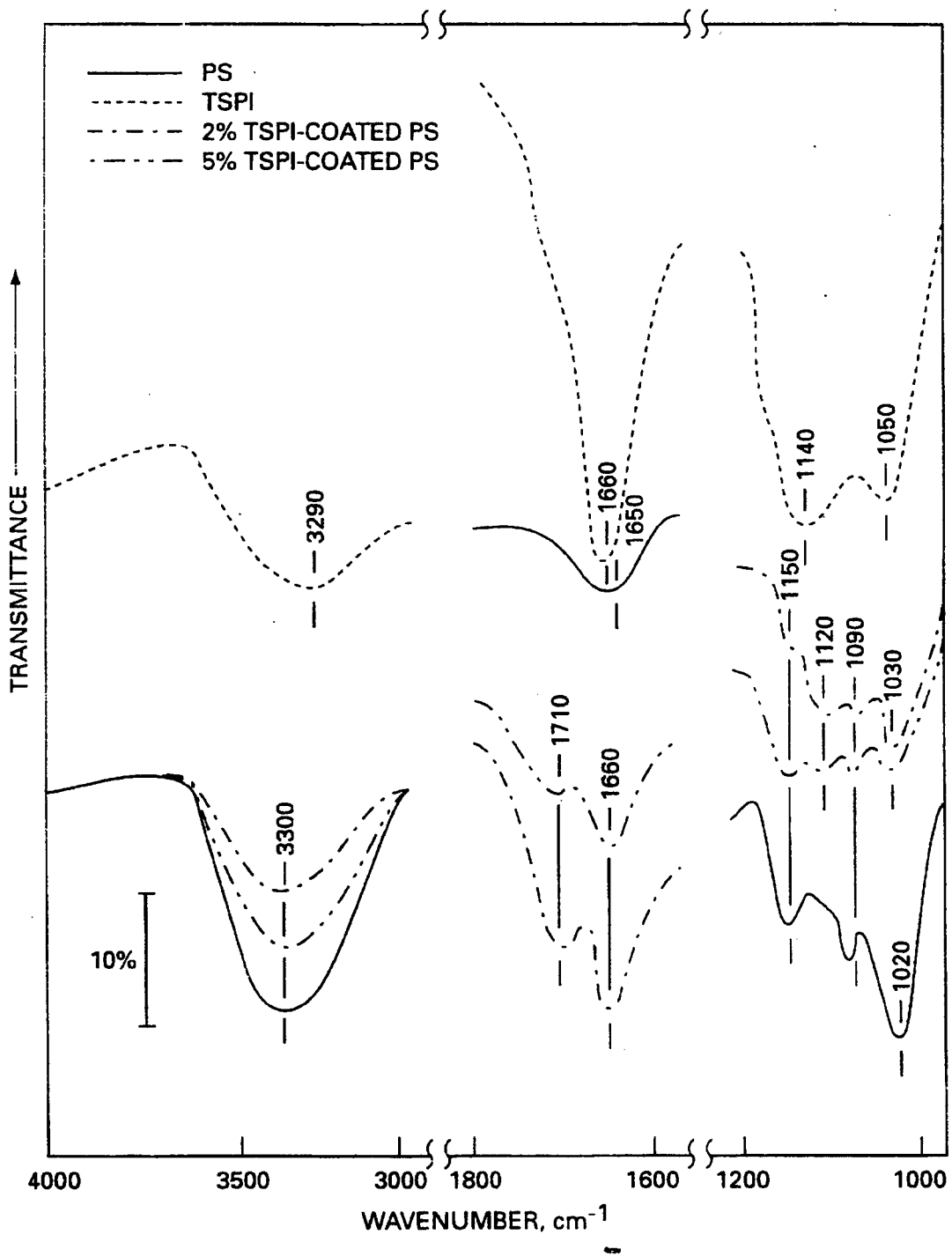
PS
TSPI
2% TSPI-COATED PS
5% TSPI-COATED PS
TRANSMITTANCE
3290
1660
1650
1140
1050
1150
1120
1090
1030
1710
1660
3300
10%
1020
4000
3500
3000
1800
1600
1200
1000
WAVENUMBER, cm-1

FIGURE 1

FIGURE 2a

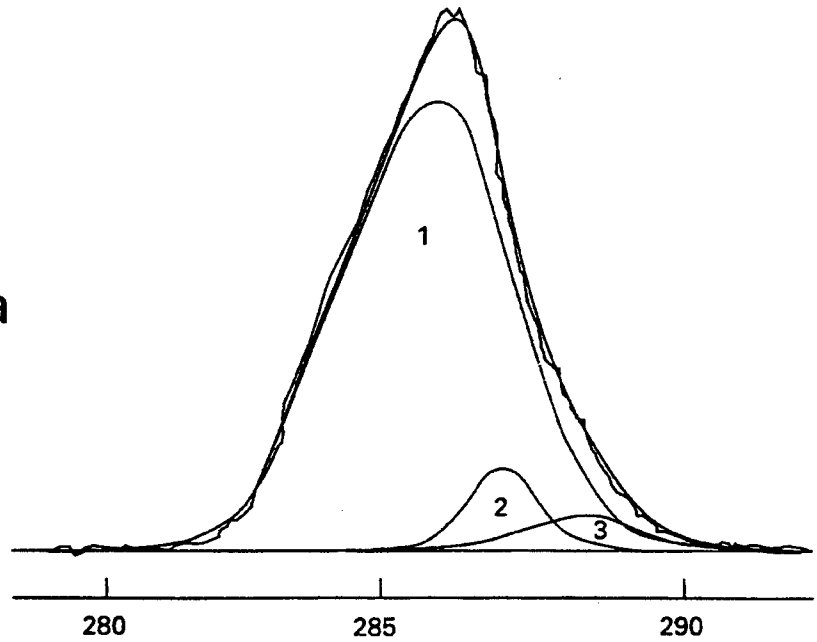

FIGURE 2b

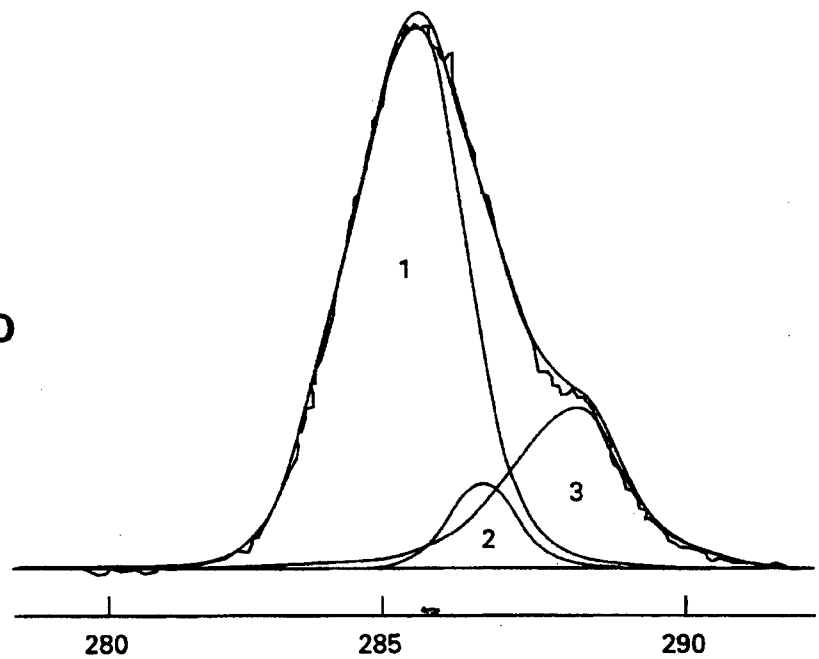

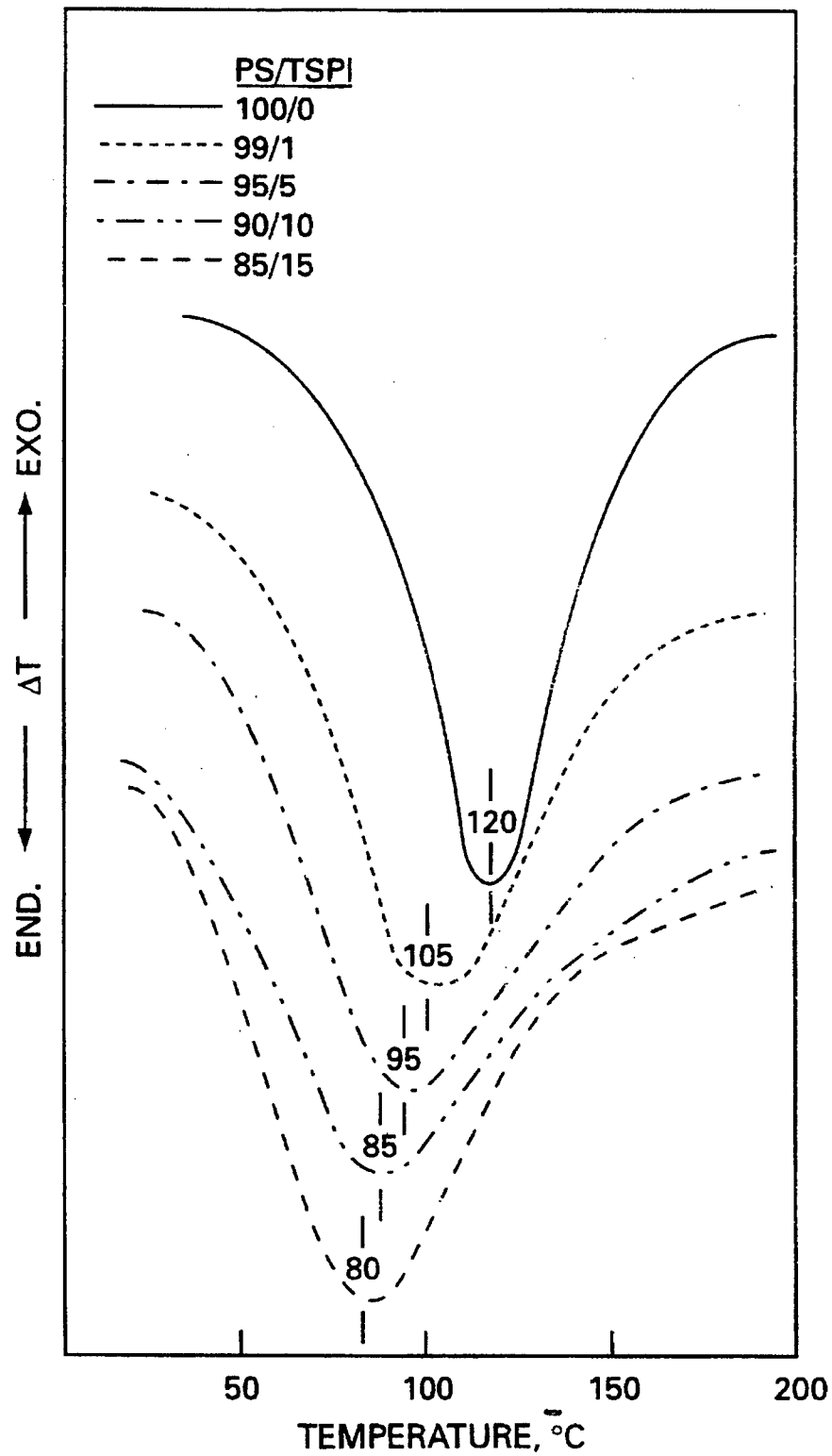
PS/TSPI
100/0
99/1
95/5
90/10
85/15
END. ΔT EXO.
120
105
95
85
80
50
100
150
200
TEMPERATURE, °C

FIGURE 3

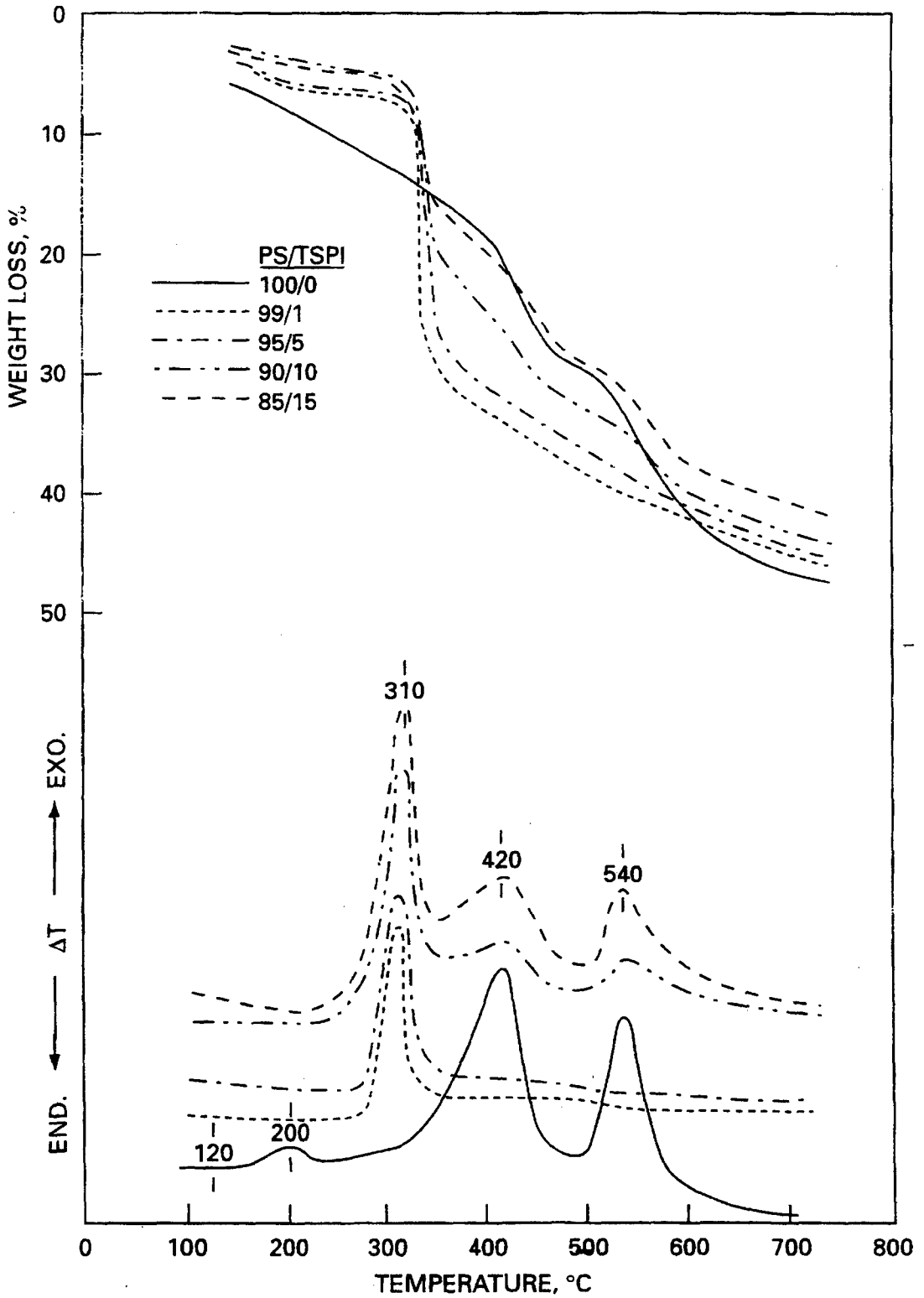
WEIGHT LOSS, %
0
10
20
30
40
50
PS/TSPI
100/0
99/1
95/5
90/10
85/15
310
420
540
200
120
END. ← ΔT → EXO.
0
100
200
300
400
500
600
700
800
TEMPERATURE, °C

FIGURE 4

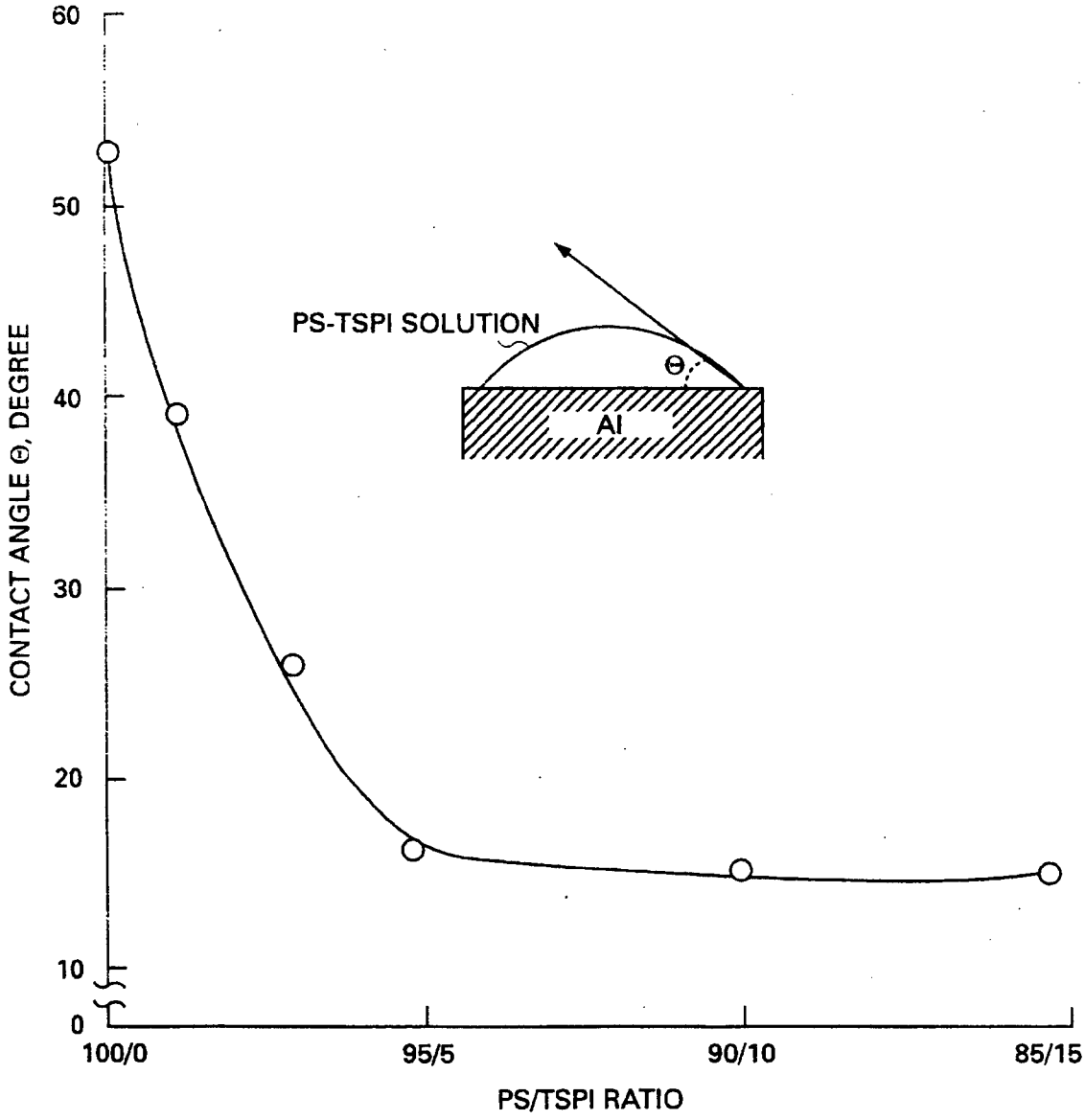
60
50
40
30
20
10
0
CONTACT ANGLE Θ, DEGREE
PS-TSPI SOLUTION
Θ
Al
100/0
95/5
90/10
85/15
PS/TSPI RATIO

FIGURE 5

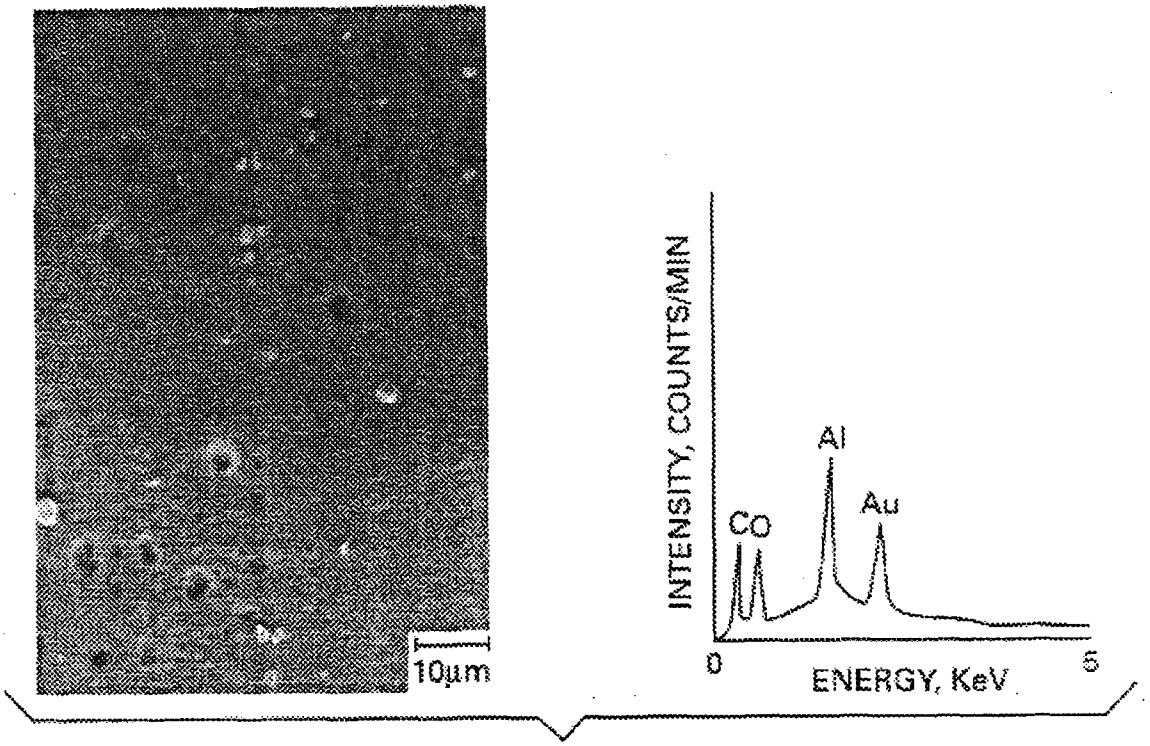

FIGURE 6a

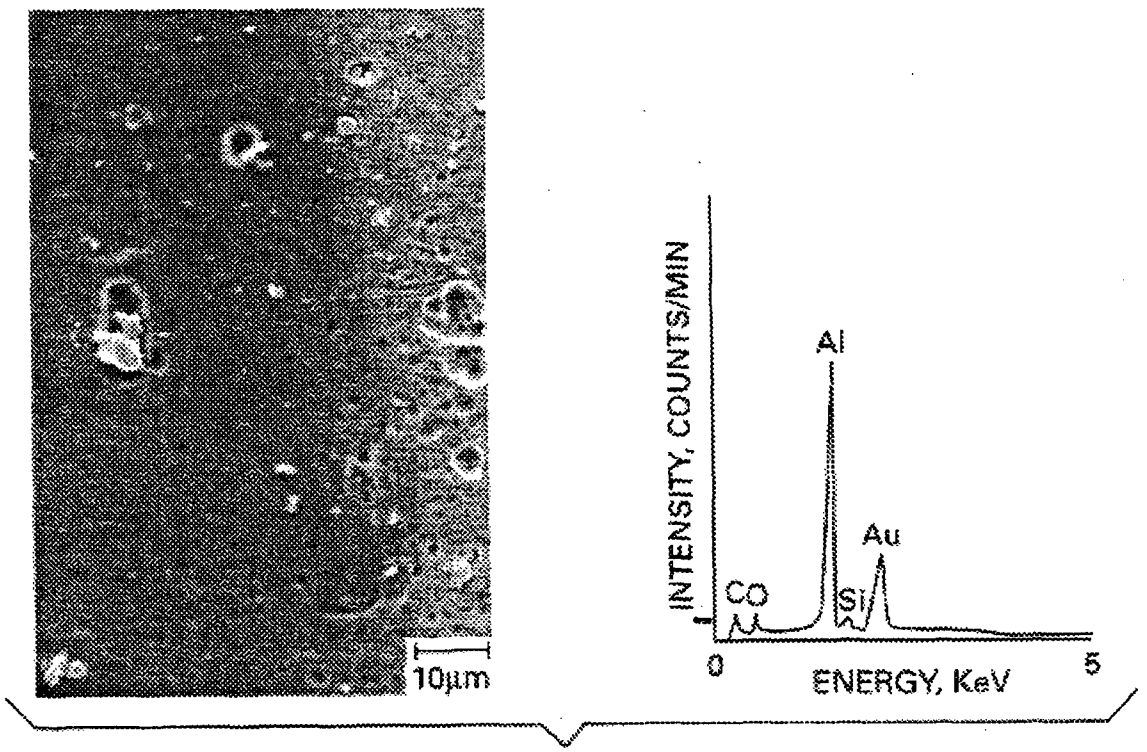

FIGURE 6b

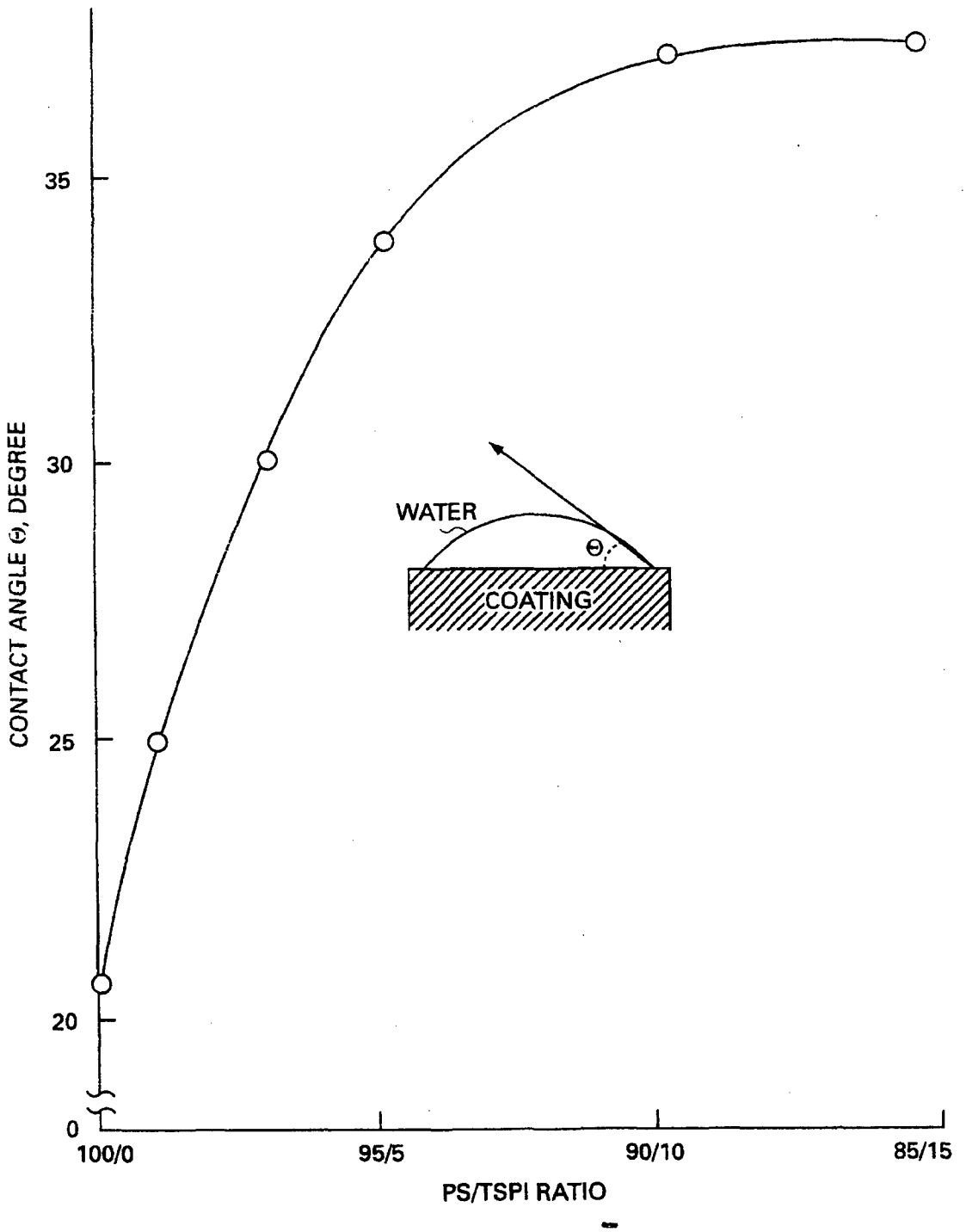
CONTACT ANGLE Θ, DEGREE
35
30
25
20
0
WATER
Θ
COATING
100/0
95/5
90/10
85/15
PS/TSPI RATIO

FIGURE 7

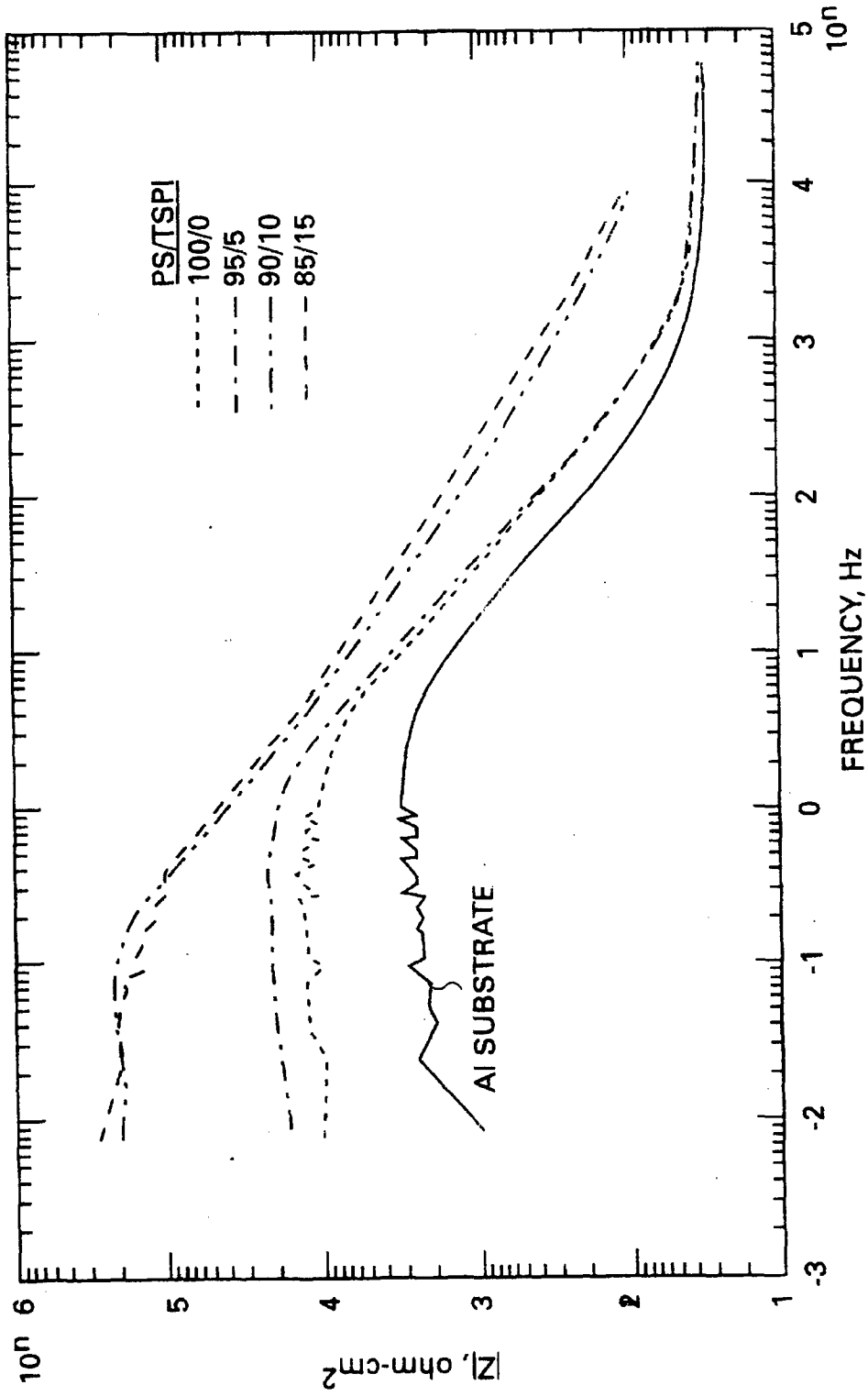
PS/TSPI
100/0
95/5
90/10
85/15
Al SUBSTRATE
|Z|, ohm-cm²
FREQUENCY, Hz
10^6
5
4
3
2
1
-3
-2
-1
0
1
2
3
4
5
10^n

FIGURE 8

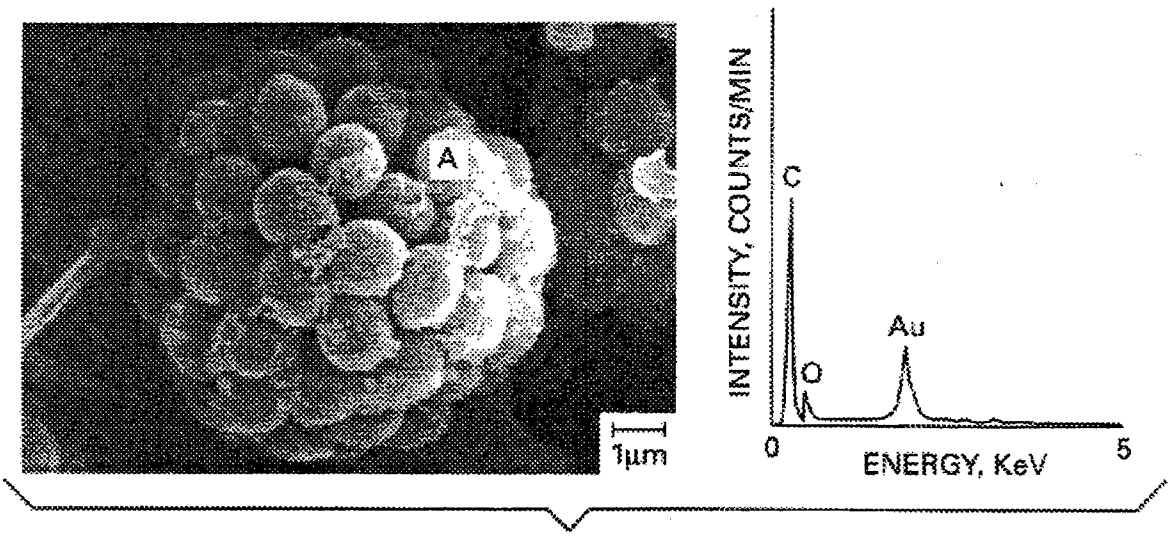

FIGURE 9a

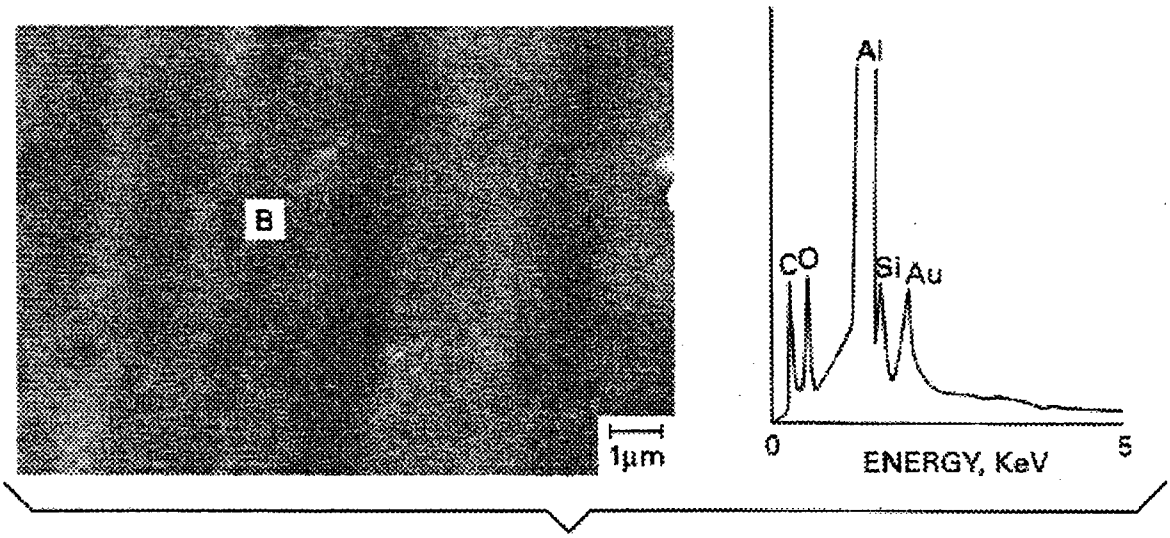

FIGURE 9b

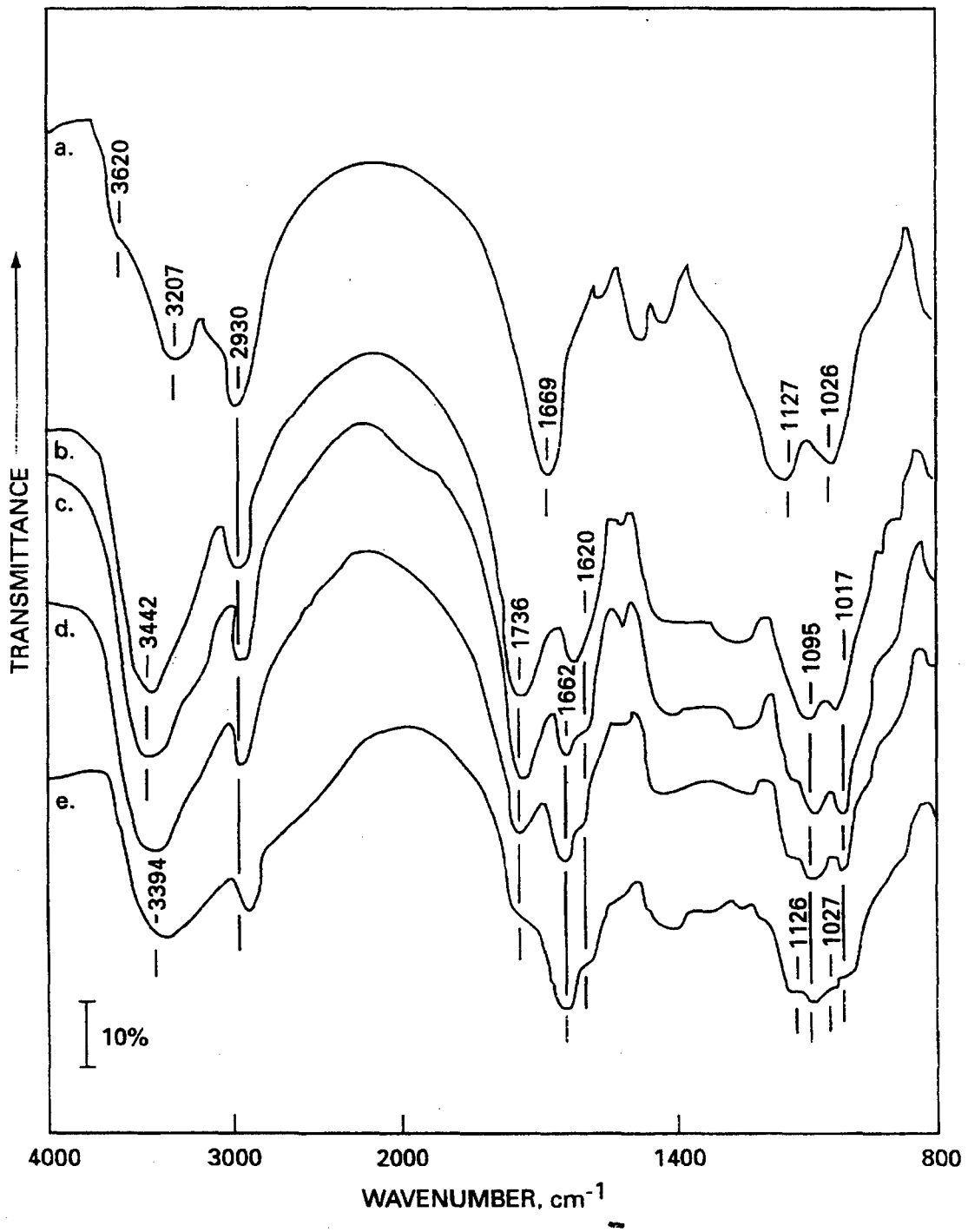
a.
b.
c.
d.
e.
3620
3207
2930
1669
1127
1026
3442
1736
1620
1662
1095
1017
3394
1126
1027
10%
TRANSMITTANCE
4000
3000
2000
1400
800
WAVENUMBER, cm-1

FIGURE 10

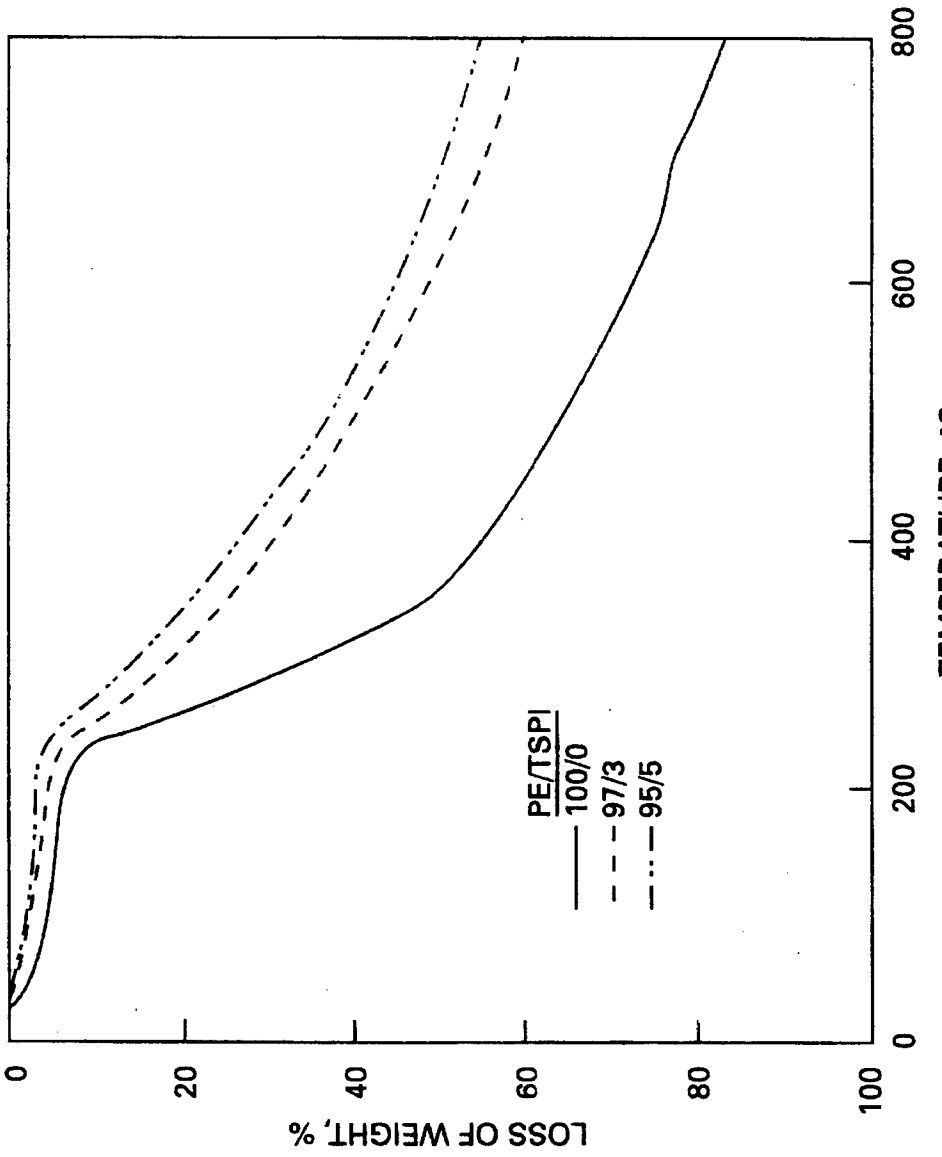
LOSS OF WEIGHT, %
0
20
40
60
80
100
TEMPERATURE, °C
0
200
400
600
800
PE/TSPI
100/0
97/3
95/5

FIGURE 11

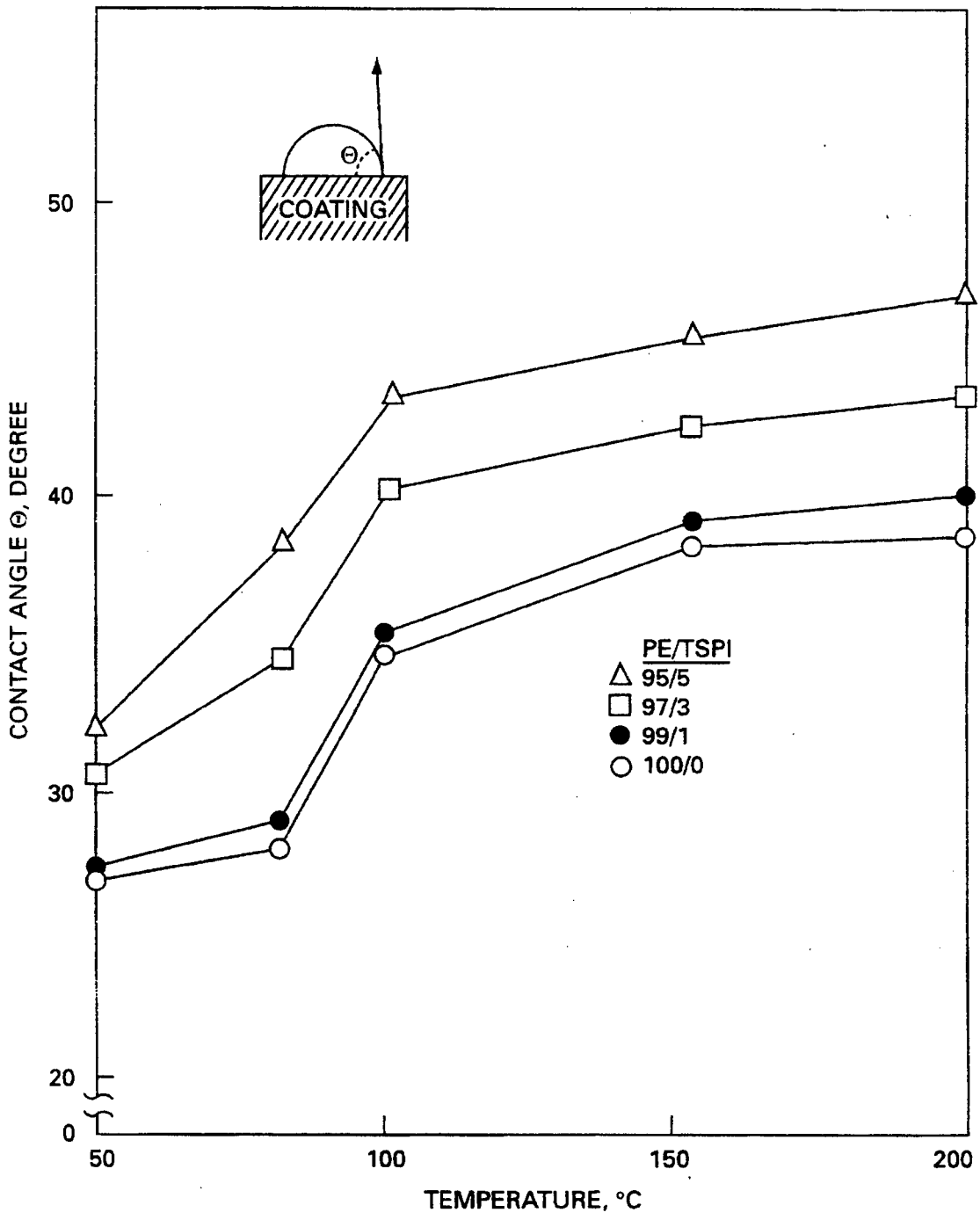
Θ
COATING
50
40
30
20
0
CONTACT ANGLE Θ, DEGREE
50
100
150
200
TEMPERATURE, °C
PE/TSPI
95/5
97/3
99/1
100/0

FIGURE 12

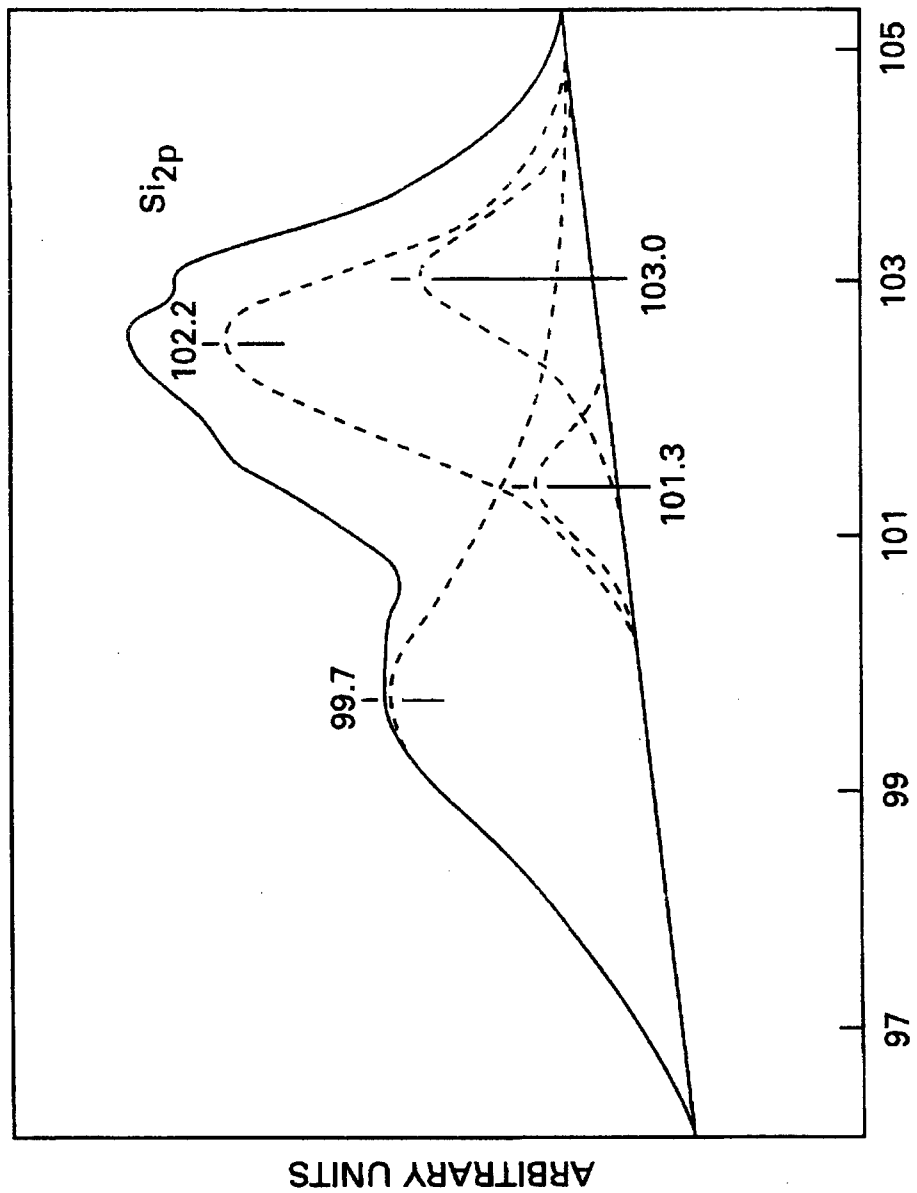
Si2p
102.2
103.0
101.3
99.7
97
99
101
103
105
BINDING ENERGY, eV
ARBITRARY UNITS

FIGURE 13

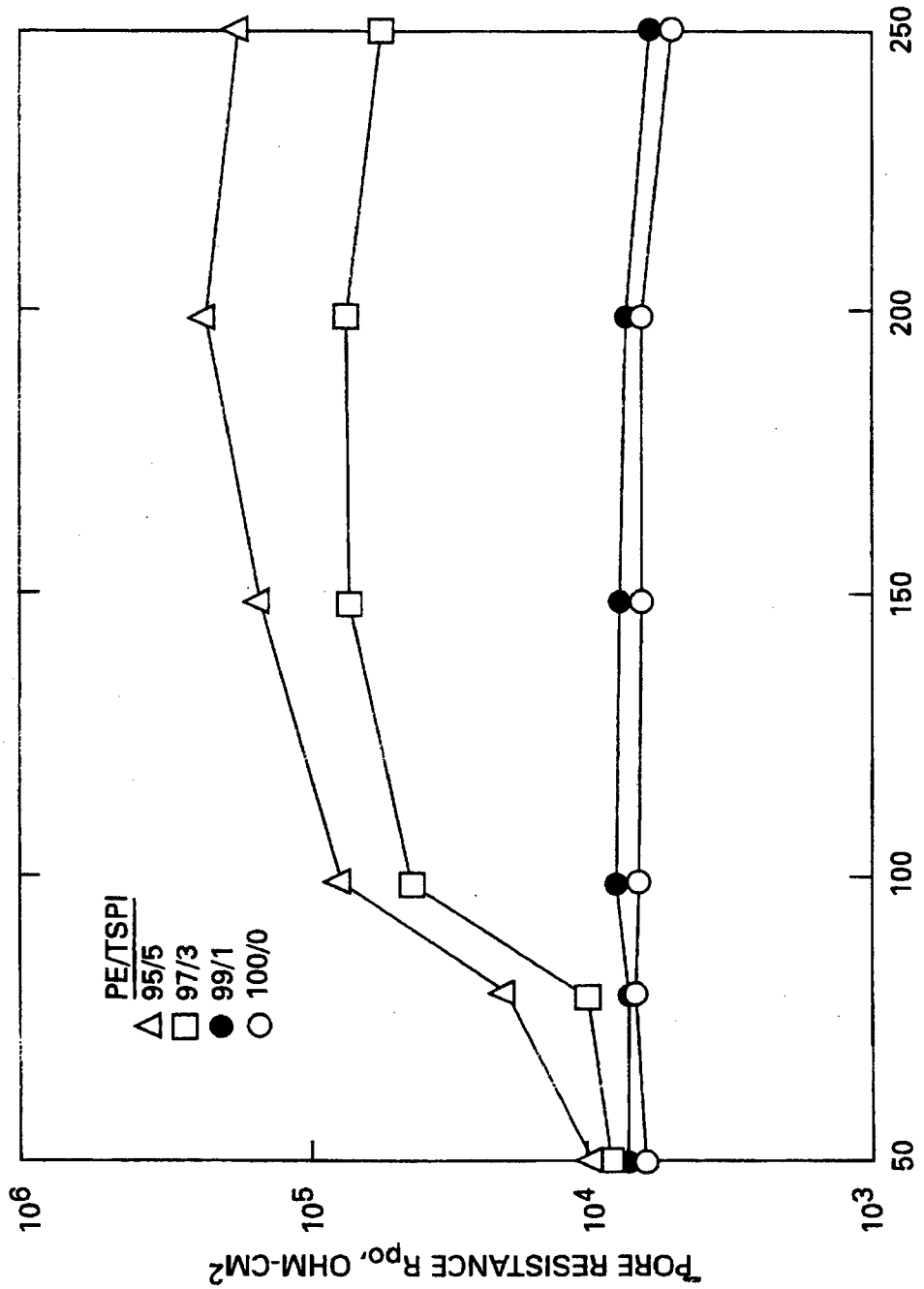
PE/TSPI
95/5
97/3
99/1
100/0
10^6
10^5
10^4
10^3
PORE RESISTANCE R_{po}, OHM-CM2
50
100
150
200
250
TEMPERATURE, °C

FIGURE 14

ORGANOSILOXANE-GRAFTED NATURAL POLYMER COATINGS

This invention was made with Government support under Contract No. DE-ACO2-76CH00016, between the U.S. Department of Energy and Associated Universities, Inc. The invention also has received support from U.S. Army Research Office Program MIPR-ARO-112-93. The Government has certain rights in the invention.

BACKGROUND OF THE INVENTION

This invention relates to a new family of polysaccharide graft polymers, methods of making and using the graft polymers to provide corrosion resistant coatings having antimicrobial properties. More specifically, the new family of polysaccharide graft polymers is provided by reacting a polysaccharide source with an antimicrobial agent.

Water-soluble or dispersable natural polymers, such as starches and cellulosics, are among the most abundant natural resources on both molecular and weight basis, with about 400 billion tons produced photosynthetically in the United States each year. Worldwide, by the year 2000, it has been estimated that natural polymer products will reach about 2000 million tons. Because sources of natural polymers come from seeds and roots of plants, both renewable and abundant agricultural resources, which are also comparatively inexpensive and relatively stable in quality and price. As a result, using natural polymers as an extender and replacement for synthetic polymers might reduce our dependence on petrochemically-derived products.

The hydroxy structures of natural polymers display an excellent affinity to polar substrates, such as cellulose. Thus, although the major consumer of natural polymers are the paper and food industries, these polymers are also widely applied as coatings for paper, and as adhesives in cellulose-based corrugation board, multiwall bags and foil lamination. In using natural polymers as adhesives, susceptibility of the solution adhesive solution to water is a major drawback which must be overcome. Some improvement of water-resistance can be obtained by incorporating water-soluble polymers, such as polyvinyl alcohol and acetate, and thermosetting resins such as ureaformaldehyde or resourcinol-formaldehyde into natural polymers.

Research has been conducted in the past on organosiloxane-containing polysaccharides and polysaccharide graft polymers. For example, U.S. Pat. Nos. 4,973,680 and 5,004,791 to Billmers disclose organosiloxane-containing polysaccharide derivatives and polysaccharide graft polymers usefull in glass fiber forming size compositions, and paper making, adhesives, paper, textile additives as thickeners, sealants, coatings, binders and films. Billmers discloses polysaccharide graft polymers having the structure of

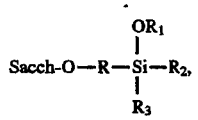

and a polysaccharide graft polymer having the structure Sacch-O—$(G)_n$—$(M)_n$—wherein Sacch- is a polysaccharide; m is 0 or 1; G is the residue of a polymerizable, unsaturated monomer which is bonded to the polysaccharide by an ether or ester linkage; n is greater than 1; and M is the residue of one or more polymerizable, unsaturated, monomer(s), at least one of which is a siloxane-containing monomer, which have been grafted to polysaccharide by free radical polymerization. The polysaccharides disclosed in the '791 and '680 references include starches, gums, cellulose and cellulose derivatives. The organosiloxane compounds used to modify polysaccharides are all trimethoxy or triethoxy silane derivatives.

Several investigators reported that another way to modify starch with synthetic polymers or monomers at molecular level is graft copolymerization in an aqueous or non-aqueous medium. Starch structures were modified through the reaction of the hydroxyl groups with functional groups of synthetic polymers, such as carboxylic acid, anhydride, epoxy, urethane, or oxazoline, and by free-radical ring-opening polymerization occurring between the glucose rings and vinyl monomers.

In the above attempts, it has been found, however, that coatings made of natural polymers such as commercial starch, have many undesirable features. The following characteristics have been found:

(i) microorganisms readily settle and grow on coatings made of natural polymers;

(ii) the coatings have hydrophilic characteristics which form mechanically weak films; and

(iii) they also display poor wetting and adhesive properties to metals and other polymer substrates.

Accordingly, there is still a need in the art of coatings for inexpensive, environmentally benign natural polymer coatings which are both corrosion resistant and have antibacterial properties.

It is therefore an object of the present invention to provide chemically modified natural polymer coatings which are inexpensive, environmentally safe and which at the same time strongly adhere to metals such as aluminum, magnesium and zinc, provide anticorrosion protection and cannot be easily attacked by bacteria.

SUMMARY OF THE INVENTION

The present invention, which addresses the needs of the prior art, provides a new family of compounds which are useful as antibacterial corrosion protective coatings for light weight metals such as aluminum, magnesium, zinc, steel and alloys thereof. The new family of compounds include a polysaccharide graft polymer having the structure below

I

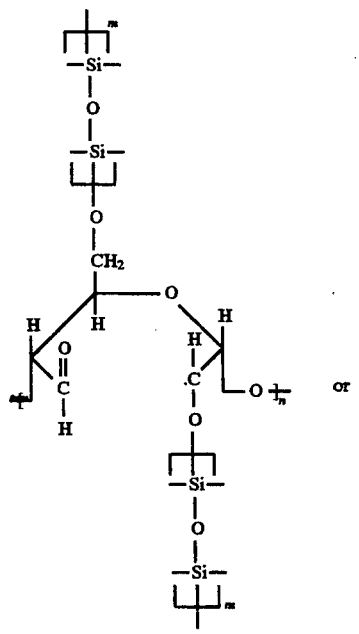

-continued

II

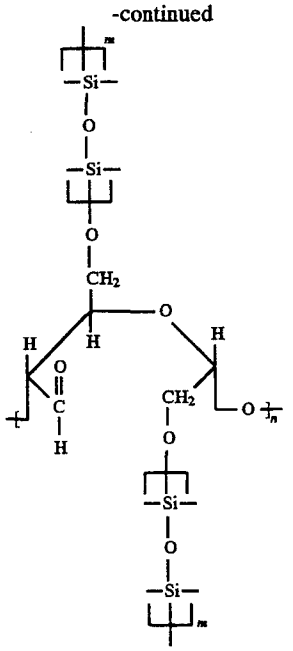

wherein m and m are greater or equal to 500. The present invention also provides methods of making the polysaccharide graft polymers of the invention by reacting a polysaccharide source with an antimicrobial agent under conditions of hydrolysis-condensation. The polysaccharide source and the antimicrobial agent are in colloidal aqueous solutions. The hydrolysis-condensation reaction occurs from about 50° C. to about 250° C. The polysaccharide source can be selected from water dispersable commercial starches and cellulosics. Starches include corn, wheat, rice, tapioca, potatoes and sago. Cellulosics include such esters or ethers as cellulose xanthate, methylcellulose, hydroxyethyl cellulose and carboxymethyl-cellulose. Useful antimicrobial agents include N[3-(triethoxysilyl)-propyl]-4,5-dihydroimidazole, β-trimethoxysilylethyl-2-pyridine, β-trimethoxysilylethyl-4-pyridine, 2-[2-trichlorosilyl)ethyl]pyridine, 4-[2-(trichlorosilyl)ethyl]pyridine, N-[3-(triethoxysilyl)propyl]-4-5-dihydroimidazole, 3-bromopropyltrimethoxysilane; 3-iodopropyltrimethoxysilane; (3,3,3-trifluoropropyl) trimethoxysilane; (3,3,3-trifluoropropyl)triethoxysilane; tridecafluoro-1,1,2,2-tetrahydrooctyl-1-triethoxysilane.

As a result of the present invention, a new family of compounds is provided. The compounds are useful as antibacterial corrosion protective coatings for light weight metals. TSPI-modified natural polymer films deposited on aluminum substrates display a superior level of corrosion protection for the substrate. For example, the coatings of the present invention had an impedance of greater than 10^6 ohm-cm^2 after a 20-day exposure to a 0.5N NaCl solution at 25° C., a 1000-hr salt-spray resistance, and a grate protection at both anodic (inhibits pitting) and cathodic sites. The extent of such resistance to corrosion was far better than that of conventional anodic oxide and Cr-conversion coatings. Hence, the modified natural polymer coatings of the present invention have high potential as substitutive material for Cr-incorporating coatings which are also known to be environmentally hazardous.

Other improvements which the present invention provides over the prior art will be identified as a result of the following description which sets forth the preferred embodiments of the present invention. The description is not in any way intended to limit the scope of the present invention, but rather only to provide a working example of the present preferred embodiments. The scope of the present invention will be pointed out in the appended claims.

BRIEF DESCRIPTION OF THE DRAWINGS

FIG. **1** shows SRFT-IR spectra for bulk PS and TSPI coating films, and 2% and 5% TSPI-coated PS films.

FIGS. **2**(*a*) and **2**(*b*) show XPS C_{1s} core-level spectra at (a) for bulk PS and at (b) for TSPI-modified PS coating surfaces at 200° C.; the peak positions for each curves 1, 2, and 3 correspond to 285.0, 286.5, and 288.0 eV, respectively.

FIGS. **3** illustrates a shift in the endothermal temperature of PS to low values when the proportion of TSPI to PS was increased.

FIG. **4** shows TGA and DTA curves for 200° C.-heated bulk PS and TSPI-modified PS polymers.

FIG. **5** illustrates contact angles of various different PS/TSPI ratio solutions which were dropped on surfaces of aluminum substrates.

FIG. **6** shows SEM micrographs coupled with EDX spectra for 200° C.-treated film surfaces with 100/0 (top) and 95/15 (bottom) PS/TSPI ratios.

FIG. **7** illustrates contact angle of a water droplet on 200° C.-treated coating films with different PS/TSPI ratios.

FIG. **8** shows Bode-plots for bare aluminum substrate, and aluminum specimens coated with films having 100/0, 95/5, 90/10, and 85/15 PS/TSPI ratios.

FIGS. **9**(*a*) and **9**(*b*) show SEM-EDX examination of coating surfaces derived from PE/TSPI solutions having ratios of 100/0 (top) and 97/3 (bottom) after leaving them for two months in culture flasks at 25° C.

FIG. **10** illustrates FT-IR spectra for 100° C.-treated PE/TSPI ratio coatings as follows: 0/100 at (a), 100/0 at (b), 99/1 at (c), 97/3 at (d), and at 95/5 (e).

FIG. **11** illustrates TGA for the TSPI-modified and -unmodified PE polymers in air at a rate of 10° C./min.

FIG. **12** shows changes in the contact angle of film surfaces made from films having various different PE/TSPI ratios as a function of temperature.

FIG. **13** shows XPS Si_{2p} core-level spectrum for the 97/3 ratio PE/TSPI coating at interference with aluminum substrate.

FIG. **14** shows changes in pore resistance, R_{po}, as a function of temperature for various PE/TSPI ratio coatings deposited on aluminum substrates.

DETAILED DESCRIPTION OF THE INVENTION

The present invention provides a new family of polysaccharide graft polymers, methods to make and use as corrosion-protective coatings for lightweight metal substrates. More specifically, the present invention provides natural polymers such as starch and cellulosics which have been modified with antimicrobial agents to form water impermeable corrosion resistant coating films which have antimicrobial properties.

All compounds utilized to prepare the new family of polymers of the present invention can be synthesized or are commercially available. For example, useful commercial starches include corn, wheat, rice, tapioca, potatoes and sago. Cellulosics include cellulose and its derivatives, typically esthers or ethers, cellulose xanthate, methylcellulose, hydroxyethylcellulose and carboxymethyl-cellulose.

Starch is a mixture of amylose and amylopectin. Amylose is a linear homopolysaccharide which is made up of several

hundred glucose units linked by (1→4)-alpha-D-glycosidic linkages. Amylopectin is a branched homopolysaccharide of glucose units with (1→6)-alpha-D-glycosidic linkages at the branching points and (1→4)-alpha-D-glycosidic linkages in the linear region. The hydrated linear amylose molecules inherently tend to align. Once the aligned configuration is formed, intramolecular hydrogen bonds generated between the linear chains lead to an agglomeration and crystallization of amylose chains, thereby resulting in a low solubility in water. Similarly, the molecular arrangement of linear portions in branched amylopectin introduces the same degree of crystallinity into hydrated starch. However, the solubility of amylopectin in water is much higher than that of amylose. Typical starches have a proportion of 20% to 30% amylose and 70% to 80% amylopectin.

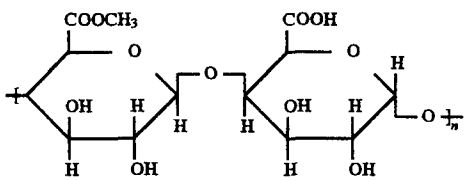

Pectin (PE) is a natural polymer also known as polygalacturonic acid methyl esther. PE has the formula shown above, wherein n is greater or equal to 500 and has a molecular weight of 20,000 to 30,000. Pectin was obtained from Scientific Polymer Products, Inc.

In order to modify the natural polymers used in the present invention, antimicrobial agents were used. For example, monomeric N-[3-(triethoxysilyl) propyl]-4,5,-dihydroimidazole (TSPI) was obtained from Huls America, Inc. or Petrarch Systems Ltd. Other useful antimicrobial agents include β-trimethoxysilyl ethyl-2-pyridine, β-trimethoxysilyl ethyl-4-pyridine, 2-[2-trichlorosilyl (ethyl]pyridine, 4-[2-(trichlorosilyl) ethyl]pyridine. Other useful antimicrobial agents include halogen-substituted silanes, such as, for example: 3-bromopropyltrimethoxysilane; 3-iodopropyltrimethoxysilane; (3,3,3-trifluoropropyl) trimethoxysilane; (3,3,3-trifluoropropyl) triethoxysilane; tridecafluoro-1,1,2,2-tetrahydrooctyl-1-triethoxysilane.

U.S. Pat. No. 4,540,777 to Amort, et al., discloses a method for the modification of starch with organofunctional alcoxysilanes and/or alkyl alcoxysilanes, in an aqueous medium. The modification of starch is performed by bringing the starch into intimate contact with hydrolyzates of the silanes in the presence of alkyl aluminates or alkyl hydroxides.

The organosilanes which could be used as modifying agents in '777 reference to Amort, et al. have the following general formula:

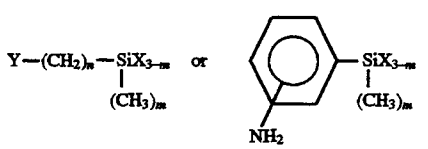

in which y represents substituted or unsubstituted amino group, or a moiety from the group H, CH_3, —Cl, $CH{=}CH_2$, —SH; X is an alcoxy moiety with a maximum of six carbon atoms; M can be 0, 1 or 2, and n takes values of 1, 2 or 3. An example of organofinctional silane includes gamma-chloropropyltrimethoxysilane. The starch disclosed in '777 reference to Amort, et al. can be used for hydrophobation and oleophobation of cellulosic material and is suitable as binder for mineral fibers, textile adjuvants, sizes for various paper products, and as fillers for plastics. The method disclosed in the '777 reference requires the presence of alkali aluminates and alkali hydroxides. Additionally, starch modified by gamma-chloropropyl trimethoxysilane does not provide the corrosion protection which is provided by bromine, iodine and fluorine substituted silanes. Moreover, the graft polymers of the present invention are prepared in the absence of alkali aluminates and alkali hydroxides.

The water-based coating systems of the present invention have been prepared by mixing solutions in two phases. One phase consisted of natural polymers dissolved in water and the other phase of a salt solution which contains an antimicrobial agent such as TSPI, water, methanol and hydrochloric acid. The resulting TSPI modified natural polymer coating films were capable of protecting lightweight metals against corrosion. Metals which can be protected with the coating films of the present invention include aluminum, magnesium, zinc, steel and alloys thereof.

Simple dip, spray or spin-coating methods can be used to deposit precursor solution layers onto the metal substrates. Heating the coated metal at temperatures from about 50° C. to about 250° C. for about 120 minutes allowed the formation of corrosion resistant coating films of the present invention.

EXAMPLES

The examples below further illustrate the various features of the invention, and are not intended in any way to limit the scope of the invention which is defined in the appended claims.

EXAMPLE 1

In this experiment, polyorganosiloxane (POS)-grafted polysaccharide copolymers were synthesized through a heat-catalyzed dehydrating condensation reaction between hydrolysates of potato starch (PS) as source of polysaccharide and N-[3-(triethoxysily)propyl]- 4,5, -dihydroimidazole (TSPI) as the antimicrobial agent and a source of the graft-forming POS at 200° C. in air. The grafting of POS onto PS followed by the opening of glycosidic rings significantly improved the thermal and hydrophobic characteristics of PS.

The experiment was also directed to evaluating the ability of antimicrobial TSPI-modified starch films to protect aluminum alloys from corrosion. The evaluations were carried out by AC electrochemical impedance spectroscopy and salt-spray resistance. The resulting data were then correlated with several other physico-chemical factors, such as the spreadability of the modified starch aqueous solution on surfaces of aluminum substrates. The magnitude of susceptibility of solid coating film surfaces to moisture, the molecular conformation of the modified starch, its thermal decomposition, and the surface morphology of films were also studied. In addition, the effect of TSPI as antimicrobial agent on preventing the settlement and growth of microorganisms in starch aqueous solution was also investigated.

1. Materials

The starch used was potato starch (PS) from ICN Biomedical, Inc. For modifying PS, monomeric N-[3-(triethoxysily)propyl]-4,5, -dihydroimidazole (TSPI) was used as supplied by Huls America, Inc. A 1.0 wt % PS solution dissolved in deionized water at 80° C. was modified by incorporating various amounts of the TSPI solution consisting of 9.5 wt % TSPI, 3.8 wt % CH_3OH, 1.0 wt %

HCl, and 85.7 wt % water. Six ratios of PS/TSPI solutions of 100/0, 99/1, 97/3, 95/5, 90/10, and 85/15 by weight were utilized. The lightweight metal substrate was a 6061-T6 aluminum (Al) sheet containing the following chemical constituents: 96.3 wt % Al, 0.6 wt % Si, 0.7 wt % Fe, 0.3 wt % Cu, 0.2 wt % Mn, 1.0 wt % Mg, 0.2 wt % Cr, 0.3 wt % Zn, 0.2 wt % Ti, and 0.2 wt % other elements.

2. Coating Technology

The aluminum surfaces were coated by TSPI-modified and unmodified PS films in the following sequence. The aluminum substrates were immersed for 20 minutes at 80° C. in an alkaline solution consisting of 0.4 wt % NaOH, 2.8 wt % tetrasodium pyrophosphate, 2.8 wt % sodium bicarbonate, and 94.0 wt % water in order to remove surface contaminants. The alkali-cleaned aluminum surfaces were washed with deionized water at 25° C. for 5 min, and dried for 15 min at 100° C. Then, the substrates were dipped into a soaking bath of solution at room temperature, and withdrawn slowly. The wetted substrates were then heated in an oven for 120 min at 200° to yield thin solid films.

3. Measurements

PS solutions are suitable nutrients for fungal and bacterial growth. Adding TSPI has had the effect of preventing the growth and colonization of microorganisms. This observation was verified by using scanning electron microscopy (SEM). The surface tension of the unmodified and TSPI-modified PS solutions was measured with a Cenco-DuNouy Tensiometer Model 70535. Solutions with an extremely high or low pH have been found improper for use as coatings of metal surfaces because of the corrosion of metal by such solutions. Thus, it was very important to measure the pH of coating solutions, prior to depositing them on the surface of a metal.

To understand the molecular structure of TSPI-modified PS, the films deposited on aluminum surfaces were investigated by specular reflectance fourier transform infrared (SRFT-IR) spectrophotometer, and x-ray photoelectron spectroscopy (XPS). The combined techniques of differential scanning calorimetry (DSC), thermogravimetric analysis (TGA), and differential thermal analysis (DTA) were used to assess the changes in the melting point of PS as a function of TSPI concentrations, and also to search the thermal decomposition characteristics of modified and unmodified PS polymers. The degree of crystallinity of the polymers was estimated by using x-ray powder diffraction (XRD). The changes in the magnitude of wettability and spreadability of PS solutions modified with various amounts of TSPI on aluminum surfaces were recorded by measuring the contact angle within the first 30 seconds after dropping the solution on their surfaces. The same technique was employed to obtain the water-wettability of polymer film surfaces which provided information on the degree of susceptibility to moisture of modified and unmodified PS film surfaces. Information on the surface morphology and chemical composition of films deposited to aluminum substrates was obtained by SEM and energy-dispersive x-ray (EDX) analysis.

AC electrochemical impedance spectroscopy (EIS) was used to evaluate the ability of coating films to protect aluminum from corrosion. The specimens were mounted in a holder, and then inserted into an electrochemical cell. Computer programs were prepared to calculate theoretical impedance spectra and to analyze the experimental data. Specimens with a surface area of 13 cm^2 were exposed to an aerated 0.5N NaCl electrolyte at 25 ° C., and single-sine technology with an input AC voltage of 10 mV (rms) was used over a frequency range of 10 KHz to 10^{-2} Hz. To estimate the protective performance of coatings, the pore resistance, R_{po}, was determined from the plateau in Bode-plot scans (impedance, ohm-cm^2 vs. frequency, Hz) that occurred at low frequency regions. The salt-spray tests of the unmodified and modified PS-coated Al panels (75 mm×75 mm, size) were performed in accordance with ASTM B 117, using a 5% NaCl solution at 35° C.

4. Properties of Coating Films

a. Growth of Microorganisms

PS polymers contain C, H, and O, among other elements which are suitable nutrients for fungal and bacterial growth. When PS comes into contact with water, inevitably the growth of microorganisms already present in the water is stimulated. As a result, bacterial colonies flourish. A serious problem in using such colonized polymer solutions as coating materials is caused by microbial bioparticles incorporated into layers of dried coating film which promote the rate of water transportation. The coating films become wet and fail as corrosion-protective coatings. Thus, adding an antimicrobial agent to a PS solution is needed to prevent the growth of microorganisms.

In the present invention, monomeric TSPI was employed as an antimicrobial agent. To assess its effectiveness on inhibiting microbial growth, 20 grams aqueous solutions having PS/TSPI ratios of 100/0 and 97/3 were placed in culture flasks, and then left for two months at 25° C. in atmospheric environments. Subsequently, these solutions were deposited on aluminum substrate surfaces by dip-withdrawal coating methods, and then dried for 24 hours in a vacuum oven at 40° C. to form solid films for SEM observations. The SEM image obtained from the unmodified PS coating disclosed a continuous coverage of extensive fungal clusters over the aluminum substrate. A strikingly different feature was observed when PS was modified with a 3 wt % TSPI solution. There was no fungal growth in the films having a 97/3 PS/TSPI ratio. This finding indicated that the incorporation of TSPI as an antimicrobial agent prevented the growth of microorganisms in PS solutions.

b. Surface Tension as a Function of pH

TABLE 1

Changes in Surface Tension and pH of PS Solutions Modified with TSPI Solutions

PS/TSPI ratio	Surface tension dynes/cm	pH
100/0	72.3	6.4
99/1	62.4	8.5
97/3	58.9	8.7
95/5	55.4	8.9
90/10	54.8	8.9
85/15	54.7	8.9

Table 1 above shows the changes in surface tension of solutions as a function of PS/TSPI ratio at 25° C., and also their pH value. The addition of TSPI solution to PS solution decreased the surface tension, from 72.3 dynes/cm for an unmodified PS solution, to 54.7 dynes/cm for a 15 wt % TSPI-modified PS. The pH of the unmodified PS solution was 6.4; however, when this solution was modified with a 1 wt % TSPI solution, its pH shifted to a weak base value. The pH values of all TSPI-modified PS solutions ranged from 8.5 to 8.9.

c. Molecular Conformation of Modified Starch

To gain information on the interfacial reaction mechanisms between PS and TSPI, and the chemical conformation of reaction products, samples of TSPI treated PS were investigated by SRFT-IR. First, a PS solution was deposited

on aluminum surfaces by dip-withdrawal coating methods, and then left for 1 hour in an oven at 100° C. to transform into a solid film. Then, the PS-coated aluminum substrates were dipped into a 2 or 5 wt % TSPI solution, and the TSPI-wetted PS coatings were treated for 2 hours with heating at 200° C. for SRFT-IR explorations.

FIG. 1 depicts the IR spectra for the 2 and 5 wt % TSPI-coated PS samples, over three frequency ranges of 4000 to 3000, 1800 to 1570, and 1220 to 970 cm^{-1}. For comparison, the spectra of 200° C.-heated bulk PS and TSPI coating films as the reference samples were also illustrated in this figure. A typical spectrum of the bulk PS reference coating showed absorption bands at 3380 cm^{-1}, revealing the OH groups in the glucose units, at 1650 cm^{-1} which were ascribed to the bending vibration of H—O—H in the adsorbed H_2O, and also at 1150, 1090, and 1020 cm^{-1}, reflecting the stretching mode of C—O—C linkages in the glycosidic rings. The spectrum of bulk TSPI film showed an OH stretching band of adsorbed H_2O at 3290 cm^{-1}, a —C=N— band of dihydroimidazole coexisting with the H—O—H bending in H_2O at 1660 cm^{-1}, a Si—O—C bond of the Si-joined alkoxy groups at 1140 cm^{-1}, and Si—O—Si linkages at 1050 cm^{-1}.

When PS was coated with 2 wt % TSPI, the particular features of the IR spectrum differed from those of the reference samples. There was a decrease in intensity of the absorption band at 3380 cm^{-1}, (ii) a development of three new bands at 1710, 1120, and 1030 cm^{-1}, and (iii) a striking reduction of intensity of the C—O—C linkage-related bands in the frequency regions of 1200 to 1000 cm^{-1}. Increasing the concentration of TSPI to a 5 wt % led to a further decrease in intensity of the OH and C—O—C bands, while a marked growth of these new bands could be seen in the spectrum. The contributor to the new band at 1710 cm^{-1} is likely to be the C=O groups. On the other hand, the Si-alkoxy compounds and siloxanes have strong bands in the ranges of 1170–1110 cm^{-1} and 1110–1000 cm^{-1}, respectively. Thus, without being bound by theory, it has been concluded that the new bands at 1120 and 1030 cm^{-1} showed the formation of Si—O—C and Si—O—Si linkages, respectively. If this interpretation is correct, Si—O—C not only belongs to that linkage in the TSPI, but also may be due to the reaction products formed by the interaction between PS and TSPI. The Si—O—Si linkage is the embodiment of forming the polysiloxane structures.

In the study of the mechanism of graft copolymerization onto polysaccharide initiated by metal ion oxidation reaction, Doba et al., in Macromolecules, 17, p. 2512, 1984 have shown that oxidation of glycol groups in the glycosidic rings by ionic metal species cleaved the glycol C—C bond. The opening of the rings caused by such a cleavage not only generated a free radical which promoted the grafting of the vinyl monomers onto the polysaccharides, but also provided the formation of C=O groups. Also, they reported that no free radicals were found at the C position of —CH_2OH groups in the glucose units. Relating this finding to the fact that the spectrum of the bulk PS film does not show a clear feature of C=O bands, the development of C=O groups in the TSPI-coated PS is thought to involve the formation of Si—O—C linkages yielded by a dehydrating condensation reaction between the one hydroxyl, OH of glycol groups and the silanol group Si—OH in the hydrolysate of TSPI, followed by opening of ring. However, there was no evidence as to whether a free radical had been generated. Moreover, such a condensation reaction may also occur between the OH of —CH_2OH group in the glucose units and the OH of silanol group to form the Si—O—C linkages. Because the polysiloxane structure is present in the reaction products, the creation of these linkages virtually demonstrated that the polyorganosiloxanes (POS) were grafted to the PS.

To further ascertain that C=O groups were generated, the XPS C_{1s} core-level excitations for the 200° C.-heated film surfaces with PS/TSPI ratios of 100/0 and 85/15 were inspected. In this core-level spectra, the scale of the binding energy (BE) was calibrated with the C_{1s} of the principal hydrocarbon-type carbon peak fixed at 285.0 eV as an internal reference standard. A curve deconvolution technique, using a Du Du Pont curve resolver, was employed to support the information on the carbon-related chemical states from the spectrum of the carbon atom. As shown in FIG. 2, the C_{1s} region of bulk PS surfaces had three resolvable Gaussian components at the binding energy (BE) positions of 285.0, 286.5, and 288.0 eV denoted as peak areas "1", "2", and "3". The major peak at 285.0 eV is associated with the C in CH_2 and CH groups as the principal component. According to established literature sources, the second most intensive peak at 286.5 eV is attributable to the C in —CH_2O— (e.g. alcohol and ether), while a very weak signal, emerging at 288.0 eV, originates from C in the C=O groups. Although the thermal treatment of PS film at 200° C. in air may introduce C=O into the PS surfaces as the oxidation product, it was assumed from the curve feature that the number is very low. In contrast, the curve structure of TSPI-modified PS film is quite different from that of bulk PS film. In particular, there is a significant growth of the C=O peak and there is a marked decay of C—O signal intensity. These findings strongly supported the results obtained from the IR study, namely, the grafting of POS onto PS promotes the development of C=O groups within the PS structure, thereby causing the opening of the glucose ring.

From this information, the graft structures set forth below is proposed. It is not clear whether the opening of the ring leads to the formation of a free radical or a saturated group.

I

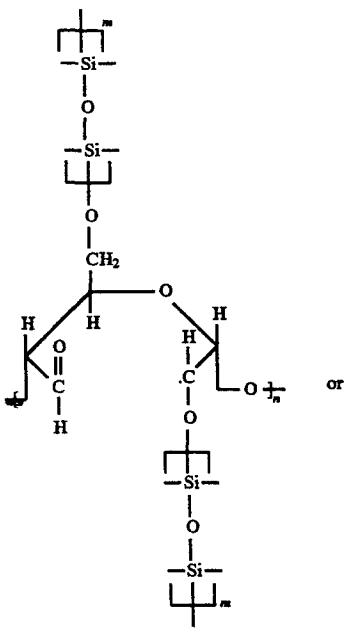

-continued

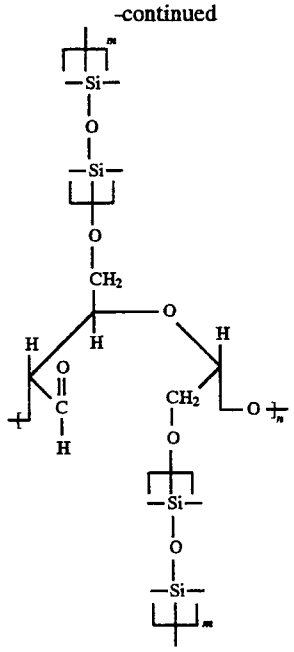

d. Thermal Characteristics

Thermal characteristics, such as melting point, thermal degradation, and stability, of 200° C.-heated samples with PS/TSPI ratios of 100/0, 99/1, 95/5, 90/10, and 85/15 have been studied. FIG. 3 illustrates the DSC endothermic phase transitions occurring in these samples at temperatures ranging from 25° C. to 170° C. As reported by Lelievre in J. Appl. Poly. Sci., 18, p. 293, 1973 and Donovan in Biopolymers, 18, p. 263, 1979, the temperature of the endothermal peak for hydrated starches depended primarily on the degree of its hydration; namely, the starch with a low degree of hydration had the endothermal peak at higher temperature. They interpreted that a shift in the endothermal peak to a high temperature site corresponds to an increase in melting point of starch. From this information, the endothermal peak at 120° C. for bulk PS (100/0 ratio) was similar to that obtained from their samples containing a minimum amount of water.

When PS was modified with TSPI, the endothermic temperature expressed as the melting point (T_m) decreases with an increasing amount of TSPI, suggesting that the T_m shifts to low temperature site as the number of POS grafts per PS chain unit is increased. In other words, the cleavage of glycol C—C bonds which occurred when POS was grafted onto glycosidic rings might cause a lowering of T_m, reflecting a low rate of PS hydration. The enthalpy, ΔH, of this phase transition was computed using the formula $\Delta H = T \cdot R \cdot A / h \cdot m$, where T, R, A, h, and m refer to temperature scale (° C./in.), range sensitivity (mcal./sec.-in.), peak area (in^2), heating rate (° C./sec), and weight of the sample (mg), respectively. The changes in ΔH as a function of the proportion of PS to TSPI are given in Table 2 below.

TABLE 2

Changes in Enthalpy which Represent the Rate of PS Hydration as a Function of PS/TSPI Ratios

PS/TSPI ratio	Enthalpy value, ΔH KJ/g
100/0	0.325
99/1	0.266
97/3	0.240

II

TABLE 2-continued

Changes in Enthalpy which Represent the Rate of PS Hydration as a Function of PS/TSPI Ratios

PS/TSPI ratio	Enthalpy value, ΔH KJ/g
95/5	0.176
90/10	0.136
85/15	0.119

From Table 2 above, it is apparent that the value of ΔH decreases with an increasing amount of TSPI incorporated into PS. Because the ΔH value reflects the total energy consumed for breaking the intermolecular hydrogen bonds generated between starch and water, it was assumed that a high degree of POS grafts might lead to a molecular configuration of PS chains with fewer hydrogen bonds.

A thermal analysis, combining TGA and DTA, revealed the decomposition characteristics during pyrolysis of 200° C.-heated samples as shown in FIG. 4. The TGA curve (top) for the bulk PS, showed a certain rate of loss in weight between 30° C. and 150° C., followed by large reductions in the two temperature ranges, 300° C.–400° C. and 450° C.–600° C., and then a small decrease between 600° C. and 700° C. The loss in weight occurring at each individual stage in the four-step decomposition process gave the following values: about 10% at temperatures up to 200° C., about 19% between 200° C. and 450° C., about 16% between 450° C. and 600° C., and about 3% between 600° C. and 700° C. By comparison with the TGA curve of bulk PS, the changes in the feature of the curve were seen in samples in which TSPI was incorporated. The addition of TSPI to PS greatly reduced the weight loss in the first decomposition stage. Considering that the weight loss at temperatures up to 200° C. was due mainly to dehydration of the samples, it is believed that the samples heated to 200° C. and which had a high proportion of TSPI to PS had a lesser uptake of moisture. For all the TSPI-modified PS samples, the onset temperature of the second decomposition stage was near 280° C. Of particular interest were also the features of curves obtained for samples 99/1 and 95/5 PS/TSPI ratio. These curves were different from those obtained for samples having 90/10 and 85/15 having PS/TSPI ratios; namely, the latter samples had two additional decomposition stages at temperatures ranging from 310° C. to 600° C.; by contrast, the 99/1 and 95/5 ratio PS/TSPI samples were characterized by a large decrease between 280° C. and 340° C., followed by a gradual loss in weight after 340° C. In these additional stages, one of the decompositions occurred between 310° C. and 470° C., and the other was in the ranges from 470° C. to 600° C. These additional decomposition stages have been assigned to POS polymers. Thus, a high proportion of TSPI to PS appeared to provide an individual POS formation segregated from the POS-grafted PS polymer systems. If this interpretation is correct, the decomposition occurring between 280° C. and 340° C. could correspond to the formation of POS-grafted PS polymers as the reaction products. In fact, no such decomposition was found from bulk PS samples.

Significantly, the DTA curves (bottom) accompanying the TGA data strongly supported the information described above. The curve of bulk PS indicated the presence of three prominent endothermic peaks at 95° C., 410° C., and 500° C. Because a DTA endothermic peak represents the phase transition temperature caused by the thermal decomposition of chemical compounds, the peak at 95° C. reveals the dehydration of PS, while the removal of carbonaceous groups from the PS structure may be associated with the peaks at 410° and 500° C. In contrast, the 99/1 and 95/5 ratio

of PS/TSPI samples had only two endothermic peaks at 95° C. and 310° C. The former peak appeared to be due to the elimination of water from the TSPI-modified PS polymers, and the latter could reveal the decomposition of POS-grafted PS polymers. No peaks at 410° C. and 500° C. were recorded on the DTA curves. As expected, the peak intensity at 95° C. decreased with an increasing amount of TSPI, suggesting that a highly grafted POS onto PS lead to a low rate of hydration of PS. Assuming that the peak at 310° C. was related to the grafted PS polymers, the growth of its line intensity resulting from the incorporation of a large amount of TSPI into PS indicated that the extent of POS grafting was promoted by an increased amount of TSPI. The peaks at 400° C. and 540° C. for the 90/10 and 85/15 ratio samples were assignable to the phase transition temperatures of POS itself isolated from the grafted PS. The intensity of these peaks increased with an increase in the proportion of TSPI to PS, implying that the extent of non-grafted bulk POS existing in the whole polymer structure increased as an excessive amount of TSPI was added to PS.

It is well documented that the hydration of starch introduces crystallinity into the amylose portion and linear branching of amylopectin. Thus, the degree of crystallinity of unmodified and TSPI-modified PS samples were investigated after heating at 200° C., by XRD. The resulting XRD patterns, ranging from 0.256 to 0.590 nm, (not shown) revealed that all the samples were essentially amorphous. Because the formation of an amorphous phase was due mainly to the low rate of hydration of starch, it was assumed that the two major factors, the treatment at 200° C. and the opening of glycosidic rings by grafting of POS onto the PS, may cause a poor hydration of starch.

5. Characteristics of Coated Surfaces

Based upon the information described above, the characteristics of the TSPI-modified PS coating films deposited onto surfaces of aluminum substrate were analyzed next. The characteristics to be investigated involved the magnitude of wettability and spreadability of PS solutions modified with TSPI onto aluminum surfaces, the morphological features and elemental compositions of the coating films, and the susceptibility of the film surfaces to moisture. All of the data obtained were correlated directly with the results from the corrosion-related tests, such as electrochemical impedance spectroscopy (EIS) and salt-spray resistance tests.

a. Wettabilitv of Coated Surfaces

In forming uniform, continuous coating films, the magnitude of wettability and spreadability of the alkali-cleaned aluminum surfaces by TSPI-modified PS solutions was among the most important factors governing good protective-coating performance. In an earlier study on the chemical composition of aluminum surfaces treated with a hot alkali solution. I have reported that such surface preparation method introduces an oxide layer into the outermost surface sites of aluminum. See Sugama, T., et al., in J. Coat. Tech., 65, p. 27, 1993. Hence, the magnitude of the wettability of the unmodified and TSPI-modified PS solutions over the aluminum oxide layers was estimated from average values of the advancing contact angle, θ (in degrees), on this surface. A plot of θ as a function of the PS/TSPI ratios is shown in FIG. 5. Because a low contact angle implied better wetting, the resultant θ-ratio data exhibited an interesting feature, namely, the wetting behavior was improved by increasing the proportion of TSPI to PS. In fact, a considerable low θ value of <18°, compared with that of the 100/0 ratio, was measured from the 95/5, 90/10, and 85/15 ratio PS/TSPI solutions, suggesting that the chemical affinity of the PS solution for the aluminum oxide surfaces was significantly improved by incorporating TSPI into it.

The surface image and elemental analyses for 200° C.-treated 100/0, 95/5, 90/10, and 85/15 ratio films over the aluminum substrates were carried out by SEM and EDX. The SEM image of 100/0 ratio film shown in FIG. 6 at the top) disclosed the morphological feature as a rough, thick coating film. The EDX spectrum, concomitant with the SEM micrographs, for this film, indicated the presence of four dominant lines of C, O, Al, and Au. The detected Au corresponds to that used as the sputtering material over the film surfaces. Because EDX is useful for quantitative analysis of elements which exist in the subsurface layer of up to about 1.5 μm in thickness, the aluminum element virtually belongs to the underlying substrate, while the C and O elements are assignable to the PS film. Hence, the thickness of this film is less than 1.5 μm. In contrast, the SEM image of coatings derived from the 95/5 ratio showed a continuous film covering the aluminum substrate as illlustrated at the bottom of FIG. 6. The disclosure of a rough underlying aluminum surface expressed the formation of a thin, transparent film. As expected, the EDX spectrum of this film had a dominant peak for Al, and weak C, O, and Si signals which revealed the formation of POS-grafted PS polymer films. Relating this finding to the fact that the spreadability of PS solution over the Al was significantly improved by incorporating TSPI, such a high magnitude of spreadability by TSPI-modified PS solutions perhaps provided the fabrication of thin coating film on Al. However, no determination of film thickness was made in this experiment. By comparison with that of the 95/5 ratio PS/TSPI film, no distinctive features were seen in the SEM images (not shown) from the 90/10 and 85/15 ratio PS/TSPI films. The EDX spectra for these films demonstrated that a very thin film was formed from 90/10 and 85/15 ratio solutions because of the indication of a firther intense Al signal.

b. Susceptibility of Coated Surfaces to Moisture

One important factor which is indispensable for good protective coating systems is good hydrophobic characteristics, namely the film coated surfaces are not susceptible to moisture. To obtain information on these characteristics, we measured the contact angle of a water droplet on the 200° C.-treated 100/0, 95/15, 90/10, and 85/15 ratio of PS/TSPI covered aluminum film surfaces. For instance, if the contact angle was low, we concluded that the film is susceptible to moisture. A high degree of susceptibility could allow the hydrolytic decomposition of the film and the penetration of water through the coating layers.

A plot of the contact angles against the changes in PS/TSPI ratio is shown in FIG. 7. The data set forth in FIG. 7 shows that a decrease in this ratio enhanced the contact angle, corresponding to a low degree of wettability of the film surface. The highest value of contact angle in this test series was obtained from the 90/10 and 85/15 ratios of PS/TSPI coatings, reflecting their low susceptibility to moisture.

All these data were correlated directly with the results from the electrochemical impedance spectroscopy (EIS) for the 100/0, 95/5, 90/10, and 85/15 ratio of PS/TSPI coated aluminum specimens at 200° C. An uncoated Al substrate was also used as the reference sample.

FIG. 8 compares the Bode-plot features (the absolute value of impedance, |Z|, ohm-cm^2 vs. frequency, Hz) of these specimens before exposure. As regards the overall impedance curve our tests focused on the impedance value of element |Z|, which can be determined from the plateau in the Bode plot occurring at sufficiently low frequencies. The impedance of the uncoated aluminum substrate was ≈3.0×10^3 ohm-cm^2 at a frequency of 0.0 Hz. Once the aluminum surface was coated with unmodified and TSPI-modified PS films, the impedance in the terms of pore resistance, R_{po}, of the coatings increased by one or two orders of magnitude over that of the substrate. The R_{po} values reflect the magnitude of ionic conductivity generated by the electrolyte passing through coating layers; namely, a high value of R_{po}

corresponds to a low degree of penetration of electrolyte into the coating film. The data demonstrated that the changes in the magnitude of conductivity depend on the PS/TSPI ratios. The data also showed that the curve feature of 90/10 ratio-derived coating closely resembled that of the 85/15 ratio PS/TSPI coating, suggesting that the ability of 90/10 ratio coating to prevent the penetration of electrolyte is almost the same as that of 85/15 ratio. From the comparison of R_{po} values at 5×10^{-2} Hz, the effectiveness of these ratios in ensuring a low degree of penetration of electrolyte was in the following order; 85/15=90/10>95/5>100/0. Thus, the 85/15 and 90/10 ratio-derived PS/TSPI coating films displayed a good protective performance of aluminum against corrosion.

c. Salt Spray Resistance Tests

To support the data obtained from EIS, salt-spray resistance tests were carried out for all coated specimens. The trace of rust stain was generally looked for in evaluating the results from salt-sprayed specimens.

TABLE 3

Salt-Spray Resistance Tests for TSPI-Modified PS Coatings

PS/TSPI ratio	Salt-spray resistance Hr
100/0	24
99/1	24
97/3	24
95/5	48
90/10	288
85/15	288

As shown in Table 3 above, the results were reported as the total exposure time at the date of the generation of rust stain from Al surfaces. The surfaces of the 100/0, 99/1, and 97/3 ratio coatings were corroded after exposure to salt fog for only 24 hours. By comparison with these coatings, a better protective performance for 48 hours was obtained from the 95/5 ratio-coated specimens. In contrast, the deposition of the 90/10 and 85/15 PS/TSPI ratio coatings onto aluminum contributed remarkably to protecting it from salt-induced corrosion for 288 hrs. This finding was similar to the data obtained on EIS, namely, the most effective thin coating film for protecting aluminum alloys against corrosion can be prepared by using the solutions having ratios of 90/10 and 85/15 PS/TSPI ratios.

In conclusion, in applying the polyorganosiloxane (POS) polymers grafted onto polysaccharide as thin coating films, adequate protection from corrosion to aluminum alloys was provided. The precursor hydrolysate solutions with a pH of 8.5–8.9 were prepared by incorporating monomeric N-[-3-(triethoxysilyl)propyl]-4.5, -dihydroimidazole (TSPI) as source of graft-forming POS into a 1.0 wt % potato starch (PS) aqueous solution as source of polysaccharide. The monomeric TSPI solutions consisted of 9.5 wt % TSPI, 3.8 wt % CH_3OH, 1.0 wt % HCl, and 85.7 wt % water. In this system, TSPI played an important role in preventing the settlement and growth of microorganisms in PS aqueous solution. One of the important properties for TSPI precursor solution was that the surface tension of PS hydrolysate could be reduced by adding TSPI hydrolysate, thereby assuring its excellent wetting behavior on aluminum surfaces.

The high magnitude of wettability was responsible for fabricating a thin solid film over aluminum surfaces. When the precursor solution-solid phase conversion occurred at 200° C. in air, the grafting of TSPI-derived POS polymer onto PS was produced by dehydrating condensation reactions between silanol groups in the hydrolysate of TSPI, and the OH groups of glycol and CH_2OH in the glucose units.

Such reactions of silanol with one OH of glycol groups also led to the cleavage of glycol C—C bonds, causing the opening of glycosidic rings. Thus, an increase in the number of POS grafts shifted the melting point of PS to a low temperature site, thereby forming the molecular configuration of PS chains with few hydrogen bonds between PS and water. Although the onset of major thermal decomposition of POS-grafted PS polymers began near 280° C., the loss in weight of POS-PS copolymers occurring between 280° C. and 700° C. depended mainly on the number of POS grafts; a high degree of grafting corresponded to a low rate of weight reduction. However, the addition of an excessive amount of TSPI to PS caused the phase segregation of non-grafted POS polymers from its copolymer phases.

The most effective amorphous coating films for preventing the corrosion of aluminum surfaces were derived from precursor solutions with PS/TSPI ratios of 90/10 and 85/15. These coating films deposited onto an aluminum surface displayed a low susceptibility to moisture, improved impedance, Ω-cm^2 by two orders of magnitude over that of an uncoated aluminum substrate, and conferred salt-spray resistance for 288 hours.

EXAMPLE 2

In this example, environmentally benign natural polymers in water-based coating material systems were provided to protect aluminum (Al) substrates from corrosion. Polygalacturonic acid methyl ester or pectin (PE) which belongs to a family of natural polymers was modified with N-[3-(triethoxysilyl)propyl]-4.5-dihydroimidazole (TSPI). The water-based coating systems were prepared by mixing solutions of two phases; one was PE dissolved in water, and the other was a sol solution, consisting of TSPI, water, CH_3OH, and HCl. In this system, TSPI played an important role in preventing the settlement and growth of microorganisms in PE aqueous solution.

1. Materials

The materials used to make the polysaccharide graft polymers and coatings including these polymers have been synthesized as set forth below or are readily commercially available.

Polygalacturonic acid methyl ester,

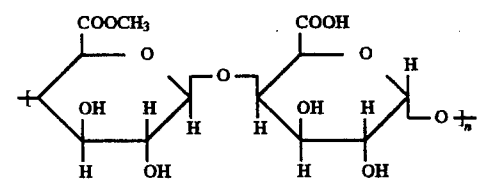

(pectin, PE), with M.W. 20,000–30,000, obtained from Scientific Polymer Products Inc., was used as the natural polymer. For modifying this polymer, monomeric N-[3-(triethoxysilyl)propyl]-4.5,-dihydroimidazole (TSPI),

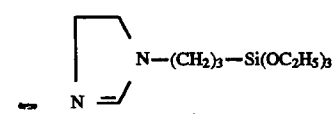

was supplied by Petrarch Systems Ltd. The estimated purity level of these organic reagents was greater than 99.8%. A 0.7 wt % PE solution dissolved in deionized water was modified by incorporating various amounts of TSPI solution consisting of 9.5 wt % TSPI, 3.8 wt % CH_3OH, 1.0 wt % HCl, and 85.7 wt % water. Six ratios of PE/TSPI solutions were used, namely, 100/0, 99/1, 97/3, and 95/5 by weight, corresponding to pH value of 3.40, 3.68, 6.37, and 7.55, respectively.

The lightweight metal substrate was 6061-T6 aluminum (Al) sheet, containing the following chemical constituents: 96.3 wt % Al, 0.6 wt % Si, 0.7 wt % Fe, 0.3 wt % Cu, 0.2 wt % Mn, 1.0 wt % Mg, 0.2 wt % Cr, 0.3 wt % Zn, 0.2 wt % Ti, and 0.2 wt % other.

2. Coating Method

Aluminum surfaces were coated by TSPI-modified and unmodified PE films in the following sequence. As the first step to remove surface contaminants, the aluminum substrates were immersed for 20 min at 80° C. in an alkaline solution consisting of 0.4 wt % NaOH, 2.8 wt % tetrasodium pyrophosphate, 2.8 wt % sodium bicarbonate, and 94.0 wt % water. The alkali-cleaned aluminum surfaces were washed with deionized water at 25° C. for 5 minutes, and dried for 15 minutes at 100° C. Then, the substrates were dipped into a soaking bath of solution at room temperature, and withdrawn slowly. The wetted substrates were heated in an oven for 120 min at either 50°, 80°, 100°, 150°, 200°, or 250° C. to yield thin solid films. Because the PE solution is a suitable nutrient for fungal and bacterial growth, the effect of adding TSPI was to prevent the growth and colonization of microorganisms.

3. Measurements

The antibacterial properties of the coatings of the present invention were measured by using scanning electron microscopy (SEM) and energy-dispersion X-ray (EDX). The changes in chemical conformation of PE modified with different amounts of TSPI were investigated by fourier transform infrared (FT-IR) spectrophotometer. To determine the maximum allowable temperature needed for fabricating the coating films, the onset of thermal decomposition in modified and unmodified PE polymers was measured using thermogravimetric analysis (TGA) in air. The changes in magnitudes of water-wettability of PE film surfaces with various amounts of TSPI were recorded by measuring the contact angle within the first 30 seconds after dropping water on their surfaces. The resulting data provided information on the degree of susceptibility to moisture of modified and unmodified PE film surfaces. Information on the bond structure assembled at interfaces between modified PE film and Al was obtained using X-ray photoelectron spectroscopy (XPS). These data were correlated directly with the corrosion-related information.

AC electrochemical impedance spectroscopy (EIS) was used to evaluate the ability of coating films to protect Al from corrosion. The specimens were mounted in a holder, and then inserted into an electrochemical cell. Computer programs were prepared to calculate theoretical impedance spectra and to analyze experimental data. Specimens with a surface area of 13 cm^2 were exposed to an aerated 0.5N NaCl electrolyte at 25° C., and single-sine technology with an input AC voltage of 10 mV (rms) was used over a frequency range of 10 KHz to 1 MHZ. The lower frequency limit was chosen because of time limitations. To estimate the protective performance of coatings, the pore resistance, R_{po}, was determined from the plateau in Bode-plot scans (impedance, ohm-cm^2 vs. frequency, Hz) that occurred at low frequency regions.

4. Characteristics of Coating Films

a. Growth of Microorganisms

PS polymers contain C, H, and O, among other elements as suitable nutrients for fungal and bacterial growth. When the PS polymer comes into contact with water, inevitably the growth of microorganisms already present in the water is stimulated, and bacterial colonies are formed. A serious problem in using such colonized polymer solutions as coating materials is caused by microbial bioparticles incorporated into layers of dried coating film which particles promote the rate of water transportation. The coating films become wet and fail as corrosion-protective coatings. Thus, adding an antimicrobial agent to the PE solution is needed to prevent the growth of microorganisms and the accumulation of water into the coating materials.

In the present invention, monomeric TSPI was employed as an antimicrobial agent. To assess its effectiveness on inhibiting microbial growth, 20 gram aqueous solutions having PS/TSPI ratios of 100/0, 99/1, and 97/3 were placed in culture flasks, and then left for two months at 25° C. in atmospheric environments. Subsequently, these solutions were deposited on aluminum substrate surfaces by dip-withdrawal coating methods, and then dried for 24 hours in a vacuum oven at 40° C. to transform them into solid films for SEM observations.

FIG. **9** shows SEM micrographs, coupled with EDX examinations of the surfaces of PE/TSPI coatings in a ratio of 100/0 at the top and 93/3 at the bottom. The SEM image from an unmodified PE coating disclosed a continuous coverage of extensive fungal clusters over the aluminum substrate. As expected, the EDX spectrum for the cluster denoted as site A showed the presence of only two organic elements, C and O, corresponding to microorganisms formed in the TSPI unmodified coating. There was no signal for the element aluminum which could have originated from the underlying substrate. Because EDX is useful for quantitative elemental analysis within a subsurface layer up to ≈1.5 μm thick, the microbial biofilms deposited on the aluminum appear to have been more than 1.5 μm thick. The element Au which was detected by EDX came from the Au coating film which had been deposited on the surface of the SEM sample. The SEM image of the 99/1 ratio PE/TSPI film is not shown in this figure; however, the morphology of its surface was similar to that of the 100/0 ratio film, revealing fungal clusters randomly distributed over the aluminum substrate.

A strikingly different feature was observed when PE was modified with a 3 wt % TSPI solution; there was no fungal growth in the films having a 97/3 ratio of PE/TSPI.

The EDX spectrum at site B had a dominant line of aluminum and moderate lines of C, O, Si, and Au. Because the aluminum and silicon elements belong to the substrate and TSPI, respectively, the thickness of this film is probably less than ≈1.5 μm. Nevertheless, this finding strongly suggested that the incorporation of a proper amount of TSPI as an antimicrobial agent prevented the growth of microorganisms in the PE solution.

To understand why the TSPI-incorporated PE solution causes microbial inertness, the chemical reaction products occurring between PE and TSPI in an aqueous medium were studied. Three solutions with PE/TSPI ratios of 99/1, 97/3, and 95/5, were poured into test tubes, and left for 24 hours at room temperature to yield a suspension of colloidal reaction products. The colloidal products were separated by filtration, and subsequently converted into a solid state by heating them for 20 hours in a N_2 saturated oven at 100° C.

Finally, disks for FT-IR analysis, over the frequency ranges from 4000 to 800 cm^{-1}, were prepared by mixing 200 mg of KBr and 3 mg to 5 mg of powdered solid reaction product that had been crushed to a size of less than 0.074 mm. Also, IR spectra were taken of 100° C.-treated pure PE and TSPI as the reference samples. The results from these samples are shown in FIG. **10**.

The hydrolysis of TSPI as catalyzed by HCl not only converted ethoxysilyl groups, Si—(OC_2H_5), into silanol groups, Si-OH, but also promoted the cleavage of the N-CH_2—linkage in TSPI, thereby generating the isolated imidazoline derivative,

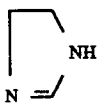

and the propylsilanol hydrolysate containing Cl-substituted end groups. The dehydrochlorinating and dehydrating condensation reactions between the hydrolysate finally induced the formation of polyorganosiloxane (POS) network structure. A typical spectrum 10(a) of 100°C.-treated bulk TSPI specimens reveals the formation of POS and imidazoline derivatives. The representative absorption bands can be interpreted as follows: O—H in the silanol groups at 3620 cm^{-1}; N—H in the imidazoline rings at 3287 cm^{-1}; C—H in the methylene chains and imidazoline at 2930 cm^{-1}; C=N in the imidazoline at 1669 cm^{-1}; Si—O—C in the Si-joined alkoxy groups at 1127 cm^{-1}; and, Si—O—Si in the polymeric siloxane at 1026 cm^{-1}. The spectrum of 100° C.-dried PE, 10(b), had six prominent peaks at band positions of 3442, 2930, 1736, 1620, 1095, and 1017 cm^{-1}.

The first four bands in the PE structure correspond to the OH, CH_3, C=O, and hydrogen-bonded C=O, respectively as is more specifically described in Bellamy, L. J., "The Infrared Spectra of Complex Molecules, vol., 3rd edition by Chapman & Hall, London, 1975. The bands at 1095 and 1017 cm^{-1} are assignable to the C—O—C stretching vibration within the PE structure. When PE was modified with a 1 wt % TSPI solution (99/1 ratio PE/TSPI), the peculiar feature of its spectrum, shown in 10(c), was the development of a new frequency at band position of 1662 cm^{-1}, while the hydrogen-bonded C=O band at 1620 cm^{-1}became a shoulder peak. This new band, corresponding to a shift in the high frequency site by 42 cm^{-1} above that of hydrogen-bonded C=O, presumably reflected the formation of newly developed hydrogen bonds by interactions between silanol, OH in the TSPI hydrolysate, and C=O in the PE. This interpretation was supported by the fact that the signal intensity of the C=O band at 1736 cm^{-1} decayed considerably with an increase in the concentration of TSPI. For instance, sample (e) as shown in FIG. **10** with a 95/5 PE/TSPI ratio showed that the peaks at 1662 and 1736 cm^{-1} were converted into a predominant and a shoulder one, respectively. Thus, the rate of formation of hydrogen bonds between silanol and C=O appeared to be enhanced when highly concentrated TSPI was incorporated into PE. Conversely, a decrease in proportion of PE to TSPI markedly reduced the intensity of PE's OH band in the frequency range of 3442 to 3304 cm^{-1}. Of particular interest was the appearance of an absorption band at 1126 cm^{-1} on the spectrum (e) of sample with a 95/5 ratio. Because this band revealed the presence of a Si—O—C linkage, one possible interpretation for the attenuation of the OH band implicated in the development of new frequency at 1126 cm^{-1}, was that the silanol groups not only had a chemical affinity with the C=O in PE to form the hydrogen bonds, but also favorably reacted with OH in PE to yield Si—O—C linkages. The latter pathway is explicable as a dehydrating condensation reaction between OH in silanol and OH in PE. The growth of a peak at 1027 cm^{-1} in the spectrum of the 95/5 PE/TSPI sample, was assigned as originating from the siloxane band, Si—O—Si; this suggested that the POSs were grafted onto the PE polymer chain. The number of POS branches per PE chain and the length of POS grafts were related to the concentration of TSPI incorporated into the PE solution.

Assuming that all of functional OH and C=O groups in PE react with TSPI, a hypothetical structure of the PE copolymer with its POS grafts is illustrated below.

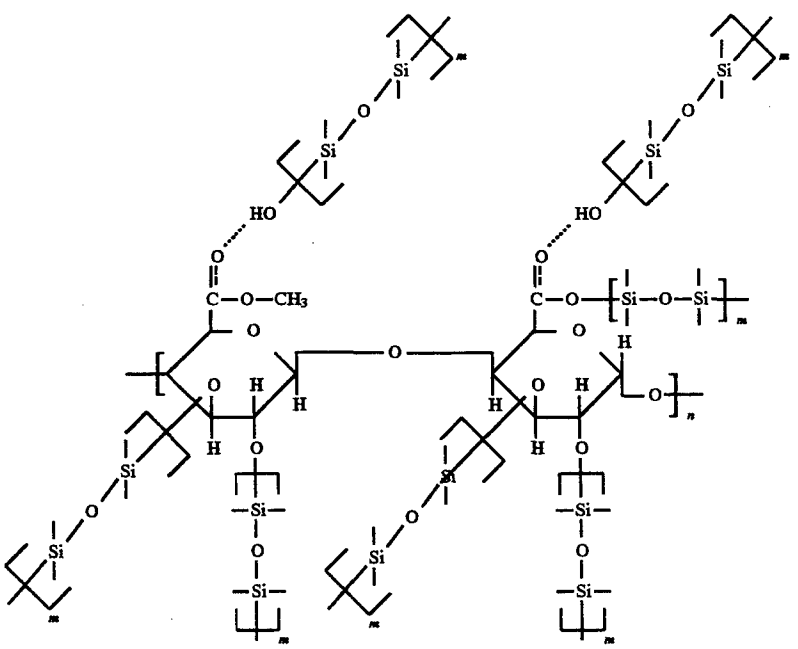

Without being bound by theory, it is believed that the reason for why TSPI-modified PE inhibits microbial growth is due to a combination of two factors. One factor is the chemical bonding between functional groups in PE and silanol groups in POS. The other factor is the alteration in molecular configuration of PE by grafting POS. The former factor not only serves in eliminating hydrophilic groups, such as OH and COOH in PE, but also contributes to an increase in the pH of the PE solution because of the decrease in numbers of COOH acid groups.

b. Thermal Characteristics

Before surveying the ability of the PE copolymers with POS grafts to protect aluminum (Al) substrates from the NaCl-related corrosion, their thermal behavior using TGA was investigated. FIG. **11** illustrates TGA curves showing the thermal-decomposition characteristics of modified and unmodified PE polymers which had been pre-heated at 100° C. for 10 hours. All these samples displayed a slight weight loss in the initial temperature range from 25° C. to 150° C., which may reflect the liberation of moisture chemisorbed onto the copolymers. The curves indicate that the amount of liberated moisture depended on the PE/TSPI ratios; namely, the uptake of moisture decreased with decreasing ratio, suggesting that PE polymers modified with a large amount of TSPI were less susceptible to attack by moisture. The onset temperatures of decomposition were obtained by finding the intersection point of the two linear extrapolations. Thus, thermal decomposition of the unmodified PE polymers (100/0 ratio) began near 270° C. Similar onset temperature was recorded on the TGA curves of the TSPI-modified PE polymers with ratios of 97/3 and 95/15. However, the total weight loss at 400° C. was markedly reduced as the amount of TSPI was increased; weight loss in the 95/5 ratio polymer was only 25%, corresponding to a lowering more than twice that of the bulk PE polymer. Thus, the thermal stability of PE polymer was improved by incorporating a certain amount of TSPI. In other words, the increased number of POS branches and the extended length of POS grafts in the PE chain significantly improved the thermal stability of PE polymers.

c. Wettability of Coated Surfaces

In making water-impermeable coating films, the magnitude of the wettability of the film surfaces by water is among the most important factors governing a good protective performance. The degree of water-wettability of the TSPI-modified and unmodified PE film surfaces was estimated from the average value of the advancing contact angle on these surfaces. The films deposited on the aluminum surfaces were prepared by heating them in an oven for 2 hours at 50°–250° C.

FIG. **12** depicts the changes in contact angle, θ, as a function of the film-treating temperatures, for the 100/10, 99/1, 97/3, and 95/15 ratio PE/TSPI polymers. The resultant θ-temperature curves demonstrated that the contact angle depends primarily on the PE/TSPI ratio and treatment temperature of the films; a high contact angle was observed in films with a low ratio of PE/TSPI treated at elevated temperatures. Because a high contact angle correlates with a lowering of wetting, the 200° C.-treated film surfaces with a 95/15 ratio had the least susceptibility to moisture. This finding strongly supported the characteristics previously discussed, namely, that modification of PE with TSPI removed hydrophilic OH and COOH groups in the PE. Thus, incorporating a large amount of TSPI into PE promoted the rate of dehydrating condensation reactions between the OH in PE and the silanol OH in TSPI, thereby increasing the number of POS branches per PE chain. In contrast, a further increase in temperature to 250° C. caused a drop in θ for all film surfaces. This enhancement in water-wetting behavior may be due to thermal decomposition of the film because the onset temperature for thermal decomposition for all these polymers is about 270° C.

d. The Interfacial Bond Structures and Reaction Products Formed at Interfaces Between Coatings and Metals

The chemistry at interfaces between a coating and the substrate it coats is one of the important factors governing the ability of polymers to protect metals against corrosion. Several other investigators have reported that imidazole type compounds are effective in affording some corrosion protection to metals, such as copper, iron, and aluminum. The corrosion-inhibiting activity of this compound was due mainly to the formation of a water-insoluble imidazole complex with metals derived from the adsorption of imidazole rings onto metal oxide surfaces. See, for example Dugdale, I., et al., in Corrosion Science, 3, p. 69, 1963; Mayanna, S. M., et al., in Corrosion Science, 15, p. 627, 1975; Yoshida, S., et al., in Journal of Material Science, 78, p. 6960, 1983.

The complete coverage of the oxide surfaces by complex layers retarded the rate of cathodic reactions, known as oxygen-reduction reactions, thereby inhibiting corrosion of the metals. As described previously, the HCl-catalyzed hydrolysis of TSPI led to the isolation of the imidazoline derivative from TSPI. Thus, if the concept of other researchers is correct, the metal surfaces might have preferentially reacted with the imidazoline derivative to form water-insoluble complexes with metal, rather than with POS. XPS was employed to obtain this information.

Samples according to the present invention were prepared in the sequence described below. The aluminum substrate was dipped into a 97/3 ratio PE/TSPI solution, and then, the solution-covered aluminum was dried for 1 hour in an oven at 80° C. to form a water-soluble xerogel film. Most of the xerogel film was removed from the aluminum surface by immersing it in deionized water. Subsequently, the film-devoid aluminum side was dried for 1 hour in N_2 gas at 100° C. for XPS examination. An XPS survey scan of the Al side indicated the presence of four different atoms, Al, Si, C, and O, corresponding to Al_{2p}, Si_{2p}, C_{1s}, and O_{1s} core-level excitation peaks. The alkali-cleaned Al surfaces not only have Al and O atoms attributed mainly to the formation of Al_2O_3, but also include elemental Si. Thus, Al, and some Si and O atoms originated from the substrates. Assuming that the Si, C, and O atoms are attributable to residual POS-grafted PE copolymer film adhering to the substrate, this film was thin enough to see the photoemission signal from the underlying Al substrate. XPS is commonly used to identify the chemical compositions and states for superficial layers at the penetrating depth of photoelectron, from 50 to 500 nm, suggesting that the thickness of such residual film may be no more than 500 nm. However, the peak for N element originating from N in the imidazoline derivatives was too weak to be detected in the N_{1s} core-level region. Thus, although imidazoline may be adsorbed on metal surfaces, imidazoline complexes with metal were susceptible to dissolution in water. In contrast, POS grafts adsorpted to metals formed water-insoluble structures, indicating that the POS grafts could have had a strong affinity for the Al_2O_3 layers that were present at the outermost surface site of aluminum.

XPS was used in order to understand the characteristics of the POS grafts and the role they played in promoting atomic linkages with Al_2O_3. The XPS Si_{2p} region exciting at the film-Al_2O_3 interfaces is shown in FIG. **13**. The deconvoluted curve for this sample revealed four Gaussian compounds at the BE position of 99.7, 101.3, 102.2, and 103.0 eV. According to Loreny, W. J., et al., in Corrosion Science, 21, p.647, 1981, the peak at 102.2 eV as the major line was assignable to the Si in the siloxane groups, Si—O—Si, and the secondary intense line at 99.7 eV originated from the elemental Si in the underlying aluminum substrate. The weakest peak at 101.3 eV as the minor component was due to the Si in the silanol groups, Si—OH. Of particular interest was the excitation of 103.0 eV line, belonging to the silicate

groups. Considering that the silicate compounds were implicated in forming water-insoluble complexes consisting of Si, O, and metals, this interesting peak was assignable to the Si in the Si—O—metal linkages. Because the metal comes from the aluminum substrate, it was assumed that such a linkage, in terms of interfacial covalent oxane-bond structure, might be formed by interactions at interfaces between POS and Al_2O_3.

All the information described above was correlated directly with the results from the electrochemical impedance spectroscopy (EIS) for 100/0, 99/1, 97/3, and 95/5 ratio-PE/TSPI coated aluminum specimens as a function of film-treating temperatures up to 250° C. EIS curves for these specimens in a 0.5N NaCl solution at 25° C. were representative of the Bode-plot features (the absolute value of impedance, |Z|, ohm-cm^2 vs. frequency, Hz). Particular attention in the overall EIS curve was given to the impedance value as the element |Z|, which can be determined from the plateau in the Bode plot occurring at sufficiently low frequencies. The impedance of the uncoated bare aluminum substrate was $\approx 5.0\times10^3$ ohm-cm^2 at a frequency of 0.5 Hz.

Once the aluminum surfaces were coated with bulk PE and grafted PE copolymers, the impedance at the same frequency, in terms of the pore resistance, R_{po}, of the coatings, increased by some degree of magnitude over that of the substrate as shown in FIG. 14. For instance, the R_{po} value of the 50° C.-treated bulk PE coating was somewhat higher than that of the bare aluminum. When PE was grafted with POS, the R_{po} for the coating treated at the same temperature increased with the increased proportion of TSPI to PE. The R_{po} values reflect the magnitude of ionic conductivity generated by the electrolyte passing through the coating layers; namely, a high value of R_{po} corresponds to a low degree of penetration of electrolyte into the coating film. Comparing R_{po} values, the effectiveness of PE/TSPI ratios in ensuring a low degree of penetration of electrolyte was in the following order: 95/5>97/3>99/1>100/0. In addition, an increase in treatment temperature, especially for the 95/5 and 97/3 PE/TSPI ratio coatings, contributed significantly to increasing the R_{po} value. Thus, treatment at 200° C. increased R_{po} by one or two orders of magnitude over that of the 50° C.-treated coatings. Temperature had little effect on the R_{po} for the 100/0 and 99/1 ratio coatings. As expected, a temperature at 250° C. was too high to be employed for assembling the coating films because of the thermal degradation of PE polymers, thereby resulting in a decrease in R_{po}.

In conclusion, the major reason for the antimicrobial activity of TSPI was due to two factors: 1) chemical bonding between the functional groups, such as OH and C=O, in PE, and the silanol hydrolysate derived from hydrolysis of TSPI, and 2) grafting of polyorganosiloxane (POS), formed by dehydrating condensation reactions between neighboring silanols, into the PE polymer chain. Such a grafted copolymer structure was formed by the condensation reaction between silanol end groups in POS and OH groups in PE, and also by hydrogen bonding between silanol hydrogen and C=O oxygen. The formation of POS-grafted PE copolymers not only conferred thermal stability on the copolymer conformation, but also, they were less susceptible to moisture because hydrophilic groups, such as OH and COOH, had been removed from PE. Furthermore, the silanol end groups in the POS grafts favorably reacted with the Al_2O_3 at the metal's outermost surface side to form interfacial covalent oxane bonds in terms of a water-insoluble bonding structure.

EXAMPLE 3

To ascertain whether TSPI acted properly as an antimicrobial agent for other natural polymers, such as potato starch, amylopectin, and hydroxyethyl cellulose, the ability of TSPI-modified starch, amylopectin, and cellulose coatings to protect aluminum (Al) alloys against corrosion was examined.

In TSPI-starch systems, the coating films were deposited onto aluminum substrate surfaces in accordance with the following sequence: the alkali-cleaned aluminum substrates were dipped for a few seconds into mixed aqueous solutions consisting of 98 to 60 wt % TSPI solution (9.5 wt % starch dissolved in water at ≈90° C.) and 2 to 40 wt % TSPI solution (9.5 wt % TSPI, 3.8 wt % CH_3OH, 1.0 wt % HCl and 85.7 wt % water) at temperatures, ranging from 90° C. to 25° C. After dipping, the substrates were withdrawn and then dried for 10 to 300 minutes at temperatures of up to 200° C.

In TSPI-amylopectin systems, the alkali-cleaned aluminum substrates were dipped for a few seconds into mixed aqueous solutions of 0.2 to 2.5 wt % amylopectin dissolved in water at 80° C. and 2 to 40 wt % TSPI solution (9.5 wt % TSPI, 3.8 wt % CH_3OH, 1.0 wt % HCl and 85.7 wt % water) at temperatures, ranging from 80° C. to 25° C. After dipping, the substrates were withdrawn and then dried for 10 to 300 minutes at temperatures of up to 200° C.

In TSPI-cellulose systems, the alkali-cleaned aluminum substrates were dipped for a few seconds into mixed aqueous solutions of 0.2 to 2.5 wt % cellulose dissolved in water at 80° C. and 2 to 40 wt % TSPI solution (9.5 wt % TSPI, 3.8 wt % CH_3OH, 1.0 wt % HCl and 85.7 wt % water) at temperatures, ranging from 80° C. to 25° C. After dipping, the substrates were withdrawn and then dried for 10 to 300 minutes at temperatures of up to 200° C.

Regarding the corrosion protection of the aluminum alloy, the coating systems developed above were compared to conventional coating systems as shown in Table 4.

TABLE 4

COATING	FILM THICKNESS	IMPEDANCE, OHM-CM^2	SALT-SPRAY RESISTANCE, HR
Blank Al	—	10^2	24
Anodic Oxide	≈10 μm	10^3–10^4	≈300
Cr-Conversion (Alodine 600)	Unknown	10^4	≈500
Polybutadiene	≈8 μm	10^5–10^6	>2000
Natural Polymers of Invention	0.5–1.0 μm	10^5–10^6	>1000

As illustrated in Table 4 above, the extent of such resistance to corrosion was far better than that of conventional anodic oxide and Cr-conversion coatings. Thus, TSPI-modified natural polymer coatings have great potential as substitutive materials for the Cr-incorporated coatings which are known to be environmentally hazardous.

We claim:

1. A polysaccharide graft polymer comprising a structure of Formula I or Formula II

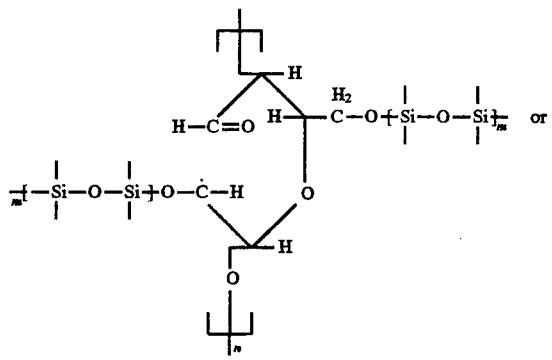

I

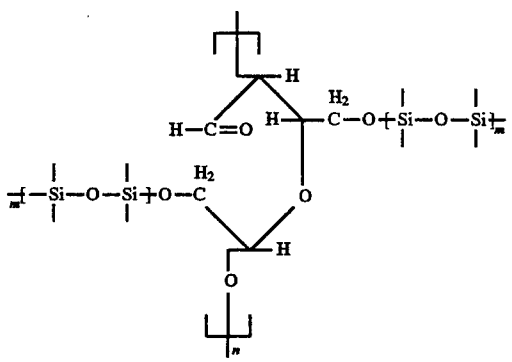

II

wherein the polysaccharide is selected from the group consisting of water dispersable starches, cellulose, cellulose esters or cellulose ethers, the segment is provided by an antimicrobial agent selected from the group consisting of halogen substituted silanes, N[3-(triethoxysilyl)-propyl]-4,5-dihydroimidazole, β-trimethoxysilylethyl-2-pyridine, β-trimethoxyxilyethyl-4-pyridine, 2-[2-trichlorosilyl) ethyl]pyridine, and 4-[2-((trichlorosilyl)ethyl] pyridine], and m and n are ≧500.

2. A method of making a polysaccharide polymer having a structure of Formula I or Formula II

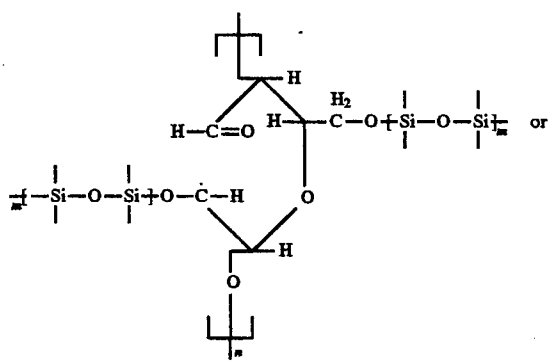

-continued

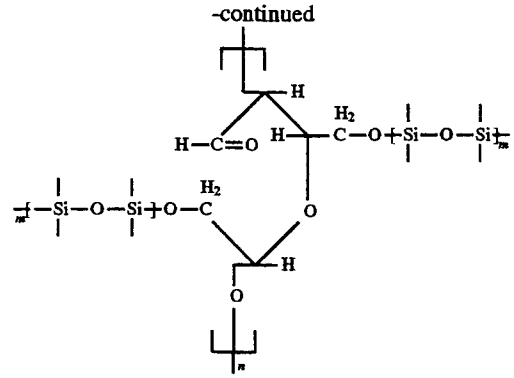

which comprises reacting a polysaccharide selected from a group consisting of water dispersable starches, cellulose, cellulose esters and cellulose ethers with an antimicrobial agent selected from the group consisting of halogen substituted silanes, N[3-(triethoxysilyl)-propyl]-4,5-dihydroimidazole, β-trimethoxysilylethyl-2-pyridine, β-trimethoxyxilylethyl-4-pyridine, 2-[2-trichlorosilyl)ethyl] pyridine, and 4-[2-(trichlorosilyl)ethyl]pyridine, under conditions of heat catalyzed dehydrating condensation.

3. The method of claim 2 wherein said polysaccharide source and said antimicrobial agent are colloidal aqueous solutions.

4. The method of claim 2, wherein said reaction occurs from about 50° C. to about 250° C.

5. The method of claim 2, wherein said polysaccharide source is selected from the group consisting of water dispersible starches and cellulosics.

6. The method of claim 2 wherein said polysaccharide source is from about 60 wt % to about 98 wt % and said antibacterial agent is from about 2 wt % to about 40 wt %.

7. The polymer of claim 1, wherein said halogen substituted silane is selected from the group consisting of: 3-bromopropyltrimethoxysilane; 3-iodopropyltrimethoxysilane; (3,3,3-trifluoropropyl) trimethoxysilane; (3,3,3-trifluoropropyl)triethoxysilane; tridecafluoro-1,1,2,2-tetrahydrooctyl-1-triethoxysilane.

8. The method of claim 2, wherein said halogen substituted silane is selected from the group consisting of: 3-bromopropyltrimethoxysilane; 3-iodopropyltrimethoxysilane; (3,3,3-trifluoropropyl) trimethoxysilane; (3,3,3-trifluoropropyl)triethoxysilane; tridecafluoro-1,1,2,2-tetrahydrooctyl-1-triethoxysilane.

9. A corrosion resistant coating having antimicrobial properties which comprises a polysaccharide graft polymer having a structure of Formula I or Formula II

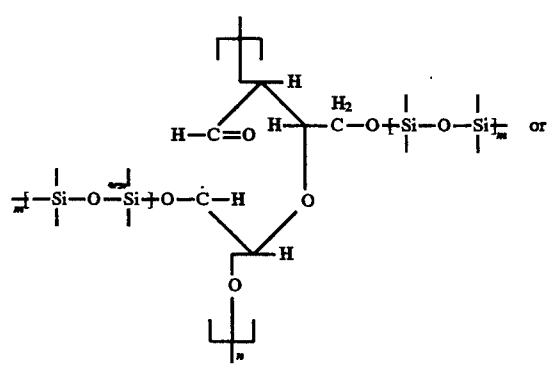

I

-continued

II

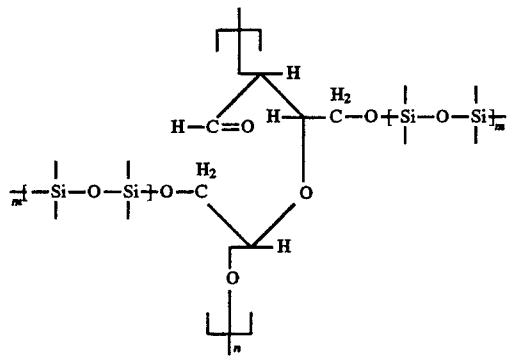

wherein the polysaccharide is selected from the group consisting of water dispersable starches, cellulose, cellulose esters or cellulose ethers, the segment is provided by an antimicrobial agent selected from the group consisting of halogen substituted silanes, N[3-(triethoxysilyl)-propyl]-4,5-dihydroimidazole, β-trimethoxysilylethyl-2-pyridine, β-trimethoxyxilylethyl-4-pyridine, 2-[2-trichlorosilyl) ethyl]pyridine, and 4-[2-(trichlorosilyl)ethyl]pyridine], and m and n are ≧500.

10. The coating of claim **9**, wherein said halogen substituted silane is selected from the group consisting of: 3-bromopropyltrimethoxysilane; 3-iodopropyltrimethoxysilane; (3,3,3-trifluoropropyl) trimethoxysilane; (3,3,3-trifluoropropyl)triethoxysilane; tridecafluoro-1,1,2,2-terahydrooctyl-1-1-triethoxysilane.

11. A method of rendering a metallic surface of a substrate resistant to corrosion which comprises:

coating a metallic surface of a substrate with a coating including a polysaccharide graft polymer having the structure of Formula I or Formula II

I

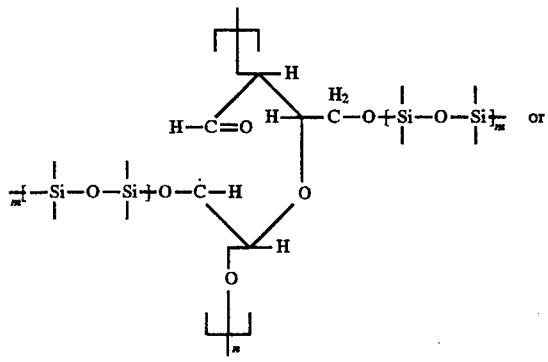

or

II

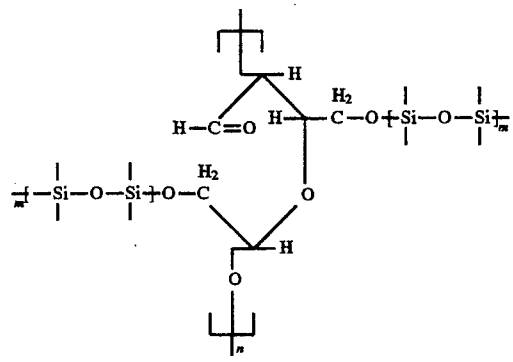

wherein the polysaccharide is selected from the group consisting of water dispersable starches, cellulose, cellulose esters or cellulose ethers, the segment is provided by an antimicrobial agent selected from the group consisting of halogen substituted silanes, N[3-(triethoxysilyl)-propyl]-4,5-dihydroimidazole, β-trimethoxysilylethyl-2-pyridine, β-trimethoxysilylethyl-4-pyridine, 2-[2-trichlorosilyl) ethyl]pyridine, and 4-[2-(trichlorosilyl)ethyl]pyridine], and m and n are ≧500.

12. The method of claim **11**, wherein said halogen substituted silane is selected from the group consisting of: 3-bromopropyltrimethoxysilane; 3-iodopropyltrimethoxysilane; (3,3,3-trifluoropropyl) trimethoxysilane; (3,3,3-trifluoropropyl)triethoxysilane; tridecafluoro-1,1,2,2-tetrahydrooctyl-1-triethoxysilane.

* * * * *